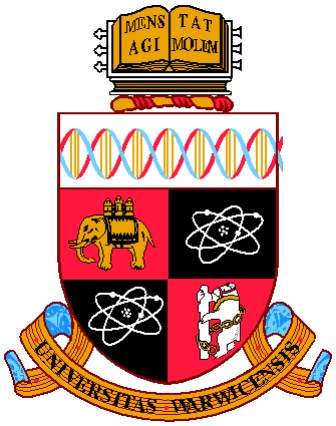

The role of NF-Y subunits in transcriptional regulation of the plant defense response

By

Maura Di Martino

Thesis

Submitted to the University of Warwick
for the degree of
Doctor of Philosophy

Life Sciences

September 2018

Table of Contents

List of Figures

List of Tables

Acknowledgement

Firstly, I would like to thank Professor Katherine Denby for her excellent supervision and input throughout this project, I have learned so much during this PhD experience. Secondly a huge thank you to my second supervisor Dr. Emily Breeze for all the support and the precious suggestions and to my third supervisor Dr. Alex Jones for her guidance on proteomics analysis.

In addition, I would like to thank my awesome lab group: Elspeth, Iulia, Dr. Sarah, Dr. Adam, Dr. Claire, Dr. Rachael and Dr. Gill, for all the help in the lab but especially to be such amazing friends and colleagues. I could not ask for more, I have learned many things from each and every one of them.

Also thank you to Murray Grant group (University of Warwick) for the *P. syringae* screening and Prof. Ben Holt (University of Oklahoma) for providing me NF-Y KO seeds.

In addition, I would like to thank the Bioscience Technology Facility of University of York for their assistance during this project.

Thank you to the MIBTP for funding and Prof. John Walsh and Dr. Patrick Schafer for being my advisory panel and for their suggestion along the way.

A huge thanks to my family for their love and support over the years, and to all my friends with a special thanks to Abi, without her none of this would have been possible. Finally, thank you to Piero for being supportive, patience and such amazing husband and to my little miracle… I can't wait to meet you!

Declarations

This thesis is presented in accordance with the regulations for the degree of Doctor of Philosophy. It has been composed by myself and has not been submitted in any previous application for any degree. All of the work in this thesis has been undertaken by myself except where otherwise stated.

Abstract

Transcriptional reprogramming plays a significant role in the defense of plants against pathogen infection. In this work, we established that NF-Y transcription factors (TF) act as important regulators of plant immunity. The eukaryotic NF-Y TF is a highly conserved heterotrimeric complex composed of three subunits, NF-YA, NF-YB and NF-YC, which directly bind CCAAT elements in target gene promoters to regulate their expression. In Arabidopsis, a multi-gene family encodes each subunit of the complex, having 10 NF-YA, 10 NF-YB and 10 NF-YC which can hypothetically combine into 1000 unique combinations. This research investigated the combinatorial mechanism of action of NF-Y complexes during the plant defense response against the necrotrophic pathogen *Botrytis cinerea*. A comprehensive investigation into the formation of these hetero-trimers revealed the ability of NF-YB2 and NF-YC2 to dimerize *in planta.* Other potential leaf complexes were also discovered confirming the combinatorial capability of NF-Y members. In agreement with the assembly mechanism observed in mammals, subcellular localization performed on Arabidopsis transgenic lines stably expressing NF-Y GFP tagged proteins, detected NF-YA2 exclusively in the nucleus and NF-YB2 and NF-YC2 in both nucleus and cytoplasm. Detailed functional analysis of knockout and overexpressor mutants identified NF-YA2 as a key regulator in the plant defense against *B. cinerea* as well as an overlapping functionality between NF-YB2 and NF-YB3 subunits. Additionally, evolutionary analysis in combination with a comparative expression analysis between Arabidopisis, tomato and lettuce NF-Ys during *B. cinerea* infection, suggested a possible conserved function of some members of NF-YA and NF-YB orthologues genes during the plant defense response.

Abbreviations

35S	Cauliflower mosaic virus promoter
ABA	Abscisic acid
ABF	ABRE-binding factor
ABRE	Abscisic acid response element
AGO1	Argonatute 1
AS	Alternative Splicing
bp	Base pair
B. cinerea	*Botrytis cinerea*
BiCAP	Bimolecular complementation affinity purification
BiFC	Bimolecular fluorescence complementation
BiFP	BIFC in Planta
BIK1	Botrytis Induced Kinase 1
BiP3	BINDING PROTEIN 3
bos1	*Botrytis susceptible 1*
BSA	Bovine serum albumin
bZIP	Basic leucine-zipper protein

CaMV	Cauliflower mosaic virus
CATMA	Complete Arabidopsis Transcriptome MicroArrays
CCT	CO, CO-like, TIMING OF CAB EXPRESSION 1
CDPK	Calcium-dependent protein kinase
cDNA	cDNA
CERK1	Chitin Elicitor Receptor Kinase 1
CFU	Colony forming units
CDS	Coding DNA sequence
ChIP	Chromatin immunoprecipitation
CO	COSTANS
Co-IP	co-immunoprecipitation
COI1	CORONATINE-INSENSITIVE 1
Col-0	*Arabidopsis thaliana* Columbia ecotype 0
CORE	CONSTANT RESPONSE ELEMENT
CRC	CRUCIFERIN C
DAMP	Damage-associated molecular pattern
DAS	Days after sowing

DE	Differentially expressed
DEG	Differentially expressed genes
DNA	Deoxyribonucleic acid
DPB3/4	DNA POLYMERASE II SUBUNIT B3/B4
DREBA2A	DREHYDRATION- RESPONSIVE ELEMENT BINDING PROTEIN 2A
E. coli	*Escherichia coli*
EIN3	Ethylene-insensitive3
EIL1	Ethylene-Insensitive3-Like 1
ER	Endoplasmic reticulum
ERF	Ethylene response factor
ERSE	ER stress response element
ET	Ethylene
ETI	Effector Triggered Immunity
E-YFP	Split YFP
FT	FLOWERING LOCUS-T
GA	gibberellic acid
GFP	Green fluorescent protein

Hpa	*Hyaloperonospora arabidopsidis*
HPI	Hours post-inoculation
HR	Hypersensitive response
IAA	Indole-3-acetic acid
JA	Jasmonic acid
JAZ	Jasmonate ZIM-domain
KO	Knockout mutant
LB	Lysogeny broth
LD	Long day
LEC1	LEAFY COTYLEDON1
L1L	LEC1-LIKE
limma	Linear models for microarrays
LYM2	Lysin Motif Domain 2
MAMP	Microbe-Associated Molecular Pattern
MAPK	Mitogen-activated protein kinase
miRNA	MicroRNA
MKS1	MAP kinase 4 Substrate 1

MS	Murashige Skoog
MS	Mass spectrometry
NASC	Nottingham Arabidopsis Stock Centre
N. benthamiana	*Nicotiana benthamiana*
NB-LRR	Nucleotide binding leucine rich repeat
NC2	Negative cofactors 2α/β
NF-Y	Nuclear factor Y
NFYBE	NF-Y BINDING ELEMENT
NHR	Non-host resistance
OE	Overexpressor mutant
OGs	Oligogalaturonides
ORA59	octadecanoid-responsive AP2/ERF 59
ORF	Open reading frame
PAMP	Pathogen-associated molecular patterns
PCR	Polymerase chain reaction
PDF1.2	PLANT DEFENSIN 1.2
PGs	Endopolygalaturonase

PGIPs	Endopolygalaturonase inhibiting proteins
PIF4	PHYTOCHROME-INTERACTING FACTOR4
PPI	Protein-protein interaction
P. syringae	*Pseudomonas syringae*
PRESTA	Plant Responses to Environmental STress: Arabidopsis
PRR	Pattern recognition receptors
PTI	PAMP-triggered immunity
REF6	RELATIVE OF EARLY FLOWERING 6
RGA	REPRESSOR OF *ga1-3*
RGL2	RGA-LIKE2
RLK	Receptor-like kinase
RNA	Ribonucleic acid
RNAi	Ribonucleic acid interference
ROS	Reactive oxygen species
RPBG1	Responsiveness To Botrytis Polygalacturonases 1
RT	Reverse transcription
RT-PCR	Reverse transcription PCR

SA	Salicylic acid
SD	Short day
SDS-PAGE	Sodium dodecyl sulfate polyacrylamide gel electrophoresis
SID2	SALICYLIC ACID INDUCTION DEFICIENT 2
SOBIR1	Suppressor Of Bir 1
SOC	Super optimal broth with catabolite repression
SOC1	SUPPRESSOR OF OVEREXPRESSION OF CO 1
SUS2	SUCROSE SYNTHASE 2
Tuba	Alpha-Tubulin
UBQ5	Ubiquitin
uORF1p	Open Reading Frame 1 peptide
UPR	Unfolded protein response
UTR	Untranslated region
WAK1	Wall Associated Kinase 1
WT	Wild-type
Y1H	Yeast one-hybrid
Y2H	Yeast two-hybrid
Y3H	Yeast three-hybrid
YFP	Yellow fluorescent protein
XTH21	XYLOGLUCAN ENDOTRANSGLUCOSYLASE/HYDROLASE 21

Chapter 1

1. Introduction

1.1 Global food security

By 2050, agriculture will need to feed more than nine billion people, requiring roughly double the amount of crops grown today. However, the demographic increment is not the only reason why more food is necessary. The spread of the middle class across the world is influencing a higher demand for meat and other protein-rich foods, increasing the pressure to grow more animal feed crops (FAO 2009). Meeting these rising demands will require a considerable increment in global food production, stretching the Earth's resources such as arable land and water. Nowadays, most of all continents are facing land degradation and water scarcity, due to farming practices and climate change. This causes loss of arable land and water resource depletion, which negatively affects crop production (Lobell and Gourdji 2012), having a deleterious impact on agriculture and food supply. In addition, climatic changes influence all life stages of the plant pathogen and modify host susceptibility, contributing to the spread of many plant diseases (Atkinson and Urwin 2012, Bebber et al. 2014). Overall, this means that plants, which are sessile organisms, will be gradually exposed to a variety of hostile environmental conditions. It is estimated that most of global food production losses are caused by different environmental stresses, such as drought, high salinity and pathogen attack (Food and Agriculture Organization of the United Nations. 2013). Worldwide average of 25% of crop losses are determined by pests and pathogens, such as bacteria, fungi, oomycetes, viruses, nematodes, and insects, to which crops are exposed (Global Food Security 2015). Counteracting crop losses associated with plant disease, while promoting environmental sustainability, is one of the fundamental challenges for plant scientists in order to ensure global food security.

Nowadays to control plant disease both at pre- and post-harvest, the use of chemicals compounds is the most common method. A large variety

of chemicals are available on the market, depending on the pathogen that they affect, such as fungicides, bactericides, viricides. However, the fact that food production heavily relies on chemical control of pathogens is worrying for human health, since many pesticides have been related with health and environmental issues (Goulson 2014, Hayes et al. 2006, Mnif et al. 2011, Sanborn et al. 2007, Zheng et al. 2016). Many studies have reported several health effects associated with accidental or intentional exposure to chemical compounds which include dermatological, neurological, carcinogenic, reproductive and endocrine effects (Nicolopoulou-Stamati et al. 2016). Furthermore, such pesticides are responsible to contaminate soil and consequently water through runoff from treated plants, damaging beneficial soil microorganisms. Moreover these chemicals can also affect non-target vegetation and non-target organisms affecting the wildlife (Aktar et al. 2009).

This evidence emphasizes the necessity of a more sustainable approach, such as the production of genetically disease resistant crops to reduce the dependence of agriculture on pesticides. A biotechnological approach would meet this challenge by providing genetically engineered plants. Hence a better understand of the transcriptional regulatory mechanisms by which plants respond to biotic stress would allow for the genes involved in host defense to be introduced or removed into crop genomes, using methods such as genetic modification or genome editing.

1.1.1 *Botrytis cinerea*: a risk to the future of food security

Botrytis cinerea is a necrotrophic fungal pathogen able to infect over 230 plant species worldwide causing severe damage, both pre- and post-harvest (Dean et al. 2012). The cost of the losses caused by this fungal disease, also called gray mold, is difficult to estimate because of the broad stages of the production and retail chain where infection can occur. However, it is estimated to be one of the major globally economically important fungal pathogens (Dean et al. 2012). Worldwide the conventional way to control *B. cinerea* consists of multiple

fungicide applications during the seasonal crop cycle. However the intensive use of fungicide has caused a significant increase of fungicide resistance in fungal pathogens with *B. cinerea* amongst them (Bardas et al. 2010, De Miccolis Angelini et al. 2014, Korolev et al. 2011, Latorre and Torres 2012). Hence, understanding how plants naturally defend themselves against this pathogen would enable to identify key genes involved in the host defense, allowing to exploit the plant genetic resistance to control the disease using a biotechnology approach. Moreover *B. cinerea* represents a good model to study the interaction between plant and necrotrophic pathogen, since it is easy to propagate in a laboratory environment and has a simple life cycle compared to other fungal pathogens (Schumacher 2012).

1.2 Plant defense response against pathogens

Plants have evolved a sophisticated multilayer defense system to protect themselves against a variety of pathogens. The successful colonization of plant by phytopathogens is quite rare with most of the plant species showing resistance to whole microbial species (Gurr and Rushton 2005, Hein et al. 2009, Ingle et al. 2006). When an entire plant species is resistant to a complete microbial species, it is called non-host resistance (NHR), while when members of a susceptible host plant species evolve the capability to resist against a specific pathogen attack, this is called cultivar resistance. NHR is the most prevalent form of plant disease resistance, relying on structural and chemical barriers, such as plant cell wall, waxy cuticles and the production of antimicrobial compounds. Another common plant disease resistance system are inducible defenses (Ingle et al. 2006), which depend on the plant's ability to recognize molecules associated with pathogen infection by pattern recognition receptors (PRRs). These host receptor-like kinases detect conserved molecules called MAMPs (microbe-associated molecular patterns) or PAMPs (pathogen-associated molecular patterns) characteristic of many microbes (Boller and Felix 2009). These receptors can also recognize molecules known as DAMPs (damage associated molecular patterns),

which are released upon damage of plant architecture. In plants the identification of these molecules initiates the activation of a basal defense called PAMP Triggered Immunity (PTI) in an attempt by the plant to prevent colonization by the pathogen. This system is able to counteract the infection through multiple defense responses such as Reactive Oxygen Species (ROS) production, intracellular Ca^{2+}, Mitogen-activated protein kinase (MAPK) and Calcium-dependent protein kinase (CDPK) signaling cascades, callose accumulation, closing of stomata and activation of defense genes (Asai et al. 2002, Nicaise et al. 2013).

Pathogens have evolved secreted effector molecules that act to suppress PTI for a successful colonization of the plant. In some cases, effectors are detectly by resistance (R) genes in the host plant which are able to identify the microbial effectors or their action on other plant proteins, in a gene-for-gene manner, initiating an effector-triggered immunity (ETI) (Jones and Dangl 2006). This defense mechanism generally involves a hypersensitive response (HR), which aims to stop the spread of the pathogen.

The 'zig-zag' model proposed by Jones and Dangl (2006) illustrates the interaction between pathogen and effectors during the course of the infection (Figure 1.1), describing the multitude of defense mechanism that the plant is able to produce. Plant pathogens such as the hemi-biotrophic pathogen *Pseudomonas syringae*, the oomycete pathogen, *Phytophthora infestans* and the biotrophic pathogen *Hyaloperonospora arabidopsidis* (*Hpa*) have evolved an advanced secretion systems which bring the effector proteins into the plant cell to suppress the defense response (Alfano 2009, Bardoel et al. 2011, Cunnac et al. 2009, Pel et al. 2014, Pieterse et al. 2012). However, there is no evidence that the plant trigger an ETI defense mechanism in response to *B. cinerea* infection. Indeed, no effectors have been shown to be recognized in a gene for gene manner. However, Govrin & Levine (2002) have proposed that the cell death induced by this necrotrophic pathogen is a sort of hypersensitive response (HR) (Govrin and Levine 2002), which secrete proteins and other molecules to aid the infection and manipulate the host.

It was reported that *Botrytis cinerea* releases small RNAs (sRNAs) to silence specific mRNAs with a role in the plant defense response (McLoughlin et al. 2018, Weiberg et al. 2013). Specifically, it has been shown that *B. cinerea* B05.10 is able to secrete sRNAs into Arabidopsis and *Solanum lycopersicum* tissue, which bind to Argonaute (AGO) proteins and guide the RNA-induced silencing complex (RICS) to suppress key *B. cinerea* defense genes present in the host plant (Weiberg et al. 2013). Indeed, Weiberg et al. (2013) reported that *ago1* knockout mutants do not show a decrease in expression levels of these defense genes, such as mitogen activated protein kinase (MPK2 and MPK1), oxidative stress related gene peroxiredoxin (PRXIIF) and cell wall associated kinase (WAK). In contrast, plants constitutively overexpressing *B. cinerea* sRNA showed an enhanced susceptibility to the necrotrophic pathogen compared to wild type plants.

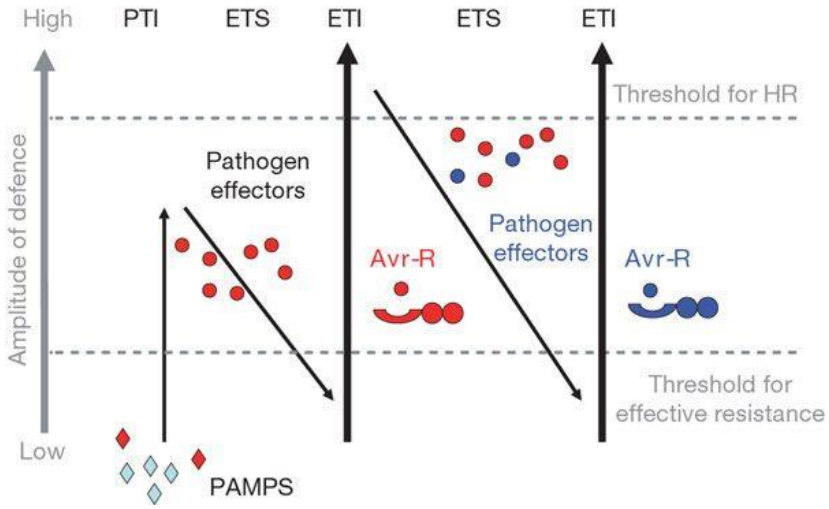

Figure 1.1 - The Zig-Zag model describes the plat immune-system (Jones and Dangl 2006). Phase 1 - Plants detect MAMPs or PAMPs (red diamonds) through PRRs to activate PAMP-triggered immunity (PTI). Phase 2 - Pathogens effectors interfere with PTI allowing pathogen's colonization and triggering effector-triggered susceptibility (ETS). Phase 3 - The effector recognition by NB-LRR protein initiate the effector-triggered immunity (ETI), increasing disease resistance and causing a hypersensitive cell death response (HR). Phase 4 - The natural selection drives the development of different effector genes able to suppress ETI and the consequent evolution of new resistance genes to trigger ETI. Figure from Jones and Dangl (2006).

1.2.1 Plant defense against *B. cinerea*

Plants use constitutive and inducible responses to defend themselves from *B. cinerea* colonization. Constitutive responses involve the production of physical barriers (cell walls and waxy cuticles) to prevent hyphal penetration, which, when bypassed by the pathogen, triggers the inducible responses. Induced responses depend on pathogen detection by the host plant. When the plant is attacked by *B. cinerea*, plant cells secrete chitinases that release chitin fragments from fungal cell walls which are recognized via the receptor kinase Chitin Elicitor Receptor Kinase 1 (CERK1) and Lysin Motif Domain 2 (LYM2), acting as MAMPs (Miya et al. 2007, Wan et al. 2008, Zhang L. et al. 2014). This recognition triggers the plant innate immunity against the pathogen helping to limit the infection (Figure 1.2). The degradation of the cell wall during the infection due to the action of *B. cinerea* endopolygalaturonase (BcPGs) and host endopolygalaturonase inhibiting proteins (PGIPs), releases oligogalaturonides (OGs) which are recognized as DAMPs by the Wall Associated Kinase 1 (WAK1) (Brutus et al. 2010). In addition, BcPGs, recognized by the receptor like protein Responsiveness To Botrytis Polygalacturonases 1 (RPBG1) (Zhang L. et al. 2014), function as MAMPs themselves. After the detection of these MAMPs and DAMPs by PRRs, the signal is transduced to downstream components by other receptor-like kinases (RLKs). For example, SOBIR1 (Suppressor Of Bir 1) a membrane bound receptor-like kinase interacts with Botrytis Induced Kinase 1 (BIK1) localized in the cytoplasm; they both have a key role in the host defense response against *B. cinerea* infection, since plants with a mutation in SOBIR1 or BIK1 are more susceptible (Zhang W. et al. 2013). Subsequently, the chitin receptor (CERK1) interacts with BIK1, this interaction allows BIK1 to leave the receptor and move towards cytoplasmic proteins involved in the activation of protein kinase (MAPK) signaling cascade systems (Lu et al. 2010). At the beginning of the cascade MAPKKK is activated by phosphorylation of a downstream MAPK kinase (MAPKK) which then activates and phosphorylates MAPKs. This MAPK signaling cascades is essential in plant immunity against several pathogens, playing an important role in PTI. How

the signaling cascades is triggered varies according to the pathogen, for example by bacterial flagellin or fungal chitin. However MPK3, MPK4, MPK6 are conserved and play an important role in plant defense response (Rasmussen et al. 2012).

MPK3 and MPK6 are essential for camalexin synthesis, an antifungal compound produced by the plant during *B. cinerea* infection (Ferrari et al. 2007). Hence, *mpk3* and *mpk6* single mutants show an increased susceptibility against *B. cinerea* (Galletti et al. 2011, Ren et al. 2008). Moreover, MPK4 is very important in the plant defense response, as it is involved in salicylic acid (SA) and jasmonic acid (JA) cross talk, which are key hormones during the infection. Hence, *mpk4/mpk6* double mutant show a decreased resistance to *B. cinerea* (Schweighofer et al. 2007). The phosphorylation of MAPKs determines a transcriptional response to the pathogen attack; hence a differential expression of significant number of genes is visible after the infection (Windram et al. 2012). Specifically, it has been reported that Arabidopsis undergoes drastic changes to its transcriptome and approximately 30% of its genome is differentially expressed 48 hours post infection with *B. cinerea* (Tao et al. 2003, Windram et al. 2012).

However, still very little is known about MAPK pathways and transcriptional regulation. Probably, the MAPK at the bottom of the cascade is capable to activate a specific set of transcription factors (TFs) and so trigger the transcriptional response. For example, WRKY DNA-Binding Protein 33 (WRKY33) TF is necessary for defense against *B. cinerea*. It has been shown that MPK4 interact with MAP kinase 4 Substrate 1 (MKS1) and with WRKY33 (Qiu et al. 2008). After the infection, MKS1 and WRKY33 are released from the trimer and activate camalexin biosynthetic genes and *WRKY33* itself in a feedback loop mechanism (Qiu et al. 2008), positively regulating the plant defense response. According to this, overexpression of MKS1 enhanced plant susceptibility against *B. cinerea*, indicating it acts as a negative regulator of the defense response against the necrotrophic pathogen (Fiil and Petersen 2011).

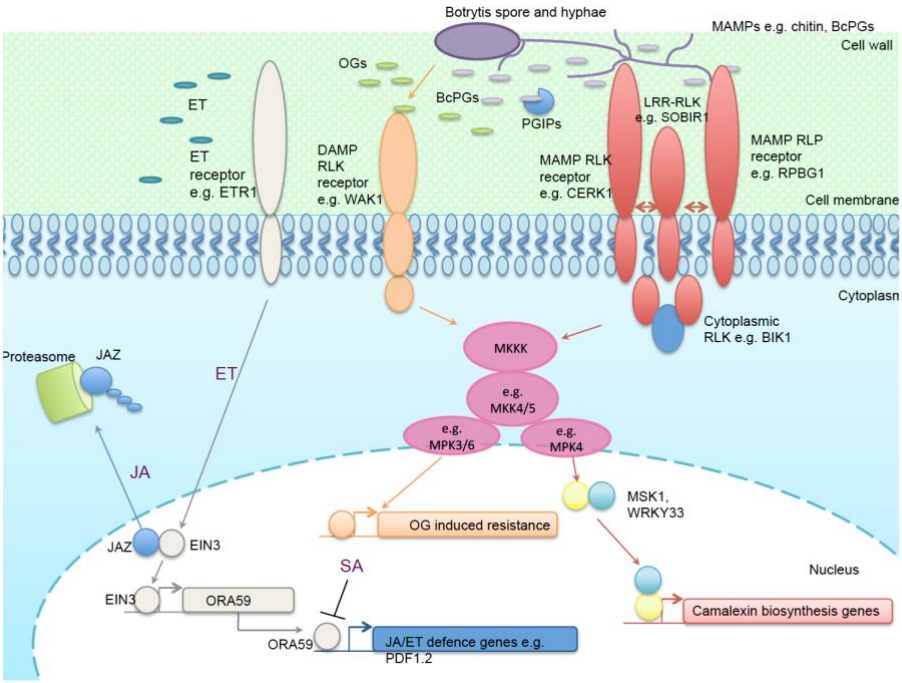

Figure 1.2 – Pathogen perception and initial signaling events during *B. cinerea* infection (Windram et al. 2015). Receptor like kinases (RLKs) and receptor like proteins (RLPs) detect MAMPs and DAMPs. This interaction initiate the signal transduction to kinase cascades. MAPKs are very important for DAMP-induced resistance and specifically MPK4 for the activation of WRKY33 TF, which activates the expression of camalexin biosynthetic genes. Then cross talk between phytohormones such as ET, SA and JA is essential in the plant defense response. In this figure, after the infection with *B. cinerea* the production of ET stabilizes the TF EIN3. The production of JA activates the degradation of the repressive JAZ proteins by the proteasome, leading the transcriptional cascade of JA and ET relate defense genes downstream of EIN3. The accumulation of ORA59 protein is repressed by SA. → indicates positive regulation and ⊣ indicates negative regulation. Figure from Windram et al. (2015).

1.2.2 Hormone crosstalk fine-tunes Arabidopsis defense response during *B. cinerea* infection

After infection by a bacteria or fungus, the plant coordinates a transcriptional reprogramming leading to differential expression of a large number of genes involved in many cellular process.

This reprogramming trigger the production of secondary metabolites such as camalexin which have an antimicrobial effect, and generate several signaling molecule, called phytohormones, to communicate the infection. These molecules have a key role in the defense response. Specifically, it is known that salicylic acid (SA), jasmonic acid (JA), ethylene (ET) and abscisic acid (ABA) play a role in the plant defense response against the necrotrophic pathogen *B. cinerea* (Audenaert

et al. 2002, Thomma et al. 1998, Thomma et al. 1999). During the infection, hormonal pathways share a high level of cross talk, which depends on many factors such as pathogen lifestyle, environmental stresses and host plant. For instance, JA seems to confer resistance to necrotrophic pathogens, while SA is more important against (hemi)biotrophic pathogens (Glazebrook 2005). Active JA-isoleucine is detected by a receptor complex formed by CORONATINE-INSENSITIVE 1 (COI1) and jasmonate ZIM-domain (JAZ) proteins (Sheard et al. 2010). Hence, it was reported that Arabidopsis COI1 knockout mutants have increased susceptibility to necrotrophic fungi such as *Botrytis cinerea* (Lorenzo et al. 2003, Thomma et al. 1998), while the resistance to the hemibiotrioph *P. syringae* increased. This is in line with high level of SA found in these mutants, supporting the hypothesis of an antagonistic relationship between JA and SA (Kloek et al. 2001). Additionally, it was discovered that Arabidopsis mutants lacking in SALICYLIC ACID INDUCTION DEFICIENT 2 (SID2), or expressing the bacterial gene nahG which leads to SA degradation, show an increased susceptibility to hemibiotrophic pathogens such as *P. syringae*. The perception of phytohormones leads to the activation of downstream TFs, which play an important role in phytohormone signaling mediation.

For example, the binding between JAZ protein and Ethylene-insensitive 3 (EIN3) and Ethylene-Insensitive3-Like 1 (EIL1) TFs (Figure 1.2), which are central activators of the ET response, is hypothesized to contribute to the cross-talk between the JA and ET pathways (Zhu et al. 2011). TFs such as Ethylene-Responsive Transcription Factor 1 (ERF1) is EIN3 target, inducing the expression of key defense genes such as PLANT DEFENSIN 1.2 (PDF1.2) (Pre et al. 2008) and octadecanoid-responsive AP2/ERF 59 (ORA59), JA/ET dependent genes, which inhibit the infection disease.

1.2.3 Changes in Arabidopsis transcriptome in response to *Botrytis cinerea*

TFs are proteins that regulate gene transcription by binding to DNA at certain target sequence to either activate or repress the gene expression in response to a particular environmental perturbation. Many genes are controlled by group of different transcription factors, which combine in a specific combination, in a mechanism called combinatorial regulation, to turn the gene on or off.

Perhaps the most famous TF families with a known role in the defense response are WRKYs and Ethylene response factors (ERFs). WRKYs act as positive or negative regulators of plant immunity (Rushton et al., 2010) and it has been reported that WRKY3, 4, 8, 18, 33, 40, 60, and 70 effect the plant susceptibility against *B. cinerea* (AbuQamar et al. 2006, Birkenbihl et al. 2012, Chen et al. 2010, Lai et al. 2008, Xu X. et al. 2006). It was also discovered that some ERFs, such as ERF1, ERF5, ERF6, RAP2.2, and ORA59 influence *B. cinerea* immunity (Berrocal-Lobo et al. 2002, Maruyama et al. 2013, Moffat et al. 2012, Pre et al. 2008, Son G. H. et al. 2012, Zhao Y. et al. 2012). Also, it was reported that NACs (Bu et al. 2008, Wang et al. 2009), TGAs (Windram et al. 2012, Zander et al. 2010) and MYBs (Mengiste et al. 2003, Ramirez et al. 2011) TFs are involved in the plant defense response. Additionally, in the last few years, a TFs family, called NUCLEAR FACTOR Y (NF-Y), is emerging as important regulator of the plant defense response (Breeze 2014, Windram et al. 2012).

1.3 NF-Y transcription factors

NUCLEAR FACTOR-Y (NF-Y), also called CCAAT-Binding Factor (CBF) and Histone-Associated Protein (HAP), are heterotrimeric transcription factors (TF) formed by binding of single NF-YA, NF-YB, and NF-YC subunits (Dolfini et al. 2009, Testa et al. 2005). These TFs are found in all sequenced eukaryotes, where they regulate gene transcription binding with high specificity to *CCAAT cis*-regulatory elements (Dolfini et al. 2012, FitzGerald et al. 2004), which are present in approximately

25%of eukaryotic promoters (Li W. X. et al. 2008). Furthermore, chromatin immunoprecipitation data, performed on mammals, reveal additional widespread NF-Y binding in non-promoter sites, suggesting the importance of binding context. It has been reported that NF-Y are able to regulate the expression of a target gene constitutively in a specific tissue and developmental stage (Maity and de Crombrugghe 1998). Single NF-Y subunits cannot regulate the transcription independently, but they have to function as a hetero complex (Mantovani 1999). The NF-Y hetero-trimer can then act as a transcriptional activator or a repressor, and the interaction with other TFs or regulatory proteins can modulate its activity.

Although all three subunits are required to bind the DNA in the *CCAAT* box (Nardini et al. 2013), NF-YA is the subunit that creates sequence-specific contact with CCAAT boxes (Laloum et al, 2013).

In mammals, each subunit (NF-YA, NF-YB and NF-YC) is encoded by single gene which have numerous splicing forms and undergo several post-transcriptional modifications. In this organisms the function and the molecular mechanism of the NF-Y complex have been well characterized in the regulation of a diverse set of genes (Dolfini et al. 2009, Testa et al. 2005) such as cell cycle progression, endoplasmic reticulum stress and DNA damage (Benatti et al. 2016, Benatti et al. 2011, Dolfini et al. 2016, Oldfield et al. 2014).

Unlike mammals, plants have a multi-gene family encoding each subunit of the trimer as shown in Table 1.1 (Zanetti et al. 2017). For example, the model plant Arabidopsis has 10 NF-YAs, 10 NF-YBs and 10 NF-YCs (Petroni et al. 2012, Siefers et al. 2009), which are distributed across all five chromosomes (Table 1.2) and can hypothetically combine in 1000 unique possible trimer combinations. This combinatorial variety enables the specific control of a large number of genes containing CCAAT-box by the 30 representatives of NF-Y subunits in Arabidopsis. Additionally, the same gene can be transcriptionally controlled by the modulation of different combinations of the heterotrimeric NF-Y complexes binding to the corresponding promoter element (Hackenberg et al. 2012).

The difference in NF-Y genes number between animal and plants is the main reason why the molecular characterization of these TFs in plants has only started in the past decade, in contrast with animal and yeast NF-Ys which have already been well characterized (Nardini et al. 2013, Romier et al. 2003).

NF-Ys have emerged as important regulators of various developmental processes and stress tolerance in plants. Hence, Arabidopsis NF-YA genes have been shown to regulate gametogenesis, embryogenesis, seed morphology, seed germination and flowering (Quach et al. 2015). Specific members of NF-YB, particularly the LEC1 group, have been reported to be involved in embryogenesis, seed and nodule development, flowering time, cell proliferation and endosperm development. Meanwhile, NF-YC have been found to regulate flowering time, root growth, photosynthesis and photomorphogenesis (Siefers et al. 2009).

Table 1.1 – Number of genes encoding NF-Y subunits in different plant species.

Species	NF-YA	NF-YB	NF-YC	Reference
Arabidopsis thaliana	10	10	10	(Petroni et al. 2012)
Nicotiana tabacum	15	9	8	(Jin J. et al. 2014)
Solanum lycopersicum	10	27	17	(Li S. et al. 2016)
Populus trychocarpa	57	38	27	(Jin J. et al. 2014)
Setaria italica	10	15	14	(Feng et al. 2015)
Oryza sativa	10	11	7	(Thirumurugan et al. 2008)
Triticum aestivum	10	11	14	(Stephenson et al. 2007)
Brachipodium distachyon	7	17	12	(Cao et al. 2011)
Zea mays	36	28	25	(Jin J. et al. 2014)
Medicago truncatula	8	14	8	(Laloum et al. 2013)
Lotus japonicus	6	11	9	(Jin J. et al. 2014)
Glycine max	21	32	15	(Quach et al. 2015)
Phaseolus vulgaris	9	14	7	(Ripodas et al. 2014)

Table 1.2 – List of NF-Y genes identified in Arabidopsis with their corresponding chromosome positions

NF-Y gene	Source accession number	Chromosome number	Chromosome location (bp)
NF-YA1	AT5G12840	5	4050691-4053669
NF-YA2	AT3G05690	3	1676504-1679061
NF-YA3	AT1G72830	1	27405145-27408221
NF-YA4	AT2G34720	2	14649706-14651709
NF-YA5	AT1G54160	1	20217336-20219452
NF-YA6	AT3G14020	3	4641930-4644571
NF-YA7	AT1G30500	1	10804450-10806428
NF-YA8	AT1G17590	1	6050164-6052628
NF-YA9	AT3G20910	3	7326355-7328581
NF-YA10	AT5G06510	5	1984823-1987064
NF-YB1	AT2G38880	2	16238401-16240883
NF-YB2	AT5G47640	5	19309227-19310272
NF-YB3	AT4G14540	4	8344349-8345324
NF-YB4	AT1G09030	1	2908611-2909032
NF-YB5	AT2G47810	2	19582658-19583618
NF-YB6	AT5G47670	5	19314778-19316169
NF-YB7	AT2G13570	2	5655391-5656518
NF-YB8	AT2G37060	2	15575996-15577916
NF-YB9	AT1G21970	1	7727577-7729649
NF-YB10	AT3G53340	3	19774318-19776289
NF-YC1	AT3G48590	3	1800593-18010018
NF-YC2	AT1G56170	1	21024482-21025902
NF-YC3	AT1G54830	1	20451083-20452671
NF-YC4	AT5G63470	5	25415600-25417199
NF-YC5	AT5G50490	5	20560434-20561228
NF-YC6	AT5G50480	5	20557574-20558487

NF-YC7	AT5G50470	5	20555120-20555758
NF-YC8	AT5G27910	5	9940669-9941447
NF-YC9	AT1G08970	1	2882491-2884342
NF-YC12	AT5G38140	5	15220208-15222524

Many TF families have undergone significant duplication mechanism in plant lineages during the evolution process and this could lead to functional overlapping. For example, MYB transcription factors in mammals are represented by a very small family composed of only three proteins involved in cell proliferation, while in Arabidopsis more than 100 MYB TFs have been found and implicated in a full range of developmental responses (Kranz et al. 1998). Another example are MADS-box TFs where the number of genes differs significantly among taxa, hence animals and fungi have between one to five MADS-box genes (Immink et al. 2010), while angiosperm plants have more than 100 (Gramzow and Theissen 2010, Wray 2003). In eukaryotic genomes, such plants, the oligomerization tendency between TFs offers a wide range of combinatorial relationships for transcriptional regulation (Wray 2003), because of the large number of TFs. With this complexity identifying specific active TF complexes is quite challenging and for this reason many studies have been mainly carried out around functional characterization of single TFs using reverse genetic approaches, such as knockout and overexpression mutants (Kondou et al. 2010), instead of focusing on complex assembly and function during endogenous and exogenous stimuli. In the case of NF-Y TFs, many studies have elucidated the biological functions of individual NF-Y subunits in plants (Gusmaroli et al. 2001, Mantovani 1999, Petroni et al. 2012) but only two papers have identified specific and active NF-Y hetero-trimers using yeast three hybrid system (Y3H) (Liu and Howell 2010, Sato et al. 2014). The difficulty in identifying unique NF-Y complexes is increased by the ability of NF-YB and NF-YC subunits to hetero-dimerize and interact with other groups of TFs, eschewing NF-YA subunits and forming non-canonical NF-Y complexes which are able to bind the DNA at different elements other than

CCAAT target sequence in the promoter (Liu and Howell 2010, Masiero et al. 2002, Wenkel et al. 2006).

1.3.1 NF-Y complexes regulates the expression of target genes in two ways.

Previous studies reported that there are two main regulatory mechanism by which NF-Y complexes modulates the expression of target genes. In the first mechanism, which is highly conserved in yeast, animals and plants, the hetero-dimer formed by NF-YB and NF-YC assembles in the cytoplasm and then translocates into the nucleus where it interacts with an NF-YA subunit and forms the hetero-trimer (Hackenberg et al. 2012, Laloum et al. 2013). All three subunits have been shown *in vitro* to be essential for binding to the CCAAT box in the promoter regions of the target genes, through NF-YA, which is the subunit that makes sequence-specific contact with the CCAAT element (Dolfini et al. 2012, Frontini et al. 2004, Mantovani 1999, Petroni et al. 2012, Sato et al. 2014). For example, it was reported that in Arabidopsis a complex formed of NF-YA4, NF-YC2 and NF-YB3 binds to the *CCAAT* box of BINDING PROTEIN 3 (BiP3) promoter region and regulates the expression of ER stress-induced genes (Liu and Howell, 2010).
In the second mechanism, the NF-YB and NF-YC hetero-dimer interact with other specific TFs to form a complex, regulating the expression of various target genes binding to specific *cis*-element in their promoters (Kumimoto et al. 2010, Wenkel et al. 2006, Yamamoto et al. 2009). In this mechanism, it was hypothesized that NF-YA subunits can inhibit the expression of target genes by competing for binding to the NF-YB/NF-YC heterodimer, preventing the formation of the NF-YB/NF-YC/non-NF-Y TF complex. For example, a complex formed by NF-YB9, NF-YC2 and bZIP67 binds to the promoter of ABA-response elements (ABREs) to regulate the expression of *SUCROSE SYNTHASE 2* (*SUS2*) and *CRUCIFERIN C* (*CRC*) and promotes seed development (Yamamoto et al. 2009). In this case NF-YA subunits compete with bZIP67 and suppress the expression of CRC forming a complex constituted by NF-YA, NF-YB9 and NF-YC2. This suggest a combinatorial

capability of each member of the NF-Y TFs family which can play different roles in plant according to endogenous and exogenous stimuli (Adrian et al., 2010).

1.3.2 Protein structure of NF-Y subunits

Each NF-Y member has a highly-conserved domain to allow the interaction between subunits and to enable the DNA binding. Crucially it has been reported that the NF-YA subunit, which is localized in the nucleus, has the capability to bind the *CCAAT* box in the promoter region of the target gene (Calvenzani et al. 2012, Laloum et al. 2013, Nardini et al. 2013, Petroni et al. 2012). Additionally, protein structure analysis has showed that the core domain of NF-YA subunits contains two α-helices A1 and A2 (Figure 1.3). A1 α helix at the N-terminal is composed of 20 amino acids and recognizes NF-YB and NF-YC subunits, while the A2 α helix at the C-terminal constitutes of 21 amino acids and it is responsible for sequence-specificity recognition of the *CCAAT* element (Laloum et al. 2013, Petroni et al. 2012). Both NF-YB and NF-YC subunits contain the conserved Histone Fold Domain (HFD), which is closely related in structure and sequence similarity to H2B and H2A histones, respectively (Dolfini et al. 2012, Laloum et al. 2013, Petroni et al. 2012) and is responsible for protein-DNA and protein-protein interactions (Frontini et al. 2004, Kahle et al. 2005, Laloum et al. 2013).

The HFD domain contains at least three α-helices (α1, α2, and α3). In NF-YB the α1 helices contain the putative DNA-binding domain (Laloum et al. 2013), α2 and α3 are responsible for the hetero-dimerization between the two subunits (Frontini et al. 2004, Zemzoumi et al. 1999) while αC in mammals is responsible for the interaction with other protein (Laloum et al. 2013, Romier et al. 2003).

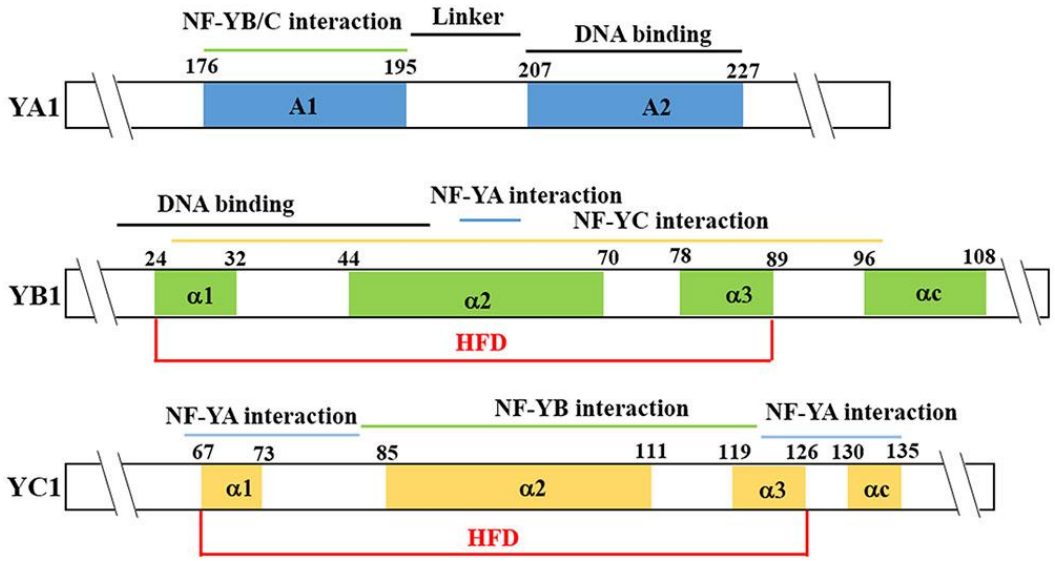

Figure 1.3 - Representation of NF-Y protein structure. The figure illustrates NF-YA1, NF-YB1 and NF-YC1 as examples. NF-YA conserved domain is formed by two α-helices: A1 and A2. A1 helix at the N-terminal is involved in the interaction with NF-YB and NF-YC subunits. A2 helix is at C-terminal functions in specific recognition of the *CCAAT* box element. NF-YB and NF-YC contain the Histone Fold Domain (HFD) involved in the DNA-binding and in the protein-protein interaction. Figure from Zhao et al. (2016).

1.3.3 NF-Y complex assembly

The assembly of NF-YB/NF-YC heterodimer in the cytoplasm is crucial for the translocation to the nucleus of the NF-YB subunit, since only NF-YA and NF-YC subunits have shown to have a nuclear localization signal (NLS) in subcellular localization experiment performed on transiently transformed Arabidopsis leaves (Hackenberg et al. 2012, Howell et al. 2010). In mammals, NF-YB and NF-YC subunits dimerize on a head-to-tail manner, through their HFDs (Figure 1.3), which involve the α1 helix of the NF-YB protein, a conserved tryptophan at the end of the α2 helix of NF-YC and a hydrophobic core formed by the α2 helices (Romier et al. 2003). This dimerization produce the surface for NF-YA association and provide a sequence-specific DNA-binding in the *CCAAT* box (Nardini et al. 2013).

In plants because each NF-Y is encoded by multigene families, most of what is known about the mechanism of NF-Y complex assembly comes from yeast two-hybrid (Y2H) and yeast-three-hybrid (Y3H) systems, used to investigate how Arabidopsis NF-Y subunits interact and assembly in hetero-trimers (Calvenzani et

al. 2012, Hackenberg et al. 2012, Sato et al. 2014). Generally, in these studies it was shown that the dimerization cannot occur between NF-YA and NF-YB members or between NF-Y subunits belonging to the same subfamily (Calvenzani et al. 2012, Hackenberg et al. 2012). However, *in vitro* analysis only allows us to investigate theoretical interaction between NF-Y members, not considering where and when the protein is expressed *in planta*. Hence, only few NF-Y complexes have been verified *in vivo,* perhaps due to their dynamic nature, which makes them hard to be detected.

Additionally, it has been reported that NF-Y subunit can interact with other proteins forming non-canonical complexes. For instance, NF-YC1, NF-YC3, NF-YC4, NF-YC9 and NF-YB2 and NF-YB3 are required for the regulation of CONSTANS (CO) during flowering time (Kumimoto et al. 2010, Wenkel et al. 2006). Hou et al. (2014) found that NF-Y complexes composed by NF-YA2, NF-YB2 and NF-YC9, interact with CO in the photoperiod pathway and with REPRESSOR OF *ga1-3* (RGA) and RGA-LIKE2 (RGL2) in the gibberellin (GA) pathway to regulate the transcription of SOC1, a crucial gene in flowering time (Hou et al. 2014). Another example of non-canonical complexes is composed by NF-YC9, also called LEAFY COTYLEDON1 (LEC1), which interact with PHYTOCHROME-INTERACTING FACTOR4 (PIF4), an important gene involved in plant development post-germination, to control hypocotyl elongation-related genes (Huang et al. 2015b).

1.3.4 NF-Ys phylogenies and alignments

As described previously, many studies have focused on individual *NF-Y* genes function, however the existence of a functional and active NF-Y complex *in planta* remains elusive. Siefers et al. (2009) presented phylogenic trees (Figure 1.4) and alignment (Figure 1.5, 1.6, 1.7) for each Arabidopsis NF-Y subfamily (NF-YA, NF-YB and NF-YC) suggesting 36 total Arabidopsis NF-Y genes (10 NF-YA, 13 NF-YB, and 13 NF-YC homologues). Conversely, it has been shown that some of the classified Arabidopsis NF-Y genes, such as NF-YB11, NF-YB12, NF-YB13, and NF-YC10, NF-YC11, NF-YC12, NF-YC13, are clearly outliers in the phylogenetic

analyses of NF-Y proteins, since they do not contain the functional NF-Y domain region. Subsequently, Petroni et al. (2012) proposed a new classification and nomenclature of Arabidopsis NF-Ys where these outlier were reclassified as negative cofactors 2α/β (NC2) (Mermelstein et al. 1996) and as DNA POLYMERASE II SUBUNIT B3/B4 (DPB3/4) (Ohya et al. 2000). Hence, a new classification with only 30 Arabidopsis NF-Ys in total (10 NF-YA, 10 NF-YB, and 10 NF-YC homologues) was proposed. In line with this, Figure 1.6 and 1.7 show that NF-YB11, NF-YB12, NF-YB13, and NF-YC10, NF-YC11, NF-YC12, NF-YC13 are phylogenetically distant, since they do not display conservation of required amino acids, suggesting an altered protein functionality (Siefers et al. 2009).

The alignment in Figure 1.5 shows that NF-YA proteins present a conserved NF-YB/NF-YC interaction domain, and a DNA-binding domain across various lineages (Siefers et al. 2009). Additionally, functionally required amino acids, which were determined from the literature, (Maity and de Crombrugghe 1992) are highly conserved across different eukaryotes, suggesting that the function of this subunit is conserved.

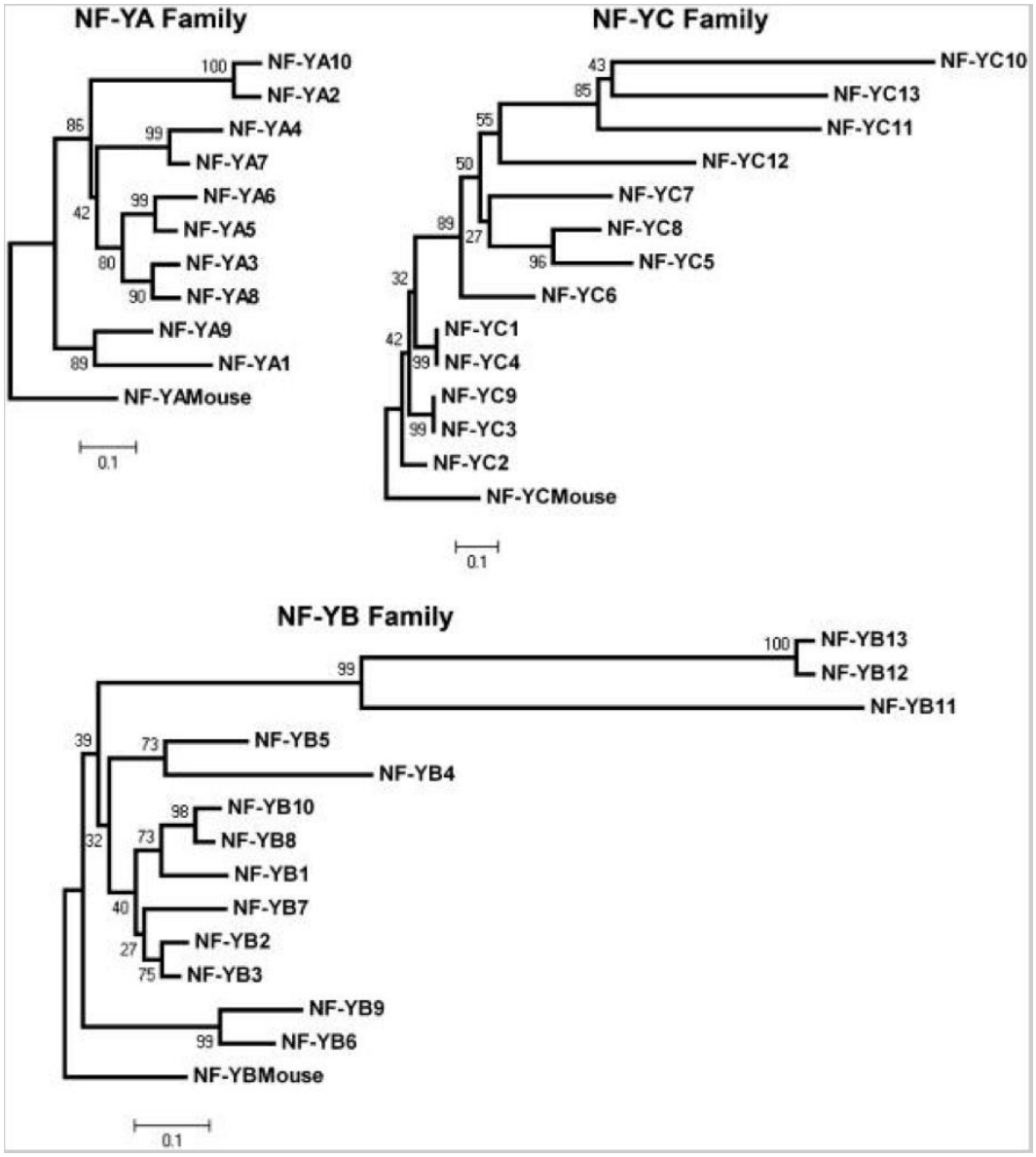

Figure 1.4 – NF-Y phylogenies. Phylogenetic trees for each subfamily were created by neighbor joining. Figure from Siefers et al. (2009)

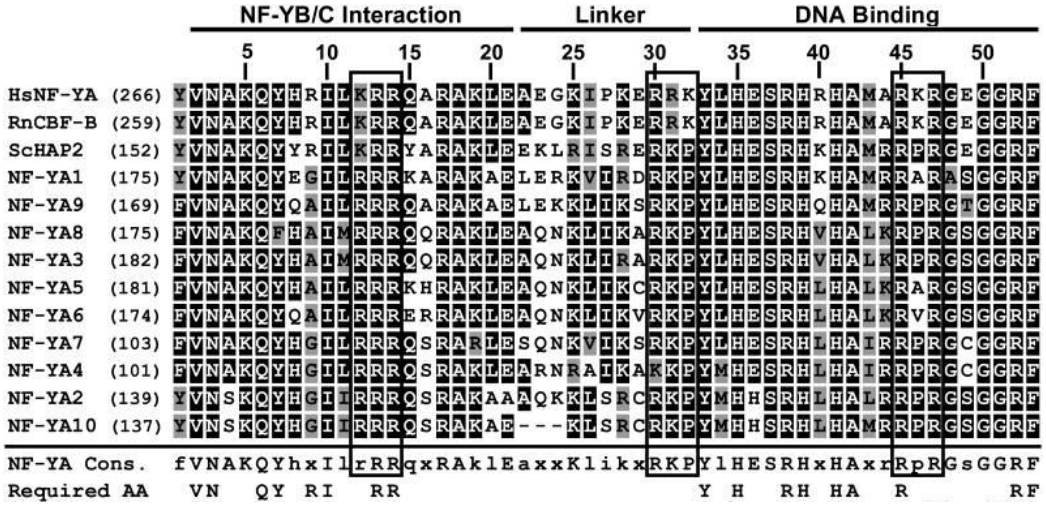

Figure 1.5 - Arabidopsis NF-YA subfamily alignment. Sequences correspond to the conserved regions in NF-YA proteins across different taxa (Hs, *Homo sapiens*; Rn, *Rattus norvegicus*; Sc, *Saccharomyces cerevisiae*). The black boxes represent the nuclear localization signals that are required for binding to importin β. In NF-YA Cons. (consensus) line, uppercase letters symbolize identity >80% of NF-YA sequences, lowercase letters > 50% identity, and x represent < 50% identity. Required amino acid (AA) residues are from the literature (Xing et al., 1993). Figure from Siefers et al. (2009).

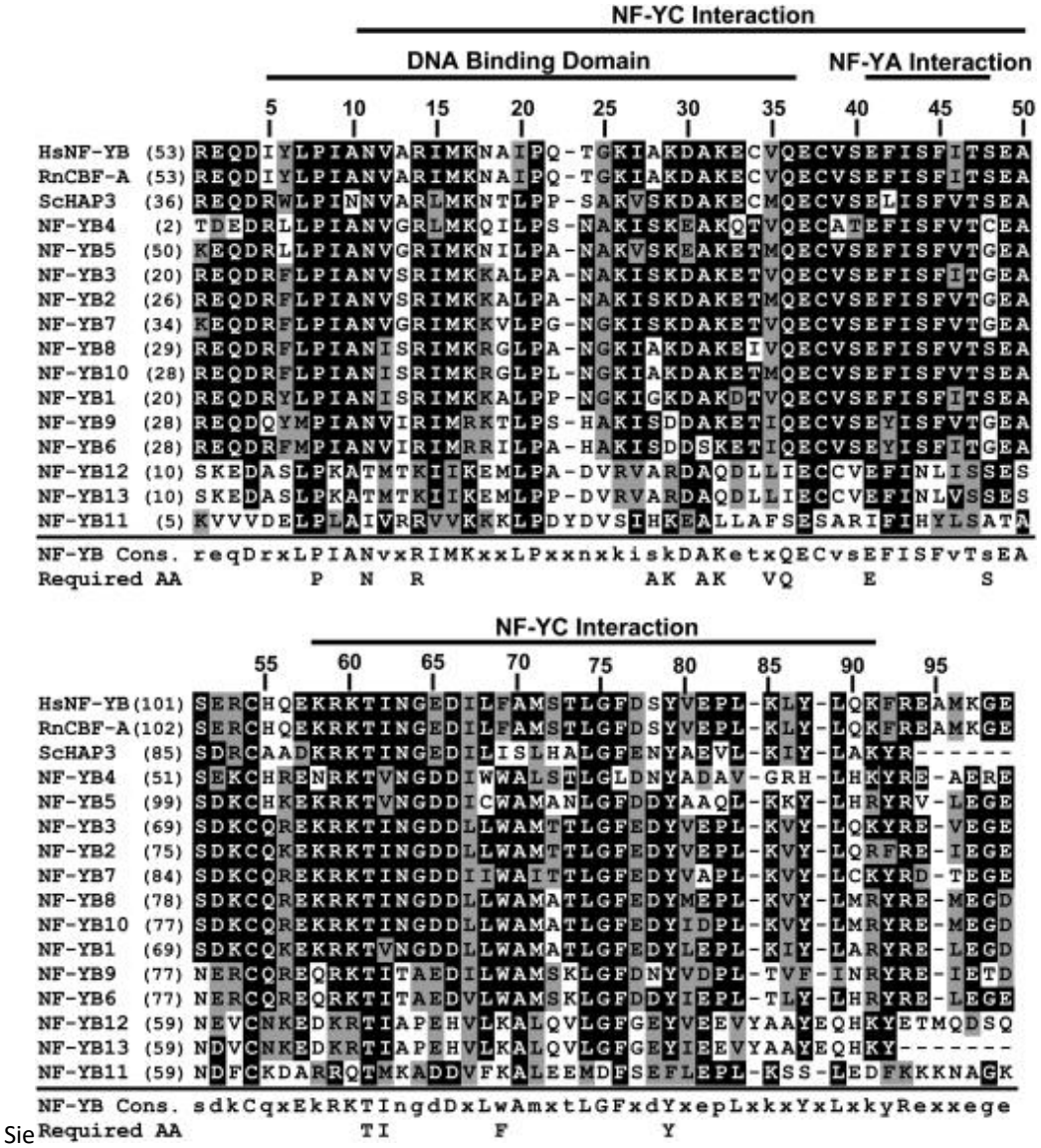

Sie

Figure 1.6 - Arabidopsis NF-YB subfamily alignment. Sequences correspond to the conserved regions in NF-YB proteins across different taxa (Hs, *Homo sapiens*; Rn, *Rattus norvegicus*; Sc, *Saccharomyces cerevisiae*). In NF-YB Cons. (consensus) line, uppercase letters symbolize identity >80% of NF-YB sequences, lowercase letters > 50% identity, and x represent < 50% identity. Required amino acid (AA) residues are from the literature (Xing et al., 1993). Figure from Siefers et al. (2009)

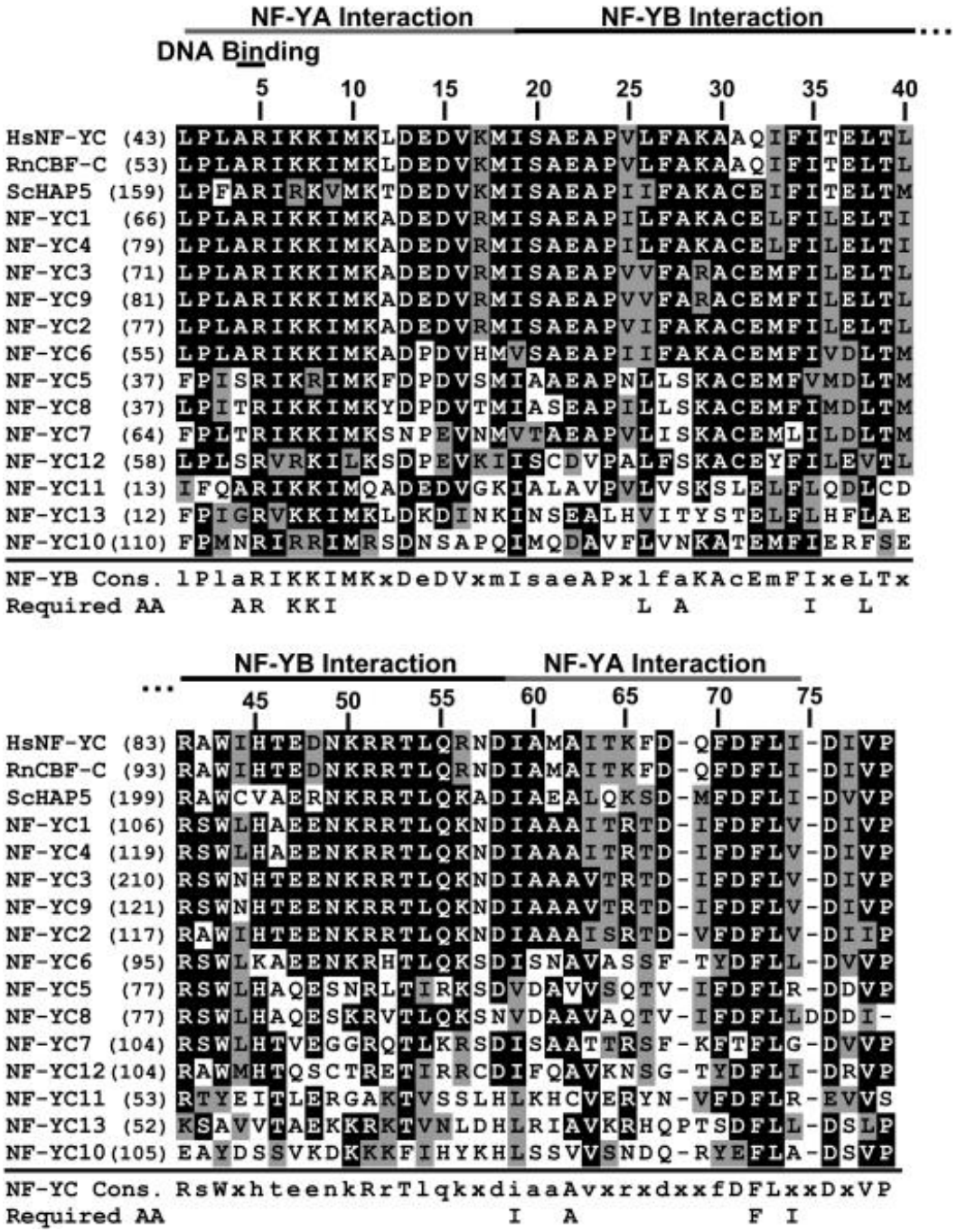

Figure 1.7 - Arabidopsis NF-YC subfamily alignment. Sequences correspond to the conserved regions in NF-YC proteins across different taxa (Hs, *Homo sapiens*; Rn, *Rattus norvegicus*; Sc, *Saccharomyces cerevisiae*). In NF-YC Cons. (consensus) line, uppercase letters symbolize identity >80% of NF-YC sequences, lowercase letters > 50% identity, and x represent < 50% identity. Required amino acid (AA) residues are from the literature (Xing et al., 1993). Figure from Siefers et al. (2009).

1.3.5 NF-Y TFs and regulatory mechanism

Specific NF-Y subunits are known to be regulated by a number of different mechanisms. In mammals, it has been reported that protein levels of NF-YA change during the cell cycle, while the amount of NF-YB and NF-YC proteins is quite constant, suggesting that NF-YA subunit regulate the heterotrimeric complex (Bolognese et al. 1999). Recently, a review has been published suggesting a model to explain transcriptional and post-transcriptional regulation of NF-YA gene in plant (Zanetti et al. 2017). This model represented in Figure 1.8 indicates that at the transcriptional level NF-YA subunits are regulated by alternative splicing (AS NF-YA mRNA) (Filichkin et al. 2010) which retains the first intron in the 5'sequence, leading the translation of the upstream Open Reading Frame 1 peptide (uORF1p). Subsequently, uORF1p binds to and destabilize both AS NF-YA and NF-YA mRNAs. The fully spliced NF-YA mRNAs is then recruited to the translational machinery which leads to the translation of the main ORF (mORF) and the synthesis of NF-YA subunit, which translocate into the nucleus to form the heterodimer with NF-YB and NF-YC subunits. NF-YA mRNAs are also post transcriptionally regulated being the target of miR169/Argonatute 1 protein (AGO1) complex, which levels are modulated according to different developmental and stress conditions (Lee H. et al. 2010, Xu M. Y. et al. 2014b, Zhou et al. 2008). Seven of the ten NF-YA subunits (NF-YA1, NF-YA2, NF-YA3, NF-YA5, NF-YA8, NF-YA9, NF-YA10) were predicted *in silico* to be regulated by miR169, which target the NF-YA 3'UTR (Jones-Rhoades and Bartel 2004). A natural antisense NAS mRNA determines the production of small interference RNA (nat-siRNAs), which inhibit the transcription of miR169 enhancing NF-YA mRNA levels by yet undetermined mechanisms. For example, different members of miR169 family are repressed when N and Pi are limited (Leyva-Gonzalez et al. 2012, Pant et al. 2009) and under abiotic stresses such as drought (Gao et al. 2015), enhancing the expression levels of several NF-YA subunits, while cold and salinity increase the expression of miR169 and reduce NF-YA expression level through the synthesis of nat-siRNAs. Consequently, overexpression of miR169 gene leads

reduced levels of NF-YA transcripts (Leyva-Gonzalez et al. 2012). Moreover, it was hypothesized that, as in mammals, when NF-YA subunit is translocated into the nucleus undergoes post-translational modification such as phosphorylation, ubiquitylation and acetylation, that affect DNA binding or protein stability (Chae et al. 2004, Manni et al. 2008, Yun et al. 2003). However, there is no experimental evidence to prove that plant NF-YAs are subjected to post-translational modifications. Additionally, it was hypothesized that as in animals NF-YA subunits in plant undergo another level of regulation represented by long non-coding RNAs (IncRNAs) which could sequester NF-YA in the nucleus and prevent DNA binding. Hence, there is strong evidence supporting post-transcriptional regulation of the plant NF-YA subunits, in agreement with studies carried out on mammalian NF-YA subunit.

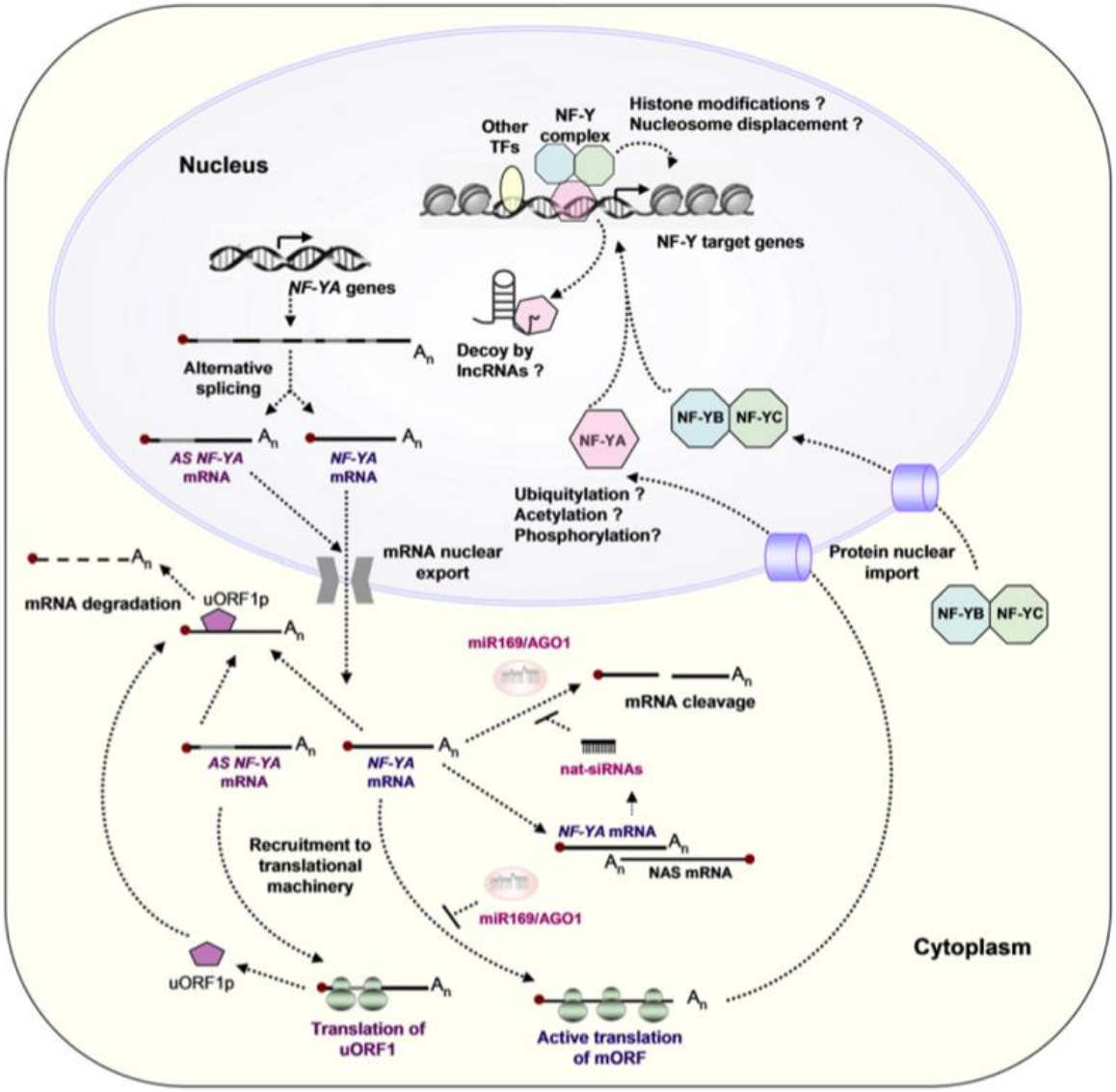

Figure 1.8 – Overview of multiple levels of transcriptional and post-transcriptional regulation of NF-Ys proposed by Zanetti et al. (2017)

1.3.6 NF-Y and plant pathogens

Not much evidence has been achieved regarding the role of NF-Y in response to pathogen attack. However, a few reports highlighted the involvement of these TFs during the plant defense response. For example, it was reported recently that in Arabidopsis miR169 is involved in defense against a bacterial infection caused by *Ralstonia solanacearum*, one of the most devastating plant pathogens, which can infect a wide range of host plants (Hanemian et al. 2016). Mutations in *clavata 1* (*clv1*) and *clavata 2* (*clv2*) *receptor kinase,* which are LRR-receptor-like proteins, confers enhanced resistance not only to a broad range of *R. solanacearum* strains but also to *the* oomycete *Hyaloperonospora arabidopsidis.* The phenotype observed in both *clv1* and *clv2* is due to the drastic reduction of miR169 accumulation and the consequent up-regulation of several NF-YAs. In line with this, it was also shown that overexpression of miR169 eliminates the resistance phenotype of *clv1* and *clv2* (Hanemian et al. 2016). Additionally, another study reported that in gravepine miR169 is negatively regulated by virus infection (Singh et al. 2012). Recently, Rey et al. (2016) identified a new role of *Medicago truncatula* NF-YA1 in compatibility to *Aphanomyces euteiches*, a root pathogenic oomycete (Rey et al. 2016). Indeed, *Mtnf-ya1* knock-out mutants were more resistant to the pathogen, showing a visible increment of their root apparatus compared to their wild type background. Interestingly, susceptible lines can be turned into resistant lines by overexpression of miR169 or by RNAi approaches, reducing MtNF-YA1 transcript level. Comparative transcriptome analysis between wild type plants inoculated with *A. euteiches* and *Mtnf-ya1* KO mutants revealed exactly the same number of differentially expressed genes. This suggests that *MtNF-YA1* act as a repressor of responses triggered in wild type plants by *A. euteiches* infection. On the other hand, previous studies showed that MtNF-YA1 is a key regulator involved of the symbiotic Rhizobium–legume interaction (Combier et al. 2006, El Yahyaoui et al. 2004). Taken together, these data strongly suggest that MtNF-YA1 gene might facilitate the symbiotic rhizobia infection by the suppression of defense responses.

1.3.7 The biological functions of NF-Y subunits

1.3.7.1 Embryogenesis

Plant embryogenesis is the developmental stage that occurs after the fertilization of an ovule to produce a fully developed plant embryo (Braybrook and Harada 2008). NF-Y TFs play a central role in embryogenesis. For example, it has been reported that NF-YB9, also known as LEAFY COTYLEDON1 (LEC1) (Lee H. et al. 2003) and the closely related NF-YB6, also known as LEC1-LIKE (L1L) (Kwong et al. 2003), play multiple roles in embryogenesis being exclusively expressed during seed development in Arabidopsis (Gusmaroli et al. 2001, Junker et al. 2012, Yamamoto et al. 2009). NF-YB9 is necessary to maintain the destiny of the embryonic cells and inhibit premature seed germination, while NF-YB6 affect embryogenesis inducing embryogenesis genes and cellular differentiation (Huang et al. 2015a, Lee H. et al. 2003). In fact, loss-of-function mutants of NF-YB9 and NF-YB6 give defective embryo development phenotypes and have delayed germination compared to wild type, suggesting that they negatively influence seed dormancy (Kwong et al. 2003, Warpeha et al. 2007). Phenotype of Arabidopsis knock out and over expression mutants in combination with tissue specific expression patterns reported that many NF-Y genes are involved in embryogenesis. For example, Siriwardana et al. (2014) showed that *NF-YA1, NF-YA2, NF-YA3, NF-YA4, NF-YA6, NF-YA7, NF-YA8*, and *NF-YA9* are expressed in the embryo and can affect embryo development, being consistent with the phenotype of Arabidopsis lines overexpressing *NF-YA1, NF-YA9, NF-YA5* and *NF-YA6* which showed defects in pollen, embryo and seed development. However, no phenotypes were observed in the corresponding single or double knock-out mutants (Mu et al. 2013). Moreover NF-Y play redundant role in embryogenesis and seed development. For instance, *nf-ya3/nf-ya8* double mutants are embryo lethal, while *nf-ya3* and *nf-ya8* single mutants do not have a different phenotype than wild type (Fornari et al. 2013), suggesting an overlapping functionality between NF-YA3 and NF-YA8. It has been reported that also NF-YC subunits are involved in seed germination through ABA responses. However different NF-YC

subunits show different sensitivity to ABA, for example Arabidopsis *nf-yc4* knock out mutants are hypersensitive to ABA during seed germination (Warpeha et al. 2007), while *nf-yc3*/n*f-yc9* double mutants have shown to be hyposensitive (Kumimoto et al. 2013). These findings revealed that many NF-Y subunits are involved in embryo and seed development, however most studies focus on single subunit, hence how these subunits act in complex to regulate these processes is still not well known.

1.3.7.2 Regulation of photoperiod-dependent flowering

Many studies have highlight the key role of NF-Y TFs in flowering response. For example, it was reported that NF-YB2 and NF-YB3 subunits are highly related proteins involved in floral transition through the regulation of FLOWERING LOCUS-T (FT) gene (Kumimoto et al. 2008). Additionally, NF-YC3, NF-YC4 and NF-YC9 subunits were found to be crucial for photoperiod-dependent flowering in Arabidopsis (Kumimoto et al. 2008), in fact CONSTANS (CO) needs these three subunits to initiate the transcriptional activation of FT. Moreover, Y2H analysis revealed that NF-YC3, NF-YC4 and NF-YC9 subunits can physically interact with NF-YB2 and NF-YB3 subunits, forming at least six different complexes which can interact with CO and then regulate the transcription of FT (Kumimoto et al. 2010). CO is an important flowering regulator and belongs to a family of proteins termed CO-LIKE (COL), which carry a CCT (CO, CO-like, TIMING OF CAB EXPRESSION 1) domain (Robson et al. 2001, Strayer et al. 2000). The CCT domain have high sequence similarity with DNA binding domain of NF-YA subunit (Romier et al. 2003, Wenkel et al. 2006). Hence Siefers et al. (2009) hypothesized a model, called replacement model, where NF-YA is a competitor of CO for NF-YB/NF-YC binding. Consequently, this competition regulates FT through the formation of two independent complexes: the activator complex CO/NF-YB/NF-YC, which positively regulate the expression of FT and the repressor complex NF-YA/NF-YB/NF-YC, which negatively regulate the expression of FT (Siefers et al. 2009, Wenkel et al. 2006). However, this sequence similarity between NF-YA and CO

does not involve the *CCAAT* box (Nardini et al. 2013), thus CO is not able to bind the DNA in the *CCAAT* box but it can bind the DNA at the CONSTANT RESPONSE ELEMENTs (CORE) (Tiwari et al. 2010). Interestingly, even if CO was shown to be unable to directly bind the *CCAAT* box on the FT promoter, it was observed that a mutation in this element prevent flowering induction (Cao et al. 2014), suggesting an important involvement of *CCAAT* element in flowering. Based on this, Cao et al. (2014) proposed a new model called recruitment model (Figure 1.9A) for the activation of FT. This model includes the interaction between CO and FT promoter at the CORE elements and a separate interaction between the NF-Y trimer and the *CCAAT* box. Subsequently, CO and the NF-Y trimeric complex interact through the formation of a chromatin loop which brings together the two complexes, suggesting that the NF-Y hetero-trimer functions as distal transcriptional activator of FT. More recently Siriwardana et al. (2016) also suggested a model (Figure 1.9B) where NF-YA subunits are positive regulators of flowering, differing from previous studies. Additionally, a complex composed by NF-YA2/NF-YB2/NF-YC3 was shown to promote flowering binding the *CCAAT* box *in vitro* (Siriwardana et al. 2016). These evidences raise the chance that two different protein complexes: CO/NF-YB/NF-YC and NF-YA/NF-YB/NF-YC interact with each other to activate FT, binding both proximal CORE and distal *CCAAT* elements, respectively.

It is important to consider that NF-Y TFs regulate flowering by not only interacting with CO but, according with recent studies, they can also interact with FLOWERING LOCUS T (FLC) or SUPPRESSOR OF OVEREXPRESSION OF CO 1 (SOC1), suggesting other mechanisms (Hou et al. 2014, Xu M. Y. et al. 2014b). Specifically, Hou et al (2014) proposed a mechanism in response to a “stress induced flowering pathway” where NF-Y regulate the expression of FLC under abiotic stress conditions. According to this hypothesis NF-YA2 directly binds and activates FLC under physiological conditions, on the contrary under abiotic stress conditions NF-YA2 transcripts are degraded by miR169, reducing FLC activity and activating genes normally suppress by FLC, including FT. However, this is in contrast with Michaels et al. (2001) where it was reported that *flc* knock out mutants did not

reveal alteration in flowering time. Hence, further investigations are needed to better understand this pathway. The alternative mechanism of NF-Y TFs in promoting flowering proposed by Hou et al (2014) suggests that the hetero-trimer interacts with CO in the photoperiod pathway and with DELLAs in the gibberellin pathway, to control the transcription of SOC1, a key gene in flowering. Specifically, it was reported that NF-YA2 mediates the interaction with a novel regulatory element called NF-Y BINDING ELEMENT (NFYBE) in the *SOC1* promoter to regulate its transcription. When the flowering signal is absent (no GA) (Figure 1.9C) the transcription of SOC1 is inhibited by the trimethylation of H3K27me3 and DELLAs interact with the NF-Y complex preventing the NF-Y binding to the NFYBE at the SOC1 locus. When GA are present (Figure 1.9D), GA degrade DELLAs allowing NF-Y to bind to the NFYBE. NF-Y TFs demethylate the SOC1 promoter through recruiting the H3K27 demethylase RELATIVE OF EARLY FLOWERING 6 (REF6) promoting SOC1 expression. Cao et al. (2014) also suggest that in long day (LD) conditions, CO proteins interact with NF-Y complexes even if DELLA proteins are present. The complex composed of NF-Y hetero-trimer and CO binds to the NFYBE in the SOC1 promoter, facilitating the demethylation of H3K27me3 and promoting the expression of SOC1 (Figure1.9E).

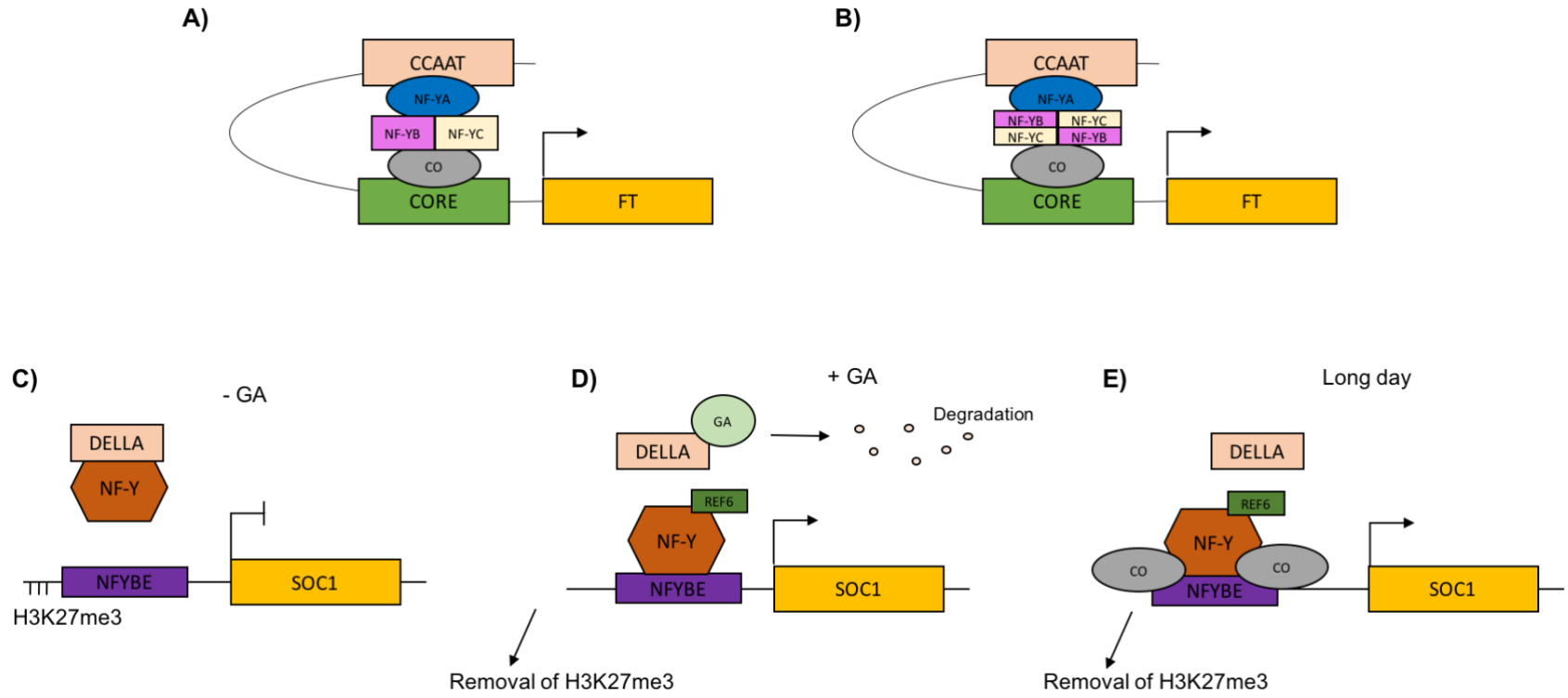

Figure 1.9 – NF-Y regulate photoperiod and GA dependent flowering. A) Recruitment model (Cao et al. 2014) B) Siriwardana et al. (2016) proposed a model where two different complexes (NF-YA/NF-YB/NF-YC and CO/NF-YB/NF-YC) cooperatively activate FT by binding *CCAAT* and CORE elements; C) In the absence of GA (-GA) DELLA protein interact with NF-Y and inhibit the expression of SOC1 (Hou et al. 2014); D) In the presence of GA (+GA) DELLA proteins are degraded relasing the NF-Y complex and promoting the expression of SOC1 (Hou et al. 2014); E) Under LD conditions, CO protein form a complex with NF-Y and bind to the SOC1 regulatory regions and promoting its expression (Hou et al. 2014).

1.3.7.3 NF-Ys in abiotic stresses

NF-Y TFs are involved in stress responses in Arabidopsis and other plants (Han et al. 2013, Laloum et al. 2013, Petroni et al. 2012, Xu L. et al. 2014a). For example, it was reported that Arabidopsis plants overexpressing NF-YA2, NF-YA3, NF-YA5, NF-YA7, NF-YA10 or NF-YB1 showed to have increased drought tolerance (Leyva-Gonzalez et al. 2012, Li W. X. et al. 2008, Nelson et al. 2007). Additionally, transcriptional profile of Arabidopsis constitutively overexpressing NF-YA2, NF-YA5 and NF-YB1 revealed that each of these genes altered different groups of genes, suggesting that they are involved in independent regulatory pathways during drought stress (Leyva-Gonzalez et al. 2012, Li W. X. et al. 2008, Nelson et al. 2007). In plants ABA inhibits seed germination to prevent excessive energy consumption under hostile conditions (Lopez-Molina et al. 2001). Abiotic stresses such as drought and high salinity trigger the biosynthesis of ABA, hence plants that are hypersensitive to ABA are more tolerant to these stresses. In Arabidopsis, salt stress conditions induced NF-YA1, NF-YA2, NF-YA7, NF-YA10 and when these genes are overexpressed the plant was hypersensitive to exogenous levels of ABA (Leyva-Gonzalez et al. 2012, Li Y. J. et al. 2013). Moreover, Leyva-Gonzalez et al. (2012) reported that under nutrient deficiency conditions, such as low N and Pi, the expression of miR169 is suppressed inducing NF-YA2, NF-YA7 and NF-YA10. Moreover, many studies have highlight the pivotal role of NF-Y TFs during temperature stress (Sato et al. 2014, Shi et al. 2014). For instance, plants overexpressing NF-YA2 or NF-YC1 were shown to be more tolerant to cold. Additionally, NF-YC1 subunit regulates the transcription of a key enzyme involved in cell wall development called XYLOGLUCAN ENDOTRANSGLUCOSYLASE/ HYDROLASE 21 (XTH21), which, when overexpressed or knocked-out, generates resistant or tolerant plants to freezing, respectively.

Additionally, under stress conditions the plant cell ENDOPLASMATIC RETICULUM (ER) triggers an unfolded protein response (UPR), which mitigates the ER stress caused by the ER protein folding machinery as the demands for protein folding exceed the capacity of the system (Liu and Howell 2010). It was shown that the

hetero-trimer formed by NF-YA4, NF-YB3 and NF-YC2 interact *in vitro* with bZIP28 to activate UNFOLDED PROTEIN RESPONSE (UPR) associated genes, which are involved in response to environmental stress condition such as pathogen attack or developmental stimuli (Vitale and Ceriotti 2004). It was observed that UPR genes have ER stress response element (ERSEs) in their promoter (Yoshida et al. 2000) and in mammals, it was demonstrated that a complex constituted by NF-Y trimer and the bZIP dimer bind to the ERSE element (Yoshida et al. 2000, 2001).

1.3.8 NF-Y as a key regulator in multiple stress responses

1.3.8.1 The PRESTA project

This research is based on dataset generated by a previous project called PRESTA (Plant Responses to Environmental STress in Arabidopsis). PRESTA was a large project that brought together plant biologists, theoreticians and bioinformaticians from different universities in the UK. It investigated the transcriptional networks underlying stress responses in Arabidopsis using a systems biology approach. The study was conducted across seven different stresses: *Botrytis cinerea* infection (Windram et al. 2012), long day senescence (Breeze E. et al. 2011), *Pseudomonas syringae* infection (Lewis et al. 2015), drought (Bechtold et al. 2013), high light and short day senescence. This systems approach was focused on the generation of large microarray datasets that follow gene expression changes over time in response to multiple stresses, generating a dynamic dataset. Indeed, the PRESTA datasets compared the treated to untreated tissue at different time points across the duration of the stress, clarifying the chronology of transcriptional events involved in eliciting the stress response. This methodology permitted to generate high-resolution time-series expression data profiles for the majority of genes in Arabidopsis, which enabled the generation of transcriptional network models. In doing this, this system allowed prediction of regulatory relationships between differentially expressed TFs and identification of key regulators of Arabidopsis stress responses from the networks.

1.3.8.2 NF-Y subunits are differentially expressed during multiple stresses

The PRESTA dataset revealed that NF-Y genes are differentially expressed under multiple stresses as shown in Figure 1.10 (Breeze, 2014). All NF-YA genes were shown to be differentially expressed in at least one treatment, with NF-YA1, NF-YA2, NF-YA4, NF-YA7 and NF-YA10 showing significant changes under four or five stresses. It is also visible that NF-YB and NF-YC subunits showed a differential expression across different treatments, however, in comparison with NF-YA subunits, it is less substantial, since it does not involve all different treatments or subunits. Figure 1.10 represents the general trend of the expression of NF-Y subunits across each stress, according to the direction of the arrow. This figure considers the NF-Y classification performed by Siefers et al. (2009) with 36 NF-Y subunits in total, instead of the new classification done by Petroni et al. (2012) with 30 NF-Y subunits. Hence, NF-YB11, NF-YB13, NF-YC10, NF-YC11 and NF-YC13 are not going to be considered. Among 36 NF-Ys, it was observed that 20 are differentially expressed during *B. cinerea* infection with 10 genes up-regulated and 10 genes down-regulated (Windram et al., 2012). This supports the involvement of the NF-Ys, particularly the NF-YA subunits, in a fundamental regulatory role in the plant defense response.

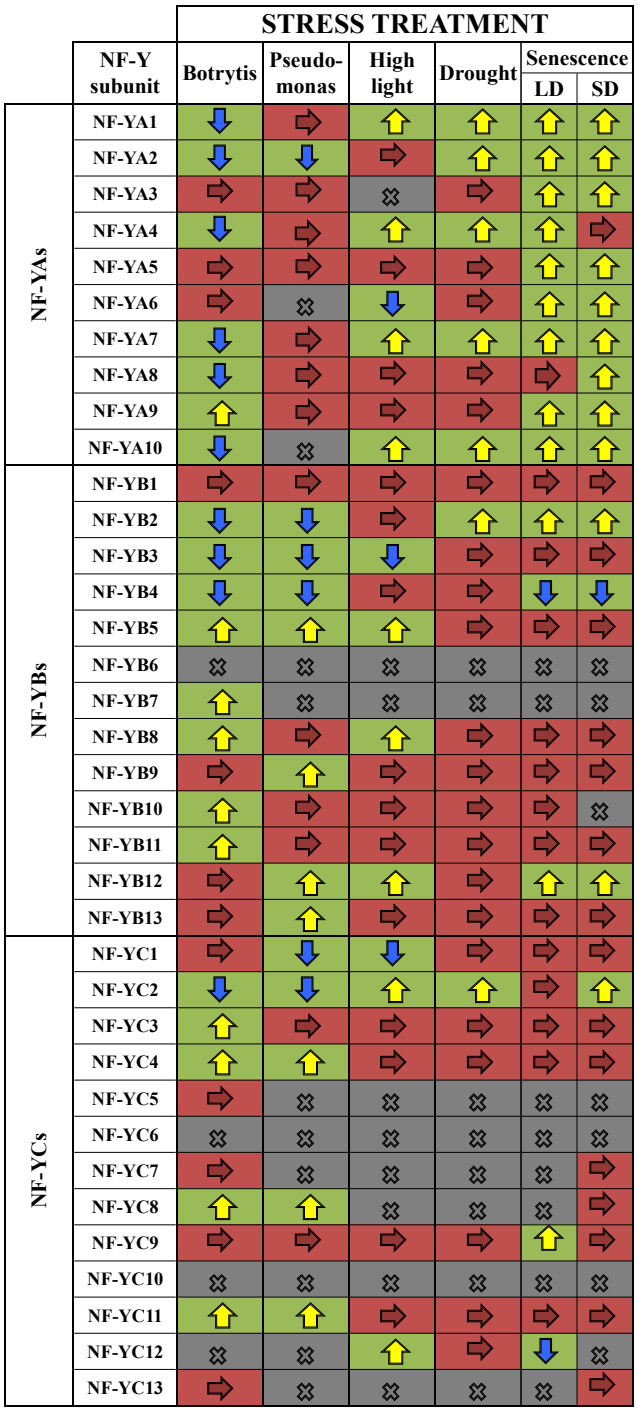

Figure 1.10 - Differential expression of the NF-Y genes in the PRESTA datasets. Differentially expressed genes, compared with stress treated and control samples, for each stress were identified. Red box indicates NF-Y genes constitutively expressed over the time series, green box indicates differentially expressed genes, grey box (with crosses) indicates not expressed genes. The color of the arrow indicates the direction of gene expression: yellow= up-regulated; blue= down-regulated. The senescence datasets have no control case. Figure from Breeze (2014).

1.3.8.3 Y2H

The ability of each of the NF-Y subunits to interact with each other was investigated *in vitro* using the Y2H assay by Emily Breeze (2014). However, this method does not allow more than two proteins to be co-expressed and hence if the formation of the NF-YB/NF-YC hetero-dimer is a prerequisite for the binding of the NF-YA subunit, binary protein interaction with NF-YA subunits will not be detected. The NF-Y Y2H results obtained are in line with other two publications: Calvenzani et al. (2012) and Hackenberg et al. (2012). All these datasets are similar in terms of the high proportion of NF-YB/NF-YC interactions identified, and the limited detection of any NF-YA/NF-YB interactions. Hence, generally, NF-YB and NF-YC subunits were seen to hetero-dimerize promiscuously. Hetero-dimerization was also observed between NF-YA and NF-YC subunits, while the dimerization between NF-YA/NF-YB subunits was not identified. This analysis gave important information on the possible dimer combinations between NF-Y subunits, and so in this study was used to predict putative hetero-trimer complexes.

1.4 Context of this work

As explained in the introductory section above, NF-Y TFs have been shown to be involved in multiple developmental and stress responses. Knowing the multigene family for each subunit, it was hypothesized that different hetero-trimer combinations have evolved specialized regulatory functions. Additionally, it was reported that NF-YB and NF-YC can form non-canonical trimeric complexes interacting with other TFs and enhancing the combinatorial complexity of NF-Y family in plant. Hence, these complexes might bind different DNA element rather than the *CCAAT* motif (Hou et al. 2014, Liu and Howell 2010, Mendes et al. 2013, Wenkel et al. 2006). This expanded combinatorial complexity makes the NF-Y family an attractive target for future research, however to identify a specific and functional hetero-trimer is exceedingly challenging.

The aim of this PhD work was to identify one or more functional NF-Y trimers with a role in the plant defense response. In order to do this effectively, a more focused approach was taken in which detailed functional analysis was performed on a small subset of NF-Y genes. The subset of NF-Ys selected for further study were chosen on the basis of the microarray dataset results during *B. cinerea* and *P. syringae* infection (Figure 1.11) obtained by the PRESTA consortium in combination with previous Y2H analysis. The NF-Y genes selected for further study were NF-YA2, NF-YB2 and NF-YC2, for the reasons outlined below:

NF-YA2

NF-YA2 is an obvious choice for further study, in fact it was shown to be a major hub in both drought and senescence and because of its putative regulation of several other NF-Y genes (Breeze, 2014). Furthermore, it is differentially expressed in multiple stresses (Figure 1.10) and it has TDNA insertion lines exhibiting reduced expression of the target transcript, thus aiding functional analysis. Moreover, previous study showed that NF-YA2 knock-out and overexpressor mutants have altered endogenous levels of JA, a key phytohormone during the plant defense response against *B. cinerea* infection (Breeze et al. in preparation). This result together with the misregulation of JA biosynthetic genes observed in the *nf-ya2* KO mutant (Breeze, 2014), strongly suggests the involvement of NF-YA2 in the JA biosynthesis pathway. In agreement with this, *nf-ya2* mutant exhibit an altered susceptibility to the necrotrophic pathogen *B. cinerea*. Based on these evidences it was hypothesized that *NF-YA2* is a good candidate gene involved in plant immunity against necrotrophic pathogens.

NF-YC2

PPI data identified NF-YC2, as obvious targets for further study since this subunit was the only one capable of interacting with NF-YA2 subunit in Y2H analysis.

Furthermore NF-YC2 was selected due to its differential expression in most of the PRESTA time series datasets.

NF-YB2

Preliminary Mass Spectrometry analysis performed on Arabidopsis lines overexpressing NF-YC2 identified NF-YB2 as an interacting protein. Providing a useful starting point for testing potential trimer combinations *in vivo.* Furthermore, Arabidopsis TDNA insertion lines are available for functional experiments.

In summary, a putative trimer formed by NF-YA2, NF-YB2 and NF-YC2 was hypothesized. All three subunits showed to be down regulated during *B. cinerea* and *P. syringae* infection compared with mock controls (Figure 1.11) and this considerable differential expression suggests that they may be playing an important role in the plant defense response.

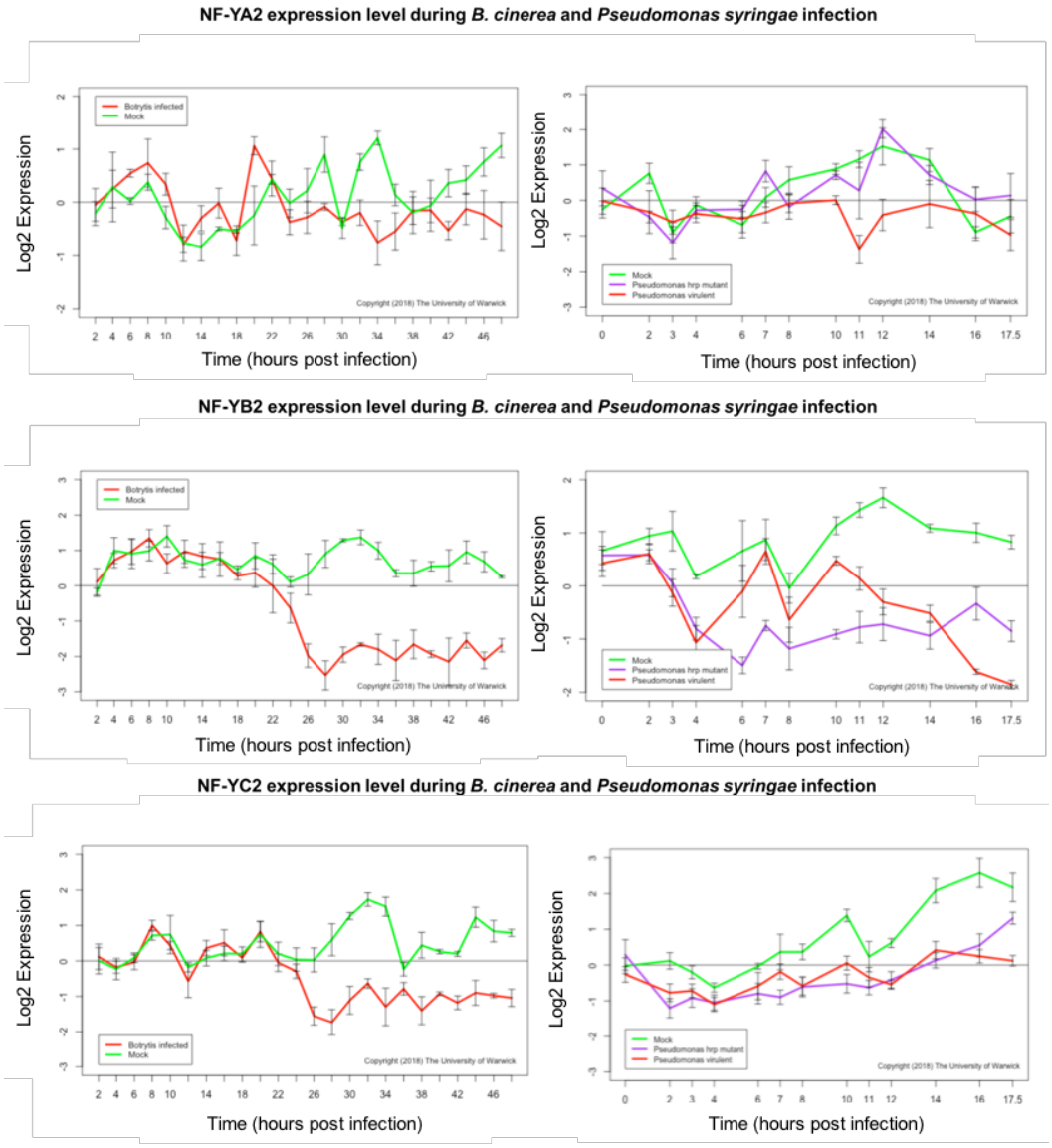

Figure 1.11 - Expression of NF-YA2, NF-YB2 and NF-YC2 during *Botrytis cinerea* infection, *Pseudomonas syringae* infection and mock treatment, as determined by the high-resolution time-course microarray (Windram et al. 2012). Each graph shows the mean $\log_2$ normalized expression over time for both the treated (red and purple) and untreated (green) samples. In the *Pseudomonas* plot, green is mock data, purple is *hrpA* infection and red is *Pst DC3000* infection. Error bars are presented in the form of deviation from the mean, based on 1 standard error calculated from the standard deviation.

1.5 Aims and objectives

The overall aim of this research is to improve our knowledge on functional NF-Y complexes in physiological conditions and specifically during the plant defense response.

In particular, the research objectives are to:

- Determine the existence of the putative hetero-trimer (NF-YA2/NF-YB2/NF-YC2) *in planta*
- Identify functional NF-Y complexes during biotic stress and under unstressed conditions
- Localize NF-YA2, NF-YB2 and NF-YC2 in the plant cell
- Use transcriptome data to predict functional orthologues of the NF-Y subunits in other crops, such as lettuce and tomato, during *B. cinerea* infection.

Chapter 2

2. Materials and Methods

2.1 Materials

2.1.1 Molecular Biology Reagents

Oligonucleotides were supplied by Sigma- Aldrich or Integrated DNA Technologies (IDT; Scotland, UK). Polymerase chain reaction (PCR) was conducted using BioMix™ Red (Bioline, UK) and ACCUZYME™ DNA Polymerase (Bioline, UK); QIAprep Spin Miniprep kit, QIAquick PCR Purification Kit, QIAquick Gel Extraction Kit (Qiagen, UK). BP Clonase II and LR Clonase II enzymes were supplied by Invitrogen, UK.

2.1.2 Electrophoresis Reagents

Gels were composed of 1.2% (w/v) ultrapure agarose (Invitrogen), 1x TAE buffer (40 mM Tris base, 20 mM acetic acid, 1 mM EDTA, pH 8.0) and stained with Ethidium Bromide (Sigma Aldrich) or GelRed (Biotium Inc., U.S.A.). 1 Kb Plus DNA Ladder (Life TechnologiesTM) was used as a DNA size marker in all gels unless otherwise stated.

2.1.3 Nucleic Acid Measurements

DNA and RNA concentrations were measured using a NanoDrop ND-1000 (Thermo Scientific, UK).

2.1.4 Cell Density Measurements

Cell density measurements (OD_{600}) were taken using a Biochrom WPA CO8000 cell density meter (Biochrom Ltd., UK).

2.1.5 Vectors Used

- **pDonrZeo;** Gateway entry vector. Containing a Zeocin resistance gene for bacterial selection (Invitrogen™).
- **pGWB604;** Gateway binary destination vector containing a GFP tag N-terminally fused to the protein encoded by the gene of interest, under the control of the native promoter. It also contains a spectinomycin selectable

marker for bacteria and BASTA resistance gene for transgenic plant selection (Nakamura et al. 2010).

- **pGWB605;** Gateway binary destination vector containing a GFP tag N-terminally fused to the protein encoded by the gene of interest, under the control of a 35S promoter from Cauliflower mosaic virus. It also contains spectinomycin resistance gene for bacterial selection and BASTA resistance for transgenic plant selection (Nakamura et al. 2010).
- **pGWB606;** Gateway binary destination vector containing a GFP tag C-terminally fused to the protein encoded by the gene of interest, under the control of a 35S promoter. It also contains spectinomycin resistance gene for bacterial selection and BASTA resistance for transgenic plant selection (Nakamura et al. 2010).
- **pGWB610;** Gateway binary destination vector containing a FLAG tag N-terminally fused to the protein encoded by the gene of interest, under the control of the native promoter. It also contains spectinomycin resistance gene for bacterial selection and BASTA resistance for transgenic plant selection (Nakamura et al. 2010).
- **pGWB611;** Gateway binary destination vector containing a FLAG tag N-terminally fused to the protein encoded by the gene of interest, under the control of a 35S promoter. It also contains spectinomycin resistance gene for bacterial selection and BASTA resistance for transgenic plant selection (Nakamura et al. 2010).
- **pGWB612;** Gateway binary destination vector containing a FLAG tag C-terminally fused to the protein encoded by the gene of interest, under the control of a 35S promoter. It also contains Spectinomycin resistance gene for bacterial selection and BASTA resistance for transgenic plant selection (Nakamura et al. 2010).
- **pGWB613;** Gateway binary destination vector containing a 3xHA tag N-terminally fused to the protein encoded by the gene of interest, under the control of the native promoter. It also contains spectinomycin resistance

gene for bacterial selection and BASTA resistance for transgenic plant selection (Nakamura et al. 2010).

- **BIFP1;** Gateway destination vector in which the N terminus of Clontech E-YFP is C-terminally fused to the protein encoded in the Gateway cassette. Supplied by Francois Parcy (University Grenoble, France). It also contains spectinomycin resistance gene for bacterial selection.
- **BIFP2;** Gateway destination vector in which the N terminus of Clontech E-YFP is N-terminally fused to the protein encoded in the Gateway cassette. Supplied by Francois Parcy (University Grenoble, France). It also contains spectinomycin resistance gene for bacterial selection.
- **BIFP3;** Gateway destination vector in which the C terminus of Clontech E-YFP is N-terminally fused to the protein encoded in the Gateway cassette. Supplied by Francois Parcy (University Grenoble, France). It also contains spectinomycin resistance gene for bacterial selection.
- **BIFP4;** Gateway destination vector in which the C terminus of Clontech E-YFP is C-terminally fused to the protein encoded in the Gateway cassette. Supplied by Francois Parcy (University Grenoble, France). It also contains spectinomycin resistance gene for bacterial selection.

2.1.6 Plant Material

- **Col-0;** *Arabidopsis thaliana* accession Columbia.
- ***Solanum lycopersicum L.*** **cultivars of Micro-Tom.** Seeds were provided by JustSeed UK.
- ***Solanum lycopersicum L.*** **cultivars Ailsa craig.** Seeds were provided by JustSeed UK .
- ***p*35S:HA:GFP;** Arabidopsis Col-4 expressing GFP with an N-terminally fused HA tag (using Gateway vector Earleygate201), selected on BASTA until homozygous (transformation performed by Sarah Harvey, University of Warwick).

- ***p*35S:FLAG:GFP;** Arabidopsis Col-0 expressing GFP with an N-terminally fused FLAG tag, selected on BASTA until homozygous (seed were kindly provided by Sophie Piquerez, University of Warwick).
- ***nf-ya2*;** Arabidopsis accession Col-0 with T-DNA insertions in the NF-YA2 gene (SALK_146170). Provided by NASC and screened for zygosity.
- ***nf-yb2*;** Arabidopsis accession Col-0 with T-DNA insertions in the NF-YB2 gene (SALK_025666). Provided by Ben F. Holt III (Kumimoto et al. 2013) and screened for zygosity.
- ***nf-yb3*;** Arabidopsis accession Col-0 with T-DNA insertions in the NF-YB3 gene (SALK_150879). Provided by Ben F. Holt III (Kumimoto et al. 2013) and screened for zygosity.
- ***nf-yb2/b3*;** Arabidopsis accession Col-0 with T-DNA insertions in the NF-YB2 and NF-YB3 genes. Provided by Ben F. Holt III (Kumimoto et al. 2013) and screened for zygosity.
- ***nf-yc2*;** Arabidopsis accession Col-0 with T-DNA insertions in the NF-YC2 gene (SALK_026351). Provided by NASC and screened for zygosity.
- ***bos1;*** Arabidopsis accession Col-0 with T-DNA insertions in the MYB108 gene. Provided by Prof. Tesfaye Mengiste (Purdue Agricolture).
- **HaRxL14;** HaRxL14 cloned into pB2GW7, transformed into Col-0 and selected on BASTA until the fourth generation (transformation performed by Matthew Watson, University of Warwick).
- ***Col-0*::35S:NF-YC2-GFP;** NF-YC2 cloned into pGWB605 transformed into Col-0 and selected on BASTA until the fourth generation. Col-0::35S:NF-YC2-GFP_1 and Col-0:: 35S:NF-YC2-GFP_3 differentiate between lines derived from independent transformations (transformation performed by Emily Breeze, University of Warwick).
- ***nf-ya2*::35S:FLAG-NF-YA2;** Arabidopsis knockout mutant *nf-ya2* expressing NF-YA2 with an C-terminally fused FLAG tag (using pGWB612 Gateway vector), selected on BASTA until homozygous. *nf-ya2*::35S:FLAG-

NF-YA2_1 and *nf-ya2*::35S:FLAG-NF-YA2_2 designate independent transformants (this study).

- ***Col-0*::35S:FLAG-NF-YA2;** Arabidopsis Col-0 expressing NF-YA2 with a C-terminally fused FLAG tag (using pGWB612 Gateway vector), selected on BASTA until homozygosity. *Col-0*::35S:FLAG-NF-YA2_1 and *Col-0*::35S:FLAG-NF-YA2_2 designate independent transformants (this study).
- ***Col-0*::35S:GFP-NF-YA2;** Arabidopsis Col-0 expressing NF-YA2 with a C-terminally fused GFP tag (using pGWB606 Gateway vector), selected on BASTA until homozygous. *Col-0::35S:GFP-NF-YA2*_1 and *Col-0::35S:GFP-NF-YA2*_2 designate independent transformants (this study).
- ***Col-0*::pNF-YA2:NF-YA2-GFP;** Arabidopsis Col-0 expressing NF-YA2 with an N-terminally fused GFP tag (using pGWB604 Gateway vector), selected on BASTA until homozygous. *Col-0*::pNF-YA2:NF-YA2-GFP_1 and *Col-0*::pNF-YA2:NF-YA2-GFP_2 designate independent transformants (this study).
- ***nf-ya2*::pNF-YA2:NF-YA2-GFP;** Arabidopsis knock out mutant *nf-ya2* expressing NF-YA2 with an N-terminally fused GFP tag (using pGWB604 Gateway vector), selected on BASTA until homozygous. *Col-0*::pNF-YA2:NF-YA2-GFP_1 and *Col-0*::pNF-YA2:NF-YA2-GFP_2 designate independent transformants (this study).
- ***nf-yb2*::35S:FLAG-NF-YB2;** Arabidopsis knock out mutant *nf-yb2* expressing NF-YB2 with a C-terminally fused FLAG tag (using pGWB612 Gateway vector), selected on BASTA until homozygous. *nf-yb2*::35S:FLAG-NF-YB2_1 and *nf-yb2*::35S:FLAG-NF-YB2_2 designate independent transformants (this study).
- ***nf-yb2*::35S:GFP-NF-YB2;** Arabidopsis knockout mutant *nf-yb2* expressing NF-YB2 with a C-terminally fused GFP tag (using pGWB606 Gateway vector), selected on BASTA until homozygous. *nf-yb2*::35S:GFP-NF-YB2_1 and *nf-yb2*::35S:GFP-NF-YB2_2 designate independent transformants (this study).

- ***Col-0*::35S:GFP-NF-YC2_1;** Arabidopsis Col-0 expressing NF-YC2 with a C-terminally fused GFP tag (using pGWB605 Gateway vector), selected on BASTA until homozygous. *Col-0*::35S:GFP-NF-YC2_1 and *Col-0*::35S:GFP-NF-YC2_2 designate independent transformants (this study).

2.1.7 Microbial Strains

- **DH5α;** Chemically competent *Escherichia coli* (*E. coli)* used for transformation.
- ***Agrobacterium tumefaciens* strain GV3101**, used for stable transformation of *Arabidopsis thaliana* and transient transformation of *Nicotiana benthamiana*.
- ***Botrytis cinerea* strain pepper** (Denby et al. 2004)
- ***Hyaloperonospora arabidopsidis,*** spores of isolate Noks1 (Coates and Beynon 2010)
- ***Pseudomonas syringae* pv. *tomato* DC3000 wild type**. (Prof. Murray Grant group, University of Warwick).

2.1.8 Media and Buffers

- **Luria broth (LB) growth media for *Escherichia coli*:** 25 g of LB Broth, Miller (Fisher Scientific UK) per litre of MilliQ water, in 1.5% agar (w/v) (VWR; UK). Contains: 10 g/L Tryptone, 10 g/L NaCl and 5 g/L Yeast Extract.
- **Super Optimal broth with Catabolite repression (SOC) media for *Escherichia coli* transformation:** Liquid medium from Invitrogen™ (catalogue number 15544-034). Contains: 2% (w/v) Tryptone, 0.5% (w/v) Yeast Extract, 10 mM Sodium Chloride, 2.5 mM Potassium Chloride, 10 mM Magnesium Chloride, 10 mM Magnesium Sulphate and 20 mM Glucose.
- **YEB growth media for *Agrobacterium tumefaciens*:** 5 g/L Beef Extract, 1 g/L Yeast extract, 5 g/L Peptone, 5 g/L Sucrose, 2 mM MgSO4.

- **Murashige Skoog (MS) media:** 2.2 g Murashige Skoog nutrients (Duchefa Biochemie, Haarlem, The Netherlands) per litre of MilliQ water, 1 % (w/v) sucrose and adjusted to pH 5.9 with KOH, 0.7 % (w/v) Plant agar (Duchefa Biochemie).

2.2 Methods

2.2.1 Plant growth

Arabidopsis seeds were sown into P24 seed trays containing pre-watered soil (Levington F2 compost) and stratified at 4°C for 72 h in the dark. Trays were then covered with a transparent lid to maintain humidity and placed in a growth chamber to germinate. The lid was removed after 10 days post-sowing and seedlings thinned to one plant per pot. Plants were grown under standardized conditions of 12 or 16 hours of light, 20^{o}C, 70% relative humidity, 350ppm CO_2 and 100 µmol^{2}s^{-1} light, unless otherwise stated.

2.2.2 Plant transformation

A. thaliana plants of the Col-0 ecotype or knockout mutant for a gene of interest were grown. Floral dipping was performed by as described in Clough and Bent (1998) (Clough and Bent 1998). T0 seed was selected on soil soaked in 5 g/ml BASTA. Up to 10 resistant seedlings were transplanted and T2 seed generated. T2 seed were treated with BASTA again and lines with a 3:1 ratio of BASTA resistant:sensitive plants were selected. T3 seed was generated from resistant plants in these selected lines. Batches of T3 seed were then sown onto BASTA-socked soil and lines which showed 100% germination were deemed homozygous.

2.2.3 PCR

PCR master mix was made as described in Table 2.1. PCR was performed using the GeneAmp PCR System 9700 (Applied Biosystems), using the thermal cycling

conditions described in Table 2.2. All DNA samples were run on electrophoresis gels at 100 V for approximately 45 min.

Table 2.1 - PCR components.

Component	Volume
BioMix Red Master Mix	10 µl
Forward primer (10 µM)	1.5 µl
Reverse primer (10 µM)	1.5 µl
MilliQ H_2O	Up to a total of 20 µl

Table 2.2 - PCR Thermal Cycling Conditions.

Step	Temperature	Time	Cycles
Initial denaturation	95 °C	3 minutes	1
Denaturation	95 °C	30 seconds	
Annealing	55°C	30 seconds	30-35
Elongation	72°C	1-2 minutes (~ 1kb/min)	
Final elongation	72°C	10 minutes	1
Cooling	15°C	Indefinitely	

2.2.4 Genotyping

All T-DNA insertion lines were genotyped prior to use. Genomic DNA was extracted from 0.5 cm leaf discs using the REDExtract-N-Amp™ Plant PCR kit (Sigma-Aldrich) following the manufacturer's instructions. PCR was performed using the conditions described in Table 2.2 with the forward primer (LP) and reverse primers (RP) located in the T-DNA flanking sequences together with the appropriate left T-DNA border primer (LB) (Table 2.3). Primers were designed using T-DNA Primer Design tool (http://signal.salk.edu/tdnaprimers.2.html). By using the three primers (LBb1.3+LP+RP) for SALK lines, in wild type lines (WT) only LP-RP product is visible, in homozygous lines (HM) BP-RP product will be 410+N bp, while in heterozygous lines (HZ), both bands will be visible (Figure 2.1).

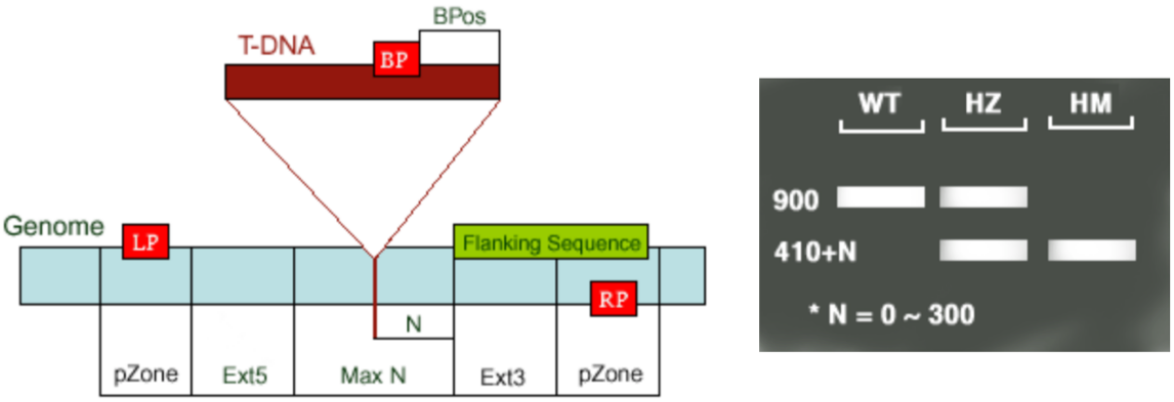

N = Difference of the actual insertion site and the flanking sequence position
MaxN = Maximum difference of the actual insertion site and the sequence
pZone = Regions used to pick up primers
Ext5, Ext3 = Regions reserved not for picking up primers
LP, RP = Left, Right genomic primer
BP = T-DNA border primer
LB = the left T-DNA border primer
BPos = The distance from BP to the insertion site

Figure 2.1 – A general representation of the position of the T-DNA and primers used for genotyping SALK lines loss-of-function mutants. On the right: representation of expected band sizes in wild type, homozygous and heterozygous lines.
Figure from http://signal.salk.edu/tdnaprimers.2.html.

Table 2.3 - Primers used for genotyping

Gene name	Forward primer sequence	Reverse primer sequence	Salk line	Insertion	BP+RP PRODUCT SIZE
NF-YB2	TGGGTCGTAAAAATAGGCATG	CAAGATCAATTCCAATCCGAC	SALK_025666	chr5 19309425	455-755
NF-YB3	TGTTACGTTAGTGGGTTGAACC	TAAAGACCGGTACGACGTTTG	SALK_150879	chr4 8344543	583-883
NF-YC2	AGCTTGTTGGAATGCCATATG	GAGGGATGGAGGAGACTGTTC	SALK_026351	chr1 21024577	434-734
NF-YA2	TTTTGGCCACTACAATAGATTATATACC	TGCAAAGAAAGGTGATGGAAG	SALK_146170	chr3 1676699	594-894

LB Primer	Sequence
Salk LBb1.3	5'- ATTTTGCCGATTTCGGAAC - 3'

2.2.5 Gateway Cloning

All cloning was performed utilizing Gateway® recombination cloning technology (Life Technologies™). pDONRZeo vector (Invitrogen) was used to generate all entry vectors. NF-YA2, NF-YB2 and NF-YC2 ORF sequences were amplified from Arabidopsis Col-0 cDNA. Only the NF-YA2 under the native promoter was amplified from Arabidopsis Col-0 genomic DNA.

Where necessary, the stop codon was removed using a QuikChange II Site-Directed Mutagenesis Kit (Agilent) and the primers shown in Table 2.6. To recombine the PCR product into the entry vector, attB-PCR product was synthesized using two-step PCR (Table 2.4 and 2.5).

Table 2.4 – Cloning: first step PCR primers

Primer	Sequence	Cycles
Forward	5'- AAAAAAGCAGGCTTC-template specific sequence (20-30bp) - 3'	15
Reverse	5'- CAAGAAAGCTGGGTC-template specific sequence (20-30bp) - 3'	

Table 2.5 – Cloning: second step PCR primers

Primer	**Sequence**	**Cycles**
Forward	5'- GGGGACAAGTTTGTACAAAAAAGCAGGCT - 3'	25
Reverse	5'- GGGGACCACTTTGTACAAGAAAGCTGGGT - 3'	

Table 2.6 - Primers to remove STOP codon

Gene	**Primer**	**Sequence**
NF-YA2	Forward	5' GCTGCAATTTCAAAACCGACCCAGCTTTCTTGTAC 3'
NF-YA2	Reverse	5' GTACAAGAAAGCTGGGTCGGTTTTGAAATTGCAGC 3'
NF-YB2	Forward	5' CGGTAGGACAAGGACTGACCCAGCTTTCTTGTAC 3'
NF-YB2	Reverse	5' GTACAAGAAAGCTGGGTCAGTCCTTGTCCTACCG 3'

PCR was performed using ACCUZYME™ DNA Polymerase (Bioline, UK) as described in Table 2.1 using the thermal cycling conditions described in Table 2.2. attB-PCR product and the pDONRZeo vector were mixed at equal amounts

(150ng) in sterile water to a final volume of 4 µl before the addition of 1 µl BP Clonase II to recombine the PCR product into the entry vector. Reactions were incubated at 25°C overnight.

2µl of BP reaction was used to transform 10 µl of DH5α competent *Escherichia coli* cells and incubate on ice for 30 minutes. The cells were heat shocked at 42°C for 30 seconds and incubate on ice for 2 minutes. 250 µl of SOC media was added and cells were incubated at 37°C for 1 hour. 150 µl of inoculum was then plated on LB media containing Zeocin (25ng/ml, Invitrogen) and incubated at 37°C overnight. Bacterial colonies were inoculated in 100 µl of sterile water. Colony PCR was performed on 1 µl of the inoculated water (primers are listed on table 2.7). Plasmids were purified and quantified. Fragments were sequenced using the M13 forward and reverse primers (Table 2.7). Positive transformants with a correctly sized colony PCR amplicon were inoculated into 5 mL LB broth containing Zeocin™ (50 µg/ml) and incubated at 37°C overnight with shaking at 220 rpm. Bacterial cells were harvested by centrifugation at 10,000 × g for 10 min and plasmid DNA (pDNA) purified using QIAprep Spin Miniprep Kit (Qiagen) according to the manufacturer's instructions with final elution into 30 µL sterile water.

LR reactions were conducted using 150 ng purified pDONRZeo vector, 150 ng Destination vector (listed in section 2.1.5) and 1 µL LR Clonase® II, sterile water was added to a final volume of 5 µL. Reactions were incubated at 25°C overnight. The LR reaction was transformed into *E. coli* strain DH5α cells and plated onto selective LB agar plates. Colony PCR was performed and plasmids were purified and quantified.

Table 2.7 - Primers used for colony PCR and sequencing

Gene	Primer	Sequence
NF-YA2	Forward	CAGAGCAGGGTAATGCTTCC
NF-YA2	Reverse	TGGTTCCGCTATTTTCCAAG
NF-YB2	Forward	GGTCGGAGAGCATCAGAGAG
NF-YB2	Reverse	TGGTTCTGCTGGTGAAGAAA
NF-YC2	Forward	CATGACCTGTTTGGGATCATC
NF-YC2	Reverse	TTGGTCACGCCTAAACCTTC

Gene	Primer	Sequence
M13	Forward	5' GTAAAACGACGGCCAG 3'
M13	Reverse	5' CAGGAAACAGCTATGAC 3'

2.2.6 *A. tumefaciens* mediated transient expression in *N. benthamiana*

2.2.6.1 Generation of *Agrobacterium tumefaciens* competent cells

A.tumefaciens strain GV3101 was inoculated into 10 ml of YEB medium containing Rifampicin (100 µg/mL) and Gentamicin (30 µg/mL) and grown at 28^{o}C with shaking at 220 rpm overnight. The next day the overnight culture was transferred into 200 ml of YEB medium with the appropriate antibiotics and incubated at 28^{o}C with 220 rpm shaking to an OD_{600} of 0.5 (approximately 4 hours). The culture was harvested by centrifugation at 2500g at 4°C for 20 minutes and re-suspended in ice cold TE buffer (10mMTris/HCl, 1mM EDTA pH 8.0). Cells were then centrifuged at 2500g at 4°C for 20 minutes and re-suspended into ice cold YEB medium. *A. tumefaciens* competent cells were aliquoted into 500 µl volumes, flash frozen in liquid nitrogen and stored at -80°C.

2.2.6.2 *Agrobacterium tumefaciens* transformation

500 µl aliquot of *A. tumefaciens* competent cells were thawed on ice. Approximately 1-2 µg of plasmid DNA was added to 100 µl of cells and mixed,

before incubation on ice for 5 minutes. The DNA-bacteria mixture was flash-frozen in liquid nitrogen for 5 minutes and then heat-shocked at 37°C for 5 minutes. Cells were left on ice for 2 minutes followed by the addition of 900 µl of YEB medium and incubated for 2 hours at 28°C with shaking. 100 µl of the transformed *A. tumefaciens* cells were plated onto YEB agar plates with Rif_{100} and $Gent_{30}$ and the appropriate destination vector selective antibiotic, then incubated at 28°C for 2 days.

2.2.6.3 Transient expression in *Nicotiana benthamiana*

Agrobacterium tumefaciens strain GV3101 containing the plasmid of interest and the p19 silencing suppressor (Voinnet et al. 2003) were grown overnight in 10 ml YEB medium with the appropriate antibiotics at 28°C and 220 rpm shaking. The next day, the cultures were harvested by centrifugation at 3000g for 10 minutes and re-suspended in 10 ml infiltration buffer (10 mM MES, 10 mM $MgCl_2$ pH 5.7). The OD_{600} was then measured and adjusted, while mixing any constructs to be co-expressed. Typically, a final OD_{600} of 0.4 was used for CO-IP or BIFC. *A. tumefaciens* expressing p19 was added to each mixture at a final OD_{600} of 0.4. 100 µM Acetosyringone was added to each cell suspension and incubated for 2-4 hours in the dark. Each cell suspension was transiently expressed in 3 weeks old *Nicotiana benthamiana* leaves by infiltration as described in Voinnet et al. 2003.

2.2.7 Bimolecular Fluorescence Complementation (BIFC) screen

Using this system, the interaction between NF-Y TFs were tested on 3-week-old *Nicotiana benthamiana* leaves. Two YFP fragments, either C and N terminal of E-YFP were co-infiltrated so that both the C and N terminus of E-YFP were present in the leaf (BIFP1 or 2 with BIFP3 or 4). Upon interaction between the two proteins, the fragments restore fluorescence, which can be detected using confocal microscopy 3 days after infiltration.

2.2.7.1 Localization of fluorescently tagged proteins by confocal microscopy

After three days of transient expression of protein constructs in *N. bethamiana*, 5 mm leaf discs were imaged using Zeiss Laser Scanning Microscope (LSM) 710 (Carl Zeiss Ltd; Cambridge, UK). Images were then processed using Fiji software (Schneider et al., 2012).

2.2.8 Biochemical techniques

2.2.8.1 Protein immunoprecipitation

Extraction and quantification of protein transiently expressed in *Nicotiana benthamiana*

In the case of protein transiently expressed in *Nicotiana benthamiana*, the whole infiltrated region was used per sample. Experiments were performed using either fresh or frozen material. Tissue was grounded using mortar and pestle and protein extraction was done using GTEN buffer (Table 2.8). GFP-Trap®_A (Chromotek) beads were used following the manufacturer's instructions to immunoprecipitate YFP re-assemble protein. Samples were quantified using Bradford reagent and comparison to a standard curve of Bovine Serum Albumin (BSA), then stored at -20^{o}C.

Table 2.8 - GTEN protein extraction buffer component

Component	Final concentration
Glycerol	10% [v/v]
Tris-HCl	25 mM
EDTA	1 mM
NaCl	150 mM
Nonidet P40	0.15% [v/v]
PVPP	2% [w/v]
DTT	10 mM
PMSF	1 mM
Protease inhibitors (Sigma P9599)	1X

Protein extraction and co-immunoprecipitation of Arabidopsis epitope tagged lines

A protocol published by Piquerez et al (2014) was used for the immunoprecipitation of plant-expressed proteins. Fully expanded Arabidopsis leaves were ground in liquid and proteins were extracted in Buffer C (2% w/v PVPP, 1% IGEPAL® CA-630) at a ratio 4:1 v/w. Starting plant material varied from 1-2 g for the identification of expressed protein to 30-40 g for the immunoprecipitation of large protein complexes and then mass spectrometry. Protein extracts were filtered through Miracloth (Millipore) and mixed with 15-30µL of appropriate affinity resin: GFP-Trap®_A (Chromotek) beads or ANTI-FLAG M2 Affinity Gel (Sigma). Immunoprecipitation was performed at 4^{o}C for 2 hours on a rotating wheel. Beads were then washed with Buffer D. All protein extraction buffers components are listed on Table 2.9.

Table 2.9 - Protein extraction buffers component (Piquerez et al. 2014)

BUFFER	Component	Final concentration
BUFFER C	Glycerol	5% [v/v]
	Tris-HCl pH 7.5	150 mM
	EDTA	5 mM
	NaCl	150 mM
	EGTA	2 mM
	PVPP	2% [w/v]
	DTT	10 mM
	PMSF	0.5 mM
	Protease inhibitors (Sigma P9599)	1% [v/v]
BUFFER D	Buffer C without PVPP	
5x SDS-PAGE loading buffer	Tris-HCl pH 6.8	60 mM
	SDS	2% [w/v]
	Glycerol	0.15% [v/v]
	Bromophenol blue	0.10% [w/v]
	DTT	50 mM

2.2.8.2 On-beads trypsin digestion

Trypsin digestion was performed to prepare immunoprecipitated proteins for mass spectrometry analysis. For the reduction of cysteine double bonds 45 µL of immunoprecipitated material was incubated for 15 minutes at 60°C in 10 mM DTT. Subsequentely 20 mM iodoacetamide (IAA) was added and incubated for 30 min in the dark for the alkylation of the cysteine bridges. Protein digestion was obtained with 0.5 mg/mL Trypsin (Promega) and overnight incubation at 37°C. Finally, 0.1% (v/v) of formic acid was added to obtain a low pH. A clear solution of trypsin digest was achieved after filtration through a 0.22 µm Costar® Spin-X® centrifuge tube filter (Sigma- CLS8169) before transferring to a glass vial for mass

spectrometry analysis. Samples were kept at -20°C until analysed by Mass Spectrometry (MS).

2.2.8.3 Identification of proteins by mass spectrometry

Co-immunoprecipitated protein from GFP or FLAG beads, were digested with trypsin and prepared for MS. An aliquot containing 6 µL of extracted peptides from each sample was analyzed by means of nano LC-ESI-MS/MS using the Ultimate 3000/Orbitrap Fusion instrumentation (Thermo Scientific) using a 120 minutes LC separation on a 25 cm column. The data were used to interrogate the *Arabidopsis thaliana* database (supplied by The Sainsbury Laboratory, Norwich) and the common Repository of Adventitious Proteins (http://www.thegpm.org/cRAP/index.html) using un-interpreted MS/MS ions searches within the Mascot software. Scaffold software was used to analyze and visualize the results from Mascot searchs. Peptide identifications were accepted if they could be established at >95.0%.

2.2.8.4 Western Blotting

4X SDS loading buffer (Table 2.10) was added to the total protein extracts and then loaded with Color Prestained Protein Standard, Broad Range Protein Ladder (BioLabs). Samples were separated by polyacrylamide gel electrophoresis (PAGE) on 12% sodium dodecyl sulfate (SDS)-PAGE (Bio-Rad) gels. The run was performed at 100 V for 1.5 h in running buffer (Table 2.10) before electroblotting using transfer buffer (Table 2.10) onto polyvinylidene difluoride (PVDF) membrane (Hybond-P; GE Healthcare, Little Chalfont, England), at 30 V overnight at 4°C. Membranes were rinsed in TBS and blocked for 1.5 h shacking in 5% [w/v] milk in TBS-Tween (0.1% [v/v]) and then probed with anti-GFP-HRP or anti-FLAG-HRP conjugated antibody (Miltenyl Biotec, Gladbach, Germany) for 3 h at room temperature. Blots were washed for 10 minutes with TBS-Tween (0.1% [v/v]) buffer for a total of 3 washes. Also 2 washes were carried out with just TBS.

Labelled-GFP or FLAG was detected using chemiluminescence with ECL Prime Western Blotting Detection Reagent (GE Healthcare) according to the manufacturer's protocol and imaged on the ImageQuant LAS 4000 (GE Healthcare) or X-ray processor.

Table 2.10 - Western blot buffers

Buffer	Final concentration
4X SDS loading buffer	50 mM Tris-HCl pH 6.8 4 ml 100% [v/v] glycerol 12.5 mM EDTA 1% [v/v] mercaptoethanol 0.02 % [w/v] bromophenol Blue 2% [w/v] SDS
Running buffer	2.4 g Tris 11.3 g Glycine
Transfer buffer	2.4 g Tris 11.3 g Glycine 20 % [v/v] Methanol

2.2.9 *Botrytis cinerea* screens

2.2.9.1 *Botrytis cinerea* sub-culture

Pepper *Botrytis cinerea* isolate spores were germinated and sub-cultured every 10-14 days on sterile tinned apricot halves in a deep petri dishes at 25^{o}C in the dark.

2.2.9.2 *Botrytis cinerea* infection of detached leaves

Botrytis cinerea spores were collected after 2 weeks in 3 ml sterile distillated water and filtered through glass wool to remove mycelium in the solution. Subsequently spores were counted using a haemocytometer and adjusted to 10^5 spores/ml in 50% [v/v] grape juice for infection of detached leaves. Plants were used at age 4 or 5 weeks, three leaves per plant were detached and place on 0.8%

(w/v) bacterial agar in three propagator trays (30 biological replicates per line). A 10 µl drop of the spore suspension was inoculated onto the center of each leaf. A control leaf from each line was mock inoculated with 50% [v/v] grape juice. Trays were covered with lids and stored at 22°C, 90% humidity and 16 h of light. Photographs of the leaves were taken at 24, 48, 64 and 72 hours post-infection (hpi). ImageJ (Schneider et al. 2012) software was used to record lesion area on all of the leaves, using the scale measure.

2.2.10 *Hyaloperonospora arabidopsidis* screens

2.2.10.1 *Hyaloperonospora arabidopsidis* subculture

Hyaloperonospora arabidopsidis isolates were stored by freezing infected seedlings at -80°C and revived by suspension in sterile distilled water, sprayed onto 10 day old Col-0 plants and grown in a sealed propagator at 18°C, with 10 hours light at 60% humidity. After 7 days of growth, infected seedlings were harvested, suspended in sterile distilled water and vortexed. Spores were isolated from plant material by filtration through miracloth, counted using a haemocytometer and light microscope and adjusted to 30,000 spores/ml. Spores were then sprayed onto Arabidopsis Col-0 and grown in a sealed propagator at 18°C, with 10 hours light at 60 % humidity.

2.2.10.2 *Hyaloperonospora arabidopsidis* Infection and quantification

P40 seed trays were used to grow plants at a density of around 30 seedlings per module. Modules around the edge of the tray were sown with Col-0 while plant lines to be screened were randomised within the inside modules. Plants were grown under short day conditions; 10 hours light, 20°C, 60% humidity. Spores were harvested as described in the subculture section and sprayed onto 14 day old Arabidopsis seedlings. Propagators were sealed and placed at 18°C, with 10 hours light at 60% humidity. At 4 days post infection dissecting microscope was used to count the number of sporangiophores per seedling.

2.2.11 *Pseudomonas syringae* screens

The screening was performed by Prof. Murray Grant group (University of Warwick).

2.2.11.1 *Pseudomonas syringae* phenotyping.

Arabidopsis mutants were infiltrated with *P. syringae* DC3000 suspensions diluted with sterile $MgCl_2$ to a final OD_{600} of 0.05. Four leaves on each of four plants were inoculated per time point. The plants were then incubated in a growth chamber under 120 µmol m-2 s- light for 10 hours, at 21°C and 60% humidity. Images of plants were taken at 2, 3, 4 and 5 days post infection (dpi) and a scale of 0-5 was used to score the leaves.

2.2.11.2 *Pseudomonas syringae* Bacterial growth.

Three leaves per plant were infiltrated with *P. syringae* DC3000 using an OD_{600} of 0.002. *P. syringae* suspensions were diluted with sterile $MgCl_2$, generated by a serial dilution from OD_{600} 0.2. Plants were incubated in a growth room under 120 µmol m-2 s- light for 10 hours, at 21°C. Samples were harvested at 4 dpi, leaf disks were excised with a cork borer size 4 and placed in a 2 ml microfuge tubes containing 1000 µl of sterile $MgCl_2$ and homogenized in a tissue lyzer for 2 x 30 sec at 25 Hz. Serial 1:10 dilutions in MgCl2 were made and 10 µl spots were plated onto KB agar containing appropriate antibiotics. Plates were sealed and grown at 28°C for 48 hours at which point colonies were counted.

2.2.12 Gene expression methods

2.2.12.1 RNA extraction

Three glass beads were added to a pre-labelled 2 ml Eppendorf tube prior to sampling. Material was ground using a mixer mill for 30 seconds at 25 Hz. RNeasy Plant Mini Kit (Qiagen) and the manufacturer's protocol was used for RNA extraction and on-column DNase digestion (RNase-Free DNase set, Qiagen),

followed by an RNA cleanup, again carried out according to the instructions (QIAgen RNeasy Mini Kit, Part 2). 1.5 µl of each sample was quantified with a Nanodrop ND-1000 spectrophotometer (Thermo scientific) and stored at -80^{o}C.

2.2.12.2 cDNA synthesis

cDNA synthesis was performed using SuperScript II Reverse Transcriptase (Invitrogen). 1 µl of 50 mM oligo(dT) and 1 µl of 10mM dNTPs were added to each RNA sample, before incubation at 65^{o}C for 5 minutes to anneal the oligos to the RNA. 4 µl of First Strand Buffer, 2 µl dithiothreitol (0.1M), 1 µl RNase OUT (Invitrogen) and 1 µl SuperScript II Reverse Transcriptase (Invitrogen) was added to each sample and then incubated at 42^{o}C for 50 minutes, followed by 70^{o}C for 15 minutes to inactivate the enzyme. cDNA samples were stored at -20^{o}C.

2.2.12.3 qPCR

Specific primers for target genes were designed for qPCR analysis to amplify 50-150 bp of the coding sequence (Table 2.11). cDNA samples were diluted 1:10 before the analysis (initial concentration of 50 ng/l). 5 ng of cDNA was mixed with 5 µl of SsoAdvanced SYBR Green Supermix (Bio-Rad) and specific primers for the target gene (200 nM), to a total volume of 10 µl. Three technical and three biological replicates were performed for each reaction. Specifically, the analysis was performed on pooled multiple plants from a single tray, which represent a single biological replicate. Three trays for each reaction were used. qPCR reaction cycles were performed on a QuantStudio Real-Time PCR (ThermoFisher) in 96-well plates. A 2-step PCR reaction was used, with a pre-cycle 95^{o}C for 3 minutes, followed by 45 cycles of 95^{o}C for 10 seconds, 55^{o}C for 30 seconds. Fluorescence of each well was recorded after each cycle. A post-reaction melt-curve was performed by heating the sample to 95^{o}C for 10 seconds, then performing a temperature gradient increase of 65^{o}C to 95^{o}C at 5 second increments. Fluorescence was measured after each temperature increase. A single melt-curve peak was confirmed visually.

Table 2.11 – Primers used for qPCR

Target gene	Direction	Oligo sequence (5'-3')
AtNF-YA2 (AT3G05690)	Forward	TGAGTAGTAGATGCCGCAAGCC
AtNF-YA2 (AT3G05690)	Reverse	TCACCTTTCTTTGCATTGGTTCCG
AtNF-YB2 (AT5G47640)	Forward	ACAACCAGAACGGACAGTCCTC
AtNF-YB2 (AT5G47640)	Reverse	ACGTTAGCGATCGGCAAGAACC
AtNF-YC2 (AT1G56170)	Forward	AGCAACAGCAACAGGGAGTGATG
AtNF-YC2 (AT1G56170)	Reverse	AGCTGCATTTACTGGCCCACTC
Ubiquitin (UBQ)	Forward	GGGTCGTCCAGTGTCCTCTATTA
Ubiquitin (UBQ)	Reverse	TCAACCAAACCACTGTACCTCAG
Alpha tubulin (Tuba)	Forward	TGACATTGAGCGCCCAACTTACA
Alpha tubulin (Tuba)	Reverse	ATCCACATTCAGAGCACCATCGA
SolyNF-YA2 (Solyc01g006930)	Forward	AACTTTCGGGCCGCATTA
SolyNF-YA2 (Solyc01g006930)	Reverse	GGTCTTTCGACGCCTTAGTATC
SolyNF-YB2 (Solyc07g065500)	Forward	CAAGACAGGTTCCTTCCCATAG
SolyNF-YB2 (Solyc07g065500)	Reverse	CTTGAACTACCTCCTTAGCATCTT
SolyNF-YC2 (Solyc01g079870)	Forward	CAGCAACCACCCTCAGATT
SolyNF-YC2 (Solyc01g079870)	Reverse	GTGTTCTCCAGTACTTCGCTAC
SolyActin	Forward	CGGTGACCACTTTCCGATCT
Soly-Actin	Reverse	TCCTCACCGTCAGCCATTTT
Soly-β-6 Tubulin	Forward	TTGGTTTTGCACCACTGACTTC
Soly-β-6 Tubulin	Reverse	AAGCTCTGGCACTGTCAAAGC

2.2.12.4 RNAseq: library preparation and sequencing

Previous to library preparation, mRNA quality was evaluated using a Nanodrop ND-1000 spectrophotometer (Thermo scientic) and an Agilent 2100 Bioanalyzer using the Agilent RNA 6000 Pico Kit. mRNA with 260/280 and 260/230 ratios of <1.8 and a clean bioanalyzer trace were sent for sequencing.

The library preparation for RNAseq was performed by the Genomics Facility at the University of York and sequencing was carried out at the Genomics centre at the University of Oxford. Libraries were made using the NEBNext Ultra II Directional RNA Library Prep Kit for Illumina after Poly (A) purification using the NEBNext Poly(A) mRNA Magnetic Isolation Module. Samples were pooled at an equimolar ratio.

Chapter 3

3. Role of NF-Y subunits in the plant defense response.

3.1 Introduction

In this chapter, a reverse genetic approach was used to investigate the function of specific NF-Y subunits. This method, extensively used in functional analysis, recognizes a gene of interest and then examines mutants in this gene to infer function (i.e. genotype to phenotype) (Page and Grossniklaus 2002). In these mutants, the target gene can be knocked out (KO) or over expressed (OE). In Arabidopsis, KO mutants are largely used to investigate a specific gene function and this approach consists of the insertion of a T-DNA fragment into the gene of interest which may disrupt gene expression. However, despite the fact that some Arabidopsis knockout mutants have shown an altered phenotype compared to wild type (Eshed et al. 2001, Simillion et al. 2002), in some cases KO mutants do not demonstrate any phenotypical alterations (Bouche and Bouchez 2001). Several reasons can explain the scarcity of phenotypes, in particular our inability to detect small alterations in plants, and gene functional redundancy, which is particularly important in transcription factors (TFs), as these are often members of large gene families with closely related genes (Riechmann et al. 2000). Also, it is important to consider that often organisms with the same genotype do not display similar phenotypes when grown in comparable conditions in different laboratories (Massonnet et al. 2010).

Another way to study the function of a TF in plants is to overexpress it using the 35S Cauliflower mosaic virus (CaMV) promoter, which increases the gene expression levels (Odell et al. 1985). However, this approach needs to be carefully considered, because the phenotype could be a consequence of the mis-expression of the TF in the plant. The change of the TF expression levels could

alter the actual function of the TF protein may be causing non-canonical protein-protein interactions (PPIs) (Moriya 2015). Moreover, in TF families that form functional complexes such as NF-Ys, overexpression of one subunit could destabilize the balance between subunits and disrupt the assembly of the complex (Viola and Gonzalez 2016). However, overexpression is a very useful tool to clarify the role of a TF in plant in combination with other supporting data such as gene expression analysis and phenotype of KO mutants, representing a complementary approach (Zhang J. Z. 2003). Indeed, despite these limitations, the reverse genetics is a powerful and widely used method to investigate gene function. The identification of altered phenotypes in the mutant in comparison to wild type, can provide valuable understanding into the role of that gene *in planta.*

3.2 Chapter aims

Based on the hypothesized putative trimer (NF-YA2/NF-YB2/NF-YC2), the aims of this chapter are to use a reverse genetic approach in which mutants with enhanced expression or lacking expression of NF-YA2, NF-YB2 and NF-YC2 will be subjected to different biotic stress screens (*Botrytis cinerea*, *Hyaloperonospora arabidopsidis* and *Pseudomonas syringae*) in order to elucidate the role of NF-Y subunits of interest during the plant defense response.

3.3 Results

3.3.1 NF-Ys knockout and overexpressor mutant resources.

To elucidate the biological function of NF-YA2, NF-YB2 and NF-YC2 through a reverse genetics approach, two types of mutants were obtained or generated for each gene.

Firstly, the NF-YA2, NF-YB2 and NF-YC2 open reading frame (ORF) was placed downstream of the 35S CaMV promoter, to drive constitutive overexpression of these genes using Gateway destination vectors (Nakamura et al. 2010). These OE vectors once cloned into *E. coli* have been sequenced to check the presence of the insert, transferred into Agrobacterium and then transformed into KO plants (for complementation) or wild type plants, using the floral dipping method (Clough and Bent 1998). All these vectors contain a Basta (a glufosinate herbicide) resistance gene for transgenic plant selection. Two independent homozygous lines for each construct have been selected and used for this study. Table 3.1 illustrates the list of Arabidopsis lines generated. A green fluorescent protein (GFP) or flagellin (FLAG) tag was also present in the vector for subsequent protein analysis.

Secondly, available loss-of-function mutants were obtained from NASC or supplied by Prof. Ben F. Holt, III (University of Oklahoma, Oklahoma). Mutants of NF-YA2 and NF-YC2 genes containing a T-DNA insertion in the coding region were identified from the SALK T-DNA insertion collection (respectively SALK_146170 and SALK_026351) and genotyped to check the homozygosity. Also, the expression level of NF-YA2 and NF-YC2 was checked in *nf-ya2* and *nf-yc2* KO mutants in leaf material from pooled multiple plants using quantitative reverse-transcription PCR (qRT-PCR) and normalized to the housekeeping genes alpha-Tubulin (Tuba) and Ubiquitin (UBQ5) (Figure 3.3). *nf-yb2* (SALK_025666), *nf-yb3* (SALK_150879) and the double mutant *nf-yb2/nf-yb3* provided by Prof. Ben F. Holt were previously described (Cao et al. 2011, Kumimoto et al. 2013), and the genotype was verified by PCR. Three plants for each of KO lines were genotyped and 100% of them showed to be homozygous (Figure 3.4).

Figure 3.1 shows a schematic representation of all gene constructs generated in this study. Additionally, Figure 3.2 shows NF-YA2, NF-YB2, NF-YB3 and NF-YC2 gene structure and T-DNA locations.

In this chapter *nf-yb3* and the double mutant *nf-yb2/nf-yb3* were also analyzed to test the overlapping functionality between NF-YB2 and NF-YB3 hypothesized by Kumimoto et al. (2013).

Table 3.1 - List of Arabidopsis lines generated in this study. Table shows construct, tag and background plant for each line. Two independent homozygous lines for each construct have been selected.

Construct	Tag	Background plant	Line name
35S:FLAG:NF-YA2	FLAG	*nf-ya2*	*nf-ya2*::35S:FLAG-NF-YA2_1 *nf-ya2*::35S:FLAG-NF-YA2_2
35S:FLAG:NF-YA2	FLAG	Col-0	*Col-0*::35S:FLAG-NF-YA2_1 *Col-0*::35S:FLAG-NF-YA2_2
35S:GFP:NF-YA2	GFP	Col-0	*Col-0*::35S:GFP-NF-YA2_1 *Col-0*::35S:GFP-NF-YA2_2
pNF-YA2:NF-YA2:GFP	GFP	Col-0	*Col-0*::pNF-YA2:NF-YA2-GFP_1 *Col-0*::pNF-YA2:NF-YA2-GFP_2
pNF-YA2:NF-YA2:GFP	*GFP*	*nf-ya2*	*nf-ya2*::pNF-YA2:NF-YA2-GFP_1 *nf-ya2*::pNF-YA2:NF-YA2-GFP_2
35S:FLAG:NF-YB2	FLAG	*nf-yb2*	*nf-yb2*::35S:FLAG-NF-YB2_1 *nf-yb2*::35S:FLAG-NF-YB2_2
35S:GFP:NF-YB2	GFP	*nf-yb2*	*nf-yb2*::35S:GFP-NF-YB2_1 *nf-yb2*::35S:GFP-NF-YB2_2
35S:NF-YC2:GFP	GFP	*Col-0*	*Col-0*::35S:NF-YC2-GFP_1 *Col-0*::35S:NF-YC2-GFP_3
35S:GFP:NF-YC2	GFP	*Col-0*	*Col-0*::35S:GFP-NF-YC2_1 *Col-0*::35S:GFP-NF-YC2_2

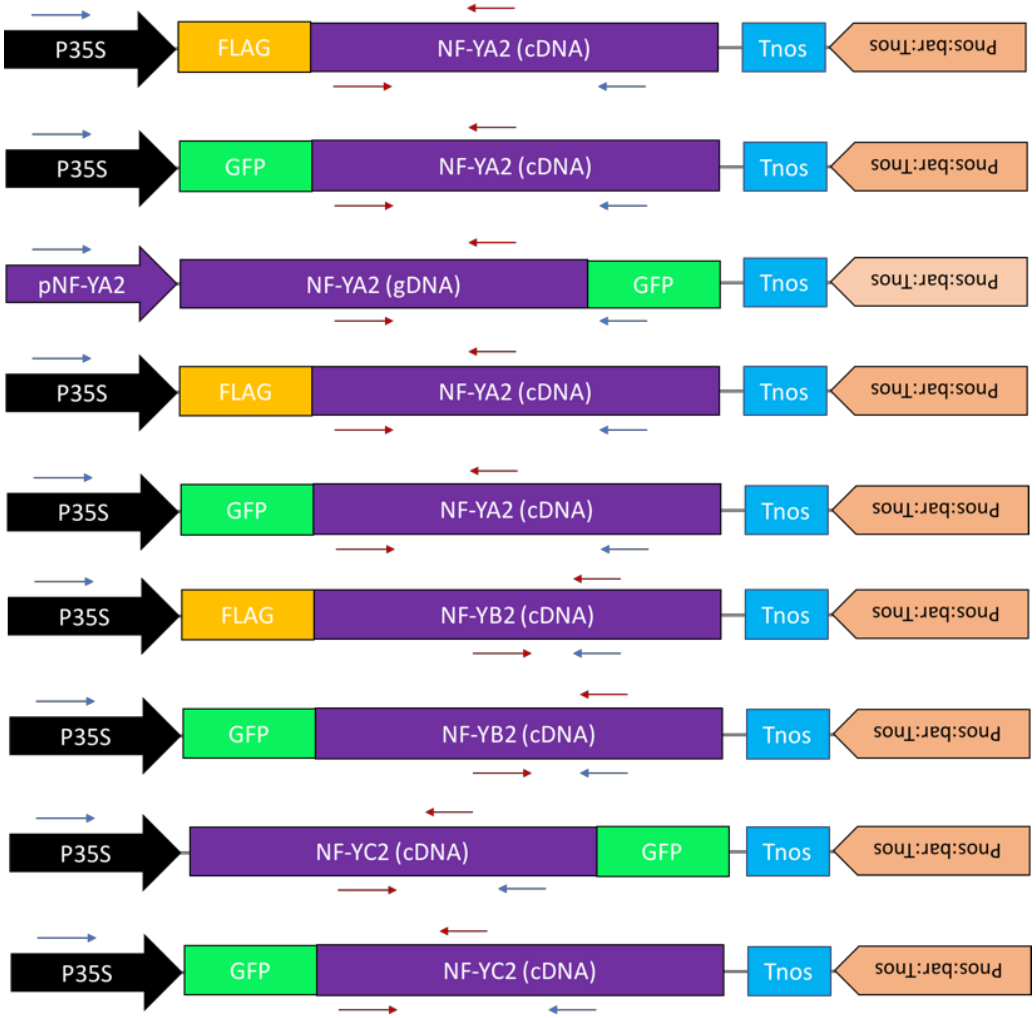

Figure 3.1 – Schematic representation of all gene constructs generated. Red arrows indicate position of primer pair used for q-PCR, while blu arrows indicate primers used for genotyping.

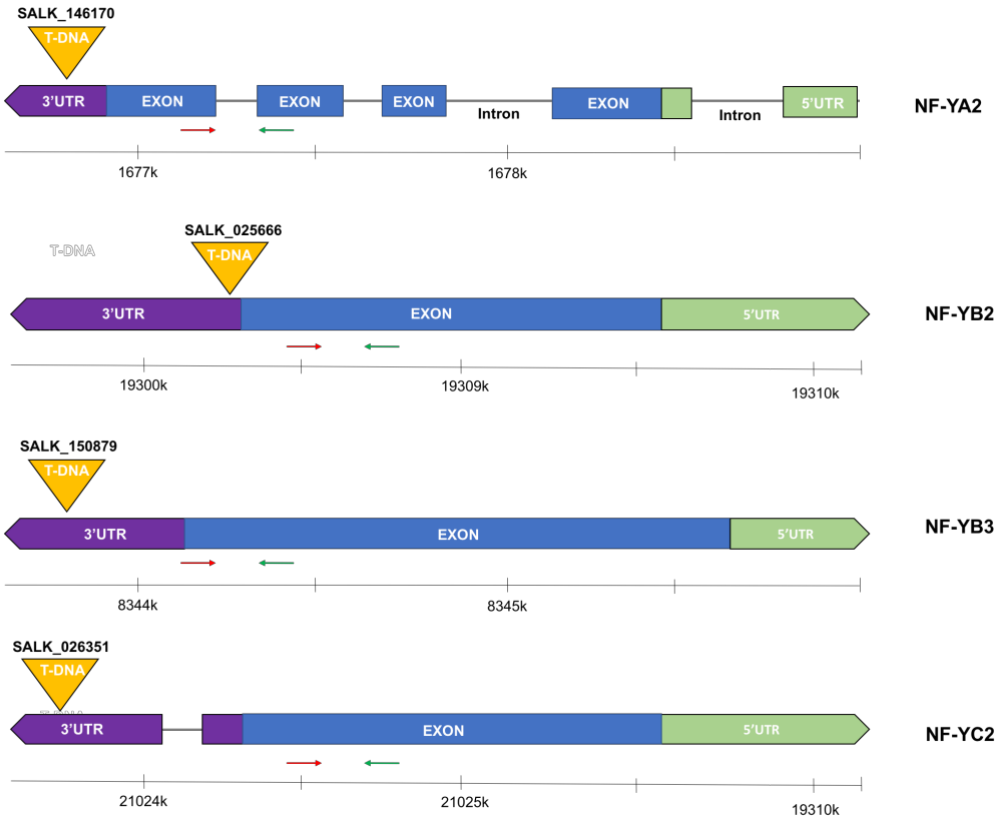

Figure 3.2 – NF-YA2, NF-YB2, NF-YB3 and NF-YC2 gene structure and T-DNA locations. Schematic of the annotated (TAIR10) gene model for NF-YA2, NF-YB2, NF-YB3 and NF-YC2 showing the relative size and positions of the 5' UTR, exons, introns and 3' UTR, together with the reported locations of the T-DNA insertions for the NF-YA2, NF-YB2, NF-B3 and NF-YC2 loss-of-function mutants. Green and red arrows indicate positions of primer pairs used for q-PCR. Ruler indicates the chromosome location of each gene.

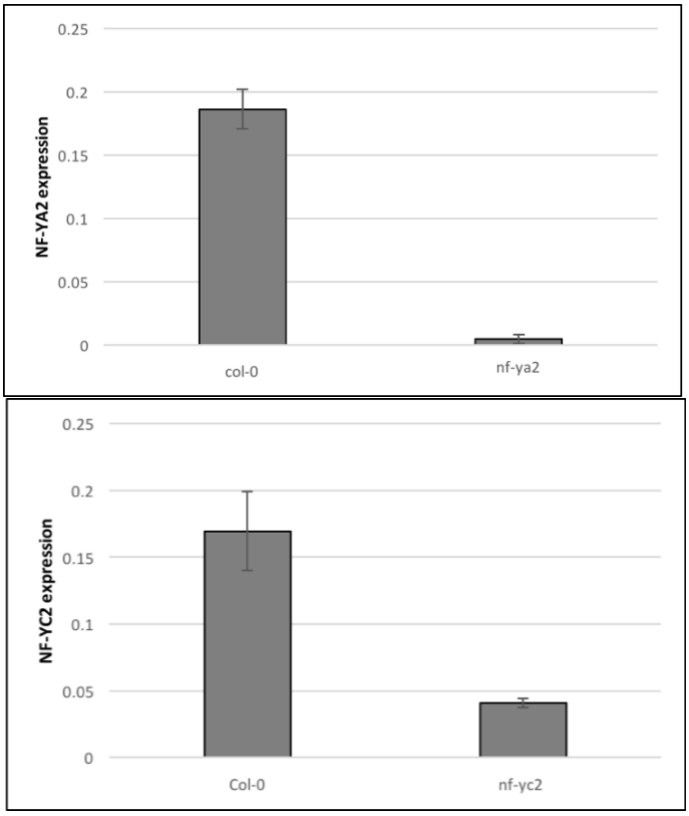

Figure 3.3 – q-PCR expression analysis confirmed that Arabidopsis NF-YA2 (SALK_146170) and NF-YC2 (SALK_026351) are knockout mutants. Relative expression of NF-YA2 and NF-YC2 genes in *nf-ya2* and *nf-yc2* KO mutants compared to the wild type Col-0 was determined by quantitative RT-PCR. Gene transcript levels were calculated using the comparative 2-ΔΔC(T) method (Livak and Schmittgen 2001) and normalized to the expression of the two housekeeping genes alpha-Tubulin and (Tuba) and Ubiquitin (UBQ5). Data are presented as the relative expression from 3 technical and 3 biological replicates. The analysis was performed on pooled multiple plants leaf material.

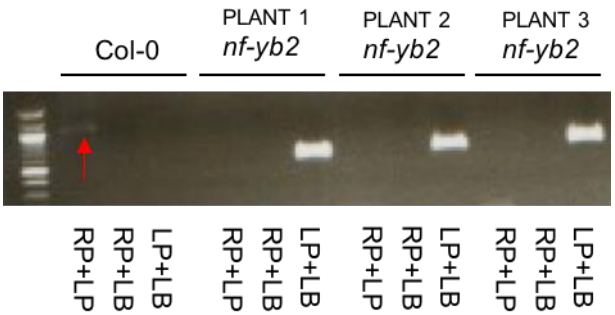

Figure 3.4 – Representative PCR gel for genotyping of *nf-yb2* KO line. Three plants for each of KO line were genotyped. All of them showed to be homozygous. Only Col-0 showed a band in the RP+LP primers combination (indicated by arrow). The single band in LP+LB primers combination confirm the homozygosis of KO plants (LP=left primer; RP=right primer; LB=Left border primer Salk: Lbb1.3).

3.3.2 Morphology appearance of NF-YA2, NF-YB2 and NF-YC2 OE and KO lines

Plants were grown to check for large-scale morphological differences between lines. *Arabidopsis thaliana* NF-Y KO and OE lines were grown in long day conditions (16 h day length) for five weeks as reported in Windram et al. (2012). Col-0 was used as control. *nf-ya2*, *nf-yb2, nf-yc2* and the double mutant *nf-yb2/nf-yb3* lines were indistinguishable morphologically from the wild type Col-0 plants, while *nf-yb3* showed a slightly bigger size (Figure 3.5). The phenotype of *nf-yb2* seen here is consistent with a previous report where it was observed that *nf-yb2* KO mutants are not significantly different from wild type (Ballif et al. 2011).

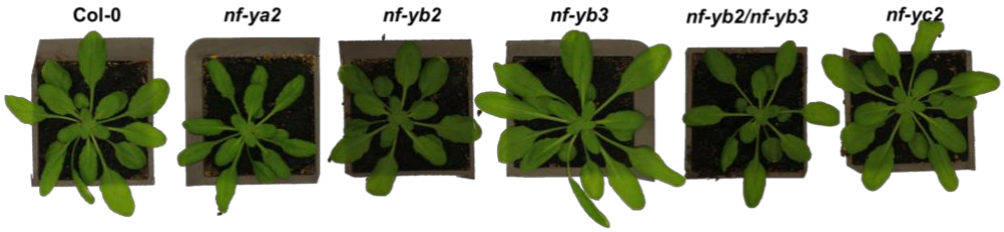

Figure 3.5 – Representative images showing morphology of the *nf-ya2*, *nf-yb2*, *nf-yb3*, *nfyb2/nf-yb3* and *nf-yc2*, compared to the wild type Col-0, rosettes at 5 weeks after sowing. Plants were grown in soil under long day (LD) conditions (16 hours of light) at 20°C, 70% relative humidity and 100 $\mu mol^2.s^{-1}$ light

The phenotype of Arabidopsis plants overexpressing NF-YA2, NF-YB2 and NF-YC2 was also investigated. Col-0 or the relative KO mutant was used as background plant. The morphology of NF-YA2 OE lines (Col-0::35S:FLAG-NF-YA2_1, Col-0::35S:FLAG-NF-YA2_2, Col-0::35S:GFP-NF-YA2_1, Col-0::35S:GFP-NF-YA2_2) in Col-0 background, were analyzed and all of them showed to be phenotypically similar to Col-0 (Figure 3.6). On the other hand *nf-ya2::*35S:FLAG-NF-YA2_1*, nf-ya2::*35S:FLAG-NF-A2_2, with *nf-ya2* as genetic background plant, appeared to be smaller, with zig-zagged leaves in both lines. Unexpectedly, the NF-YA2 OE lines generated in this study did not show severe dwarfism as found in Siriwardana et al. (2014). For this reason, the expression of NF-YA2 in the OE lines was checked using quantitative reverse-transcription PCR (qRT-PCR) and normalized to the

housekeeping genes alpha-Tubulin and (Tuba) and Ubiquitin (UBQ5) (Figure 3.7). Higher NF-YA2 expression, relatively to the background plant, was found in both lines, confirming the over expression of NF-YA2 gene. Specifically, the NF-YA2 OE transgenic plants in the *nf-ya2* background (*nf-ya2::*35S:FLAG-NF-YA2) showed a very high expression level compared to Col-0, while the NF-YA2 OE mutant in the Col-0 background (Col-0::35S:FLAG-NF-YA2) showed a moderate increase in expression compared to the wild type plant.

Lines where *nf-ya2* KO plants were complemented with the pNF-YA2:NF-YA2-GFP construct showed the same morphology as the background plant (Figure 3.6). In these lines the expression level of NF-YA2 was checked and it appeared to be very low compared to Col-0 plants (Figure 3.8). This result confirmed that full complementation of *nf-ya2* KO plants with pNF-YA2:NF-YA2-GFP construct did not occur.

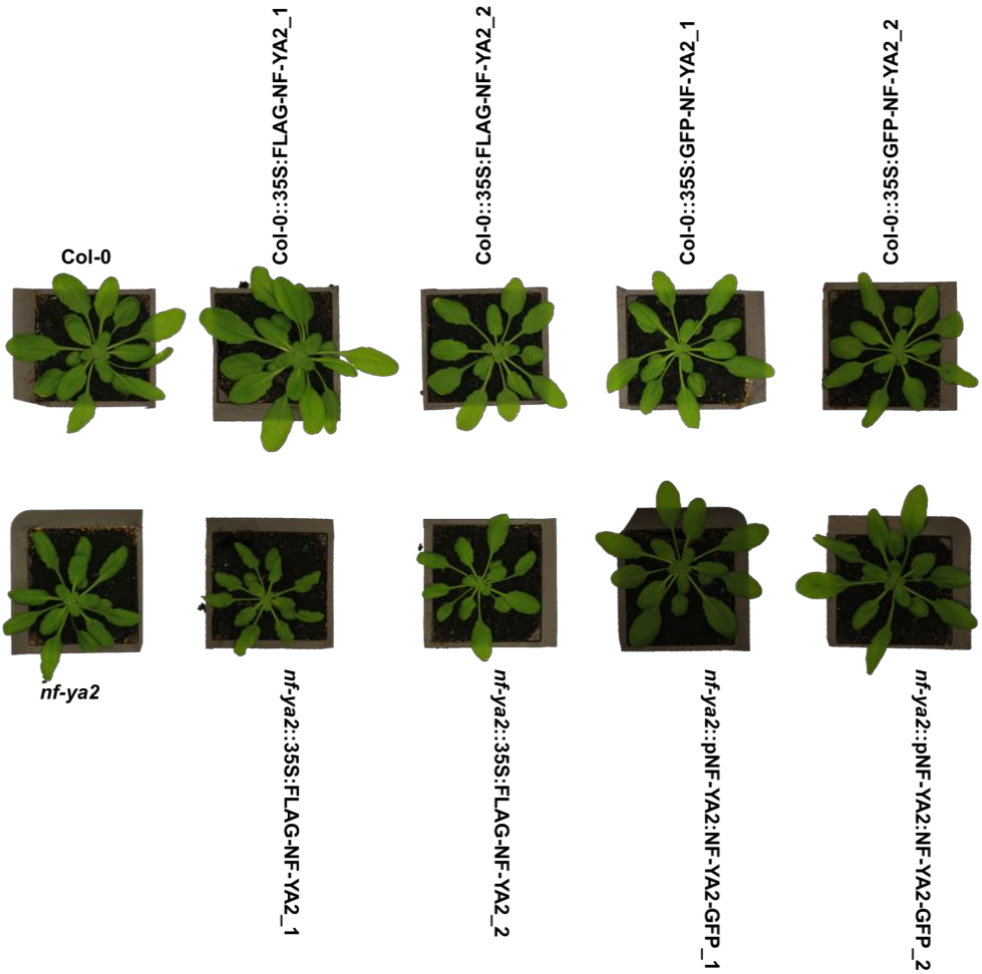

Figure 3.6 - Morphological appearance of 5 weeks old NF-YA2 lines generated, compared to the background plants. Plants were grown in soil under LD conditions (16 hours of light) at 20ºC, 70% relative humidity and 100 $\mu mol^2.s^{-1}$ light. Independent lines were analyzed. The first row shows the morphology of NF-YA2 OE lines: Col-0::35S:FLAG-NF-YA2_1, Col-0::35S:FLAG-NF-YA2_2, Col-0::35S:GFP-NF-YA2_1, Col-0::35S:GFP-NF-YA2_2 with Col-0 as background plant. The second row indicates all NF-YA2 lines generated with *nf-ya2* as background plant: the NF-YA2 OE lines (*nf-ya2*::35S:FLAG-NF-YA2_1, *nf-ya2*::35S:FLAG-NF-A2_2), with smaller and zig-zagged leaves, and the complementary lines (*nf-ya2*::pNF-YA2:NF-YA2-GFP_1, *nf-ya2*::pNF-YA2:NF-YA2-GFP_2) with a similar phenotype as *nf-ya2*.

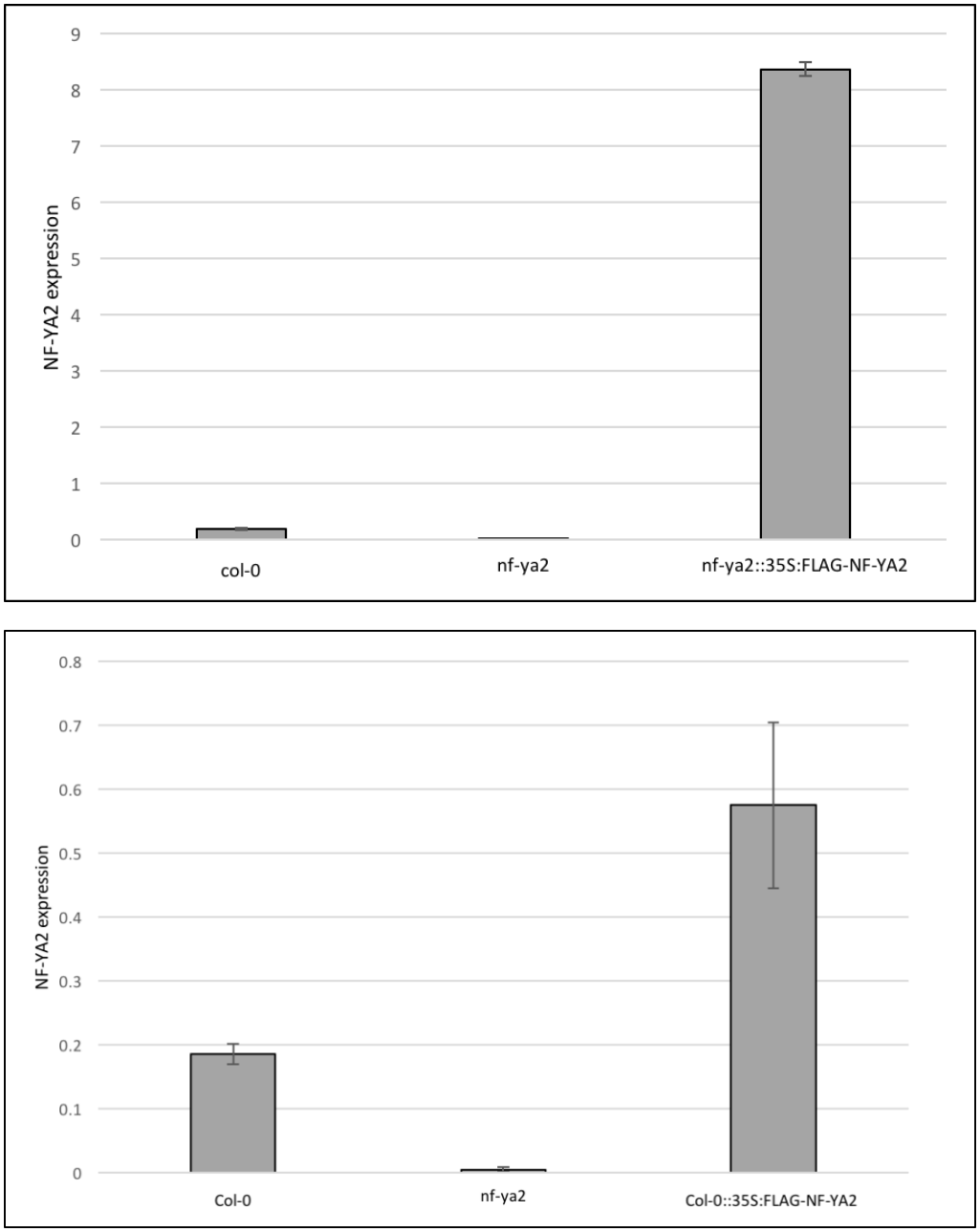

Figure 3.7 – q-PCR expression analysis of Arabidopsis *nf-ya2*::35S:FLAG-NF-YA2 and Col-0::35S:FLAG-NF-YA2 lines showed overexpression of NF-YA2 gene. Relative expression of NF-YA2 in NF-YA2 OE mutants compared to the wild type Col-0 and *nf-ya2* KO mutant was determined by quantitative RT-PCR. Gene transcript levels were calculated using the comparative 2-ΔΔC(T) method (Livak and Schmittgen 2001) and normalized to the expression of the two housekeeping genes alpha-Tubulin and (Tuba) and Ubiquitin (UBQ5). Data are presented as relative expression from 3 technical and 3 biological replicates. The analysis was performed on pooled multiple plants leaf material.

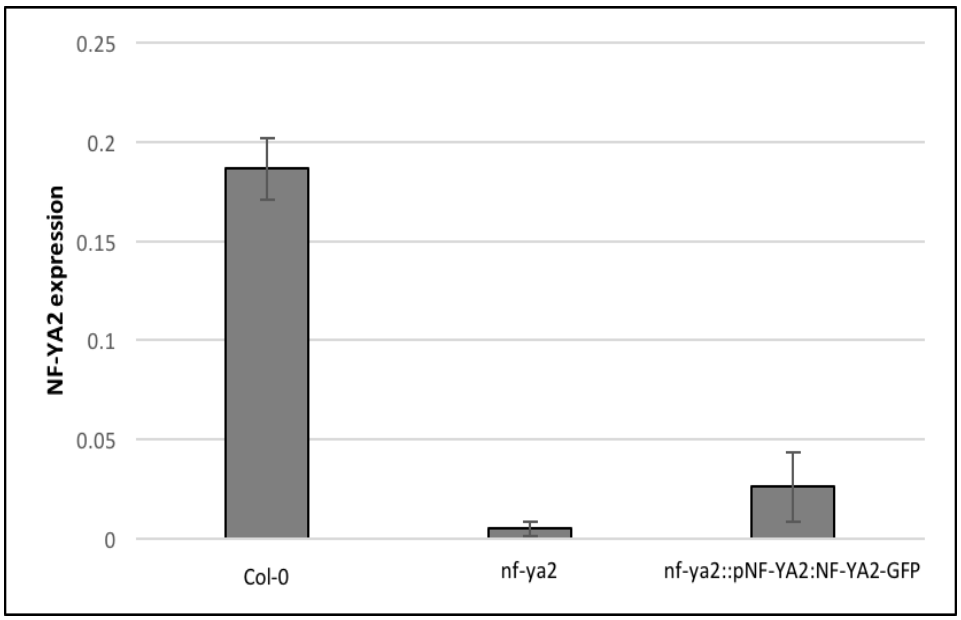

Figure 3.8 – q-PCR expression analysis of Arabidopsis *nf-ya2*::pNF-YA2:NF-YA2-GFP lines did not show the same expression level of NF-YA2 gene compared to Col-0. Relative expression of NF-YA2 in *nf-ya2*::pNF-YA2:NF-YA2-GFP mutants compared to the wild type Col-0 and *nf-ya2* KO mutant was determined by quantitative RT-PCR. Gene transcript levels were calculated using the comparative 2-ΔΔC(T) method (Livak and Schmittgen 2001) and normalized to the expression of the two housekeeping genes alpha-Tubulin and (Tuba) and Ubiquitin (UBQ5). Data are presented as relative expression from 3 technical and 3 biological replicates. The analysis was performed on pooled multiple plants leaf material.

The phenotypes of Arabidopsis NF-YB2 OE lines (*nf-yb2*::35S:GFP-NF-YB2_1, *nf-yb2*::35S:GFP-NF-B2_2 and *nf-yb2*::35S:FLAG-NF-YB2_1, *nf-yb2*::35S:FLAG-NF-B2_2) with *nf-yb2* as background plant, were also examined. Compared to *nf-yb2* plants, which are not significantly different from wild type (Swain et al. 2017), these lines showed slightly bigger leaves (Figure 3.9). This phenotype is in agreement with previous study showing that overexpression of NF-YB2 enhanced cell elongation in the root elongation zone (Ballif et al. 2011), suggesting that NF-YB2 could be involved in cell elongation and cell division process in different plant tissues.

Figure 3.9 - Morphological appearance of 5 weeks old NF-YB2 OE lines generated, compared to *nf-yb2* background plant. Plants were grown in soil under LD conditions (16 hours of light) at 20ºC, 70% relative humidity and 100 µmol^2.s^{-1} light. Independent lines were analyzed. Morphology of NF-YB2 OE lines was checked on *nf-yb2*::35S:GFP-NF-YB2_1, *nf-yb2*::35S:GFP-NF-B2_2 lines and *nf-yb2*::35S:FLAG-NF-YB2_1, *nf-yb2*::35S:FLAG-NF-B2_2 lines, all with *nf-yb2* as background plant.

Also, NF-YC2 OE lines revealed the same morphology as Col-0 plants (Figure 3.10). This data is consistent with what was observed in Hackenberg et al. (2012) where NF-YC2 overexpressors did not show phenotypical differences compared to wild type plants during plant development.

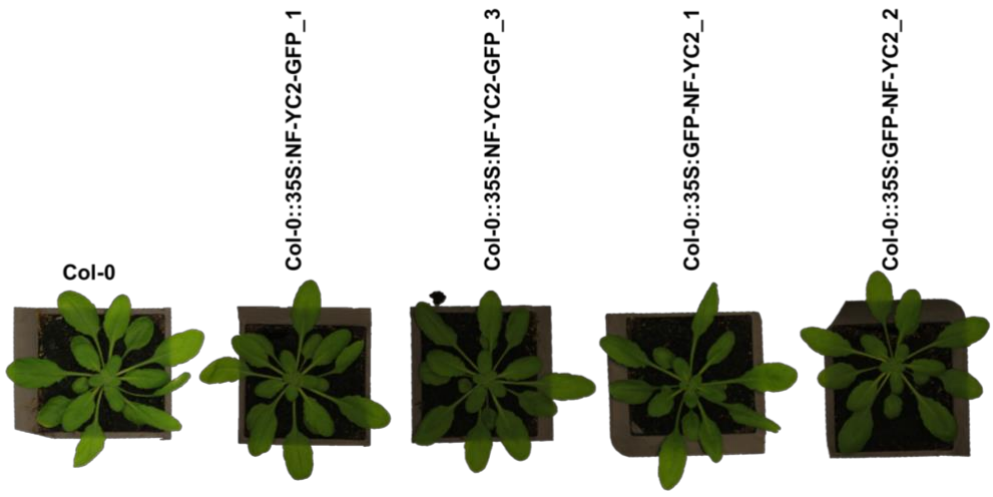

Figure 3.10 - Morphological appearance of 5 weeks old NF-YC2 OE lines generated, compared to Col-0. Plants were grown in soil under LD conditions (16 hours of light) at 20ºC, 70% relative humidity and 100 µmol^2.s^{-1} light. Independent lines were analyzed. Morphology of NF-YC2 OE lines was checked on Col-0::35S:NF-YC2-GFP_1, Col-0::35S:NF-YC2-GFP_3 lines and Col-0::35S:GFP-NF-YC2_1, Col-0::35S:GFP-NF-YC2_2 lines, all with Col-0 as background plant.

In order to determine whether NF-YA2, NF-YB2 and NF-YC2 are important TF in the plant defense response, these OE and KO mutants were tested to observe whether pathogen susceptibility is compromised compared to wild type.

3.3.3 *Botrytis cinerea* susceptibility of Arabidopsis NF-Y KO and OE lines.

Botrytis cinerea is a necrotrophic pathogen which penetrates plant epidermis and kills plant tissue to grow.

B. cinerea infection on Arabidopsis detached leaves (Windram et al. 2012) was performed on five weeks old Arabidopsis KO and OE mutants grown in LD condition as described in Windram et al. (2012). Leaves were drop inoculated with a suspension of *B. cinerea* spores and the developing lesion area was measured at 48, 64 and 72 hours post-inoculation. Col-0 wild type and *botrytis susceptible 1 (bos1*), a T-DNA insert of MYB108 showing a hypersensitive *Botrytis* and wounding response (Cui et al. 2013, Mengiste et al. 2003), were used as controls. The *B. cinerea* assay showed that the *nf-ya2* KO mutant was significantly more susceptible to *B. cinerea* than Col-0 at all three time points post-inoculation (Figure 3.11). This result can also be observed visually, in fact *nf-ya2* showed significantly larger infection area than Col-0 (Figure 3.11b). Conversely, both NF-YA2 OE lines with *nf-ya2* as the genetic background (*nf-ya2*::35S:FLAG-NF-YA2_1 and *nf-ya2*::35S:FLAG-NF-YA2_2), showed a more resistant phenotype compared to Col-0 and the *nf-ya2* mutant, however only *nf-ya2*::35S:FLAG-NF-YA2_2 line was significantly more resistant. This suggests that the insertion of the 35S:NF-YA2 construct into Arabidopsis *nf-ya2* KO mutant, increased the expression level of NF-YA2 gene, giving a similar phenotype to Col-0. Because Col-0::35S:FLAG-NF-YA2_1 and Col-0::35S:FLAG-NF-YA2_2, which have Col-0 as background plant, showed the same phenotype as the *nf-ya2* KO mutant, gene expression level of NF-YA2 in both lines was checked. This analysis showed a lower expression in Col-0::35S:FLAG-NF-YA2 lines than *nf-ya2*::35S:FLAG-NF-YA2 lines (Figure 3.7) and

this could affect plant susceptibility against *B. cinerea* and explaining the different phenotype between the two OE lines.

The increased susceptibility of *nf-ya2* KO mutant to *Botrytis* infection give a first hint about the tight regulation of this gene during the defense response. This result, together with the altered expression of JA biosynthetic in *nf-ya2* KO line, caused by its inability to synthesize JA under inductive conditions in the absence of functional NF-YA2 (Breeze Emily 2014), suggest an important role of NF-YA2 in the plant defense response.

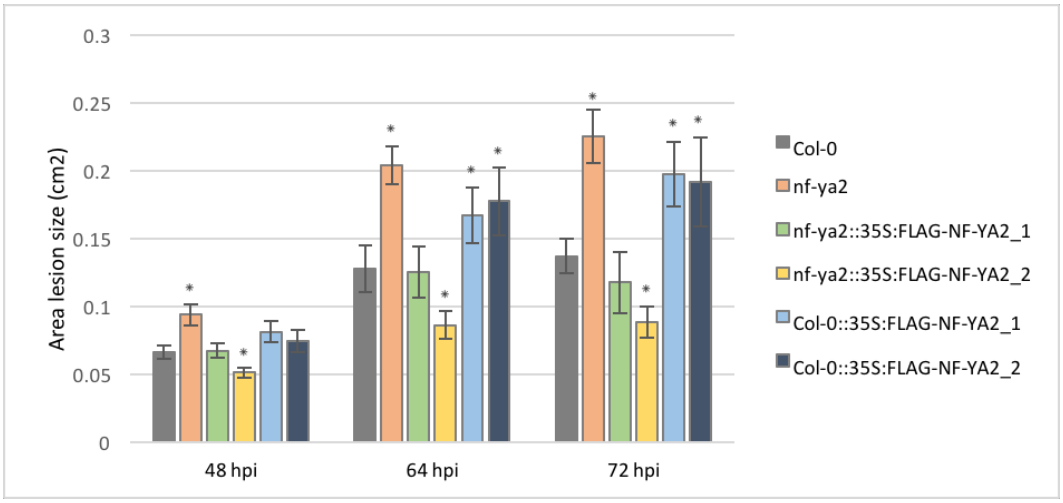

a)

b)

Figure 3.11 - Susceptibility of NF-YA2 KO and NF-YA2-FLAG OE mutants to *Botrytis cinerea* infection. Detached leaves from five weeks old Arabidopsis plants *nf-ya2*, *nf-ya2*::35S:FLAG-NF-YA2_1, *nf-ya2*::35S:FLAG-NF-YA2_2, *Col-0*::35S:FLAG-NF-YA2_1, *Col-0*::35S:FLAG-NF-YA2_2, Col-0 and *bos1* were drop inoculated with *B. cinerea* spores and lesion areas measures at 48, 64 and 72 hours post-inoculation (hpi). a) Mean lesion area, the values presented are the mean of 30 biological replicates (10 plants each line were analyzed) ± SE. Significantly different lesion sizes to Col-0 (indicated by *) at each timepoint were determined using a two-tailed Student's T- test assuming equal variance ($p<0.05$). Experiment was performed twice. b) Representative leaf images at 72 hours post infection are shown. Col-0 and *bos1* were used as controls.

Col-0::35S:GFP-NF-YA2_1 and Col-0::35S:GFP-NF-YA2_2 lines were also tested against *B. cinerea* infection, these lines showed the same susceptibility as Col-0 plants (Figure 3.12). Subsequently, quantitative PCR on leaf material from pooled multiple plants of Col-0::35S:GFP-NF-YA2 lines revealed that the expression level of NF-YA2 gene is not significantly different to Col-0 (Figure 3.13) in physiological condition, explaining the reason of the same phenotype between Col-0 and NF-YA2 OE mutants (Figure 3.12) .

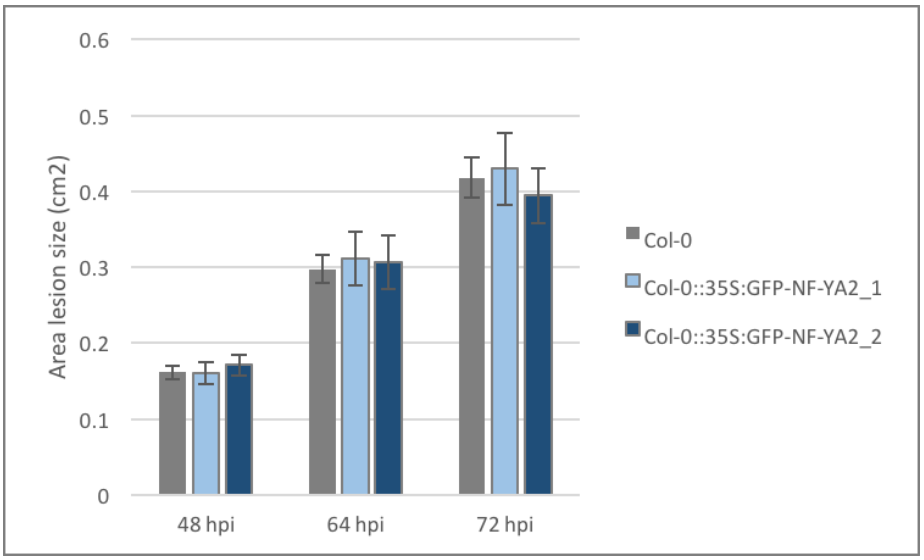

a)

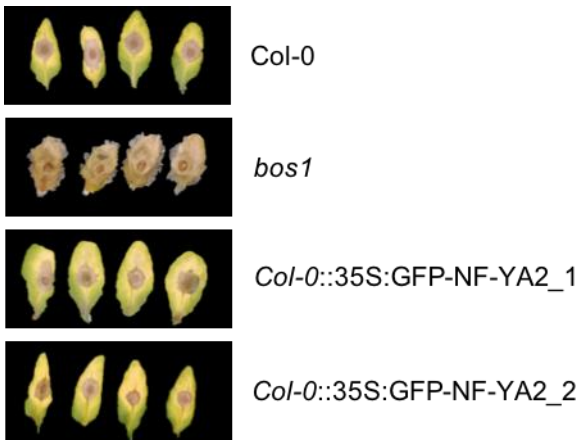

b)

Figure 3.12 - Susceptibility of NF-YA2-GFP OE mutants to *Botrytis cinerea* infection. Detached leaves from five weeks old Arabidopsis plants Col-0::35S:GFP-NF-YA2_1, Col-0::35S:GFP-NF-YA2_2, Col-0 and *bos1* were drop inoculated with *B. cinerea* spores and lesion areas measures at 48, 64 and 72 hours post-inoculation (hpi). a) Mean lesion area, the values presented are the mean of 30 biological replicates (10 plants each line were analyzed) ± SE. Experiment was performed twice. b) Representative leaf images at 72 hours post infection are shown. Col-0 and *bos1* were used as controls.

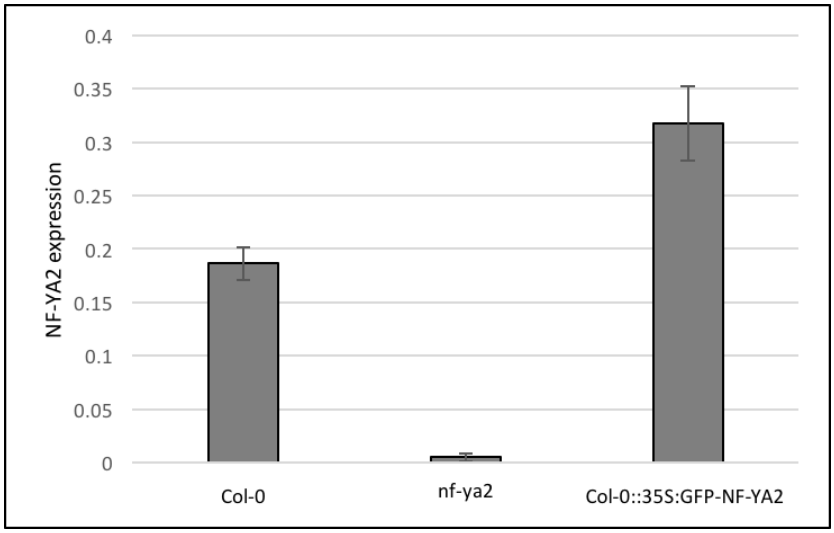

Figure 3.13 – q-PCR expression analysis of Arabidopsis Col-0::35S:GFP-NF-YA2 OE lines revealed that the expression level of NF-YA2 gene is not significantly different to Col-0. Relative expression of NF-YA2 in NF-YA2 OE mutants compared to the wild type Col-0 and *nf-ya2* KO mutant was determined by quantitative RT-PCR. Gene transcript levels were calculated using the comparative 2-ΔΔC(T) method (Livak and Schmittgen 2001) and normalized to the expression of the two housekeeping genes alpha-Tubulin and (Tuba) and Ubiquitin (UBQ5). Data are presented as relative expression from 3 technical and 3 biological replicates. The analysis was performed on pooled multiple plants leaf material.

Moreover, the susceptibility of *nf-ya2*::pNF-YA2:NF-YA2-GFP_1 and *nf-ya2*::pNF-YA2:NF-YA2-GFP_2 lines was tested against *B. cinerea*, revealing a similar phenotype to *nf-ya2* KO mutant (Figure 3.14). This result was confirmed by qPCR which showed that the level of NF-YA2 on leaf material from pooled multiple plants of *nf-ya2*::pNF-YA2:NF-YA2-GFP was very low (Figure 3.8). This suggests that the complementation of *nf-ya2* KO mutant with pNF-YA2::NF-YA2-GFP insert, did not restore the NF-YA2 expression level (Figure 3.8).

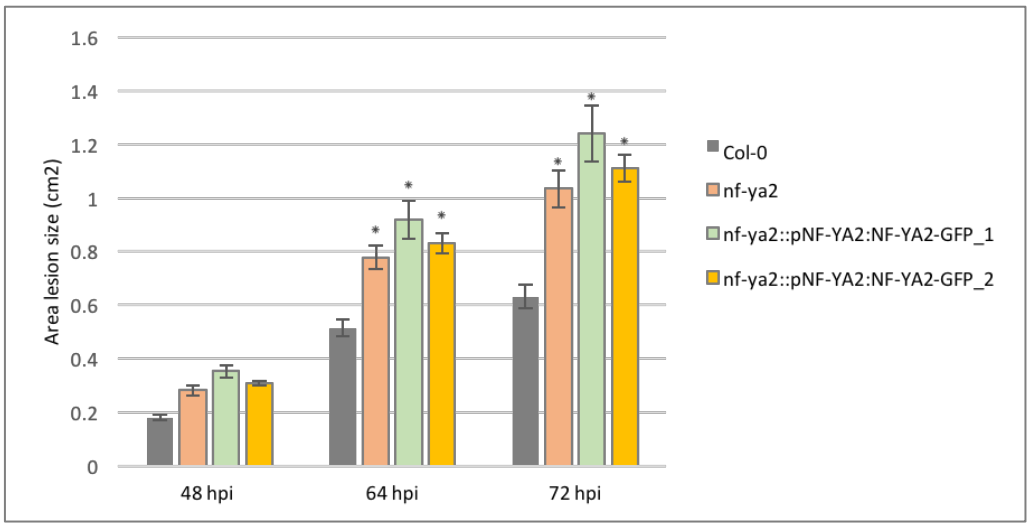

a)

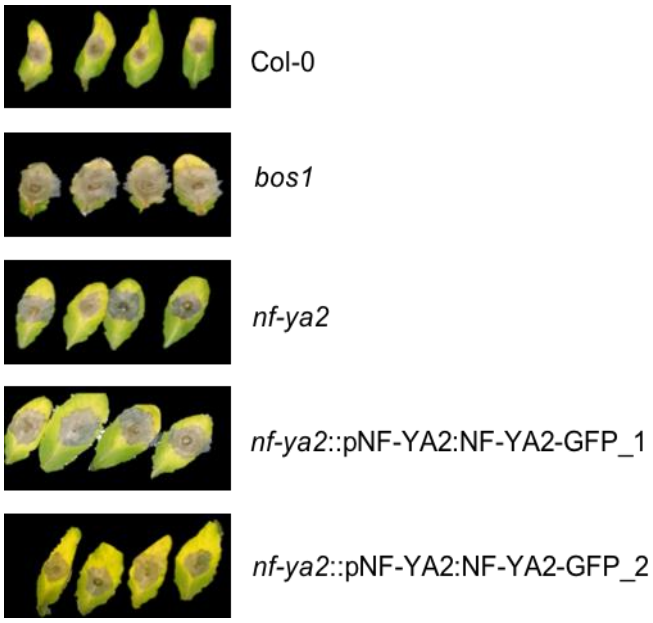

b)

Figure 3.14 - Susceptibility of *nf-ya2*::pNF-YA2:NF-YA2-GFP lines to *Botrytis cinerea* infection. Detached leaves from five weeks old Arabidopsis plants *nf-ya2*::pNF-YA2:NF-YA2-GFP_1, *nf-ya2*::pNF-YA2:NF-YA2-GFP_2, Col-0 and *bos1* were drop inoculated with *B. cinerea* spores and lesion areas measures at 48, 64 and 72 hours post-inoculation (hpi). a) Mean lesion area, the values presented are the mean of 30 biological replicates (10 plants each line were analyzed) ± SE. Significantly different lesion sizes to Col-0 (indicated by *) at each timepoint were determined using a two-tailed Student's T-test assuming equal variance ($p<0.05$). Experiment was performed twice. b) Representative leaf images at 72 hours post infection are shown. Col-0 and *bos1* were used as controls.

The *B. cinerea* assay was also performed on *nf-yb2* KO mutant, this line showed the same level of susceptibility as Col-0 during the infection at all time points (Figure 3.15). Meanwhile, the *nf-yb3* KO mutant showed slightly enhanced (but not significantly so) resistance to *Botrytis* at all three time points post inoculation. Interestingly the *nf-yb2/nf-yb3* double mutant was significantly more resistant to *B. cinerea* infection than Col-0 and *nf-yb2*. This result indicates an overlapping functionality between NF-YB2 and NF-YB3 since to get altered resistance both NF-YB2 and NF-YB3 genes need to be knocked out. In support of this result, it has been previously reported that NF-YB2 have an high protein sequence homology with NF-YB3 (Siefers et al. 2009).

Additionally, all NF-YB2 OE lines, which have *nf-yb2* as the genetic background, were more resistant than Col-0 and *nf-yb2* during *B. cinerea* infection at all time points. This result is visible in Figure 3.16, indeed the lesion size is considerably smaller than Col-0 and *nf-yb2*, and only *nf-yb2*::35S:FLAG-NF-YB2_1 showed no significant difference. The expression of NF-YB2 in *nf-yb2*::35S:FLAG-NF-YB2 and *nf-yb2*::35S:GFP-NF-YB2 lines was checked using western blot analysis (Figure 3.17).

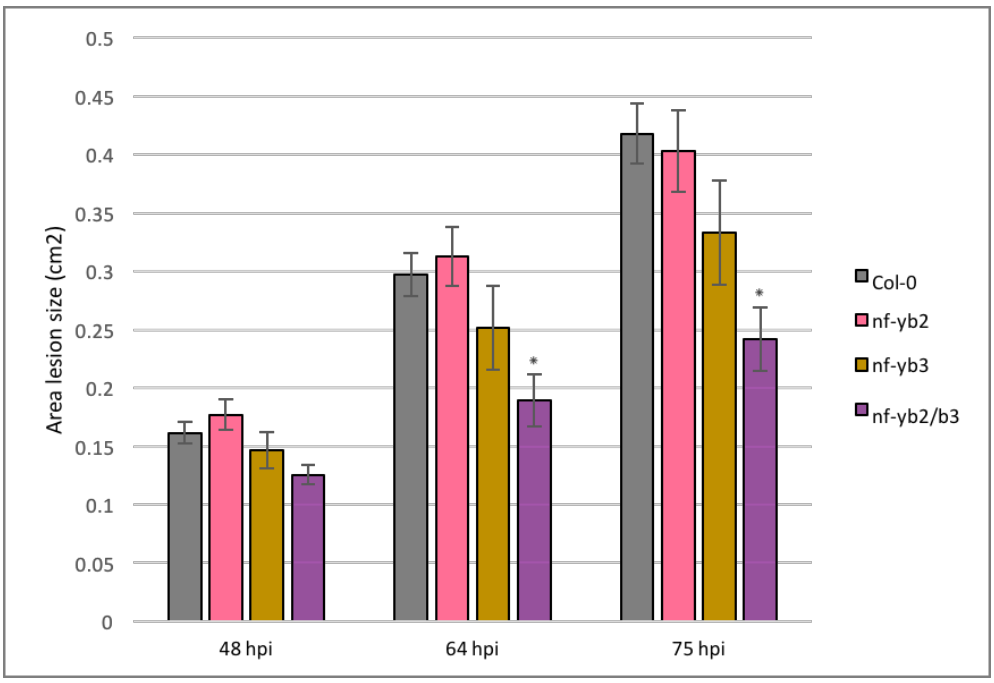

a)

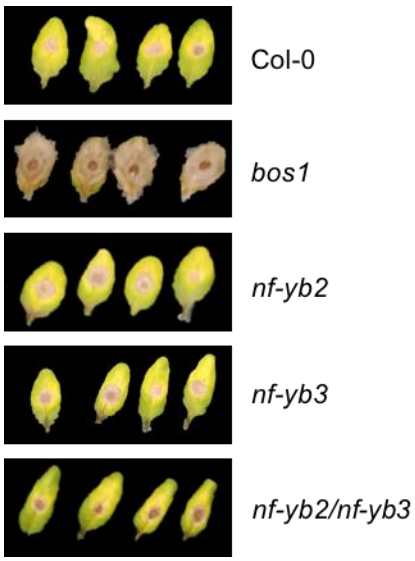

b)

Figure 3.15 - Susceptibility of *nf-yb2, nf-yb3* and *nf-yb2/nf-yb3* KO mutants to *Botrytis cinerea* infection. Detached leaves from five weeks old Arabidopsis plants *nf-yb2*, *nf-yb3* and *nf-yb2/nf-yb3*, Col-0 and *bos1* were drop inoculated with *B. cinerea* spores and lesion areas measures at 48, 64 and 72 hours post-inoculation (hpi). a) Mean lesion area, the values presented are the mean of 30 biological replicates (10 plants each line were analyzed) ± SE. Significantly different lesion sizes (indicated by *) at each timepoint were determined using a two-tailed Student's T-test assuming equal variance ($p<0.05$). Experiment was performed twice. b) Representative leaf images at 72 hours post infection are shown. Col-0 and *bos1* were used as controls.

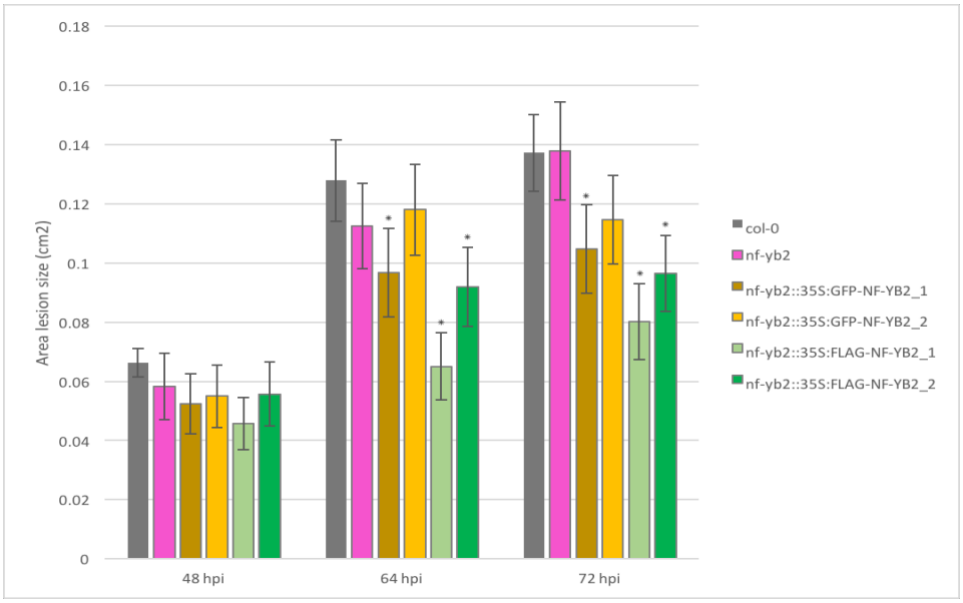

a)

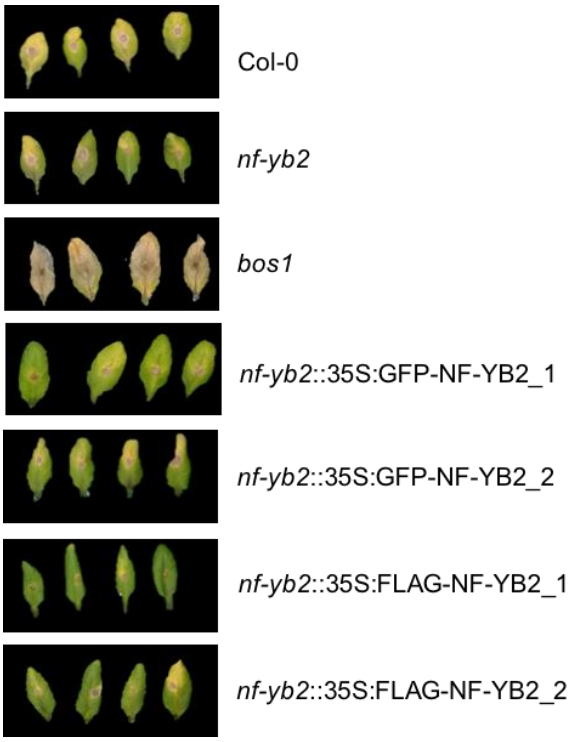

b)

Figure 3.16 - Susceptibility of NF-YB2 OE mutants to *Botrytis cinerea* infection. Detached leaves from five weeks old Arabidopsis plants *nf-yb2*::35S:GFP-NF-YB2_1, *nf-yb2*::35S:GFP-NF-YB2_2, *nf-yb2*::35S:FLAG-NF-YB2_1, *nf-yb2*::35S:FLAG-NF-YB2_2, *nf-yb2*, Col-0 and *bos1* were drop inoculated with *B. cinerea* spores and lesion areas measures at 48, 64 and 72 hours post-inoculation (hpi). a) Mean lesion area, the values presented are the mean of 30 biological replicates (10 plants each line were analyzed) ± SE. Significantly different lesion sizes (*) at each timepoint were determined using a two-tailed Student's T-test assuming equal variance ($p<0.05$). Experiment was performed twice. b) Representative leaf images at 72 hours post infection are shown. Col-0 and *bos1* were used as controls.

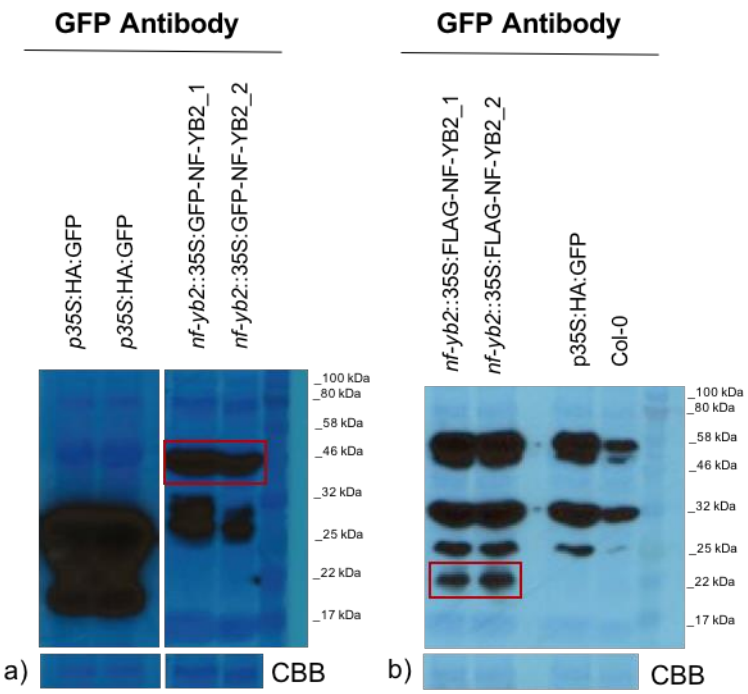

Figure 3.17 - Western blot analysis to check NF-YB2 OE lines. a) Total protein from *nf-yb2*::35S:GFP-NF-YB2_1 and *nf-yb2*::35S:GFP-NF-YB2_2 lines was extracted. Proteins were separated by SDS-PAGE and GFP-HRP antibody was used for immunoblotting. p35S:HA:GFP was used as positive control. GFP band (27 kDa) is visible in all samples. p35S:HA:GFP lines show a smaller band representing a cleaved product. The red square indicates the band corresponding to GFP-NF-YB2 protein (47 kDa). b) Total protein from *nf-yb2*::35S:FLAG-NF-YB2_1 and *nf-yb2*::35S:FLAG-NF-YB2_2 lines was extracted. Proteins were separated by SDS-PAGE and FLAG-HRP antibody was used for immunoblotting. Col-0 and p35S:HA:GFP were used as negative controls. The red square indicates the band corresponding to FLAG-NF-YB2 protein (20 kDa). Other bands in the gel are unspecific bands. Blots are representative of three experiments.

Based on the putative trimer (NF-YA2/NF-YB2/NF-YC2), NF-YC2 KO and OE mutants were also tested during *B. cinerea* infection, to check altered susceptibility. The OE lines, Col-0::35S:NF-YC2-GFP_1 and Col-0::35S:NF-YC2-GFP_3, were slightly more resistant than Col-0 to *Botrytis* at all three time points post inoculation (Figure 3.18). However, only Col-0::35S:NF-YC2-GFP_3 showed to be significantly different. On the other hand, *nf-yc2* KO mutant revealed to be considerably more susceptible than Col-0. The protein expression of these OE lines was checked by Emily Breeze (Breeze Emily 2014) and in following analysis performed in this study (Chapter 5). This similar phenotype between Col-0::35S:NF-YC2-GFP_1 and Col-0 suggests that the expression level of NF-YC2 did not increased considerably in this line to show a significantly altered

susceptibility. However, the enhanced susceptibility of *nf-yc2* could suggest an important role of NF-YC2 during the infection.

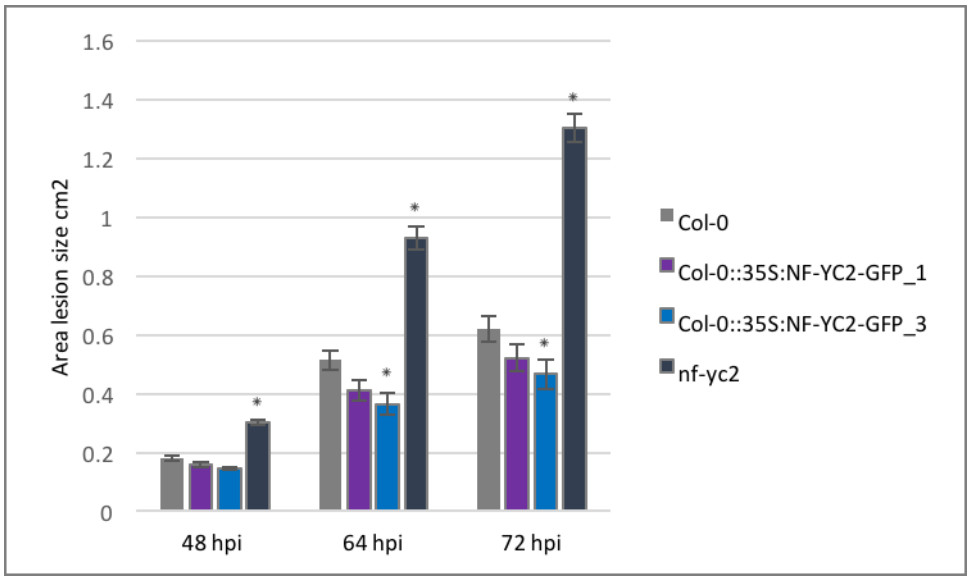

a)

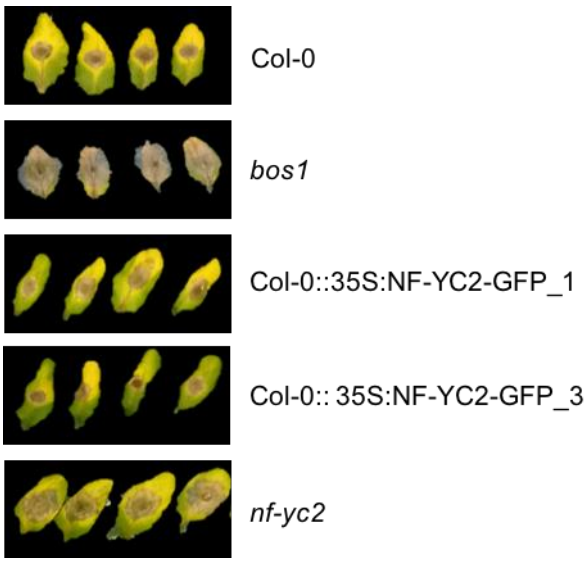

b)

Figure 3.18 - Susceptibility of NF-YC2 OE and KO mutants to *Botrytis cinerea* infection. Detached leaves from five weeks old Arabidopsis plants Col-0::35S:NF-YC2-GFP_1, Col-0::35S:NF-YC2-GFP_3, *nf-yc2*, Col-0 and *bos1* were drop inoculated with *B. cinerea* spores and lesion areas measures at 48, 64 and 72 hours post-inoculation (hpi). a) Mean lesion area, the values presented are the mean of 30 biological replicates (10 plants each line were analyzed) ± SE. Significantly different lesion sizes (indicated by *) at each timepoint were determined using a two-tailed Student's T-test assuming equal variance ($p<0.05$). Experiment was performed twice. b) Representative leaf images at 72 hours post infection are shown. Col-0 and *bos1* were used as controls.

3.3.4 *Hyaloperonospora arabidopsidis* (*Hpa*) susceptibility of Arabidopsis NF-Y KO and OE lines.

According to their lifestyles plant pathogens are often divided into biotrophs, which derive energy from living cells and necrotrophs**,** which derive energy from killed cells. Because biotrophic pathogens do not kill host plants while necrotrophic pathogens kill plant tissue rapidly, the defense response mechanism against these pathogens is very different. Indeed, in biotrophic pathogens it is largely due to programmed cell death in the plant, associated with the activation of defense responses regulated by the salicylic acid-dependent pathway. Meanwhile since necrotrophic pathogens benefit from death of host cells, they are not limited by this defense mechanism, but by responses activated by jasmonate acid and ethylene signaling pathways (Glazebrook 2005).

To elucidate the role of NF-Y subunits in the plant defense response against a biotrophic pathogen, susceptibility to *Hyaloperonospora arabidopsidis* (*Hpa*) was also tested in Arabidopsis plants constitutively overexpressing NF-Y genes or with NF-Y subunits knocked out. This oomycete is a model pathogen (Coates and Beynon 2010) which requires host tissue to be living in order to obtain nutrients. Specifically, *Hpa* spores of isolate Noks1 were sprayed on two weeks old Arabidopsis seedlings. Col-0 was used as control, in order to see whether basal defense responses were compromised and 35S::HaRxL14 was used as a positive control for enhanced susceptibility. The line 35S::HaRxL14 is *A. thaliana* ecotype Col-0 transformed with 35S::HaRxL14, which has consistently shown enhanced susceptibility and is therefore used as a positive control (Fabro et al. 2011). Sporangiophores were counted 4 days post infection using a dissecting microscope.

The *Hpa* assay on Arabidopsis NF-Y KO lines showed that *nf-ya2, nf-yb2, nf-yb3* and *nf-yc2* KO mutants were not significantly more reistant to *Hpa* than Col-0 (Figure 3.19). However, the *nf-yb2/nf-yb3* double mutant was significantly more susceptible to *Hpa* than wild type plants. This result is comparable with what was

observed during *B. cinerea* assay, and it reinforces the hypothesis of overlapping function between NF-YB2 and NF-YB3, since these subunits are very similar, sharing 94% amino acid identity in their conserved domains (Siefers et al. 2009). The high susceptibility of the positive control 35S::HaRxL14 compared to the wild type (Col-0) confirmed the reliability of this experiment.

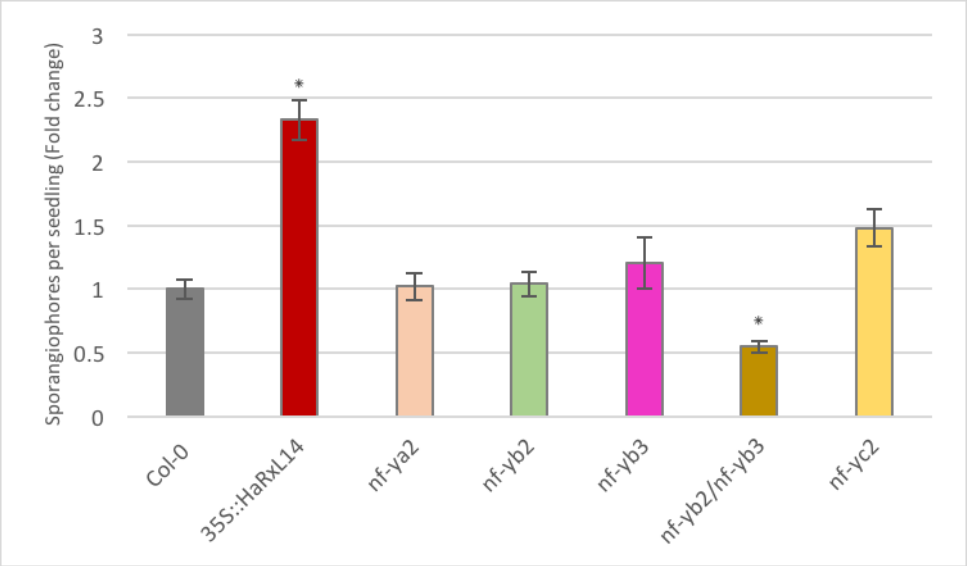

Figure 3.19 – NF-Y KO mutants do not show altered susceptibility to *Hpa.* *Hyaloperonospora Arabidopsidis* spores of isolate Noks1 were sprayed on two weeks old Arabidopsis NF-Y KO seedlings (*nf-ya2*, *nf-yb2*, *nf-yb3*, *nf-yc2* and *nf-yb2/nf-yb3*). Col-0 and 35S::HaRxL14 were used as control. Sporangiophores were counted 4 days post infection using a dissecting microscope. The values presented are the mean of sporangiophore per seedlings (45 biological replicates) normalized to Col-0. Error bars show standard error and significant differences to Col-0 using a T-test are indicated with * ($p<0.05$). The experiment was performed twice.

The *Hpa* assay on Arabidopsis *nf-ya2*::35S:FLAG-NF-YA2_1 (*nf-ya2* background plant) and Col-0::35S:FLAG-NF-YA2_1 (Col-0 background plant) lines where NF-YA2 is constitutively over expressed, did not show any significant difference in susceptibility to *Hpa* compared to wild type plants (Figure 3.20). This result, together with no difference observed in *nf-ya2*, could indicate that NF-YA2 gene is not involved in the defense response against biotrophic pathogens such as *Hpa.*

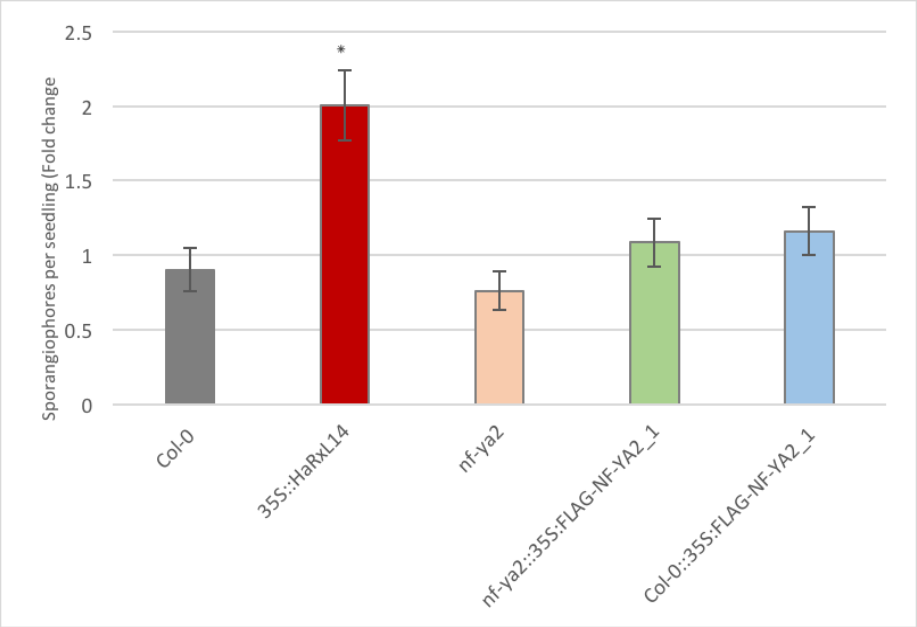

Figure 3.20 – NF-YA2 KO and OE mutants do not show altered susceptibility to *Hpa*. *Hyaloperonospora Arabidopsidis* spores of isolate Noks1 were sprayed on two weeks old Arabidopsis *nf-ya2*::35S:FLAG-NF-YA2_1 and Col-0::35S:FLAG-NF-YA2_1. *nf-ya2*, Col-0 and 35S::HaRxL14 were used as control. Sporangiophores were counted 4 days post infection using a dissecting microscope. The values presented are the mean of sporangiophore per seedlings (45 biological replicates) normalized to Col-0. Error bars show standard error and significant differences to Col-0 using a T-test are indicate with * ($p<0.05$). The experiment was performed twice.

Arabidopsis *nf-yb2*::35S:GFP-NF-YB2_1 and *nf-yb2*::35S:FLAG-NF-YB2_1 (*nf-yb2* background plant) lines overexpressing NF-YB2 gene, showed an enhanced resistance to *Hpa* infection compared to wild type plants, however only the *nf-yb2*::35S:GFP-NF-YB2_1 line was significantly different than Col-0 (Figure 3.21). This result, even if no difference was observed in *nf-yb2*, probably due to overlapping functionality between NF-YB subunits, could indicate that NF-YB2 is involved in the defense response against the biotrophic pathogen *Hpa.*

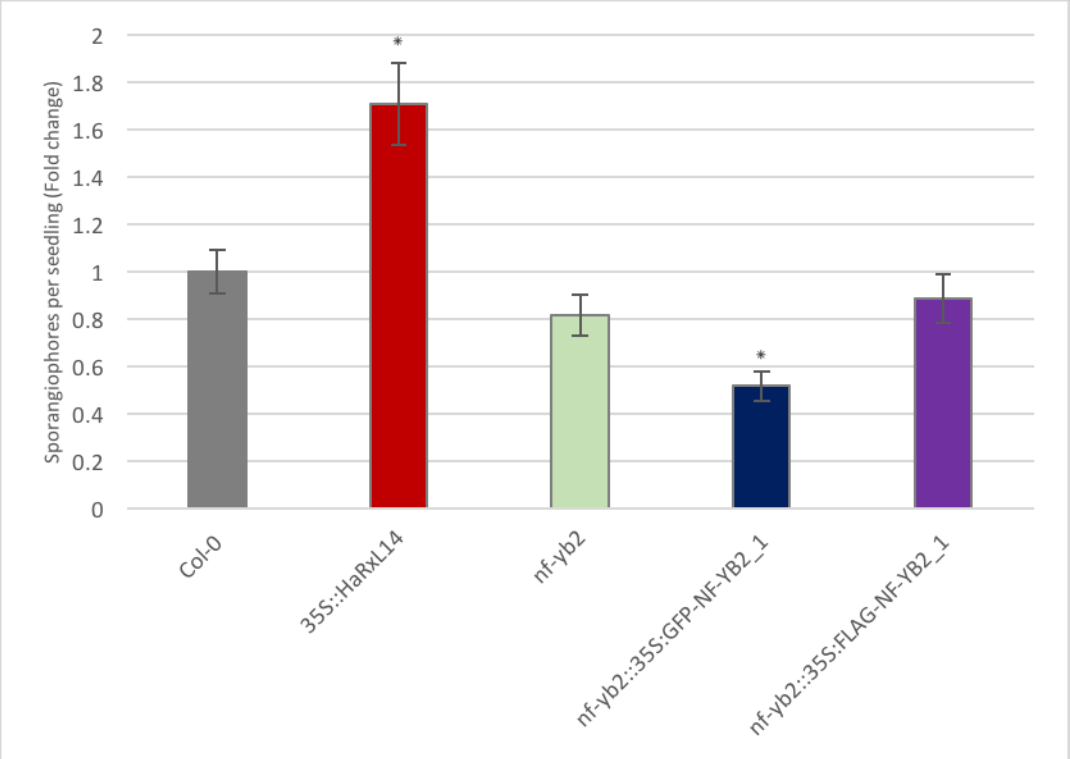

Figure 3.21 – NF-YB2 KO mutant does not show altered susceptibility to *Hpa*, while nf-yb2::35S:GFP-NF-YB2_1 mutant apperead to be more resistant. *Hyaloperonospora Arabidopsidis* spores of isolate Noks1 were sprayed on two weeks old Arabidopsis *nf-yb2*::35S:GFP-NF-YB2_1 and *nf-yb2*::35S:FLAG-NF-YB2_1. *nf-yb2*, Col-0 and 35S::HaRxL14 were used as control. Sporangiophores were counted 4 days post infection using a dissecting microscope. The values presented are the mean of sporangiophore per seedlings (45 biological replicates) normalized to Col-0. Error bars show standard error and significant differences to Col-0 using a T-test are indicate with * ($p<0.05$). The experiment was performed twice.

Also, no significant difference was observed on Arabidopsis Col-0::35S:NF-YC2-GFP_1 and Col-0::35S:NF-YC2-GFP_3 (Col-0 background plant) lines during the *Hpa* infection assay (Figure 3.22) compared to Col-0 plants. Hence, the number of sporangiophores per seedling was similar between Col-0 and the NF-YC2 OE lines. This result in combination with no difference detected in *nf-yc2*, suggests that NF-YC2 subunit is not involved in the defense response against this biotrophic pathogen.

However, having looked at these results, it is important to consider that there are 10 NF-Ys for each subfamily, which can have redundant functionality in plant, hence the phenotype observed could be caused by new protein interactions which occur when one subunit is missing or overexpressed.

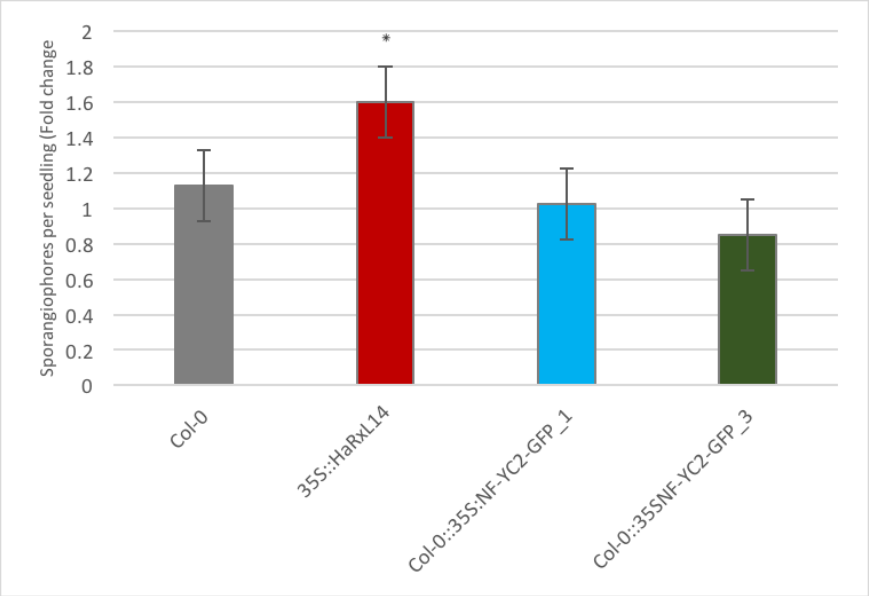

Figure 3.22 – NF-YC2 OE mutants do not show altered susceptibility to *Hpa*. *Hyaloperonospora Arabidopsidis* spores of isolate Noks1 were sprayed on two weeks old Arabidopsis Col-0::35S:NF-YC2-GFP_1 and Col-0::35S:NF-YC2-GFP_3. Col-0 and 35S::HaRxL14 were used as control. Sporangiophores were counted 4 days post infection using a dissecting microscope. The values presented are the mean of sporangiophore per seedlings (45 biological replicates) normalized to Col-0. Error bars show standard error and significant differences to Col-0 using a T-test are indicate with * ($p<0.05$). The experiment was performed twice.

3.3.5 *Pseudomonas syringae* susceptibility of Arabidopsis NF-Y KO and OE lines

A subset of NF-Y KO and OE mutants were screened by Dr's Rana Hussain and Susan Breen (Prof. Murray Grant group, University of Warwick) against the hemibiotrophic pathogen *Pseudomonas syringae*. Differentially from necrotrophs and biothrophs pathogens, hemibiotrophs have an initial period of biothrophy followed by necrotrophy. Specifically, *P. syringae* lives both on the surface and in the apoplast of the plant and to thrive in its host it overcomes the plant immune response (Block and Alfano 2011).

The aim here was to check the susceptibility of NF-Y KO and OE lines against *P. syringae* to determine whether these TFs were important in the plant defense response against this hemibiotrophic pathogen. Hence for the phenotyping, Arabidopsis mutants were infiltrated with *P. syringae* DC3000 suspensions and

then incubated in a growth chamber for 10 hours, at 21°C and 60% humidity. Images of plants were taken at 2, 3, 4 and 5 days post infection (dpi) and a scale of 0-5 was used to score the infection of the leaves (Figure 3.23a). The phenotype analysis, based on leaf visual, showed no difference in the disease severity between all lines, except *nf-ya2*::35S:FLAG-NF-YA2 lines that exhibited significantly enhanced tolerance against *P. syringae* after 4 and 5 days post infection (Figure 3.23b and Figure 3.23c).

Additionally, for the bacterial growth, three leaves per plant were infiltrated with *P. syringae* DC3000 and plants were incubated in a growth room for 10 hours, at 21°C. Samples were harvested at 4 dpi, homogenized in a tissue lyzer and serial dilutions were carried out. The colony counting showed no significant difference of bacterial growth between the KO and OE NF-Y mutants analyzed compared to Col-0. Hence, similar CFU were observed in all lines (Figure 3.24).

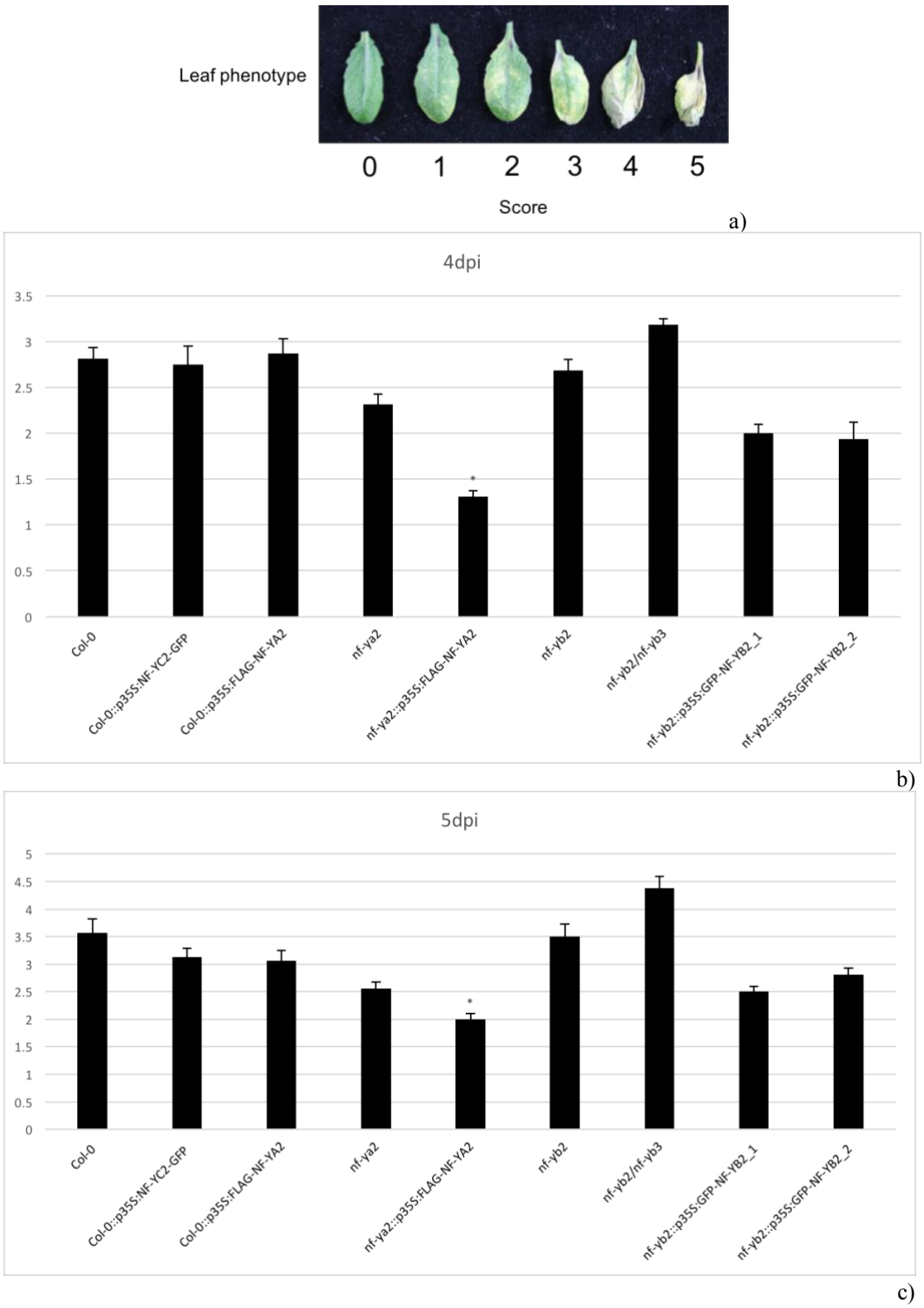

Figure 3.23 – Disease severity caused by *P. syringae* growth on Arabidopsis NF-Y KO and OE mutants. a) Scoring marker based on leaf phenotype after *P. syringae* infection. b-c) Col-0 was used as control. The disease phenotype was evaluated, based on leaf visual scoring after 4 and 5 days post infection. Error bars show standard error and significant differences to Col-0 using a T-test are indicated with * ($p<0.05$).

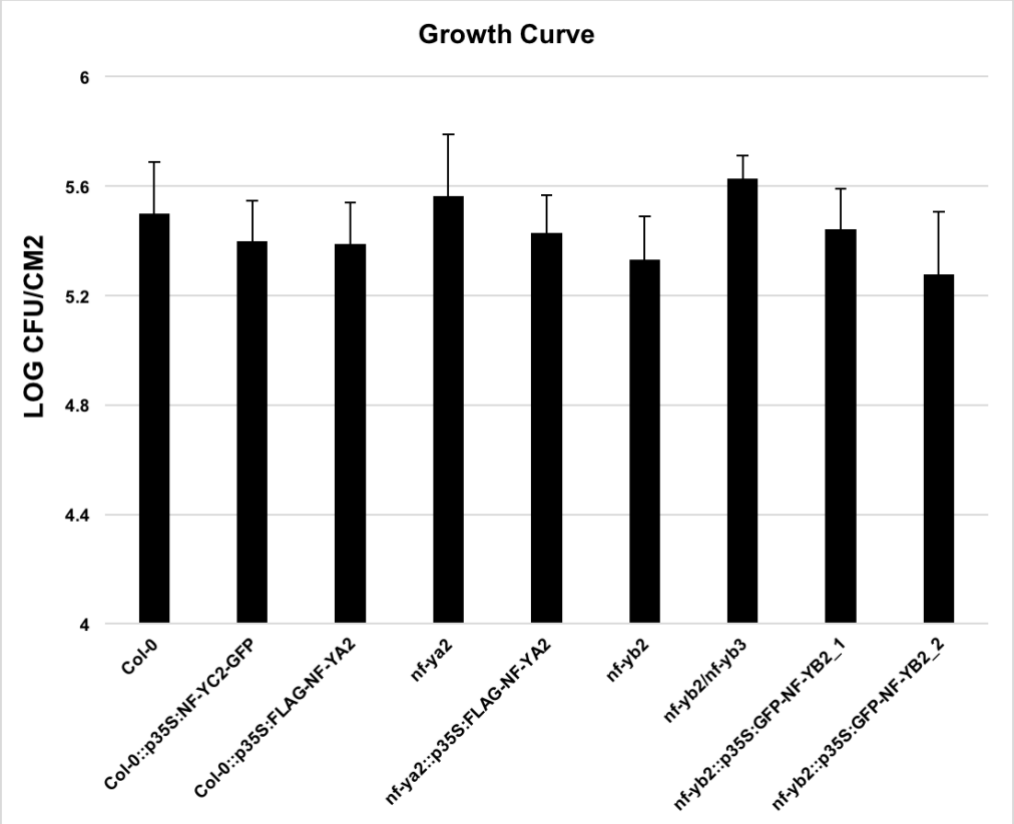

Figure 3.24 - Growth curve of *P. syringae* growth on Arabidopsis NF-Y KO and OE mutants. Col-0 was used as control. Colony counts taken sampled from 4 pooled leaves are shown using a logarithmic scale, error bars show standard error. No significant difference was observed between the treatments using a T-test (n=6).

On the base of these results it is possible to hypothesize that NF-Y subunits analyzed are not involved in the defense response against the hemibiotrophic pathogen *P. syringae*. However, this hypothesis is quite simplistic, hence it does not consider the possibility of an overlapping functionality between NF-Y subunits of the same family.

3.4 Discussion

3.4.1 Plant morphology of KO and OE NF-Y mutants did not show different phenotypes compared to wild type plants.

In this study, most of the Arabidopsis NF-Y KO and OE mutants analyzed presented a very similar morphology to wild type plants. Specifically, the phenotype of *nf-ya2*, *nf-yb2, nf-yc2* mutants and the double mutant *nf-yb2/nf-yb3* was comparable to Col-0 and only *nf-yb3* showed a bigger size. Meanwhile, between Arabidopsis plants expressing NF-YA2, NF-YB2 and NF-YC2 under the 35S promoter only *nf-ya2::*35S:FLAG-NF-YA2 lines, with *nf-ya2* as genetic background plant, were found to display an altered morphology, having a zig-zagged leafed phenotype and a smaller size (Figure 3.6).

However, the morphology of NF-YA2 OE lines generated in this study is not consistent with what was observed by Siriwardana et al. (2014), which demonstrates that overexpression of NF-YA in Arabidopsis caused severe growth retardation and developmental defects. A dwarf phenotype and a dark green color was also observed in Arabidopsis 35S:NF-YA2 seedlings and adult plants by Leyva-Gonzalez et al. (2012) compared to wild type, showing a significantly reduction of biomass (Leyva-Gonzalez et al. 2012). In contrast with these studies but in support of the results obtained in this chapter Zhang et al. (2017) found that NF-YA2 OE plants can generate more leaves than wild type plants with 24% increment of biomass. It was reported that leaf size is regulated by NF-YA2 and NF-YA10 in Arabidopsis, which are involved in leaf development through the auxin-signaling pathway, promoting leaf growth and cell expansion. Hence, NF-YA2 and NF-YA10 overexpression plants showed larger rosettes. Based on altered endogenous IAA content in NF-YA2 and NF-YA10 OE plants, it was discovered a differential accumulation of auxin signaling and it was found that the expression of YUCCA family genes was clearly different between transgenic plants and wild type plants. Specifically, YUC2, a key speed-limiting gene in auxin homeostasis, acts as a direct target of NF-YA2 and NF-YA10, hence overexpression

of NF-YA2 and NF-YA10 decreased contents of endogenous IAA through repressing the expression of *yuc2* (Zhang M. et al. 2017). Hence, the lower IAA contents in NF-YA2 OE mutants could result in an altered leaf initiation and growth in Arabidopsis. This could represent the main reason of the phenotype observed in this research, which appeared to be in contradiction with previous studies (Siriwardana et al. 2014, Leyva-Gonzalez et al. 2012). NF-YA2 OE lines generated were also validated using qPCR, which confirmed an enhanced expression of NF-YA2 gene in all lines. However, it is important to consider that there are many factors which could cause different morphology from wild type Col-0. For example, it is possible that sites of insertion of NF-YA2 construct into the genome may cause this phenotype, although this is unlikely since it is observed in all independently transformed lines. Additionally, environmental conditions can vary even between laboratories using the same equipment (Massonnet et al. 2010). Therefore, the similar phenotype between overexpressor mutants, knockout mutants and wild type plants, is likely due to gene functional redundancies with other members of the gene family, or, more simplistically, it could suggest a lack of involvement of these subunits in such traits. However, for pathogen assays this unchanged morphology between Col-0 and mutant lines is a good characteristic, since this allows susceptibility assay results which are not compromised by plant size differences.

Also, *nf-ya2*: pNF-YA2:NF-YA2-GFP lines were tested, showing a very low expression level of NF-YA2 gene. This expression pattern was similar to the background plant *nf-ya2* mutant, and consequently no differences in plant morphology were observed between *nf-ya2* KO mutants and *nf-ya2*:pNF-YA2:NF-YA2-GFP lines. This suggests that *nf-ya2* KO plants were not fully complemented with pNF-YA2:NF-YA2-GFP construct. According to the model hypothesized by Zanetti et al. (2017) showed in Figure 1.8, because NF-YA2 should be regulate at the transcriptional level by alternative splicing, providing fully spliced NF-YA mRNAs, would be a relatively simple method to increase the expression level of NF-YA2 in *nf-ya2*:pNF-YA2:NF-YA2-GFP lines. Indeed, the fully spliced NF-YA

mRNAs is the only one recruited by the translational machinery which synthetize NF-YA2 subunit, and then it is translocated into the nucleus to form a specific hetero trimer with NF-YB and NF-YC subunits. Additionally, knocking out miR169, a micro-RNA which inhibit the expression of NF-YA subunits, could be another strategy to enhance the level of NF-YA in these lines.

3.4.2 NF-Y functional redundancy in development and immunity.

When an expected phenotype is not observed in the absence of a specific gene there is the possibility that the biochemical function is redundantly encoded by two or more genes. Many studies have reported the redundant roles between NF-Y belonging the same subfamily during plant development. For example Mu et al. (2013) showed that strong phenotype was visible such as hypersensitivity to abscisic acid (ABA) during seed germination, retarded seedling growth and late flowering at different degrees. Moreover, Fornari et al (2013) reported that the closely related NF-YA3 and NF-YA8 are functionally redundant genes required in early embryogenesis. In fact, *nf-ya3* and *nf-ya8* single mutants do not display any obvious phenotypic alteration, whereas *nf-ya3/ nf-ya8* double mutants are embryo lethal. Additionally, Cao et al. (2011) and Kumimoto et al. (2008) revealed that NF-YB2 and NF-YB3 have an overlapping functionality during photoperiod-dependent flowering. A following study performed by Kumimoto et al. (2010) provided also evidence that *NF–YC3*, *NF–YC4* and *NF–YC9* are additively necessary for the proper photoperiod-dependent induction of flowering in Arabidopsis.

Hence, while some literature is available on the possible genetic redundancy between NF-Y members during plant development, much less evidence has been obtained regarding their functional redundancy in plant immunity. However, there is a substantial difference between plant development and plant immunity response. In the first one the level of a specific TF is not altered, since in

physiological condition the plant use the amount of TF available in the cell. In the second one, after a pathogen attack, the plant stress response is controlled by a complex regulatory system, involving a transcriptional gene reprogramming which alter the level of TFs in the plant cell. For this reason, identify a real overlapping functionality between TFs belonging the same family during the plant defense response is quite challenging.

In the specific case of NF-Y TFs, it is possible to hypothesize that when the plant is attacked by the pathogen the level of a specific TF change to subsequently regulate the expression of a target defense gene. Hence, the functional redundancy hypothesized in this study between NF-YB2 and NF-YB3, based on the lack of expected phenotype during *B. cinerea* infection in *nf-yb2* and *nf-yb3* single mutant, but observed in *nf-yb2/nf-yb3* double mutant, is debatable. However, previous microarray analysis performed by Windram et al. (2012) revealed that the amount of both NF-Y members in wild type plants before and after the infection is altered, suggesting a role in the plant defense response.

3.4.3 Pathogen infection assays revealed potentially important NF-Y subunits in the defense response.

To establish whether NF-YA2, NF-YB2 and NF-YC2 TFs play a role in the defense response, the first step was to investigate whether Arabidopsis KO and OE mutants of these NF-Y subunits have an altered susceptibility against the necrotrophic pathogen *Botrytis cinerea,* the biotrophic pathogen *Hyaloperonospora arabidopsidis* and the hemibiotrophic pathogen *Pseudomonas syringae*.

In this study, it was observed that significantly different phenotypes in NF-Y KO and OE mutants were observed in response to *B. cinerea* infection, while, generally, the susceptibility against *Hpa* and *P. syringae* was found to not to be compromised. Specifically, in this chapter it has been shown that *nf-ya2* KO mutants showed a significantly enhanced susceptibility to *B. cinerea,* confirming previous observation in Emily Breeze's thesis (2014). Interestingly, both NF-YA2

OE lines with *nf-ya2* as the genetic background showed a more resistant phenotype compared to Col-0 and the *nf-ya2* mutant, while NF-YA2 OE lines with Col-0 as background plant showed the same phenotype as the *nf-ya2* KO mutant. This result highlights the possibility that the overexpression of a single NF-Y subunit could alter the stoichiometry ratio compromising the formation of canonical NF-Y complexes. Hence, unknown interaction between NF-Y can interfere with plant susceptibility, giving unexpected phenotypes. The high susceptibility of *nf-ya2* observed here is consistent with the inability of *nf-ya2* mutant to synthesize JA during senescence, showing reduced endogenous JA levels, and changes in expression of several JA biosynthetic genes (Breeze et al. in preparation).

Moreover, a previous study reported that in NF-YA2 OE lines the concentration of IAA was decreased by 20% compared to wild type plants (Zhang M. et al. 2017) and according to Llorente et al. (2008) this repression of auxin signaling could compromise the resistance of Arabidopsis plants to the necrotrophic fungal pathogen *B. cinerea* (Llorente et al. 2008). In the context of this knowledge, this experiment suggests that NF-YA2 could be a key regulator in the defense response. This result is coherent with Leyva-Gonzalez et al. (2012) report which proposed a model where NF-YA subunit control a general stress response. Hence, it was found that NF-YA2 OE plants showed a delayed senescence and increased tolerance to different abiotic stresses, and it was also revealed that transcript levels of NF-YAs are induced by different stress conditions (Leyva-Gonzalez et al. 2012). Furthermore, during *Hpa* and *P. syringae* infection NF-YA2 OE and KO mutants did not show any altered susceptibility compared to Col-0, this result suggests the possibility that NF-YA2 TF play an exclusive role during the plant defense response against *B. cinerea* infection or in general against necrotrophic pathogens. However, to confirm this, further analysis using different necrotrophs are necessary.

Moreover, it has been shown here that the Arabidopsis *nf-yb2* mutant did not have altered susceptibility against *B. cinerea*, *Hpa* and *P. syringae* compared to

wild type plants. However, because the *nf-yb2/nf-yb3* double mutant was shown to have a significantly enhanced resistant phenotype compared to Col-0 during the infection by the necrotrophic pathogen *B. cinerea* and the biotrophic pathogen *Hpa*, it was hypothesized that there is an overlapping functionality between NF-YB3 and NF-YB2. Hence only when both subunits are absent it is possible to observe an altered phenotype during the infection with these pathogens compared to Col-0. In support to this theory, microarray data-set (Windram et al. 2012) showed that NF-YB2 and NF-YB3 have also the same gene expression pattern during *B. cinerea* and *P. syringae* infection, hence both genes are down-regulated. This hypothesis is consistent with previous report showing that *NF-YB2* and *NF-YB3* are redundant players in photoperiod-dependent flowering (Cao et al. 2011). Additionally, Siefers et al. (2009) found that NF-YB2 and NF-YB3 are very similar proteins with very high amino acid identity in their conserved domains.

Intriguingly, NF-YB2 OE lines also showed a more resistant phenotype compared to Col-0 and *nf-yb2* during *B. cinerea* and *Hpa* infection. This result suggests that also NF-YB2 is involved in the defense response. Hence, the overexpression of NF-YB2 allowed to overcome gene redundant function between NF-YB subunits, showing an enhanced resistance during the infection. For this reason, an altered phenotype is visible only in NF-YB2 OE mutant and not in the *nf-yb2* KO mutant, where it is probably masked by gene overlapping functionality.

B. cinerea, *Hpa* and *P. syringae* assays were also performed on NF-YC2 OE and KO mutants. This experiment showed no strong difference in pathogen susceptibility of NF-YC2 OE lines. However, *nf-yc2* KO mutant showed a significantly enhanced susceptibility against *B. cinerea* infection and a slightly enhanced *Hpa* growth, but not significant. This result could be explained by the involvement of NF-YC2 subunit in the plant defense, but further analysis need to be carried out.

According to these results and based on Leyva Gonzalez et al. (2012) model, it is possible to hypothesized that in wild type plants growing under non-stress conditions the expression of NF-YA2 is low due miR169-mediated post-

transcriptional down-regulation. Upon exposure to a necrotrophic pathogen, such as *B. cinerea*, NF-YA2 level increase due to the transcriptional activation of NF-YA2 expression and to the repression of miR169. NF-YA2 then activate defense genes involved in the plant immunity forming a complex with NF-YB2 and NF-YC2 subunits.

3.4.4 Conclusion

In conclusion, these results highlight the possibility of an important role of NF-YA2 and NF-YB2 and NF-YC2 in the plant defense response against the necrotrophic pathogen *B. cinerea*. However, the biotrophic pathogen *Hpa* and the hemibitrophic *P. syringae* assay did not show any significantly different phenotype of NF-Y mutants compared to wild type, despite previously reported microarray data (Windram et al. 2012) showing that NF-YA2, NF-YB2 and NF-YC2 were downregulated during *P. syringae* infection. However, it is important to consider that after pathogen recognition plants initiate an intricate and highly regulated network of defense mechanisms which caused extensive changes to the host transcriptome (Jones and Dangl 2006). Interestingly each mechanism is specific to different pathogens. Hence the plant defense response against necrotrophic, biotrophic, and hemibitrophic pathogens involve a distinctive pathway. For this reason, the lack of interesting phenotypes obtained in this study appears to be likely. Also, the compensatory abilities among TF families, which have been frequently reported in the literature (Jin H. and Martin 1999), represents the challenge of this research. Indeed, often the phenotype observed is due to functional redundancies with other members of the gene family. However, it is also possible that overexpression of individual NF-Y subunits generates a negative effect changing the accessibility of a subunit in the plant, affecting the stoichiometry and preventing the formation of native NF-Y complexes. Additional data, such as identification of *in vivo* physical interactions using mass spectrometry analysis or transient experiment such as BiFC and BiCAP, will be necessary to draw strong conclusions. For this purpose, in this study many

precious resources such as NF-Y-overexpressing Arabidopsis GFP or FLAG tagged lines have been generated.

Chapter 4

4. Identify protein-protein interactions between NF-YA2, NF-YB2 and NF-YC2 subunits transiently expressed in *N. benthamiana*.

4.1 Introduction

Nowadays several techniques are available to investigate protein-protein interactions *in vitro* and *in vivo,* which used in combination with a reverse genetic approach, will facilitate elucidating the role of NF-Y complexes.

Yeast two-hybrid (Y2H) (Fields and Song 1989, Walhout and Vidal 2001), represents probably the most widely used method to study protein–protein interactions (Bruckner et al. 2009), and has considerably simplified protein-protein complex identification. This assay allows the detection of interacting proteins in yeast, relying on the expression of a reporter gene (such as lacZ or HIS3), which is activated when the two proteins of interest interact together, allowing the yeast colonies to grow on a selective medium or driving a color change. However, as stated in Bruckner et al. 2009 there are many limits of Y2H technology. Firstly, proteins that are toxic to yeast cell cannot be studied using this technology. Secondly, this method is often associated with the presence of many false positive, because of proteins that are able to interact in yeast are not always able to interact in plants due to post translational modification or different cell compartment localization. Thirdly, false negative interactions are common, because this assay is able to detect pairs combination which occur only in the nucleus of the yeast cell, making interactions that happen in different cell compartments, difficult to be detected (Zhang Y. et al. 2010). Considering these limits, it is crucial to complement the Y2H analysis using other approaches *in vivo* such as Bimolecular fluorescence complementation (BiFC) assay, co-immunoprecipitation (Co-IP) and mass spectrometry (MS).

BiFC can be used to validate protein interactions pairwise *in planta* (Bracha-Drori et al. 2004, Kerppola 2008). This assay is based on reassembly of two fragments of the YFP fluorescent protein, also called Venus protein, that are fused in-frame to two different test proteins (Figure 4.1). These constructs are agro-infiltrated into *Nicotiana benthamiana* leaves, allowing the transient expression of the fusion proteins. When the two proteins interact, the two complementary fragments of YFP are brought together and the fluorescence can be detected simply by confocal microscope (Tian et al. 2011, Walter et al. 2004). The main advantage of the BiFC assay is that it is carried out in plants and highlights where in the cell the interaction occurs (Citovsky et al. 2008). However, this assay has a few disadvantages that need to be considered. First the interacting properties of protein fused with split YFP could be different from the native protein. Second if the two proteins are located in the same cell compartment, then high levels of expression may lead to fluorescence from close proximity of the two fragments rather than real protein-protein interaction. Third, auto-fluorescence of photosynthetic pigments of the plant cell often interfere with the YFP signal of the BiFC assay (Ohad et al. 2007).

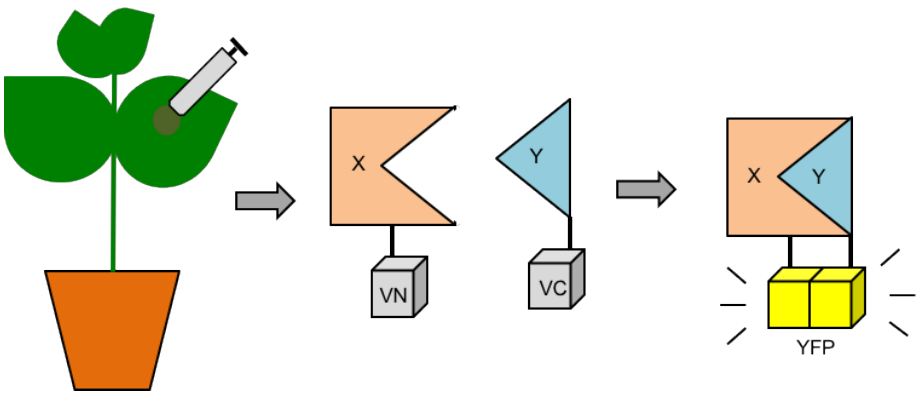

Figure 4.1 – The BiFC rationale. Schematic representation of two generic X and Y proteins fused respectively to non-fluorescent N-terminal (VN) and C-terminal (VC) fragments of the Venus (YFP) protein. If X and Y proteins interact, YFP reconstitutes and fluoresces.

In this chapter, the BiFC assay was associated with a novel method, called bimolecular complementation affinity purification (BiCAP) (Croucher et al. 2016), to characterize protein complexes in agro-infiltrated *N. benthamiana* leaves. This new technique, previously used in animal cells, exploits a neo-epitope produced by complementation of YFP protein fragments to isolate the two interacting proteins. In fact, when the two proteins are brought together using BiFC method, YFP refolds and fluoresces. Specifically, anti-GFP agarose beads (Kubala et al. 2010) recognizes a three-dimensional epitope on the β barrel of the GFP protein, which is composed by the two YFP fragments. This suggests that anti-GFP agarose beads are able to detect a neoepitope that is present only in the refolded YFP but do not exist on the individual YFP fragments. Hence, it was hypothesized that GFP beads would only bind to recombined YFP but not to individual YFP fragments. This assay provides a powerful method to isolate protein complexes while excluding individual components and competing binding partners. A further advantage of this system is the ability to visualize protein interactions *in situ*, providing confirmation of cellular context. Moreover, BICAP method in combination with mass spectrometry analysis would allow to detect interactor proteins which are specific to the dimer complex and not just to a single protein as in the standard methodology. This ability represents an important advantage to functionally characterize specific complexes in different cellular context.

Finally, co-immunoprecipitation (Co-IP) is one of the most common techniques for identifying protein-protein interactions (Masters 2004). Co-IP is a method in which a protein complex can be isolated from a cell lysate using an immobilized antibody against a tag, such as GFP, HA or FLAG, fused to one component of the protein complex. Presence of the target protein is determined by western blot, while interacting proteins can be identified using an appropriate antibody or by MS analysis. The tagged target protein can be transiently expressed in plants, for example, by agro-infiltrating the construct of interest, or stably expressed in transgenic plants.

4.2 Chapter aims

In this chapter BiFC, BiCAP and Co-IP assays on transiently transformed *N. benthamiana* leaves were used to test the existence of the putative hetero trimer (NF-YA2, NF-YB2 and NF-YC2) in *planta*. Additionally, GFP tagged constructs containing NF-YA2, NF-YB2 and NF-YC2 under the 35S promoter were transiently expressed in *N. benthamiana* leaves to investigate their subcellular localization. This will shed light on the assembly mechanism between the three types of subunits and highlight if the mechanism is conserved between plants and animals.

4.3 Results

4.3.1 NF-Ys localization in *N. benthamiana*

To clarify proteins function it is important to identify their subcellular localization to test if the assembly of the trimer occurs as in mammals. NF-YA2, NF-YB2 and NF-YC2 were visualized in the plant cell using GFP fusion construct agro-infiltrated in *N. benthamiana* leaves. Confocal imaging analysis showed that NF-YA2 is localized exclusively in the nucleus of the transformed leaf cells. In contrast NF-YB2 and NF-YC2 are localized in the nucleus and in the cytoplasm (Figure 4.2). These results perfectly fit with previous studies which have proposed a specific regulatory mechanism of NF-Y in plant (Hackenberg et al. 2012, Laloum et al. 2013, Zhao et al. 2016). Specifically, NF-YB/NF-YC dimer assembles in the cytoplasm and then translocate into the nucleus where it can form an active trimer with NF-YA. The NF-YA/B/C complex then binds to CCAAT box in the promoter region to regulate the expression of the target gene (Zhao et al. 2016). This transcriptional regulation system is highly conserved in yeast, animals and plants and can be applied to the putative trimer NF-YA2/B2/C2 object of this study (Dolfini et al. 2012, Liu and Howell 2010, Petroni et al. 2012).

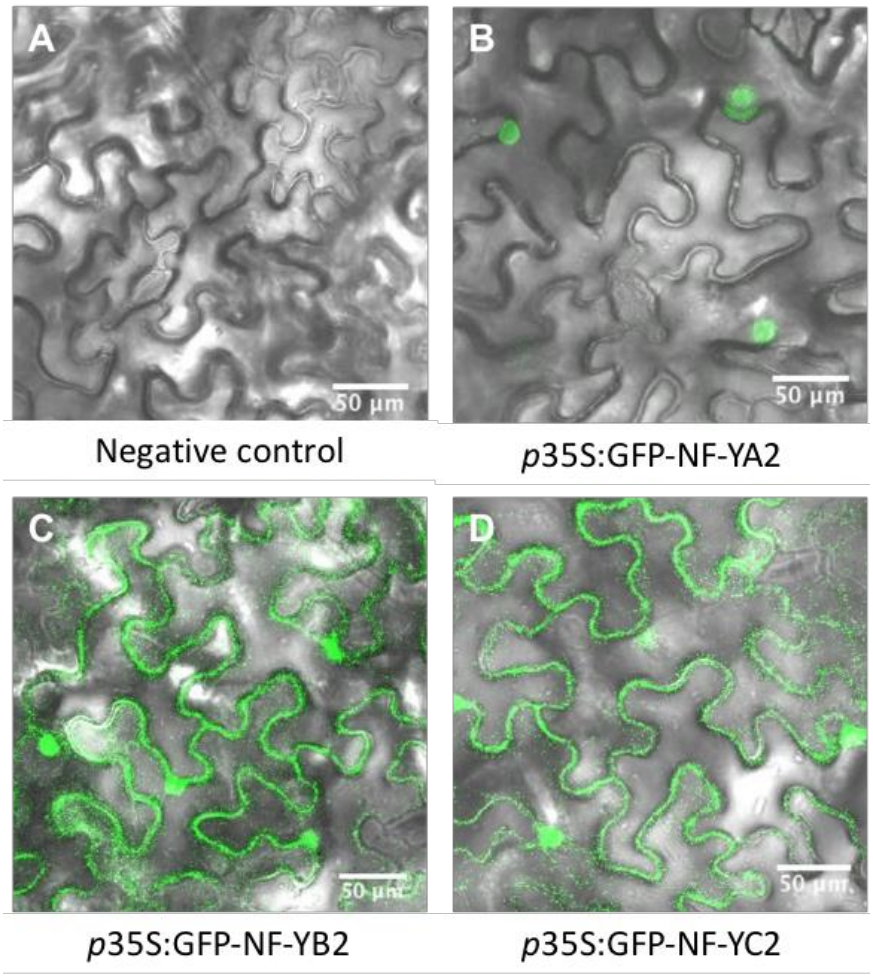

Figure 4.2 – Confocal fluorescence microscopy analysis of subcellular localization of NF-YA2, NF-YB2 and NF-YC2 fused with GFP in *N. benthamiana*. Panels display the merge image GFP + bright-field. Each *p*35S:GFP-NF-YA2, *p*35S:GFP-NF-YB2 and *p*35S:GFP-NF-YC2 construct was transferred into *A. tumefaciens* strain GV3101 and then infiltrated into *N. benthamiana* leaves. A) *N. benthamiana* leaves infiltrated with 35S:FLAG construct do not show any signal (Negative control) B) NF-YA2 is detected only in the cell nucleus. C-D) NF-YB2 and NF-YC2 are identified in nucleus and cytoplasm. Representative images from three independent experiments are shown. Scale bars, 50 µm.

4.3.2 BiFC assay to test the interaction between NF-YA2, NF-YB2 and NF-YC2 in plant.

Previous studies already tested all pair interaction between NF-Y TFs using Y2H analysis (Calvenzani et al. 2012, Hackenberg et al. 2012). These analyses showed that NF-YA2 can dimerize with NF-YC2 and NF-YC2 can dimerize with NF-YB2. The dimerization between NF-YB2 and NF-YC2 was also confirmed *in vivo* by Mass Spectrometry analysis performed on Arabidopsis NF-YC2 epitope tagged lines by Emily Breeze (thesis 2014). Following these results, BiFC method appears to be a good tool to validate the interaction between NF-YA2, NF-YB2 and NF-YC2 *in planta*.

4.3.2.1 Generation of BiFC constructs

The first step in testing pairwise interactions of NF-Y subunits is to generate clones for expression of NF-YA2, NF-YB2 and NF-YC2 fused to split YFP (E-YFP) protein. Since proteins can be tagged at either the N- or C- terminal, all pairwise combinations need to be tested because BiFC is a proximity based method and variation in resulting fusion protein structures can have repercussions on protein assembly (Kodama and Hu 2012). Hence, each NF-Y of interest (NF-YA2, NF-YB2 and NF-YC2) was cloned into four BiFC vectors, that rely on GATEWAY-cloning technology, to be able to test all possible combinations using different tag orientation (Figure 4.3).

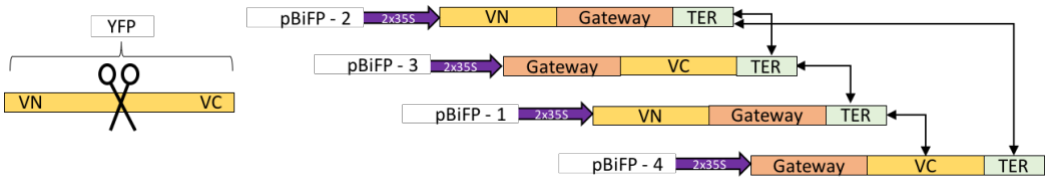

Figure 4.3 – Gateway compatible pBiFP destination vectors expressing N and C fragments of YFP fused to the interacting proteins. NF-YA2, NF-YB2 and NF-YC2 were cloned into all four vectors. Arrows show all possible pairwise combinations of the N and C fragments of YFP. (VN=N-terminal of the Venus protein; VC=C-terminal of the Venus protein).

GATEWAY compatible pBiFP (BiFC in Planta) vectors were used, kindly provided by Franois Parcy (University Grenoble, France). These vectors are based on the fluorescent protein Venus (YFP) (Nagai et al. 2002), under the CaMV35S-promoter which should lead to strong protein expression. Moreover, a set of NF-YA2, NF-YB2 and NF-YC2 FLAG-tagged and GFP-tagged constructs, again under the control of the CaMV35S promoter, were generated using Gateway binary vectors (Nakamura et al. 2010). All constructs were cloned from cDNA and sequenced. The FLAG tag is a short peptide consisting of 8 amino acids (DYKDDDDK), while the GFP tag and YFP, its genetic mutant, are proteins composed of 238 amino acids (26.9 kDa). Table 4.1 shows the size of each NF-YA2, NF-YB2 and NF-YC2 subunit in their native condition and with GFP, E-YFP and FLAG tag. These tags are recognized by several commercial antibodies and can be incorporated on either the N- or C-terminal of the protein. The small size of the FLAG tag minimizes its effect on protein function preserving protein folding, while GFP is a large tag which is extremely stable but can affect the solubility of the protein and interfere with protein folding and functionality.

Table 4.1 – Size of NF-Y proteins of interest with and without GFP, split YFP (E-YFP) and FLAG epitope tags

Protein	Protein length	Gene identifier	Size of native protein	Tag	Size of epitope tagged protein
NF-YA2	295 aa	AT3G05690	32.2 kDa	FLAG	32.2 kDa
NF-YA2	295 aa	AT3G05690	32.2 kDa	GFP	59.1 kDa
NF-YB2	190 aa	AT5G47640	20 kDa	FLAG	20 kDa
NF-YB2	190 aa	AT5G47640	20 kDa	GFP	46.9 kDa
NF-YC2	199 aa	AT1G56170	23.1 kDa	FLAG	23.1 kDa
NF-YC2	199 aa	AT1G56170	23.1 kDa	GFP	50 kDa
NF-YA2	295 aa	AT3G05690	32.2 kDa	E-YFP	45.7 kDa
NF-YB2	190 aa	AT5G47640	20 kDa	E-YFP	33.5 kDa
NF-YC2	199 aa	AT1G56170	23.1 kDa	E-YFP	36.6 kDa

4.3.2.2 Testing NF-Y subunit pairwise interaction

GATEWAY-BiFC binary vectors expressing NF-YA2, NF-YB2 and NF-YC2 cDNA were agro-infiltrated in different combinations into 4 weeks old *Nicotiana benthamiana* leaves. Equal concentrations of Agrobacterium containing each construct were mixed and infiltrated together (Leuzinger et al. 2013). All pairwise combinations between NF-YA2, NF-YB2 and NF-YC2 at N-terminal or C-terminal of the YFP were tested (Table 4.2). A strong BiFC signal was observed using confocal microscopy after three days post infection only in the p35S:YFP_N-NF-YB2 and p35S:NF-YC2-YFP_C combination. The fluorescence was detected in the cytoplasm and in the nucleus (Figure 4.4C and 4.4D). This localization reflects what has been observed in mammals (Romier et al. 2003) where NF-YB and NF-YC subunits dimerize in the cytoplasm and then translocate into the nucleus. This result is also compatible with previous Mass Spectrometry analysis on Arabidopsis Col-0::p35S:NF-YC2-GFP epitope tagged lines which showed that NF-YB2 and NF-YC2 interact *in vivo* (Breeze Emily 2014). Many controls were used to

validate the BiFC analysis, specifically p35S:NF-YB2 construct with no tag was agro-infiltrated as a negative control and no signal was detected (Figure 4.4A), while p35S:GFP was used as a positive control, showing a strong fluorescence signal in the nucleus and cytoplasm as expected (Figure 4.4B). Additionally, no fluorescence was observed when single constructs of p35S:YFP_N-NF-YB2 (Figure 4.4F) and p35S:NF-YC2-YFP_C (Figure 4.4E) were agro-infiltrated into the leaf, confirming that split YFP cannot fluoresce on its own. Hence the fluorescence detected when p35S:YFP_N-NF-YB2 and p35S:NF-YC2-YFP_C were co-infiltrated represents the re-assembly of the YFP molecule due to the interaction between the NF-YB2 and NF-YC2 proteins.

	p35S:YFP$_N$-NF-YA2	p35S:NF-YA2-YFP$_C$	p35S:YFP$_N$-NF-YB2	p35S:NF-YB2-YFP$_C$	p35S:YFP$_N$-NF-YC2	p35S:NF-YC2-YFP$_C$
p35S:YFP$_N$-NF-YA2				X		X
p35S:NF-YA2-YFP$_C$			X		X	
p35S:YFP$_N$-NF-YB2		X				X
p35S:NF-YB2-YFP$_C$	X				X	
p35S:YFP$_N$-NF-YC2		X		X		
p35S:NF-YC2-YFP$_C$	X		YFP			

Table 4.2 – Pairwise combinations of constructs tested with BiFC. Only BIFP2::NF-YB2 (p35S:YFP$_N$-NF-YB2) and BIFP4::NF-YC2 (p35S:NF-YC2-YFP$_C$) were able to interact in *N. benthamiana* (indicated as a yellow box in the table). X means no interaction. Gray boxes indicate combinations that were not tested because they contained constructs expressing the same half of YFP.

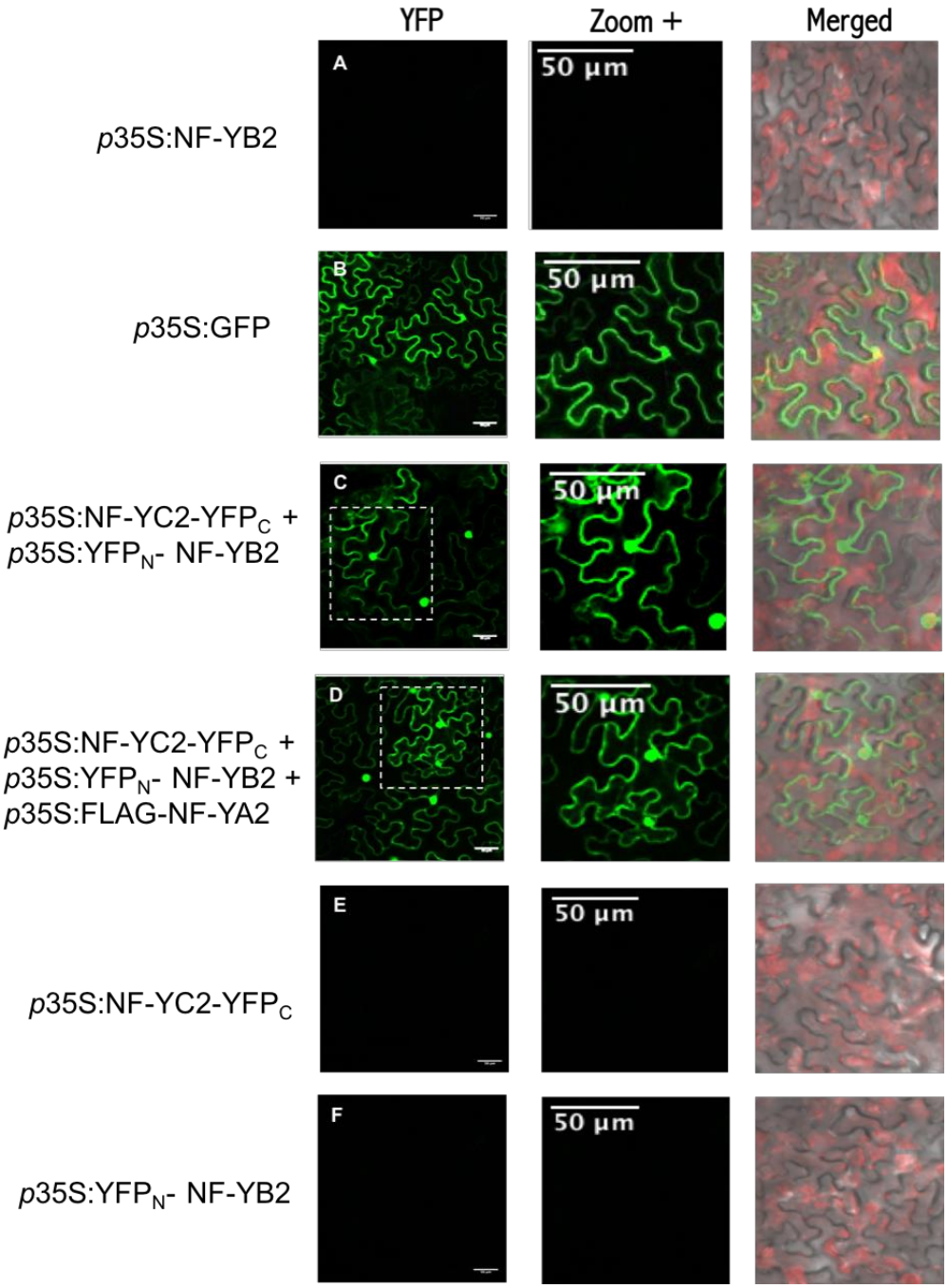

Figure 4.4 - Confocal microscopy imaging of *Nicotiana benthamiana* leaves with transient expression of YFP using BiFC assay to test pairwise interactions between NF-YA2, NF-YB2, and NF-YC2 subunits. Pictures were taken of *N. benthamiana* epidermal cells 3 days post infiltration with *A. tumefaciens* (strain GV3101) containing the indicated NF-Y constructs. Panels display: YFP fluorescence, the magnified view of the marked areas and the merged image (Chlorophyll, bright-field, YFP). A) No tagged construct (*p*35S:NF-YB2), resulting in no detectable signal, was used as a negative control. B) *p*35S:GFP construct was used as positive control. C-D) The assay revealed that NF-YB2 and NF-YC2 are able to hetero dimerize *in planta*. The fluorescence was detected in the nucleus and cytoplasm in the combination of *p*35S:NF-YC2-YFP$_C$ and *p*35S:YFP$_N$-NF-YB2. E-F) Infiltration of single constructs of *p*35S:NF-YC2-YFP$_C$ and *p*35S:YFP$_N$-NF-YB2 did not show any fluorescence. Experiments were performed three times. White scale bar represents 50 µm.

NF-YA2 did not interact with any other subunit in the pairwise tests showed in Table 4.2. Different reasons can explain this result: i) the YFP tag interferes with NF-YA2 function, ii) NF-YA2 does not interact with NF-YB2 or NF-YC2, iii) the binding of NF-YA2 is dependent on the presence of a NF-YB2/C2 dimer. In mammals, NF-YB and NF-YC subunits dimerize in the cytoplasm and are then imported into the nucleus (Kahle et al. 2005). The dimerization of NF-YB and NF-YC subunits creates a binding surface for the association of NF-YA (Romier et al. 2003). If the same process occurs in plants, then no pairwise interaction would be seen with NF-YA2, as the binding site for the NF-YA2 subunit would only be formed by the NF-YB2/C2 dimer, and hence NF-YA2 would need the other two subunits present to form the trimer. With this hypothesis in mind, all three NF-Y subunits with YFP in all different orientations and combinations were co-infiltrated. For example, NF-YA2 at the N-terminal or C-terminal of YFP, was infiltrated together with constructs of NF-YB2 and NF-YC2 (Figure 4.5), one untagged and one containing the other half of the YFP tag. No fluorescence was observed in any of these combinations between the three NF-Y subunits. This may be because NF-YA2, NF-YB2 and NF-YC2 do not form a trimer in *N. benthamiana*. However, it is also possible that steric hindrance from the tags may prevent proper complex formation. For example, split YFP could make the NF-YA2 binding site inaccessible, or split YFP may change the functionality of NF-YA2, so the tagged protein behaves differently from the native protein preventing the formation of the hetero-trimer.

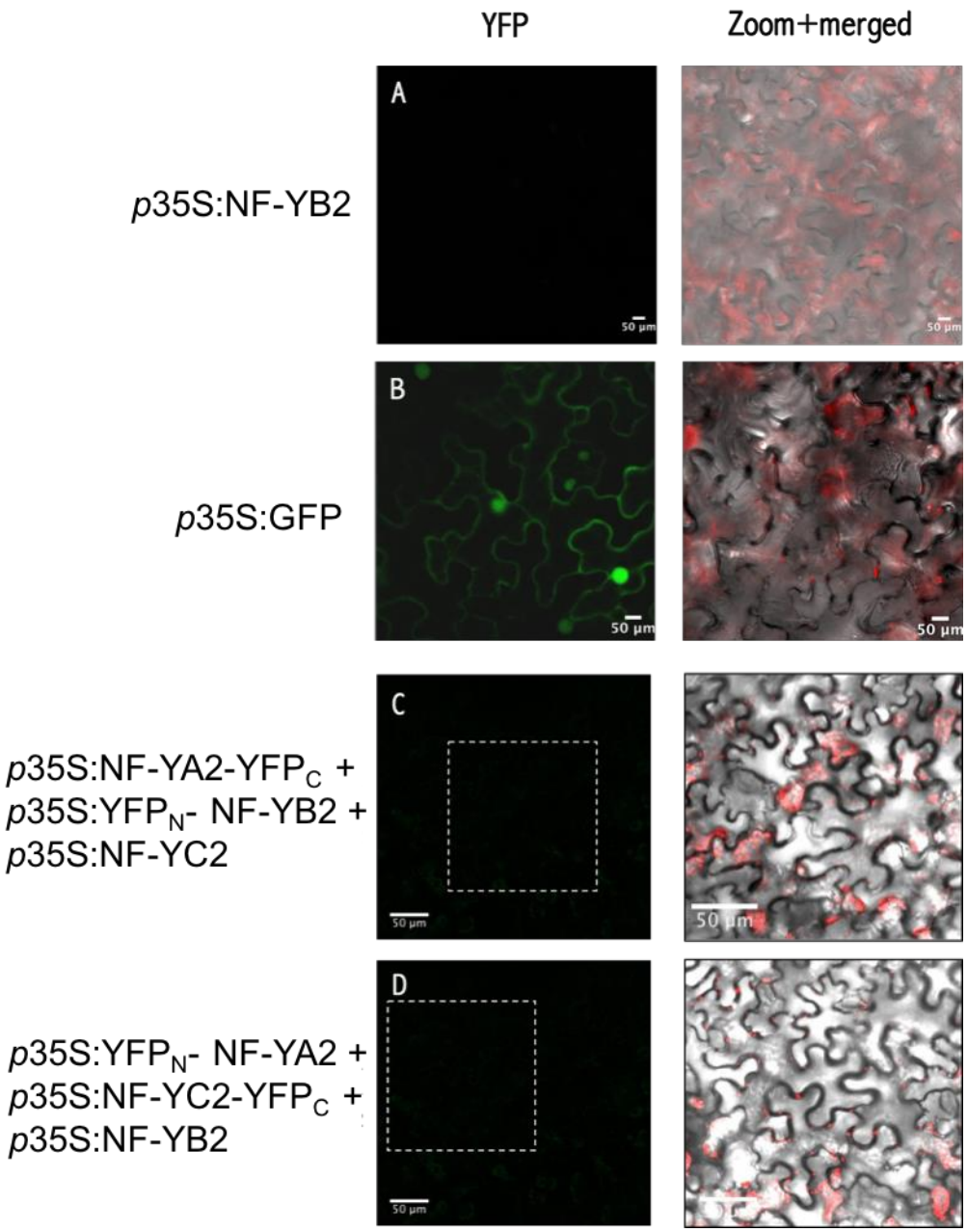

Figure 4.5 - Confocal microscopy imaging of *Nicotiana benthamiana* leaves. Examples of two combinations tested with co-infiltration of all three subunits, NF-YA2, NF-YB2 and NF-YC2, using BiFC assay. Pictures were taken of *Nicotiana benthamiana* epidermal cells 3 days post infiltration with *A. tumefaciens* (strain GV3101) containing the indicated NF-Y subunits. Panels display YFP fluorescence and merged images (Chlorophyll, bright-field). A) No tagged construct (*p*35S:NF-YB2), resulting in no detectable signal, was used as a negative control. B) *p*35S:GFP construct was used as positive control. C-D) No detectable signals were observed in either combination. Experiments were performed three times. White scale bar represents 50 µm.

4.3.3 Identification of *Nicotiana benthamiana* NF-Y orthologues genes

Because there is the possibility that the Arabidopsis NF-YA2, NF-YB2 and NF-YC2 subunits interact with the *N. Benthamiana* orthologues genes a bioinformatic identification (Table 4.3) and sequence alignment of *N. benthamiana* orthologues NF-YA2, NF-YB2 and NF-YC2 subunits was performed (Figure 4.6 and 4.7). NF-YA2, NF-YB2 and NF-YC2 in *Nicotiana benthamiana* were downloaded from the Plant Transcription Factor Database (PlantTFDB).

Table 4.3 – Genes in N. benthamiana orthologues to NF-Y subunits in Arabidopsis.

NF-Y Subunit	*Arabidopsis thaliana* gene ID	*Nicotiana benthamiana* gene ID
NF-YA2	AT3G05690	Niben101Scf04921g00005 Niben101Scf04869g07001 Niben101Scf04323g04020
NF-YB2	AT5G47640	Niben101Scf00341g02007 Niben101Scf00069g03014 Niben101Scf00919g01003
NF-YC2/NF-YC9	AT1G56170	Niben101Scf01520g05002 Niben101Scf01111g06008

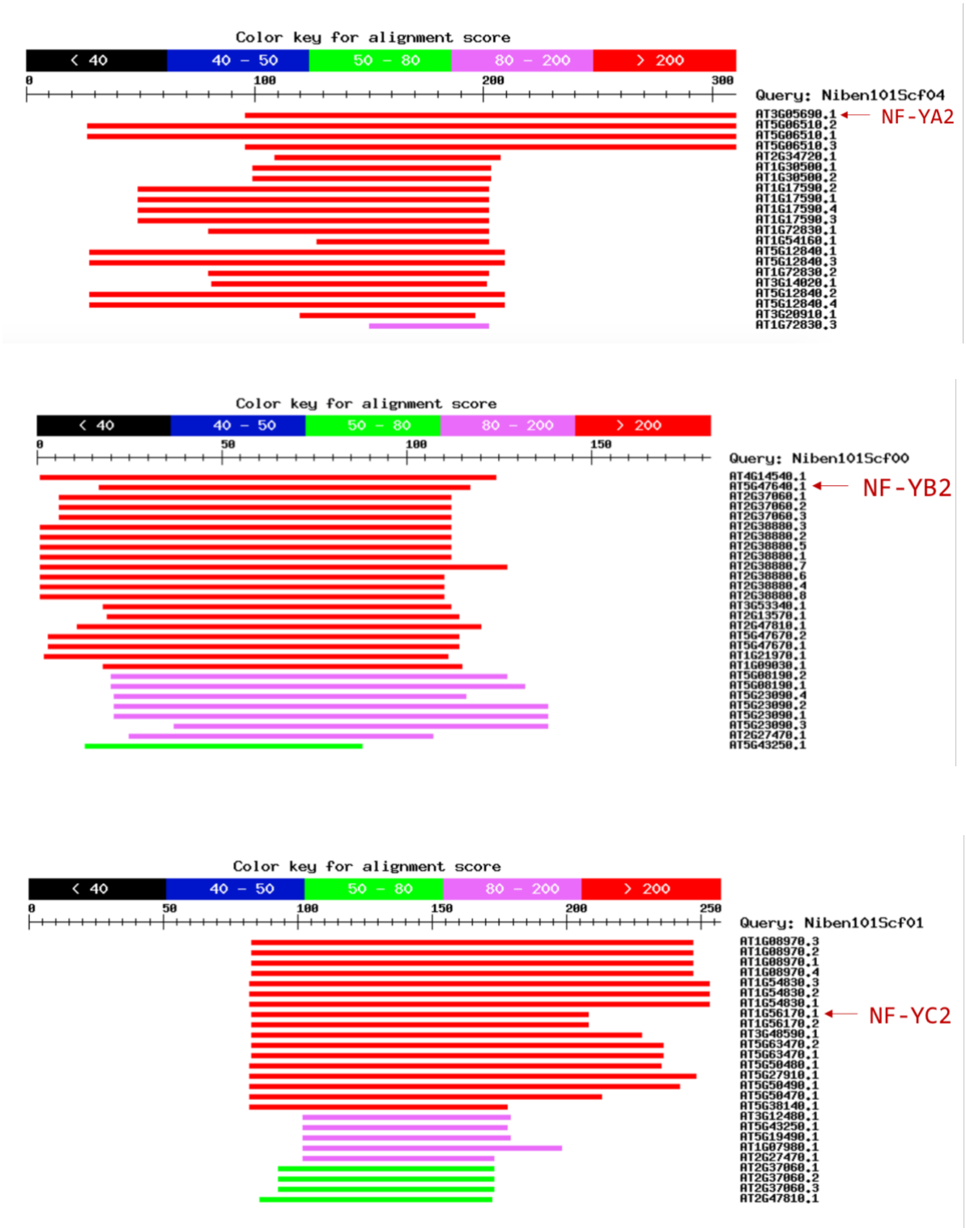

Figure 4.6 – Alignments between N. benthamiana NF-YA2, NF-YB2 and NF-YC2 orthologues gene and A. thaliana. The figure represents the alignment score according to the color: red indicate a very good alignment.

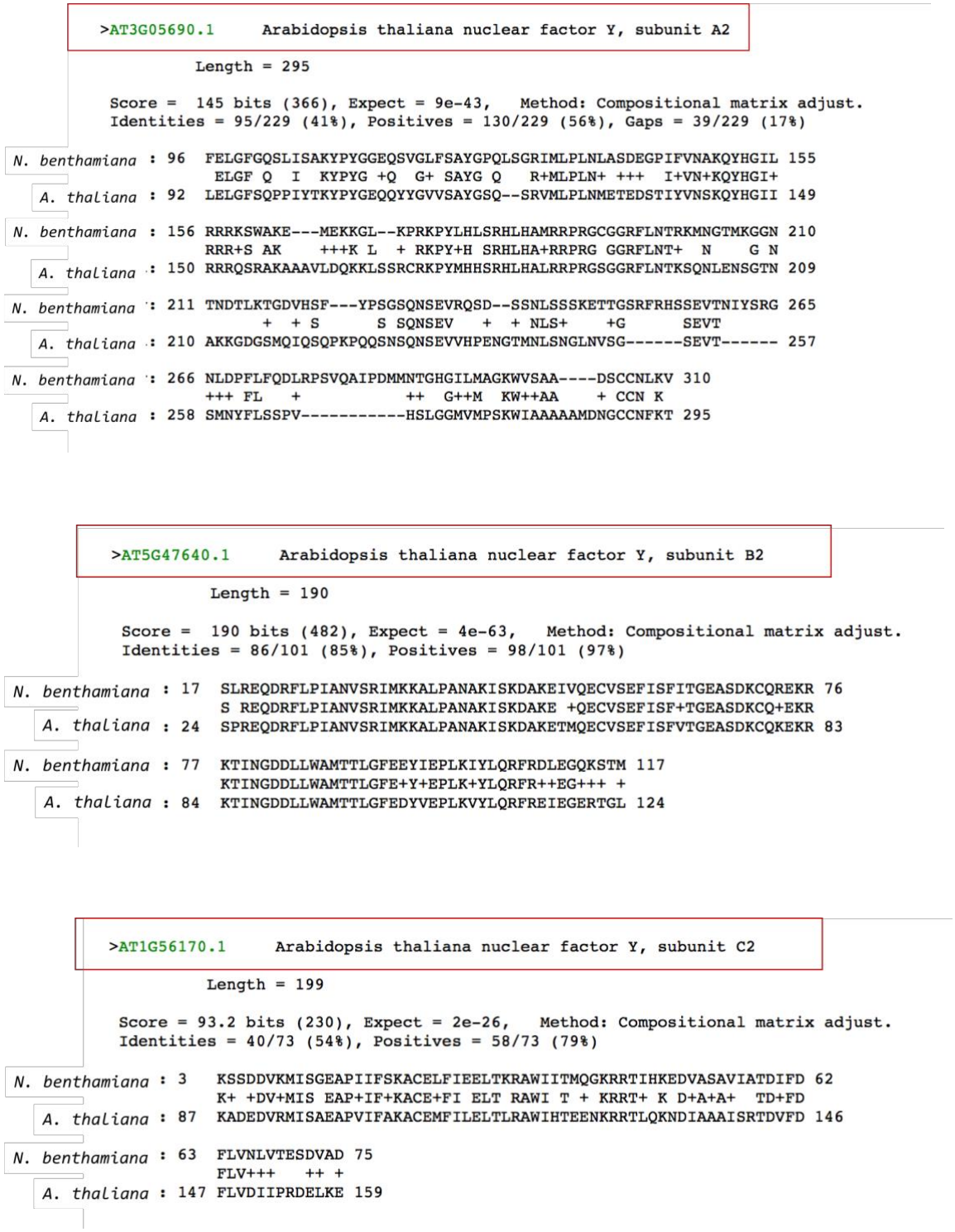

Figure 4.7– Amino acids alignments between N. benthamiana NF-YA2, NF-YB2 and NF-YC2 orthologues gene and A. thaliana. Numbers on the left indicate the amino acid position on the protein.

4.3.4 BiCAP method to isolate two interacting proteins.

After BiFC experiment, to prove that the two proteins NF-YB2 and NF-YC2 were actually interacting and not just close together, another method called BiCAP was used, which allowed the specific isolation of the two interacting subunits. Hence, total protein was extracted from *N. benthamiana* leaves co-infiltrated with *p*35S:YFP_N:NF-YB2 and *p*35S:NF-YC2:YFP_C and the two proteins fused with YFP were immunoprecipitated using GFP-trap beads which recognizes a neoepitope present on the reassembled YFP but not in split YFP. The western blot showed a YFP band only in *N. benthamiana* leaves co-infiltrated with *p*35S:YFP_N-NF-YB2 and *p*35S:NF-YC2-YFP_C but not in leaves infiltrated with either *p*35S:YFP_N-NF-YB2 or *p*35S:NF-YC2-YFP_C alone (Figure 4.8). This analysis is a validation of what was observed in the confocal microscopy (Figure 4.4) where the fluorescence was detected only in the sample containing NF-YB2 and NF-YC2 together and not when each construct containing split YFP was infiltrated alone. The band size observed (36.6 kDa) in the sample containing both NF-YB2 and NF-YC2 constructs identifies just the NF-YC2 (23.1 kDa) subunit fused with split YFP (13.5 kDa), making a protein of 36.6 kDa, because the GFP-HRP antibody recognizes only the C-terminal region of YFP (BiFP-4). Additionally, a second band at 27 kDa is observed in the same sample which is probably a cleaved product. The positive control, *p*35S:GFP-NF-YB2, showed in the western blot three bands: a band of 47 kDa which represent the NF-YB2-GFP tagged protein (20 kDa + 27 kDa), a band representing free GFP (27 kDa) and a band at 32 kDa which could be a cleaved product.

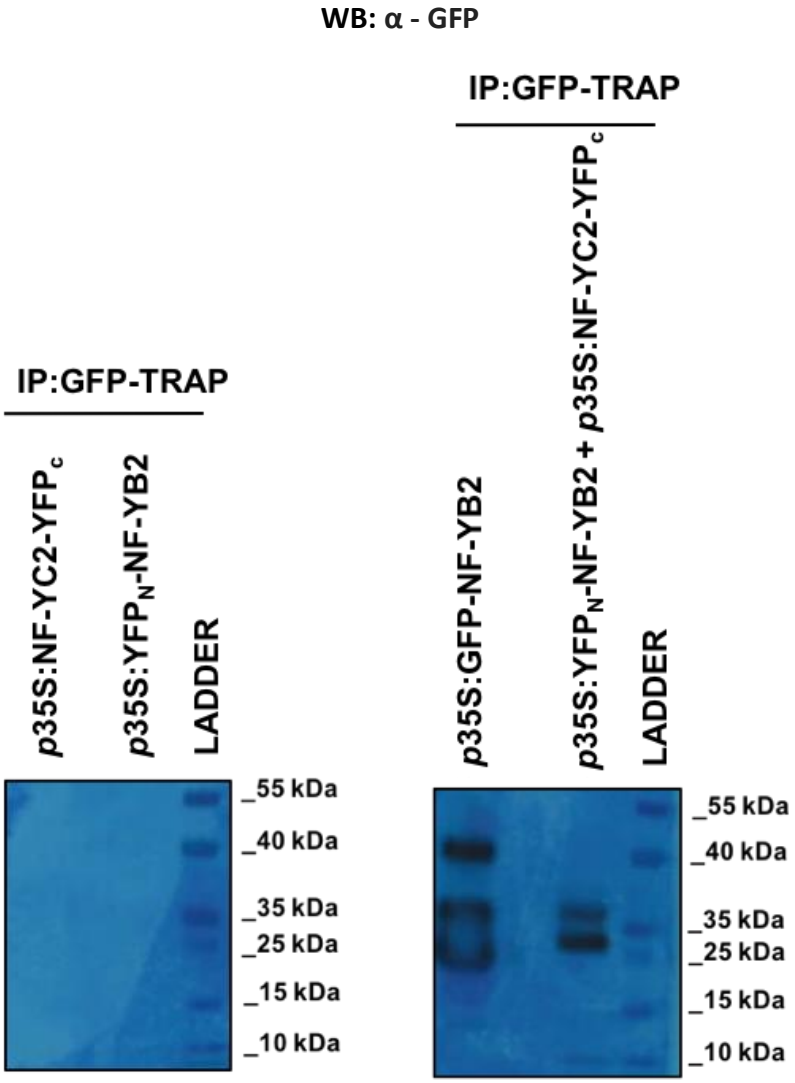

Figure 4.8 – BiCAP immunoprecipitation assay allowed the isolation of NF-YB2 and NF-YC2 hetero-dimer. Leaves were co-infiltrated with *p*35S:YFP_N-NF-YB2 + *p*35S:NF-YC2-YFP_C and infiltrated with *p*35S:YFP_N-NF-YB2 or *p*35S:NF-YC2-YFP_C alone. Proteins were immunoprecipitated using anti-GFP trap beads. The immunoprecipitated proteins were separated by SDS-PAGE and GFP-HRP antibody against C-terminal region of YFP (BiFP-4) was used for immunoblotting. *p*35S:GFP-NF-YB2 single construct was used as a positive control, showing the GFP tagged protein (47 kDa), a band representing free GFP (27 kDa) and a band representing a cleaved product (32 kDa). The infiltration of single construct *p*35S:YFP_N-NF-YB2 and *p*35S:NF-YC2-YFP_C did not show any signal. Co-infiltration of *p*35S:YFP_N-NF-YB2 + *p*35S:NF-YC2-YFP_C showed a band of 36.6 kDa, which represents NF-YC2 tagged with split YFP, and a second band at 27 kDa representing a cleavage version of the protein. Blot is representative of three experiments.

4.3.4.1 Testing proteins interaction between NF-YA2, NF-YB2 and NF-YC2 subunits in *N. benthamiana* using BiCAP assay.

Having seen that the BiCAP technique can pull down NF-YB2/C2 dimer, it was hypothesized that this method could be used in combination with NF-YA2 construct containing a smaller tag, such as FLAG tag. This method would circumvent the steric hindrance caused by the YFP tag, which may prevent the NF-YA2 interaction with the other two subunits. Hence, a *p*35S:FLAG-NF-YA2 construct was co-infiltrated into *N. benthamiana* leaves together with the other two constructs *p*35S:NF-YC2-YFP_C and *p*35S:YFP_N-NF-YB2 and to try to detect FLAG-NF-YA2 protein bound to the dimer (Figure 4.4D), two experiments were performed. In the first experiment *p*35S:NF-YC2-YFP_C and *p*35S:YFP_N-NF-YB2 were immunoprecipitated by GFP-trap beads and a western blot was performed using FLAG-HRP antibody to determine whether the NF-YA2 subunit was precipitated in a complex with NF-YB2 and NF-YC2. However, no FLAG signal was detected in the western blot analysis (data not shown).

Because in mammals, the NF-YB and NF-YC dimer forms in the cytoplasm and then moves into the nucleus where it can bind NF-YA subunit, it was hypothesized that there would be a larger amount of NF-YB2/C2 dimer in the cell than NF-YA2/B2/C2 trimer. Hence in the second experiment the NF-YA2 construct was targeted. Anti-FLAG beads were used to immunoprecipitate FLAG-NF-YA2 protein and a western blot performed using GFP-HRP antibody to determine if NF-YB2 and NF-YC2 subunits were also pulled down. It was hypothesized that if the three subunits interact *in planta* then the two YFP tagged subunits (*p*35S:NF-YC2-YFP_C + *p*35S:YFP_N-NF-YB2) would be co-immunoprecipitated with FLAG-NF-YA2, and the C terminal construct of YFP detected using the GFP-HRP antibody. However, this experiment did not demonstrate co-immunoprecipitation of the three subunits (Figure 4.9). The positive control *p*35S:GFP-NF-YB2 showed the presence of NF-YB2-GFP tagged protein of the expected size (46.9 kDa) and a second band representing free GFP (27 kDa), proving the functionality of GFP antibody. Untagged *p*35S:NF-YB2 was used as a negative control and no GFP signal was

detected. In the other samples, anti-GFP-HRP did not detect GFP signal, suggesting that FLAG beads were not able to pull down the NF-YB2/NF-YC2-YFP dimer.

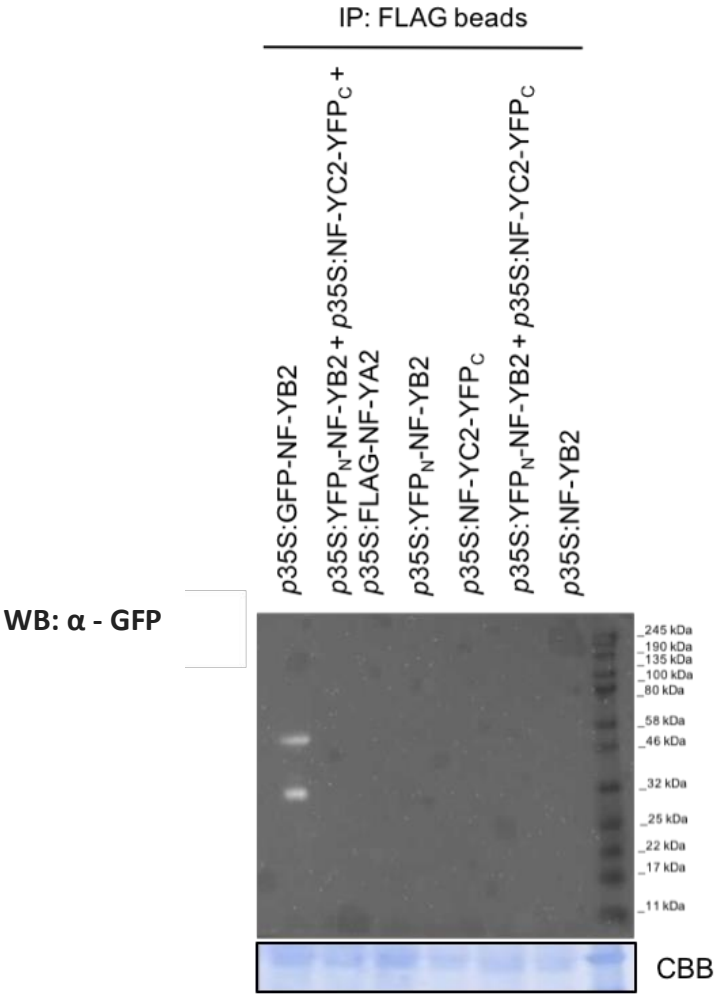

Figure 4.9 – Immunoprecipitation with FLAG beads and immunoblotting using GFP-HRP antibody. *p*35S:NF-YB2 (untagged) single construct was used as a negative control. *p*35S:GFP-NF-YB2 was used as a positive control, showing a band of the expected size of the NF-YB2-GFP tagged protein (46.9 kDa) and a second band representing free GFP (~27kDa). The infiltration of single construct *p*35S:YFP$_N$-NF-YB2 and *p*35S:NF-YC2-YFP$_C$ did not show any signal demonstrating these constructs are not immunoprecipitated by the FLAG beads. Co-infiltration of *p*35S:YFP$_N$-NF-YB2 + *p*35S:NF-YC2-YFP$_C$ and *p*35S:YFP$_N$-NF-YB2 + *p*35S:NF-YC2-YFP$_C$ + *p*35S:FLAG-NF-YA2 did not show any bands. The blot is representative of three independent experiments. The Coomassie Brilliant Blue (CBB) stained on the bottom shows the large subunits of Rubisco as an indication of total protein loading.

To prove that the FLAG beads and FLAG antibody were functional, *p*35S:FLAG-NF-YB2 and the sample containing *p*35S:NF-YC2-YFP_C + *p*35S:YFP_N-NF-YB2 + *p*35S:NF-YA2-FLAG were immunoprecipitated using FLAG beads. Western blot analysis with anti FLAG-HRP antibody was subsequently performed to detect the FLAG tagged fusion proteins (Figure 4.10). *p*35S:FLAG-NF-YB2 was used as a positive control, and resulted in a band indicating the presence of the FLAG tagged protein of the expected size (~20kDa). Untagged *p*35S:NF-YB2 was used as a negative control, and no bands were detected. In addition, infiltration of the single *p*35S:NF-YC2-YFP_C and *p*35S:YFP_N-NF-YB2 constructs, or these two constructs together, did not result in bands as expected. Meanwhile in the sample co-infiltrated with *p*35S:NF-YC2-YFP_C, *p*35S:YFP_N-NF-YB2 and *p*35S:NF-YA2-FLAG, a band of ~32 kDa, identified the tagged NF-YA2 subunit. Hence the FLAG beads successfully immunoprecipitated NF-YA2, suggesting in the previous experiment that NF-YA2 was successfully immunoprecipitated but did not co-immunoprecipitate NF-YB2 and NF-YC2 subunits.

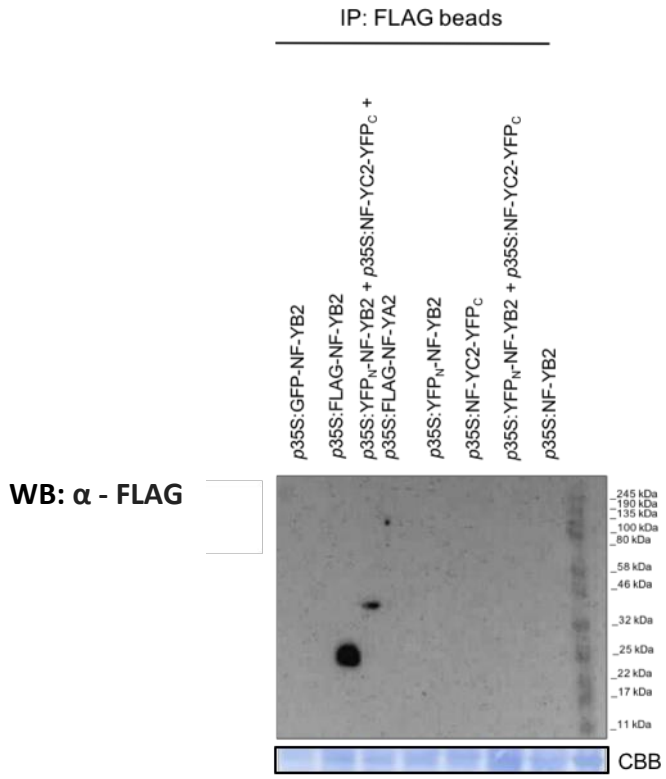

Figure 4.10 – Immunoprecipitation with FLAG beads and Immunoblotting using FLAG-HRP antibody. *p*35S:NF-YB2 (untagged) single construct and *p*35S:GFP-NF-YB2 were used as negative controls and no bands were detected. *p*35S:FLAG-NF-YB2 was used as a positive control, which showed the presence of the FLAG tagged protein of the expected size (~20 kDa). The infiltration of single construct *p*35S:YFP_N-NF-YB2 and *p*35S:NF-YC2-YFP_C and the co-infiltration of *p*35S:YFP_N:NF-YB2 + *p*35S:NF-YC2:YFP_C did not show any signal as expected. The sample co-infiltrated with p35S:YFP_N:NF-YB2, p35S:NF-YC2:YFP_C and p35S:FLAG:NF-YA2, showed a band of ~32 kDa, identifing the NF-YA2 subunit. The Coomassie Brilliant Blue (CBB) stained on the bottom shows the large subunits of Rubisco as an indication of total protein loading.

To confirm that GFP beads and anti GFP-HRP antibody were working properly, western blot analysis on the same samples as the FLAG blot (Figure 4.10) using the anti-GFP antibody after immunoprecipitation with GFP beads was performed (Figure 4.11). YFP was only detected in *N. benthamiana* leaves co-infiltrated with *p*35S:NF-YC2-YFP_C + *p*35S:YFP_N-NF-YB2 and *p*35S:NF-YC2-YFP_C + *p*35S:YFP_N-NF-YB2 + *p*35S:FLAG-NF-YA2, showing a protein band of the expected size (36.6 kDa), representing the NF-YC2 (23.1 kDa) subunit fused with split YFP (13.5 kDa) (because the antiGFP-HRP antibody recognizes the C-terminal region of YFP). No GFP signal was detected in leaves infiltrated with either *p*35S:NF-YC2-YFP_C or *p*35S:YFP_N-NF-YB2 alone as expected because the split YFP fragments should not be immunoprecipitated by the GFP beads. Infiltration of *p*35S:NF-YB2 (untagged)

single construct was used as a negative control and no bands were detected. GFP-tagged NF-YB2 and NF-YC2 were used as positive controls; both samples showed the expected size of the GFP tagged protein (47 kDa and 50 kDa respectively), a band representing free GFP (27 kDa) and a band around 32 kDa which perhaps is a cleavage version of the tagged protein.

In summary both experiments were unable to detect *in planta* interactions between NF-YA2 and the dimer NF-YB2/C2. This is consistent with the results of the BiFC assay, strengthening the evidence that NF-YA2 is not able to form a complex with NF-YB2 and NF-YC2 in *N. benthamiana*. However, there are other reasons why a true interaction may not be identified. All this work has to be done using tagged proteins and the position of the tag on NF-YB2 and NF-YC2 proteins influence whether they can form a dimer. Although one orientation allows dimer assembly, the tags may block NF-YA2 binding site or influence the conformation to prevent binding.

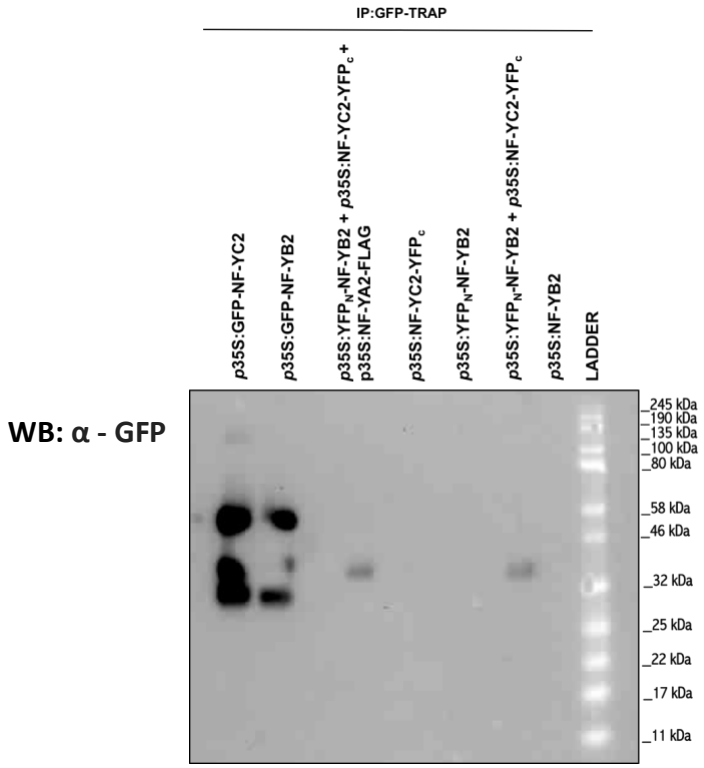

Figure 4.11– Immunoprecipitation with GFP-trap beads and immunoblotting using GFP-HRP antibody. *p*35S:NF-YB2 (untagged) single construct was used as negative control, no bands were detected. GFP-tagged NF-YB2 and NF-YC2 were used as positive control, both samples showed the expected size of the GFP tagged protein (47 kDa and 50 kDa respectively). A band representing free GFP (27 kDa) and a second band ~32 kDa, were also showed in both samples. The infiltration of single construct *p*35S:YFP_N-NF-YB2 and *p*35S:NF-YC2-YFP_C did not show any signal. Co-infiltration of *p*35S:YFP_N-NF-YB2 + *p*35S:NF-YC2-YFP_C and *p*35S:YFP_N-NF-YB2 + *p*35S:NF-YC2-YFP_C + *p*35S:FLAG-NF-YA2, showed a band of 36.6 kDa (23.1 kDa + 13.5 kDa). Blot is representative of three experiment.

4.3.5 Standard co-immunoprecipitation (Co-IP) of transiently expressed NF-YA2 epitope tagged protein in *N. benthamiana* to identify the complex.

Because using BiCAP method to prove the trimer did not detect the NF-YA2 subunit a standard co-immunoprecipitation (Co-IP) method using *N. benthamiana* leaves was performed to further validate the existence of NF-YA2/B2/C2 trimer *in planta*. This time NF-YA2, which is localized exclusively in the nucleus, was GFP tagged and NF-YB2 or NF-YC2 subunit were FLAG tagged. This would help to identify the trimer of interest if the NF-YB2/C2 dimer is able to bind

different NF-YAs or TFs than NF-YA2. So *p*35S:GFP-NF-YA2 was co-infiltrated in *N. benthamiana* using the following combinations:

1) *p*35S:GFP-NF-YA2 + *p*35S:NF-YC2-FLAG + *p*35S:NF-YB2

2) *p*35S:GFP-NF-YA2 + *p*35S:FLAG-NF-YB2 + *p*35S:NF-YC2

It was hypothesized that immunoprecipitation of GFP tagged NF-YA2 protein using GFP- trap beads should enable any associated NF-YB2 or NF-YC2 FLAG tagged subunits to be isolated. This would demonstrate that NF-YA2 is able to form a complex with NF-YB2 and NF-YC2 *in planta*. Western blots were performed on the same samples using anti-GFP and anti-FLAG antibodies. Protein samples from leaves infiltrated with *p*35S:GFP-NF-YA2 were used as a positive control. However, the anti-GFP antibody only detected a band around 27 kDa which is likely to be free GFP and a second band (~ 32 kDa) which could be a cleaved product (Figure 4.12). The full-length NF-YA2-GFP tagged protein (59 kDa) was not detected. We know from the confocal microscopy that *p*35S:GFP-NF-YA2 is expressed upon infiltration and crucially it is only found in the nucleus. Hence it is likely that the GFP-NF-YA2 protein is being cleaved during protein extraction. It is also possible that the GFP within a fusion protein is not accessible to the antibody, whereas the cleaved GFP is accessible, so the immunoprecipitation enriches for free GFP and does not pull down the intact fusion protein. The other two immunoprecipitated samples, containing *p*35S:GFP-NF-YA2 + *p*35S:NF-YC2-FLAG + *p*35S:NF-YB2 and *p*35S:GFP-NF-YA2 + *p*35S:FLAG-NF-YB2 + *p*35S:NF-YC2 also showed a single band corresponding to free GFP. Subsequently, a western blot using anti-FLAG-HRP antibody did not detect any FLAG tagged NF-Y proteins after immunoprecipitation of GFP-NF-YA2 using GFP-trap beads. Only a single band around 100 kDa (Figure 4.12B) was detected in the crude protein extraction from tissue infiltrated with *p*35S:GFP-NF-YA2 + *p*35S:NF-YC2-FLAG + *p*35S:NF-YB2. This could be an unspecific band and was not detected in repeat experiments. However, as we cannot be certain full length NF-YA2 was immunoprecipitated (Figure 4.12A) it is impossible to interpret these results in terms of NF-Y subunit interaction.

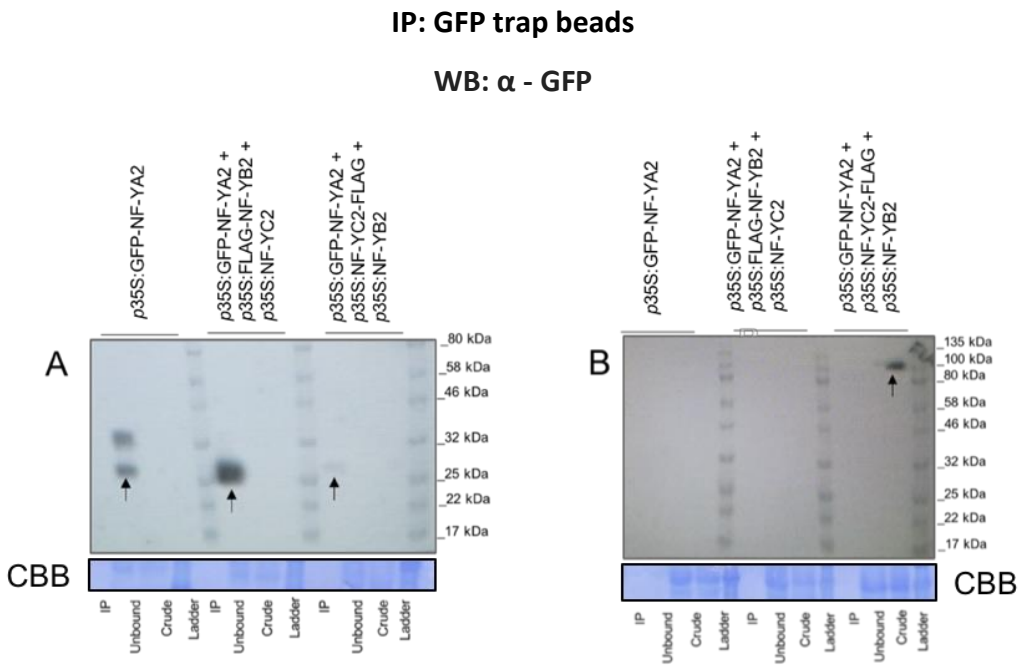

Figure 4.12- Co-immunoprecipitation (Co-IP) of transiently expressed NF-YA2-GFP tagged protein in *N. benthamiana*. GFP-tagged NF-YA2 was infiltrated using *A. tumefaciens* (strain GV3101) in *N. benthamiana* leaves and immunoprecipitated using GFP-trap beads. Crude plant extract (Crude), unbound fraction (Unbound) and the immunoprecipitated proteins (IP) were separated by SDS-PAGE. A) GFP-HRP antibody was used for the immunoblots. *p*35S:GFP-NF-YA2 showed the presence of a protein band at 32 kDa. Arrows show free GFP band (~27 kDa) in all three immunoprecipitated (IP) samples. The Coomassie Brilliant Blue (CBB) stained on the bottom shows the large subunits of Rubisco as an indication of total protein loading. B) FLAG-HRP antibody was used for the immunoblots and did not detect any NF-Ys FLAG tagged in the IP samples. An unspecific band in the crude sample containing *p*35S:GFP-NF-YA2 + *p*35S:NF-YC2-FLAG + *p*35S:NF-YB2 of around 100 kDa is visible, representing a cleaved product. The Coomassie Brilliant Blue (CBB) stained on the bottom shows the large subunits of Rubisco as an indication of total protein loading. Blot is representative of three experiments.

Confocal microscopy imaging of *N. benthamiana* leaves with transient expression of *p*35S:GFP-NF-YA2 and the other two combinations was performed to test if the expression of the three subunits together would change NF-YA2 localization and signal intensity. This analysis does not show any differences in NF-YA2 (Figure 4.13). This means that the presence of all three subunits do not change the expression of *p*35S:GFP-NF-YA2, showing a clear GFP nuclear localization in all three samples. Also, it appears that GFP is not localized in other cell

compartments besides the nucleus, so no free GFP is detectable and this could suggest that the cleavage of the protein probably occurs during the extracting process.

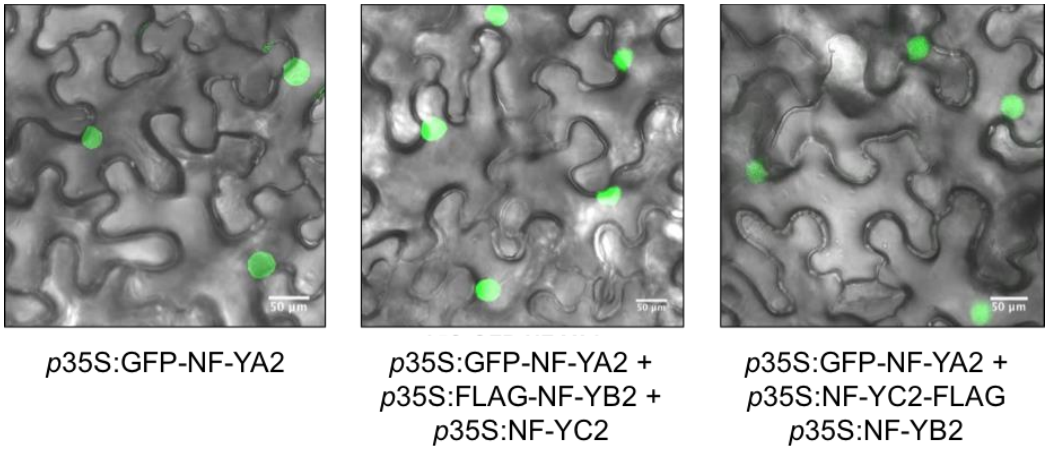

Figure 4.13 - Confocal microscopy imaging of *Nicotiana benthamiana* leaves with transient expression of *p*35S:GFP-NF-YA2. Pictures were taken of *Nicotiana benthamiana* epidermal cells 2 days post infiltration with *A. tumefaciens* (strain GV3101) containing *p*35S:GFP-NF-YA2 subunit. Panels display the merge image GFP + bright-field. Pictures represent respectively *p*35S:GFP-NF-YA2; *p*35S:GFP-NF-YA2 + *p*35S:FLAG-NF-YB2 + *p*35S:NF-YC2 and *p*35S:GFP-NF-YA2 + *p*35S:NF-YC2-FLAG + *p*35S:NF-YB2. In all three pictures NF-YA2 is localized in the nucleus and with the same signal intensity. Experiments were performed in biological replicates. White scale bar represents 50 µm.

4.4 Discussion

4.4.1 Assembly of an NF-Y trimer

BiFC assay on *N. benthamiana* cells performed in this chapter showed that NF-YB2 and NF-YC2 are able to hetero-dimerize. These results are confirmation of the Y2H analysis (Calvenzani et al. 2012) where it was tested the ability of each member of plant NF-YB and NF-YC subunits to dimerize. Specifically, it was found that NF-YB2 and NF-YC2 have a good affinity and that in general NF-YB and NF-YC subunits are able to hetero-dimerize in yeast. However, it is important to consider the possibility that the Arabidopsis NF-YA2, NF-YB2 and NF-YC2 subunits could interact with the *Benthamiana* orthologues genes, according to their high degree of sequence similarity. These promiscuous interactions between NF-Y TFs from the two species, Arabidopsis and Benthamiana, could cause artefacts due to the sequestration of NF-Y subunits, essential for their dimerization in BiFC experiments. Hence, the fact that a strong signal was observed only in the p35S:YFP_N-NF-YB2 and p35S:NF-YC2-YFP_C combination and did not occur between other subunits in different orientations, could be explained by these promiscuous interactions.

In this chapter, BiFC analysis allowed to localize the dimerization between NF-YB2 and NF-YC2, which occurs in the nucleus and in the cytoplasm. The same localization of the NF-YB/NF-YC dimer was observed in mammals where the association of the NF-Y trimer follows a strict stepwise pattern (Sinha et al. 1995). Initially, NF-YB/NF-YC dimer is formed in the cytoplasm and then it is translocated into the nucleus as hetero-dimer to recruit the NF-YA subunit and generate the functional NF-Y hetero-trimer (Kahle et al. 2005; Frontini et al. 2004). This NF-Y assembly mechanism seems to be conserved in plants.

The subcellular localization of NF-YA2, NF-YB2 and NF-YC2 on agro-infiltrated *N. benthamiana* leaves revealed that NF-YA2 is exclusively localized in the nucleus being consistent with a previous study where NF-YA2 was localized in the nucleus of Arabidopsis leaf cells transiently transformed via particle bombardment (Hackenberg et al. 2012). Meanwhile NF-YC2 and NF-YB2 were detected in both

nucleus and cytoplasm of *N. benthamiana* leaf cells. These results would confirm the hypothesis that NF-Ys in plants may behave as NF-Ys in mammals. Hence NF-YA2 is only present in the nucleus where it should join the hetero-dimer and NF-YB2 and NF-YC2 were detected in the cytoplasm as single subunits or as part of the hetero-dimer, and in the nucleus as hetero-dimer since they translocate together (Frontini et al. 2004). However previous studies showed that in Arabidopsis NF-YC2 was detected only in the nucleus after transformation of leaves using particle bombardment (Hackenberg et al. 2012) and in transgenic plant expressing constitutively tagged forms of NF-YC2 (Liu and Howell 2010). Meanwhile Arabidopsis NF-YB subunits were localized only in the cytoplasm, specifically NF-YB10 was detected in the cytoplasm of epidermal cells (Hackenberg et al. 2012) and NF-YB3 was localized in the cytoplasm of root cells (Liu and Howell 2010). This could be explained by the fact that NF-YB subunits in Arabidopsis cannot enter in the nucleus unless it dimerizes with NF-YC, in fact co-expression of a NF-YC subunit allows NF-YB to be translocated into the nucleus (Hackenberg et al. 2012).

Interestingly, NF-YB2 and NF-YC2 did not show pair interaction with NF-YA2 subunit in the BiFC assay performed in this study, suggesting that NF-YA2 may need the interphase NF-YB2/NF-YC2 to form the hetero-trimer. The same result was revealed in Y2H analysis presented by Hackenberg et al. (2012) where single NF-YB and NF-YC subunits almost never interacted with NF-YA subunits. Different approaches, such as BiCAP and standard CoIP, were used in this chapter to determine whether NF-YA2 forms an active trimer with NF-YB2 and NF-YC2. However, all of them did not demonstrate this interaction. It is important to consider that the potential interference of the tag is still an issue. Indeed, even if the GFP construct seems the most reliable, GFP tagged NF-YA2 protein appears to be unstable and cleave during extraction. Moreover, there is the possibility that the hypothesized heterotrimer is formed under a particular condition, such as pathogen attack or specific developmental plant response. In this case detect the pair interaction between NFYA2, NFYB2 and NFYC2 subunits in physiological

condition can be challenging. Hence, it would be necessary to try BiFC assay under different conditions.

4.4.2 Conclusion

In this chapter, an alternative and novel method such as BiCAP assay was used to identify NF-Y hetero-trimers. This assay brings together the advantage of the BiFC method to identify and localize protein-protein pairwise interactions, and the specificity of the co-immunoprecipitation assay. Strong evidence for dimerization of NF-YB2 and NF-YC2 were found in this study, however the BiFC and BiCAP assays in this chapter did not provide any evidence for the NF-YA2/B2/C2 hetro-trimer. Hence there is the possibility that NF-YA2, NF-YB2 and NF-YC2 are not able to interact in *N. benthamiana.* Following investigation will be done on Arabidopsis epitope tagged NF-YA2, NF-YB2 and NF-YC2, to investigate the existence of putative trimer *in planta*.

Chapter 5

5. Elucidating NF-Ys protein complexes using Arabidopsis transgenic lines.

5.1 Introduction

Considering the limitations of the BiFC method, which only enables testing of protein-protein interactions (PPIs) in a pairwise manner and can compromise the interacting properties of protein due to the steric hindrance of the tag, it is crucial to complement the BiFC results obtained in the previous chapter with alternative methods.

Nowadays there are two major methodologies to express proteins in plants. The first is the development of a stable transgenic line constitutively expressing the protein of interest, which becomes heritable in subsequent generations. The second is through transient expression of the target protein by agro-infiltration in host plant such as *Nicotiana benthamiana*. This method, without any doubt, is faster than generate stable transgenic plant lines, however these proteins are expressed in a different plant system and this can lead to artifacts.

Additionally, as mentioned previously, only few reports were able to identified active and functional NF-Y complexes (Hou et al. 2014, Liu and Howell 2010, Sato et al. 2014), combining BiFC assay with yeast-3-hybrid (Y3H) system. These methodologies suffer from some limitations considering that the interaction is tested in a heterologous environment (Cottier et al. 2011). For this reason, the use of Arabidopsis transgenic line stably expressing the protein of interest, would help to circumvent the potential problems associated with these methods, allowing to investigate protein-protein interaction *in planta*. In this context, a good assay to enable the identification of larger protein complexes *in vivo*, is the immunoprecipitation of the tagged target proteins followed by identification of other interacting proteins co-immunoprecipitated (Co-IP) using Mass

Spectrometry (MS) analysis. In order to be able to specifically purify a protein complex from a total protein extract, the target protein is fused to an affinity tag, such as FLAG or GFP tag, and captured and immobilized to an affinity resin such as anti-GFP or anti-FLAG agarose beads. This method allows non-interacting proteins to be washed off the resin, while the whole protein complex can stay immobilized. Proteins involved in the interaction after trypsin digestion are analyzed by MS, which recognizes each component using a mass spectra database (Gingras et al. 2007, Ransone 1995). There are many obvious advantages of this method. First of all, this technique does not require prior knowledge of the interacting proteins and for this reason it is ideally suited to gain new insights into a complex of interest. Second, it can be conducted under native physiological conditions, allowing to identify *in vivo* binding, since the bait protein can be purified from any tissue where it is being expressed. Third, the approach allows to pull down the whole protein complex, rather than single components at a time, and can be used in combination with cross-link methods which fix the binding between protein complex components (Vasilescu et al. 2004). Despite these numerous advantages, Co-IP assay presents some disadvantages. In fact, abundant proteins such as tubulin, actin and ribosomal proteins can be co-immunoprecipitated, together with heat shock proteins, generating a background signal; for this reason it is important to perform appropriate negative controls (Ransone 1995).

Co-IP experiments can be carried out using a specific antibody raised against the bait protein, allowing the isolation of the endogenous protein in its native context. Hence, it would not be necessary to create transgenic epitope tagged lines. However, even if this approach has been used in plants (Konig et al. 2014, Pertl-Obermeyer et al. 2014, Qi and Katagiri 2009), it is not very popular in the field. This is mostly due to the lack of availability of plant protein antibodies, together with the fact that the production of specific antibodies can be expensive and inefficient. Moreover, it is important to consider that TFs are generally part of large protein families and so getting a specific antibody for each subfamily

member can be difficult due to their high sequence similarity, while generic antibodies are usually very specific and suitable for generic purification protocols (Bontinck et al. 2018). Therefore, the use of tags such as FLAG and GFP is currently the standard practice in MS experiments. Overall, GFP and FLAG tags are the most popular for Co-IP experiments in plants due to high-quality anti-GFP and anti-FLAG antibodies currently available. Additionally, the GFP tag can also be used to perform protein localization analysis, while the FLAG tag is a very small tag minimizing its effect on protein folding and functionality.

5.2 Chapter aims

Based on these considerations, the general aim of this chapter was to analyze Arabidopsis NF-YA2, NF-YB2 and NF-YC2 epitope tagged lines (with FLAG or GFP tag at the N- or C-terminal of the target protein) using Co-IP and MS. Immunoprecipitation of the epitope-tagged protein stably expressed *in planta*, should enable identification of any bound proteins using MS. This could elucidate a NF-YA2/NF-YB2/NF-YC2 trimer *in planta* as well as identify other functional NF-Y complexes under physiological conditions. The epitope GFP tagged lines will also allow localization of NF-YA2, NF-YB2 and NF-YC2 in the plant cell.

5.3 Results

5.3.1 Subcellular localization of GFP-tagged NF-YA2, NF-YB2 and NF-YC2 stably expressed in Arabidopsis leaves.

Previous analysis (Chapter 4) performed on *N. benthamiana* leaves agro-infiltrated with *p*35S:GFP-NF-YA2, *p*35S:GFP-NF-YB2 and *p*35S:GFP-NF-YC2 constructs, revealed a nuclear localization of NF-YA2 subunit and a nuclear and a cytoplasmic localization of NF-YB2 and NF-YC2 subunits in the transiently transformed cells. The following step was then to confirm the subcellular localization observed in *N. benthamiana* using epidermal leaf cells of Arabidopsis lines stably expressing NF-Y GFP tagged proteins, described in Table 3.1. Hence, *nf-yb2*::35S:GFP-NF-YB2 and Col-0::35S:NF-YC2-GFP lines were visualized under the confocal microscope and the result, shows in Figure 5.1, indicated that NF-YB2 and NF-YC2 subunits were localized in both cytoplasm and nucleus. However, Col-0::*p*35S:GFP-NF-YA2 lines did not show fluorescence in any cell compartments (data no shown), suggesting that the *p*35S:GFP-NF-YA2 insert is not expressed in these mutants, in agreement with qPCR analysis which revealed that the expression level of NF-YA2 gene in these lines is not significantly different to Col-0 (Figure 3.13). Subsequently, *nf-ya2*::pNF-YA2:NF-YA2-GFP line was analyzed, giving a predominant signal in the nucleus. These localization, in line with the previous analysis performed on *N. benthamiana* (Chapter 4), is also consistent with previous studies, which showed that NF-YB and NF-YC in plants dimerize in the cytoplasm and then translocate to the nucleus (Laloum et al. 2013) where they can join the NF-YA to form the active hetero-trimer. According to this transcriptional regulation system reported in several papers (Hackenberg et al. 2012, Laloum et al. 2013, Zhao H. et al. 2016), the NF-Y complex composed by the tree subunit then binds to CCAAT box in the promoter region to regulate the expression of the target gene (Zhao H. et al. 2016).

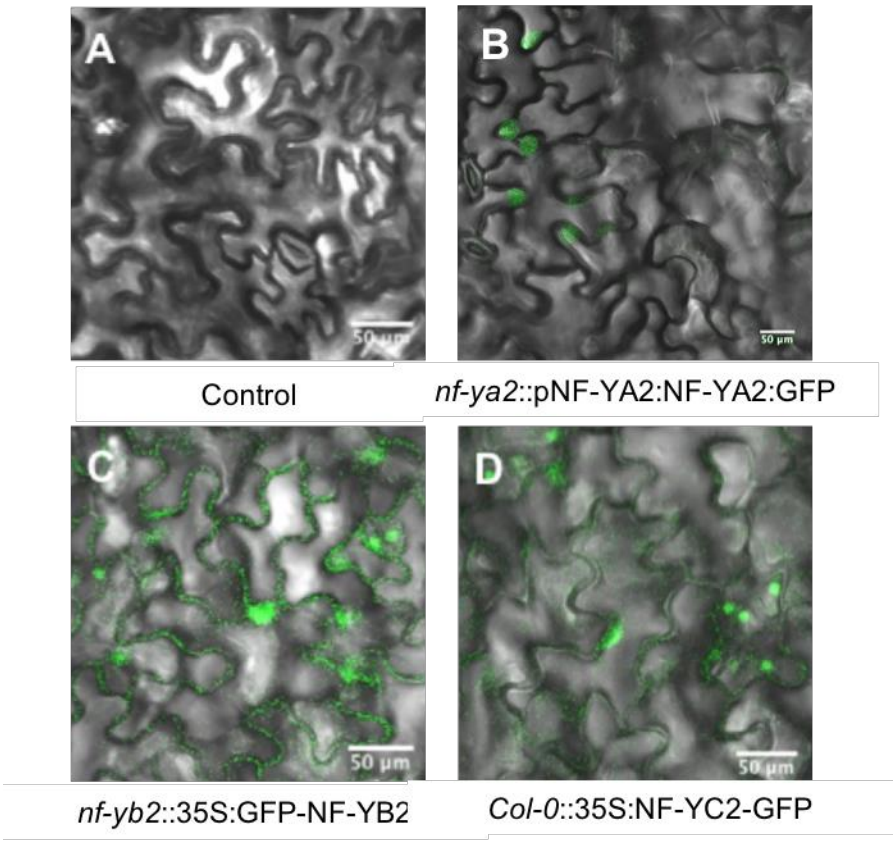

Figure 5.1 – Subcellular localization of NF-YA2, NF-YB2 and NF-YC2 GFP tagged subunits stably expressed in Arabidopsis lines. Panels display the merge image GFP + bright-field. Leaf of 4 weeks old Arabidopsis expressing NF-YA2, NF-YB2 and NF-YC2 GFP tagged were visualized under confocal microscope. A) Col-0 Arabidopsis leaves, no fluorescence is detected (Negative control) B) The florescence signal in Arabidopsis *nf-ya2*::*p*NF-YA2:NF-YA2-GFP line is predominantly detected in the nucleus. C) In Arabidopsis *nf-yb2*::*p*35S:GFP-NF-YB2 lines the fluorescence is detected in the nucleus and cytoplasm. D) In Arabidopsis Col-0::*p*35S:NF-YC2-GFP lines the GFP signal is visible in nucleus and cytoplasm. Representative images from three independent experiments are shown. Scale bars, 50 µm.

5.3.2 Co-immunoprecipitation of NF-YA2, NF-YB2 and NF-YC2 subunit.

Arabidopsis lines with NF-YA2, NF-YB2 and NF-YC2 GFP or FLAG tagged in different orientation (N-terminal or C-terminal) were generated to circumvent protein functionality issues may cause by the steric hindrance of the tag. This because due to the large size of the GFP tag, even if it is more accessible to the antibody and easy to immunodetect, it can interfere with protein folding and protein functionality. Hence, Arabidopsis epitope NF-Y FLAG tagged lines were also generated. Another factor to consider in Co-IP experiment is the tag position which can affect protein solubility. Therefore, Arabidopsis lines with the tag

placed at both N-terminal or C-terminal of the protein were used. It was reported that tags at N-terminal fusions have an enhanced protein expression and protein solubility, while at C-terminal of the protein are less likely to interfere with any signal peptides (Dyson et al. 2004). The lines generated in this study (Table 3.1) have the fusion proteins (NF-YA2, NF-YB2 and NF-YC2) under the 35S promoter, in addition Arabidopsis lines with NF-YA2 under the native promoter were generated.

5.3.2.1 Co-Immunoprecipitation of NF-YC2

Four homozygous overexpressor NF-YC2-GFP tagged lines, two N terminal tagged and two C terminal tagged lines (Col-0::p35S:NF-YC2-GFP_1, Col-0::p35S:NF-YC2-GFP_3, Col-0::p35S:GFP-NF-YC2_1, Col-0::p35S:GFP-NF-YC2_2) were grown under controlled conditions, together with p35S:HA:GFP line as a positive control. Col-0::p35S:NF-YC2-GFP_1 and Col-0::p35S:NF-YC2-GFP_3 lines were generated by Emily Breeze (2014), while Col-0::p35S:GFP-NF-YC2_1 and Col-0::p35S:GFP-NF-YC2_2 were generated in this study (see chapter 3). Two fully expanded leaves were harvested and total protein was extracted for each line. Equal amount of protein was loaded onto an SDS-PAGE agarose gel to separate the denatured proteins. Successively western blot analysis using anti-GFP was carried out to detect the expression of the NF-YC2-GFP tagged proteins in each line (Figure 5.2). A protein band of 22 kDa was detected in all of the overexpressor NF-YC2 lines analyzed, which may represent a cleaved product of the GFP. The NF-YC2-GFP labelled protein (50 kDa) was not detectable in the four lines, while the positive controls (p35S:HA:GFP line) showed two bands: a GFP band of the expected size 27 kDa and another band potentially indicating a cleaved version of the GFP (22 kDa). This result indicates a low NF-YC2 protein level, so immunoprecipitation using anti-GFP agarose beads was carried out to detect NF-YC2-GFP tagged protein.

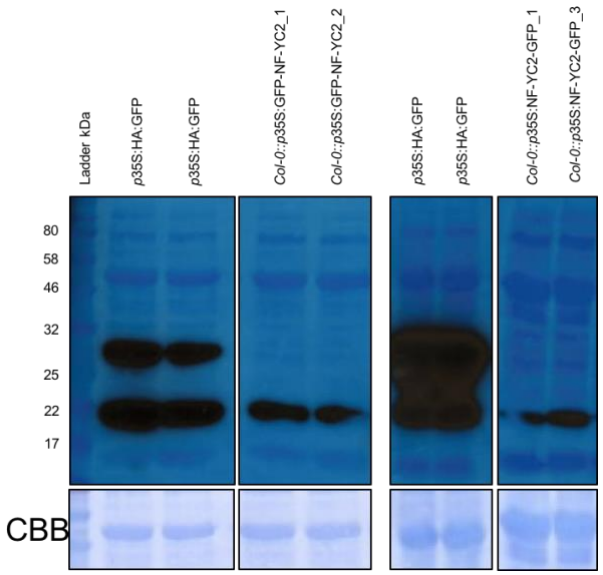

Figure 5.2 - Expression of NF-YC2-GFP in Arabidopsis epitope tagged lines. Total protein was extracted from *p*35S:GFP:HA line (positive control) and Col-0::*p*35S:NF-YC2-GFP_1, Col-0::*p*35S:NF-YC2-GFP_3, Col-0::*p*35S:GFP-NF-YC2_1, Col-0::*p*35S:GFP-NF-YC2_2 lines. Proteins were separated by SDS-PAGE and western blot was performed using anti-GFP. A band indicating HA tagged GFP (27 kDa) is visible in all positive control samples together with a second band (22 kDa) which could be a cleaved GFP product. All four NF-YC2 tagged lines present the band at 22 kDa. The Coomassie Brilliant Blue (CBB) stain on the bottom shows the large subunits of Rubisco as an indication of total protein loading.

To proceed with the biochemical characterization of NF-YC2, upper rosette leaves were harvested after 5 weeks, when the leaves were fully expanded. Approximately 20 g of leaf tissue was used to immunoprecipitate GFP-tagged proteins from the four overexpressors NF-YC2-GFP lines using anti-GFP trap beads. An aliquot of the crude total protein extracts (input), unbound protein and immunoprecipitated (IP) fractions were separated by SDS-PAGE and western blot was performed using an anti-GFP antibody. The two C-terminal fusion proteins of NF-YC2 (Col-0::*p*35S:NF-YC2-GFP_1, Col-0::*p*35S:NF-YC2-GFP_3) and the *p*35S:HA:GFP control lines showed considerable enrichment of the tagged protein following immunoprecipitation (Figure 5.3). In the IP fraction (blot on the right) a band of NF-YC2-GFP at the expected size 50 kDa (27 kDa GFP +23.1 kDa NF-YC2) was visible in both lines, Col-0::*p*35S:NF-YC2-GFP_1 line showed also a second band at 27 kDa representing free GFP. However, both NF-YC2-GFP lines did not

show bands in the crude and the unbound fraction, while the positive control (*p*35S:HA:GFP) showed the expected GFP band at 27 kDa in all three fractions, with a more significant signal in the IP.

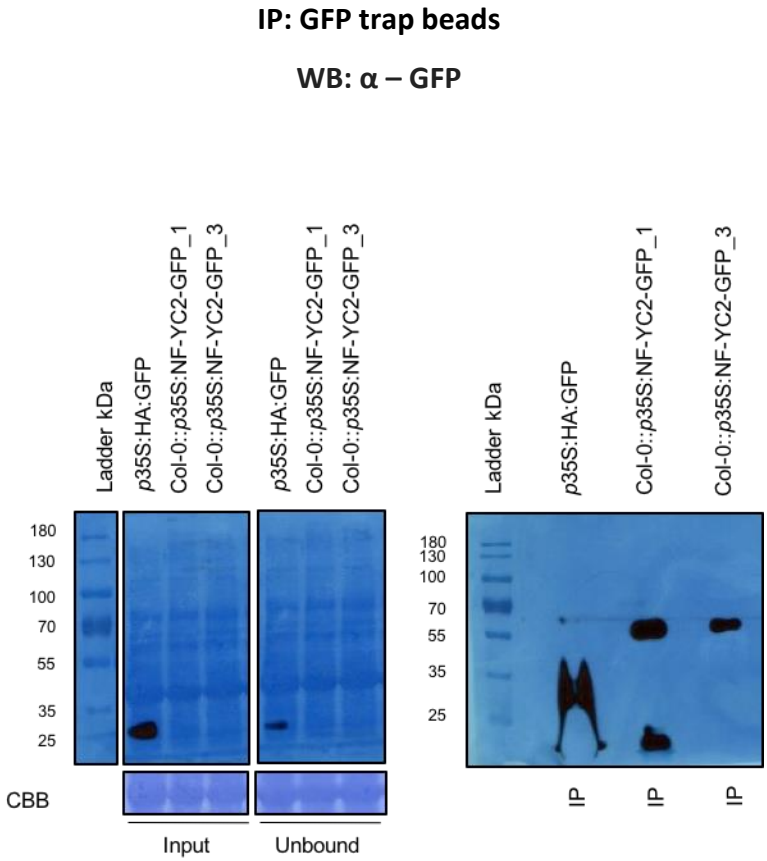

Figure 5.3 – The two C-terminal fusion proteins of NF-YC2 showed a considerable enrichment following immunoprecipitation. GFP-tagged NF-YC2 was immunoprecipitated from leaf material using anti-GFP beads. Crude plant extract, unbound fraction (blot on the left) and the immunoprecipitated proteins (blot on the right) were separated by SDS-PAGE and anti-GFP antibody was used for the immunoblots. Both Col-0::*p*35S:NF-YC2-GFP_1, Col-0::*p*35S:NF-YC2-GFP_3 show a band at 50.0 kDa representing NF-YC2-GFP protein in the IP fraction (blot on the right), a second band at 27 kDa is also visible in Col-0::*p*35S:NF-YC2-GFP_1. In the Crude and Unbound fraction of both lines no band are visible. GFP (27 kDa) band is showed in the positive control (*p*35S:HA:GFP) in all three fractions.

The two N-terminal fusion proteins of NF-YC2 (Col-0::*p*35S:GFP-NF-YC2_1 and Col-0::*p*35S:GFP-NF-YC2_2) and the *p*35S:HA:GFP control lines also showed an enrichment in the immunoprecipitation using GFP-trap beads. The western blot in Figure 5.4 shows the immunoprecipitation of NF-YC2-GFP fusion protein in Col-0::*p*35S:GFP-NF-YC2_1 and Col-0::*p*35S:GFP-NF-YC2_2 lines. A single band at 50

kDa representing NF-YC2-GFP protein in the IP fraction is shown in the Col-0::*p*35S:GFP-NF-YC2_1 line. A strong GFP signal was also detected in the IP fraction of Col-0::*p*35S:GFP-NF-YC2_2 line, showing a band at 50 kDa representing NF-YC2-GFP protein and a second one representing GFP (27 kDa). The positive control (*p*35S:HA:GFP) presented the expected GFP band at 27 kDa.

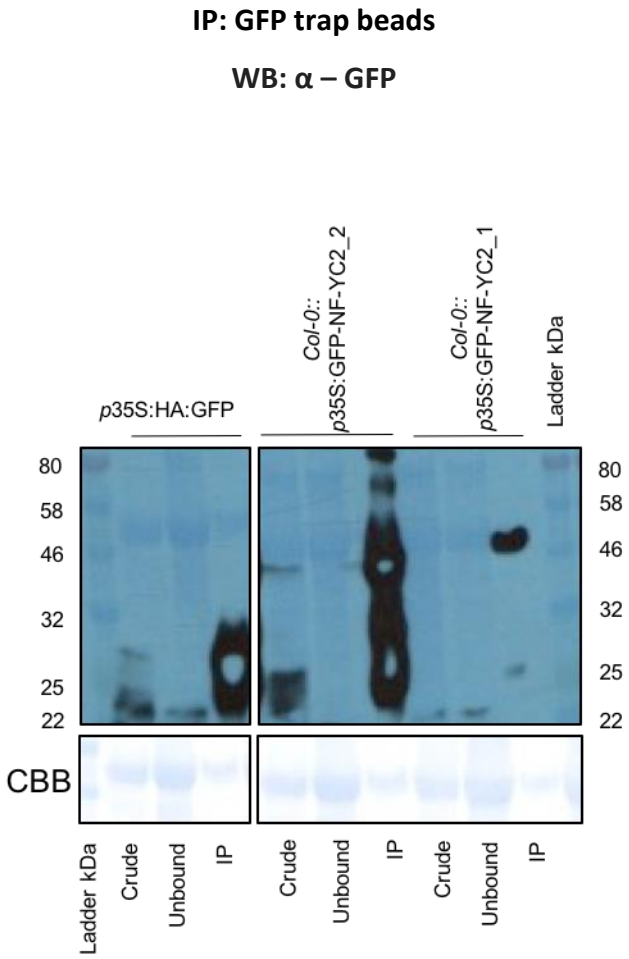

Figure 5.4 – Col-0::p35S:GFP-NF-YC2_1 and Col-0::p35S:GFP-NF-YC2_2 lines showed a considerable enrichment following immunoprecipitation. GFP-tagged NF-YC2 was immunoprecipitated from leaf material using anti-GFP beads. Crude plant extract, unbound fraction and the immunoprecipitated proteins (IP) were separated by SDS-PAGE and anti-GFP antibody was used for the immunoblots. Col-0::*p*35S:GFP-NF-YC2_1 in the IP fraction showed a single band at 50.0 kDa representing NF-YC2-GFP protein. Col-0::*p*35S:GFP-NF-YC2_2 in the IP fraction showed a very strong GFP signal: a band at 50.0 kDa representing NF-YC2-GFP protein is visible together with a band at 27 kDa representing GFP. GFP (27 kDa) band is showed in the IP fraction of the positive control (*p*35S:HA:GFP). The Crude and Unbound fraction of Col-0::*p*35S:GFP-NF-YC2_1 and *p*35S:HA:GFP show a band at 22 kDa, probably representing a cleaved version of the GFP.

After observing a clear band at the expected size (50 kDa) indicating NF-YC2-GFP protein in all four lines analyzed, samples were prepared for mass spectrometry analysis.

5.3.2.2 MS Identification of NF-YC2 interacting proteins

Co-immunoprecipitated protein from GFP-trap beads, was digested with trypsin and run on the MS for identification of NF-YC2 interacting proteins. The analysis showed a good sequence coverage for the bait corresponding to 43% (Figure 5.5). A post-translational modification such as Methionine (M) oxidation, highlighted in green, was also observed, which is commonly found in samples processed for MS and does not indicate a functionally relevant modification (Perdivara et al. 2010).

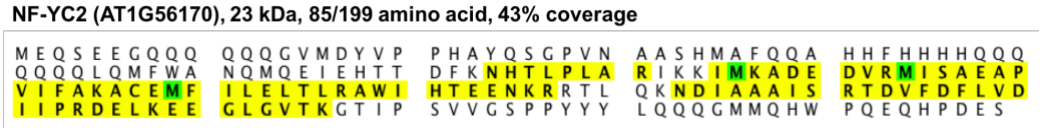

Figure 5.5 – Coverage of NF-YC2 protein sequence. Stably-expressed NF-YC2 is purified and detected successfully by mass spectrometry using beads digestion protocol. NF-YC2 sequence coverage is highlighted in yellow for peptides that were identified at least once. 43% sequence coverage was identified. Post-translational modifications such as Methionine (M) oxidation, highlighted in green arises during the sample processing.

Two experiments were carried out (Exp1 and Exp2). N-terminal and C-terminal fusion proteins of NF-YC2-GFP lines were respectively used in Exp1 and Exp2 (Table 5.1). NF-YC2 was immunoprecipitated from two independent lines in each experiment with 8 unique peptides detected in both Col-0::*p*35S:GFP-NF-YC2 lines, 10 peptides in Col-0::*p*35S:NF-YC2-GFP_1 and 8 peptides in Col-0::*p*35S:NF-YC2-GFP_3. MS detected that NF-YB2 was pulled down in both experiments along with NF-YC2. Specifically in Exp1, 5 peptides in Col-0::*p*35S:GFP-NF-YC2_1 line and 6 peptides in Col-0::*p*35S:GFP-NF-YC2_2 line of NF-YB2 were identified, while Exp2 recognized 8 unique peptides in Col-0::*p*35S:NF-YC2-GFP_1 line and 7 unique peptides in Col-0::*p*35S:NF-YC2-GFP_3 line of NF-YB2. Control samples (*p*35S:HA:GFP) did not show any of these interactions. This suggests that NF-YB2

and NF-YC2 could interact with a stoichiometric ratio 1:1. The MS identified also a good interaction between NF-YC2 and NF-YB1 subunits, since 4, 6, 4 and 5 unique peptides of NF-YB1 were found in Col-0::*p*35S:GFP-NF-YC2_1, Col-0::*p*35S:GFP-NF-YC2_2, Col-0::*p*35S:NF-YC2-GFP_1 and Col-0::*p*35S:NF-YC2-GFP_3 lines, respectively. Additionally, NF-YB10 was detected in all lines, with 2 unique peptides per line, except Col-0::*p*35S:GFP-NF-YC2_2 which showed 7 unique NF-YB10 peptides, suggesting another possible heterodimer combination with NF-YC2. However, no NF-YA2, or any NF-YA peptides, were detected in this analysis. The same result was obtained in initial experiments by Emily Breeze (2014).

In an attempt to identify an interacting A subunit, since the NF-YA2 may join the trimer in the nucleus (Kahle et al. 2005, Siefers et al. 2009) a nuclease enrichment protocol was performed on these lines to isolate nuclear proteins to try and enrich for NF-YA subunits. Additionally, formaldehyde (Sutherland et al. 2008) was used as a cross-linker to create covalent bonds between bound proteins, however, even with these modifications, MS did not detect any interaction of NF-YA subunits with NF-YC2 (data not shown).

Probability Legend:
over 95%
80% to 94%
50% to 79%
20% to 49%
0% to 19%

		Exp1			Exp2		
		*p*35S:HA:GFP	Col-0::*p*35S:GFP-NF-YC2_1	Col-0::*p*35S:GFP-NF-YC2_2	*p*35S:HA:GFP	Col-0::*p*35S:NF-YC2-GFP_1	Col-0::*p*35S:NF-YC2-GFP_3
NF-YC2 (Bait)	AT1G56170	0	8	8	0	10	8
NF-YB2	AT5G47640	0	5	6	0	8	7
NF-YB1	AT2G38880	0	4	6	0	4	5
NF-YB10	AT3G53340	0	2	7	0	2	2

Table 5.1 - Major interactors of NF-YC2. The results from two experiment (Exp1 and Exp2) involving NF-YC2 immunoprecipitation and MS. In Exp1 NF-YC2 was immunoprecipitated from two independent lines of Col-0::p35S:GFP-NF-YC2_1 and Col-0::p35S:GFP-NF-YC2_2. In Exp2 NF-YC2 was immunoprecipitated from two independent lines of Col-0::p35S:NF-YC2-GFP_1 and Col-0::p35S:NF-YC2-GFP_3. The number of exclusive unique peptide hits is shown along with a color code. Control (p35S:HA:GFP) showed no NF-Y interactions.

Table 5.2 shows other proteins identified by the MS, which represent putative NF-YC2 interactors, since they were co-immunoprecipitated together. However, these interacting proteins are not consistent across the two experiments, suggesting that they could not be real interactors of NF-YC2.

Probability Legend:
over 95%
80% to 94%
50% to 79%
20% to 49%
0% to 19%

		Exp1			Exp2		
		p35S:HA:GFP	Col-0::p35S:GFP-NF-YC2_1	Col-0::p35S:GFP-NF-YC2_2	p35S:HA:GFP	Col-0::p35S:NF-YC2-GFP_1	Col-0::p35S:NF-YC2-GFP_3
NF-YC2 (Bait)	AT1G56170	0	8	8	0	10	8
ATHDA14 | histone deacetylase 14	AT4G33470	0	4	5	0	0	0
Glycosyl hydrolases family 31 protein	AT5G11720	0	2	5	0	0	0
ATXYL1 alpha-xylosidase 1	AT1G68560	0	2	1	0	0	0
FK506-binding protein 16-2	AT4G39710	0	2	1	0	0	0
MLP-like protein 423	AT1G24020	0	1	2	0	0	0
PRXIIF, ATPRXIIF peroxiredoxin IIF	AT3G06050	0	1	2	0	0	0
PsbP family protein	AT3G56650	0	2	1	0	0	0
Clathrin, heavy chai	AT3G08530	0	0	0	0	4	3
Pectinacetylesterase family protein	AT4G19410	0	0	0	0	3	4
AOS allene oxide synthase	AT5G42650	0	0	0	0	2	2
CRD1 dicarboxylate diiron protein	AT3G56940	0	0	0	0	2	3
PSAH2 photosystem I subunit H2	AT1G52230	0	0	0	0	3	4
PL2.1 ribosomal protein L2	AT3G27830	0	0	0	0	3	2

Table 5.2 - Other putative interactors of NF-YC2. The results from two experiment (Exp1 and Exp2) involving NF-YC2 immunoprecipitation and MS. In Exp1 NF-YC2 was immunoprecipitated from two independent lines of Col-0::p35S:GFP-NF-YC2_1 and Col-0::p35S:GFP-NF-YC2_2. In Exp2 NF-YC2 was immunoprecipitated from two independent lines of Col-0::p35S:NF-YC2-GFP_1 and Col-0::p35S:NF-YC2-GFP_3. The number of exclusive unique peptide hits is shown along with a color code. Control (p35S:HA:GFP) showed no NF-Y interactions.

5.3.2.3 Co-Immunoprecipitation of NF-YB2

After obtaining evidence that NF-YC2 interacts with NF-YB2 *in planta*, Arabidopsis plants stably over expressing NF-YB2 fused to GFP and FLAG tags were generated, to confirm this interaction. Four lines containing 35S:GFP-NF-YB2 (*nf-*

yb2::*p*35S:GFP-NF-YB2_1, *nf-yb2*::*p*35S:GFP-NF-YB2_2) and 35S:FLAG-NF-YB2 (*nf-yb2*::*p*35S:FLAG-NF-YB2_1, *nf-yb2*::*p*35S:FLAG-NF-YB2_2) in *nf-yb2* knock-out mutant background, were checked for expression of NF-YB2 protein by performing immunoprecipitation followed by immunoblotting. Arabidopsis lines containing two different tags (FLAG and GFP) were used to prevent protein functionality issues that may be caused by the steric hindrance of the tag. The four homozygous overexpressor NF-YB2 tagged lines were grown under controlled conditions and immunoprecipitation of NF-YB2 GFP or FLAG tagged was performed using anti-GFP or anti-FLAG beads. Crude plant extracts, unbound and IP fractions were separated by SDS-PAGE and western blot was carried out using the relative antibody (anti-GFP or anti-FLAG). For GFP tagged lines, *p*35S:HA:GFP line was used as positive control, while for FLAG tagged lines a *p*35S:GFP:FLAG line was used. All four lines showed a significant enrichment of NF-YB2 protein following immunoprecipitation. Specifically, both *nf-yb2*::*p*35S:GFP-NF-YB2_1 and *nf-yb2*::*p*35S:GFP-NF-YB2_2 lines showed a band at the expected size 47 kDa (27 kDa GFP +20 kDa NF-YB2) representing NF-YB2-GFP in the IP fraction together with a band at 27 kDa representing free GFP and a band at 40 kDa possibly representing a cleaved product (Figure 5.6). The positive control (*p*35S:HA:GFP) showed the expected GFP band at 27 kDa in the IP fraction. The western blot in Figure 5.7 illustrates the immunoprecipitation of NF-YB2-FLAG in both *nf-yb2*::*p*35S:FLAG-NF-YB2_1 and *nf-yb2*::*p*35S:FLAG-NF-YB2_2 lines, showing a band of 20 kDa in all three fractions, being more consistent in the IP fraction. Other bands are present in the crude and unbound fractions, likely representing non-specific bands, since in this western blot Bovin Serum Albumin (BSA) was used for blocking the membrane and is known to have higher nonspecific signal compared to 5% TBS-T milk. In the positive control (*p*35S:GFP:FLAG) a band at 27 kDa is visible in the IP fraction representing the GFP-FLAG tag protein.

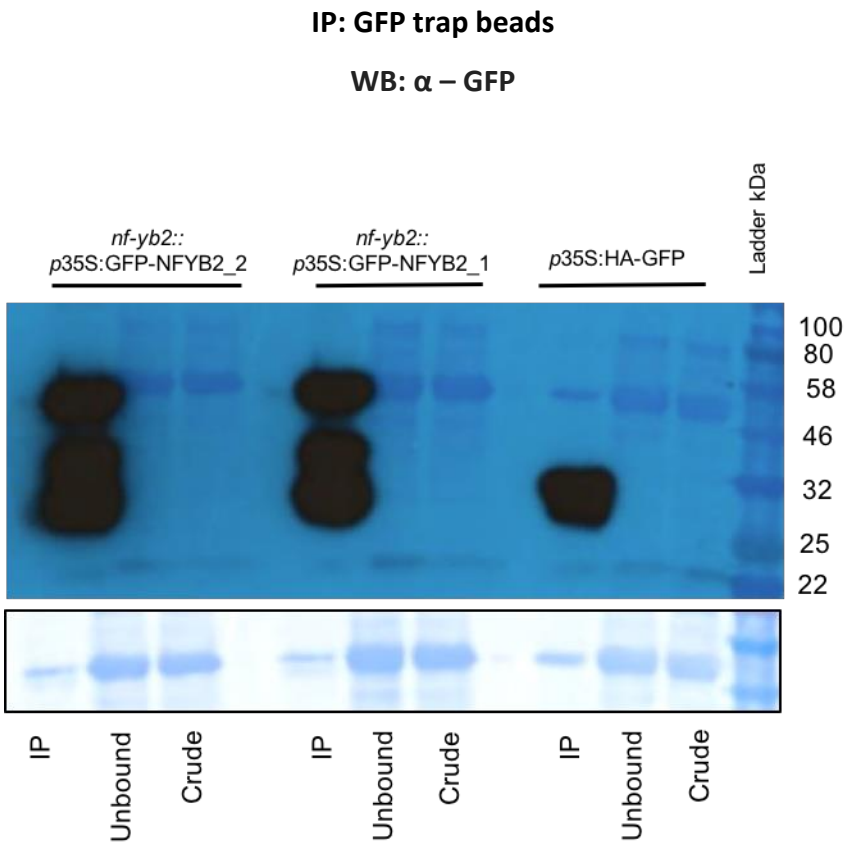

Figure 5.6 – *nf-yb2*::p35S:GFP-NF-YC2_1 and *nf-yb2*::p35S:GFP-NF-YC2_2 lines showed a considerable enrichment of NF-YB2 protein following immunoprecipitation. GFP-tagged NF-YB2 was immunoprecipitated from leaf material using anti-GFP beads. Crude plant extract, unbound fraction and the immunoprecipitated proteins (IP) were separated by SDS-PAGE and anti-GFP antibody was used for the immunoblots. Both lines in the IP fraction showed a band at 47 kDa representing NF-YB2-GFP protein. In the same fraction the band at 27 kDa is GFP and the band at 40 kDa is a cleaved product. The positive control showed the GFP band (27 kDa) in the IP fraction.

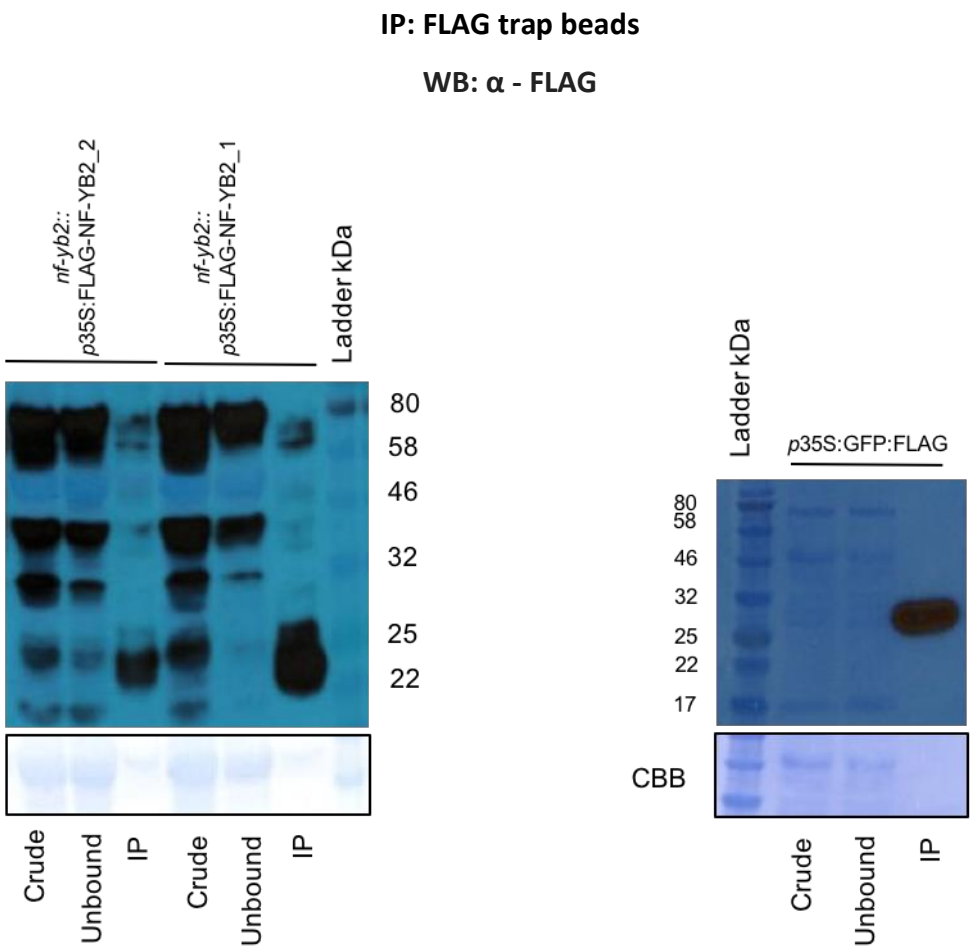

Figure 5.7 – *nf-yb2*::p35S:FLAG-NF-YC2_1 and *nf-yb2*::p35S:FLAG-NF-YC2_2 lines showed a considerable enrichment following immunoprecipitation. FLAG-tagged NF-YB2 was immunoprecipitated from leaf material using anti-FLAG beads. Crude plant extract, unbound fraction and the immunoprecipitated proteins (IP) were separated by SDS-PAGE and anti-FLAG antibody was used for the immunoblots. Both lines in all three fractions (Crude, Unbound, IP) showed a single band at 20 kDa representing NF-YB2-FLAG protein, with a stronger band in the IP sample. Other bands showed are unspecific bands since in this blot Bovin Serum Albumin (BSA) was used for blocking the membrane, this buffer facilitate nonspecific signal. The positive control (blot on the right) showed the GFP-FLAG tag protein (27 kDa) band in the IP fraction.

After seeing a strong expression pattern of NF-YB2 in the IP fraction of all lines analyzed, which showed the correct size of the tagged protein, MS analysis was performed on these samples to investigate specific NF-Y complexes functioning *in planta*.

5.3.2.4 MS Identification of NF-YB2 interacting proteins

The MS analysis showed 84% sequence coverage for the bait NF-YB2 (Figure 5.8). Interestingly, multiple post-translational modifications were identified along the protein sequence including the phosphorylation of Serine (S) and Threonine (T) and the deamidation of Asparagine (N) and Glutamine (Q) while Methionine oxidation is commonly found in samples processed for MS. The presence of these modifications could suggest an additional level of NF-YB2 regulation through post-translational modification.

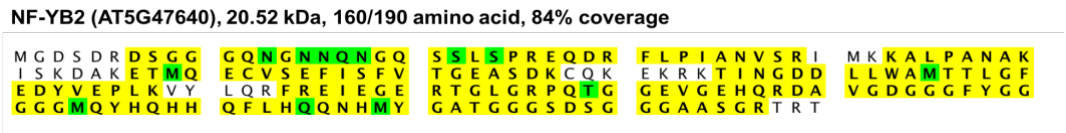

Figure 5.8 – Coverage of NF-YB2 protein sequence. Stably-expressed NF-YB2 is purified and detected successfully by mass spectrometry using beads digestion protocol. NF-YB2 sequence coverage is highlighted in yellow for peptides that were identified at least once. 84% sequence coverage was identified. Post-translational modifications, highlighted in green, such as Serine (S) and Threonine (T) phosphorylation and Asparagine (N) and Glutamine (Q) deamidation was observed. Methionine (M) oxidation arises during the sample processing.

Two experiments were carried out (Exp1 and Exp2). NF-YB2-GFP and NF-YB2-FLAG tagged lines were respectively used in Exp1 and Exp2 (Table 5.3) and NF-YB2 was immunoprecipitated from two independent lines in each experiment. Exp1 was performed twice with Exp1(Rep) as its replicate. Exp1 identified 12 unique peptides of NF-YB2 in *nf-yb2*::*p*35S:GFP-NF-YB2_1 and *nf-yb2*::*p*35S:GFP-NF-YB2_2 lines, while Exp1(Rep) recognized 10 unique peptides in both *nf-yb2*::*p*35S:GFP-NF-YB2 lines. This result is consistent with Exp2, which recognized 5 and 10 unique peptides of NF-YB2 in *nf-yb2*::*p*35S:FLAG-NF-YB2_1 and *nf-yb2*::*p*35S:FLAG-NF-YB2_2 lines respectively. The MS detected that NF-YC2 was pulled down in all three experiments along with NF-YB2, in agreement with the result obtained in the immunoprecipitation of NF-YC2 GFP tagged protein. Hence, 6 and 5 unique peptides of NF-YC2 were identified in Exp1 and Exp1(Rep) in both lines (*nf-yb2*::*p*35S:GFP-NF-YB2_1 and *nf-yb2*::*p*35S:GFP-NF-YB2_2), while 3 peptides were identified in *nf-yb2*::*p*35S:FLAG-NF-YB2_1 line and 5 peptides in *nf-yb2*::*p*35S:FLAG-NF-YB2_2 line. Furthermore, NF-YC9 was detected in all lines in

both experiments, with 9 and 10 unique peptides in *nf-yb2*::*p*35S:GFP-NF-YB2_1 and *nf-yb2*::*p*35S:GFP-NF-YB2_2 lines respectively, 7 peptides of NF-YC9 in both lines of Exp1(Rep) and 5 unique peptides of NF-YC9 in *nf-yb2*::*p*35S:FLAG-NF-YB2_1 and *nf-yb2*::*p*35S:FLAG-NF-YB2_2 lines. In addition, the MS analysis showed another possible interaction of NF-YB2 with NF-YC4, which was recognized in Exp1 and Exp2. 8 and 7 NF-YC4 unique peptides were identified in *nf-yb2*::*p*35S:GFP-NF-YB2_1 and *nf-yb2*::*p*35S:GFP-NF-YB2_2 lines respectively, while 5 NF-YC4 unique peptides were found in *nf-yb2*::*p*35S:FLAG-NF-YB2_1 line and 7 in *nf-yb2*::*p*35S:FLAG-NF-YB2_2 line. However, no NF-YC4 peptides were identified in Exp1(Rep). An interaction between NF-YB2 and NF-YC1 was identified only in Exp1(Rep) having 6 unique peptides per line. Controls samples (*p*35S:HA:GFP and *p*35S:FLAG:GFP) did not show any of these interactions. Unfortunately, again (as with the NF-YC2 pull downs) no NF-YA subunits were detected in any of these NF-YB2 pull down experiments.

Probability Legend:

- over 95%
- 80% to 94%
- 50% to 79%
- 20% to 49%
- 0% to 19%

		Exp1			Exp1 (Rep)			Exp2		
		p35S:HA:GFP	*nf-yb2::p35S:GFP-NF-YB2_1*	*nf-yb2::p35S:GFP-NF-YB2_2*	*p35S:HA:GFP*	*nf-yb2::p35S:GFP-NF-YB2_1*	*nf-yb2::p35S:GFP-NF-YB2_2*	*p35S:FLAG:GFP*	*nf-yb2::p35S:FLAG-NF-YB2_1*	*nf-yb2::p35S:FLAG-NF-YB2_2*
NF-YB2 (Bait)	AT1G56170	0	12	12	0	10	10	0	5	10
NF-YC2	AT5G47640	0	6	6	0	5	5	0	3	5
NF-YC9	AT2G38880	0	9	10	0	7	7	0	5	5
NF-YC4	AT3G53340	0	8	7	0	0	0	0	5	7
NF-YC1	AT3G48590	0	0	0	0	6	6	0	0	0

Table 5.3 - Major interactors of NF-YB2. The results from two experiments (Exp1 and Exp2) involving NF-YB2 immunoprecipitation and MS. In Exp1 NF-YB2 was immunoprecipitated from the independent lines *nf-yb2*::p35S:GFP-NF-YB2_1 and *nf-yb2*::p35S:GFP-NF-YB2_2. In Exp2 NF-YB2 was immunoprecipitated from the independent lines *nf-yb2*::p35S:FLAG-NF-YB2_1 and *nf-yb2*::p35S:FLAG-NF-YB2_2. The number of exclusive unique peptide hits is shown along with a color code. Controls (p35S:HA:GFP and p35S:FLAG:GFP) showed no NF-Y interacting peptides.

Table 5.4 displays other putative NF-YB2 interacting proteins identified by the MS, since they were co-immunoprecipitated together. However, these interactors appeared not to be consistent across all three experiments, raising doubt regarding their ability to form a complex with NF-YB2 protein. Hence, further investigation need to be done to elucidate and confirm an involvement of these proteins in this interaction.

Probability Legend:
over 95%
80% to 94%
50% to 79%
20% to 49%
0% to 19%

		Exp1			Exp1 (Rep)			Exp2		
		p35S:HA:GFP	*nf-yb2*::p35S:GFP-NF-YB2_1	*nf-yb2*::p35S:GFP-NF-YB2_2	*p35S:HA:GFP*	*nf-yb2*::p35S:GFP-NF-YB2_1	*nf-yb2*::p35S:GFP-NF-YB2_2	*p35S:FLAG:GFP*	*nf-yb2*::p35S:FLAG-NF-YB2_1	*nf-yb2*::p35S:FLAG-NF-YB2_2
NF-YB2 (Bait)	AT1G56170	0	12	12	0	10	10	0	5	10
RPS6A ribosomal protein S6	AT4G31700	0	1	2	0	0	0	0	0	0
GSTU19 glutathione S-transferase	AT1G78380	0	1	2	0	0	0	0	0	0
UQCRX/QCR9-like family protein	AT3G52730	0	1	2	0	0	0	0	0	0
ketose-bisphosphate aldolase	AT1G18270	0	0	0	0	3	5	0	1	2
NADH-ubiquinone oxidoreductase	AT4G02580	0	0	0	0	3	2	0	1	2
CCR1	AT4G39260	0	0	0	0	3	1	0	0	0
SUS1	AT5G20830	0	0	0	0	3	2	0	0	4
ATB' ALPHA	AT5G03470	0	0	0	0	3	2	0	0	0

Table 5.4 – Other putative interactors of NF-YB2. The results from two experiments (Exp1 and Exp2) involving NF-YB2 immunoprecipitation and MS. In Exp1 NF-YB2 was immunoprecipitated from the independent lines *nf-yb2*::p35S:GFP-NF-YB2_1 and *nf-yb2*::p35S:GFP-NF-YB2_2. In Exp2 NF-YB2 was immunoprecipitated from the independent lines *nf-yb2*::p35S:FLAG-NF-YB2_1 and *nf-yb2*::p35S:FLAG-NF-YB2_2. The number of exclusive unique peptide hits is shown along with a color code. Controls (p35S:HA:GFP and p35S:FLAG:GFP) showed no NF-Y interacting peptides.

5.3.2.5 Co-Immunoprecipitation of NF-YA2

Because the MS did not detect NF-YA2 when either NF-YC2 and NF-YB2 were immunoprecipitated, the immunoprecipitation of NF-YA2 tagged protein was attempted followed by MS of Co-IP. To carry out this analysis Arabidopsis lines stably expressing NF-YA2 GFP and FLAG tagged under the NF-YA2 native promoter or 35S promoter were generated (Table 3.1). Specifically, *nf-ya2*::*p*35S:FLAG-NF-YA2, *Col-0*::*p*35S:FLAG-NF-YA2 and *Col-0*::*p*35S:GFP-NF-YA2 lines were checked for expression of NF-YA2 protein using immunoprecipitation and western blot analysis. Two homozygous independent lines for each of these constructs were

grown under controlled conditions and the immunoprecipitation of NF-YA2 tagged protein was carried out using anti-GFP or anti-FLAG beads, according to the tag. For each line crude, unbound and IP fractions were separated by SDS-PAGE gel and blotted using anti-GFP or anti-FLAG antibody.

The western blot in Figure 5.9 shows that NF-YA2 could not be detected in the *nf-ya2*::*p*35S:FLAG-NF-YA2_1 and *nf-ya2*::*p*35S:FLAG-NF-YA2_2 lines, hence a band of the expected size (32 kDa) was not visible in the IP fraction. All bands observed in the crude and unbound fractions are unspecific bands, since BSA was used for blocking the membrane, which increase nonspecific protein signal but enhance the possibility of detecting low abundance protein such as NF-YA2. *nf-yb2*::*p*35S:FLAG-NF-YB2_1 was used as a positive control in this immunoblot, showing in the IP and in the crude fractions a band of the expected size 20 kDa, with a stronger signal in the IP fraction.

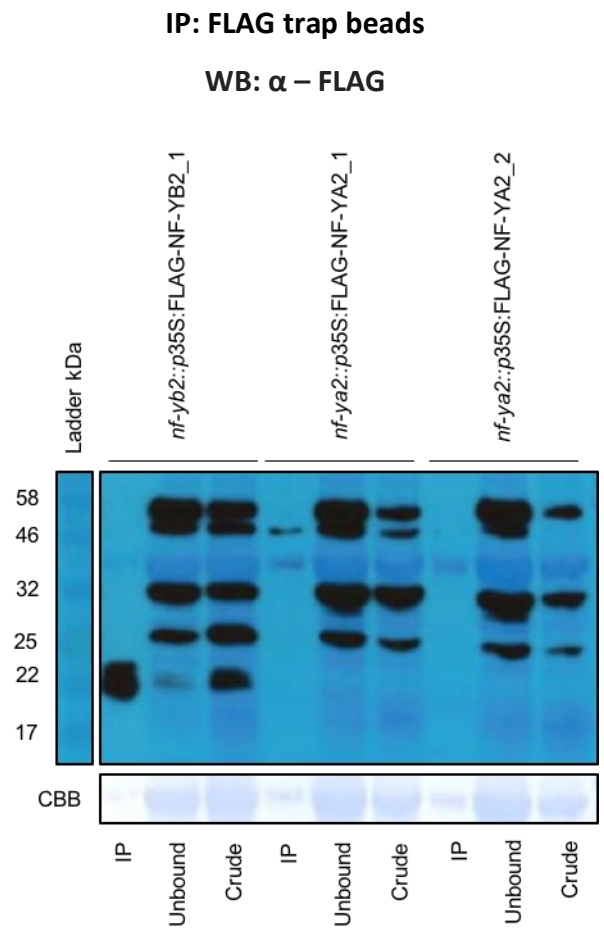

Figure 5.9 – NF-YA2 was not immunoprecipitated in *nf-ya2*::*p*35S:FLAG-NF-YA2_1 and *nf-ya2*::*p*35S:FLAG-NF-YA2_2 lines. FLAG-tagged NF-YA2 was immunoprecipitated from leaf material using anti-FLAG beads. Crude plant extract, unbound fraction and the immunoprecipitated proteins (IP) were separated by SDS-PAGE and anti-FLAG antibody was used for the immunoblots. Both lines in the IP fraction did not showed a band of the expected size 32 kDa representing NF-YA2-FLAG protein. *nf-yb2*::*p*35S:FLAG-NF-YB2_1 was used as positive control, showing a band in the IP fraction of the expected size 20 kDa.

This result is consistent with the immunoprecipitation of NF-YA2-FLAG from Col-0::*p*35S:FLAG-NF-YA2_1 and Col-0::*p*35S:FLAG-NF-YA2_2 lines (Figure 5.10), hence even in this experiment no bands representing NF-YA2 tagged protein were observed in the IP fraction. Only the positive control *nf-yb2*::*p*35S:FLAG-NF-YB2_1 showed in the IP fraction a band of the expected size 21 kDa.

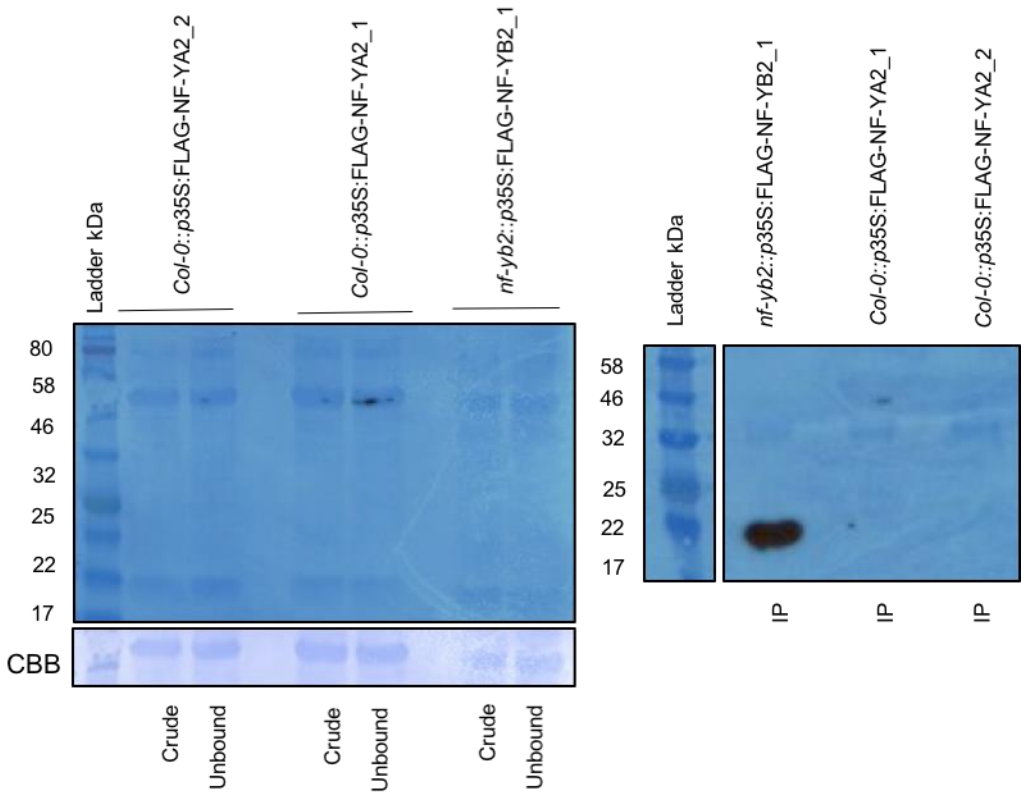

Figure 5.10 – NF-YA2 was not immunoprecipitated in *Col-0*::*p*35S:FLAG-NF-YA2_1 and *Col-0*::*p*35S:FLAG-NF-YA2_2 lines. FLAG-tagged NF-YA2 was immunoprecipitated from leaf material using anti-FLAG beads. Crude plant extract, unbound fraction and the immunoprecipitated proteins (IP) were separated by SDS-PAGE and anti-FLAG antibody was used for the immunoblots. Both lines in the IP fraction did not showed a band of the expected size 32 kDa representing NF-YA2-FLAG protein. *nf-yb2*::*p*35S:FLAG-NF-YB2_1 was used as positive control, showing a band in the IP fraction of the expected size 21 kDa.

The immunoprecipitation of NF-YA2-GFP from *Col-0*::*p*35S:GFP-NF-YA2_1 and *Col-0*::*p*35S:GFP-NF-YA2_2 lines also did not yield detectable NF-YA2 protein (NF-YA2+GFP= 59.1 kDa) (Figure 5.11). The positive control *p*35S:HA:GFP lines showed a GFP strong band of the correct size (27 kDa) in the IP fraction, suggesting the reliability of the pull down and western blot.

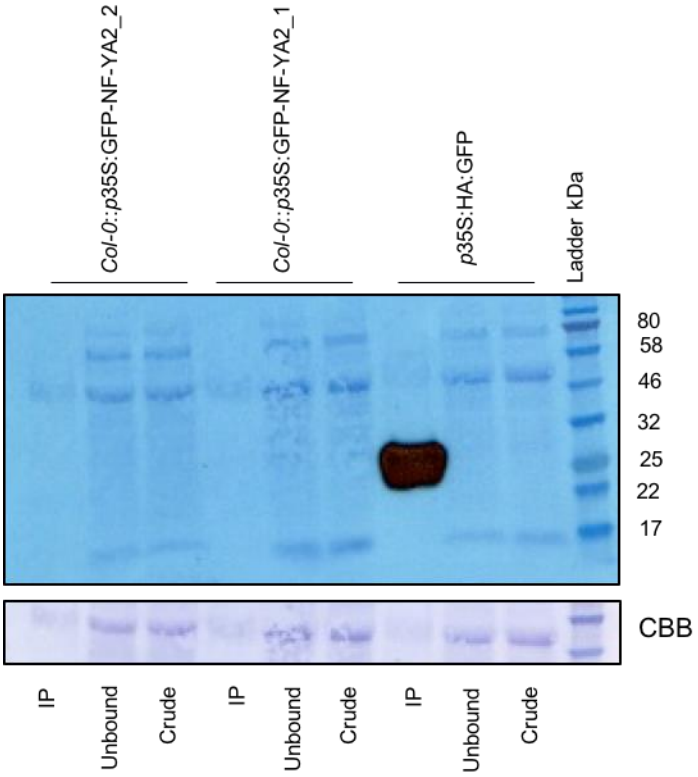

Figure 5.11 – NF-YA2 was not immunoprecipitated in *Col-0*::p35S:GFP-NF-YA2_1 and *Col-0*::p35S:GFP-NF-YA2_2 lines. GFP-tagged NF-YA2 was immunoprecipitated from leaf material using anti-GFP beads. Crude plant extract, unbound fraction and the immunoprecipitated proteins (IP) were separated by SDS-PAGE and anti-GFP antibody was used for the immunoblots. Both lines in the IP fraction did not showed a band of the expected size 59.1 kDa representing NF-YA2-GFP protein. *p*35S:HA:GFP was used as positive control, showing the GFP band in the IP fraction of the expected size 27 kDa.

These results indicate that, despite the fact that different Arabidopsis lines stably expressing GFP and FLAG tagged NF-YA2 protein were generated and analyzed, it was not possible to detect NF-YA2 protein. Indeed, NF-YA2 was not detectable even after immunoprecipitation, suggesting that the protein could be expressed at very low level.

Moreover, to prevent the possibility that the overexpression of NF-YA2 can cause cellular defect (Vavouri et al. 2009) due to overload of cellular resources, stoichiometric imbalance between subunits or promiscuous protein-protein

interactions (Moriya 2015), Arabidopsis NF-YA2 epitope tagged lines under the NF-YA2 native promoter were also generated (Chapter 3).

Two homozygous independent *nf-ya2*::pNF-YA2:NF-YA2-GFP lines were grown under controlled conditions and checked for expression of NF-YA2 protein using immunoprecipitation and immunoblotting. Immunoprecipitation of NF-YA2 tagged protein was carried out using anti-GFP beads. For each line, crude, unbound and IP fractions were separated by SDS-PAGE gel and blotted using anti-GFP antibody. The western blot in Figure 5.12 illustrates that the crude, the unbound and the IP fractions did not show any band at the expected size 59.1 kDa representing NF-YA2-GFP. A band at 20 kDa is present in all crude and unbound samples, which is probably an unspecific band being also present in Col-0 with no tag. The immunoprecipitation (blot on the right) showed only a GFP band (27 kDa) in the positive control (*p*35S:HA:GFP).

In agreement with this result qPCR analysis performed on *nf-ya2*::*p*NF-YA2:NF-YA2-GFP revealed a very low expression level of NF-YA2 gene in these lines (Figure 3.8) almost comparable to the level observed in *nf-ya2* KO mutants. Interestingly, despite the low level of NF-YA2 revealed in *nf-ya2*::*p*NF-YA2:NF-YA2-GFP lines, confocal imaging showed a GFP signal localized exclusively in the nucleus (Figure 5.1) in agreement with previous report (Laloum et al. 2013), differentially from the OE NF-YA2-GFP lines.

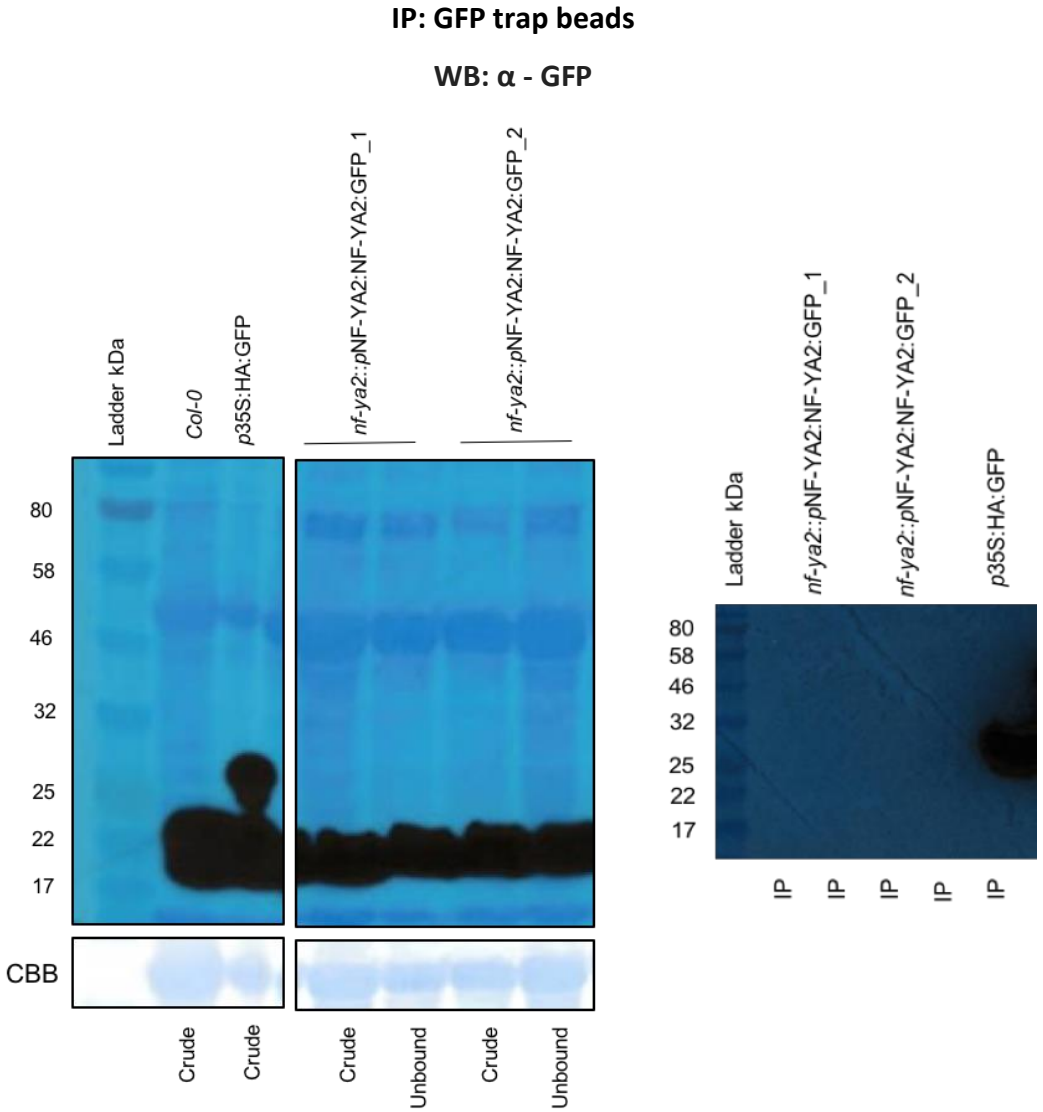

Figure 5.12 – NF-YA2 was not immunoprecipitated in *nf-ya2*::pNF-YA2:NF-YA2-GFP_1 and *nf-ya2*::pNF-YA2:NF-YA2-GFP_2 lines. GFP-tagged NF-YA2 was immunoprecipitated from leaf material using anti-GFP beads. Crude plant extract, unbound fraction and the immunoprecipitated proteins (IP) were separated by SDS-PAGE and anti-GFP antibody was used for the immunoblots. Both lines in the IP fraction did not showed a band of the expected size 59.1 kDa representing NF-YA2-GFP protein. *p*35S:HA:GFP was used as a positive control, showing the GFP band in the crude fraction of the expected size 27 kDa.

Furthermore, because the NF-YA2 level was low in *nf-ya2*::*p*NF-YA2:NF-YA2-GFP lines and only present in the nucleus, as shown in the confocal analysis, a nuclear enrichment protocol was used to enhanced the possibility of detecting NF-YA2 protein, but still no signal was visible in any protein fractions (data not shown).

As tagged NF-YA2 could not be detected in western blots, MS analysis was performed on only a few NF-YA2 lines in case this technique was able to detect very low abundance of NF-YA2 peptides and interactors.

5.3.2.6 MS Identification of NF-YA2 interacting proteins

After following the same protocol as with the NF-YB2 and NF-YC2 MS procedure, NF-YA2 was immunoprecipitated from Arabidopsis *nf-ya2*::*p*35S:FLAG-NF-YA2_1, *Col-0*::*p*35S:GFP-NF-YA2_1 and *nf-ya2*::*p*NF-YA2:NF-YA2-GFP_1 lines. One sample from each line was analyzed to investigate if it was possible to detect the NF-YA2 subunit, exploiting the high MS sensitivity. The MS identified 6 unique peptides of NF-YA2 only in the *nf-ya2*::*p*35S:FLAG-NF-YA2_1 line (Table 5.5) showing a coverage of approximately 27% (Figure 5.13). A few post-translational modifications were identified along the protein sequence such as Serine (S) phosphorylation and Methionine (M) oxidation, commonly found in samples processed for MS.

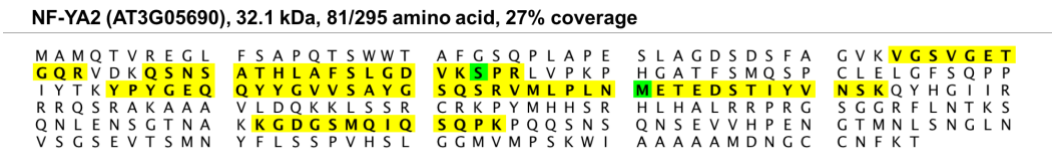

Figure 5.13 – Coverage of NF-YA2 protein sequence. Stably-expressed NF-YA2 is purified and detected by mass spectrometry using beads digestion protocol. NF-YA2 sequence coverage is highlighted in yellow for peptides that were identified at least once. 27% sequence coverage was identified. Post-translational modifications, highlighted in green, such as Serine (S) phosphorylation and Methionine (M) oxidation, which arises during the sample processing, were observed.

However, the MS did not identify other NF-YA2 interacting proteins belonging NF-Y family (Table 5.5). Additionally, because in any other NF-YA2 lines analyzed on the MS was not possible to detect any NF-YA2 peptides, following investigation on the putative NF-YA2 interactors were carried out only on *nf-ya2*::p35S:FLAG-NF-YA2_1 line.

Probability Legend:		p35S:HA:GFP	p35S:FLAG:GFP	*nf-ya2*::p35S:FLAG-NF-YA2_1	*Col-0*::p35S:GFP-NF-YA2_1	*nf-ya2*::pNF-YA2:NF-YA2-GFP_1
over 95%						
80% to 94%						
50% to 79%						
20% to 49%						
0% to 19%						
NF-YA2 (Bait)	AT1G56170	0	0	6	0	0
NF-YB2	AT5G47640	0	0	0	0	0
NF-YC2	AT2G38880	0	0	0	0	0
NF-Ys		0	0	0	0	0

Table 5.5 – The MS did not identify any NF-Y interactor subunits with NF-YA2. The results from different NF-YA2 tagged lines (*nf-ya2*::p35S:FLAG-NF-YA2_1, Col-0::p35S:GFP-NF-YA2_1 and *nf-ya2*::pNF-YA2:NF-YA2-GFP_1) involving NF-YA2 immunoprecipitation and MS. No NF-Y interactors were found. The number of exclusive unique peptide hits is shown along with a color code indicating the probability of the peptide. Controls (p35S:HA:GFP and p35S:FLAG:GFP) showed 0 NF-Y interactions.

Table 5.6 shows putative interactors of NF-YA2. Overall, MS analysis revealed that most of the interactor proteins presented here have a role in post-transcriptional regulation of NF-YA2. Specifically, 10 unique peptides of CC1-like and 8 unique peptides of U2 snRNP auxiliary factor, both splicing factors, have been identified, which are also the most abundant peptides. Moreover 6 peptides of Nucleosome assembly protein (NAP), were recognized, which are involved in regulating gene expression (Son O. et al. 2015) together with few RNA-binding proteins (RBPs) which are central regulatory factors controlling post-transcriptional RNA metabolism in plant (Lee K. and Kang 2016). Several classes of zinc-finger were also identified which have a role in DNA-binding and protein-protein interaction domains (Stege et al. 2002, Takatsuji 1998). Conversely, it was not possible to confirm these NF-YA2 interacting proteins, since it was not possible to analyze other lines. However, most of the protein identified are clearly nuclear protein and this is in line with the fact that NF-YA2 is localized in the nucleus. Following investigation to analyze the other NF-YA2 OE lines need to be carried out to confirm the consistency of these NF-YA2 interacting proteins

Probability Legend:			p35S:FLAG:GFP	nf-ya2::p35S:FLAG-NF-YA2_1
over 95%				
80% to 94%				
50% to 79%				
20% to 49%				
0% to 19%				
Nuclear factor Y, subunit A2 (Bait)	AT3G05690	32 kDa	0	6
Ribosomal protein L4/L1 family	AT3G09630	45 kDa	0	2
Glutathione S-transferase 6	AT1G02930	23 kDa	0	2
Arginine/serine-rich splicing factor 35	AT4G25500	40 kDa	0	2
Photosystem II subunit P-1	AT1G06680	24 kDa	0	2
Metacaspase 4	AT1G79340	45 kDa	0	2
RNA recognition motif and CCHC-type zinc finger domains containing protein	AT2G24590	22 kDa	0	3
Alpha/beta-Hydrolases superfamily protein	AT3G23600	26 kDa	0	3
RNA-binding (RRM/RBD/RNP motifs) family protein	AT1G02840	34 kDa	0	2
Rotamase CYP 4	AT3G62030	28 kDa	0	2
RS-containing zinc finger protein 21	AT1G23860	22 kDa	0	5
Ribosomal protein L1p/L10e family	AT2G27530	24 kDa	0	2
Pectin methylesterase 3	AT3G14310	64 kDa	0	4
Splicing factor, CC1-like	AT2G16940	63 kDa	0	10
Translation elongation factor EF1B/ribosomal protein S6 family protein	AT5G19510	24 kDa	0	2
Glutathione S-transferase PHI 9	AT2G30860	24 kDa	0	3
Eukaryotic translation initiation factor 5A-1 (eIF-5A 1) protein	AT1G26630	17 kDa	0	4
U2 snRNP auxilliary factor, large subunit, splicing factor	AT1G60900	66 kDa	0	8
Thioredoxin M-type 1	AT1G03680	20 kDa	0	4
Histone acetyltransferase of the GNAT family 2	AT5G56740	53 kDa	0	4
Nucleosome assembly protein 1;2	AT2G19480	44 kDa	0	6
SECY homolog 1	AT2G18710	59 kDa	0	2
Glycosyl hydrolase family 10 protein / carbohydrate-binding domain-containing protein	AT1G10050	118 kDa	0	4
MD-2-related lipid recognition domain-containing protein	AT3G44100	16 kDa	0	2
Glutaredoxin family protein	AT5G40370	12 kDa	0	2
Zinc finger C-x8-C-x5-C-x3-H type family protein	AT5G42820	33 kDa	0	3
Little nuclei4	AT5G65770	121 kDa	0	2
Polyketide cyclase/dehydrase and lipid transport superfamily protein	AT4G23670	18 kDa	0	3
Splicing factor PWI domain-containing protein / RNA recognition motif (RRM)-containing protein	AT1G60200	101 kDa	0	3
Pentatricopeptide repeat (PPR) superfamily protein	AT3G49140	56 kDa	0	2
Zinc knuckle (CCHC-type) family protein	AT1G75560	29 kDa	0	2
RNA-binding (RRM/RBD/RNP motifs) family protein	AT3G61860	31 kDa	0	2

Table 5.6 - Major interactors of NF-YA2. The most significant interactors are shown from all MS analyses performed. The number of exclusive unique peptide hits is shown along with a color code indicating the peptide probability.

5.4 Discussion

This chapter attempted to identify NF-YA2 interacting NF-YB and NF-YC subunits (and other proteins) as well as specifically test the existence of the trimer NF-YA2/NF-YB2/NF-YC2 *in planta*. It is well reported that each NF-Y subunit requires the collaboration of other NF-Ys and perhaps the interaction with other TFs in order to target specific genes and regulate their transcription. This suggests a significant regulatory ability of these TFs family, which can modulate the nature of the complex according to endogenous and exogenous stimuli. With this complexity, identifying the specific composition of functional NF-Y trimer *in vivo* has proven exceptionally difficult (Swain et al. 2017).

5.4.1 Localization of NF-YA2, NF-YB2 and NF-YC2 in Arabidopsis transgenic lines.

In this chapter, the subcellular localization of NF-YA2, NF-YB2 and NF-YC2 transiently expressed in *N. benthamiana* leaves in the previous chapter, was confirmed by confocal imaging of Arabidopsis leaves stably expressing NF-YA2, NF-YB2 and NF-YC2 GFP tagged protein. NF-YA2 was localized to the nucleus, while NF-YB2 and NF-YC2 were localized in both the cytoplasm and nucleus of Arabidopsis epidermal cells. This result is in line with previous studies which have proposed a specific regulatory mechanism of NF-Y in plant (Hackenberg et al. 2012, Laloum et al. 2013, Zhao et al. 2016) where NF-YB and NF-YC members dimerize in the cytoplasm and then translocate into the nucleus to join the specific NF-YA subunit, forming the hetero-trimer and starting the target gene transcription.

5.4.2 Identification of NF-Y interacting proteins

Co-IP and MS results were queried to find evidence for the existence of the NF-Y putative trimer (NF-YA2, NF-YB2 and NF-YC2). Previous publications have pointed towards the capability of NF-YB2 to dimerize with NF-YC2 in yeast (Calvenzani et al. 2012) and this interaction was confirmed *in vivo* by the BiFC assay in the

previous chapter. In this chapter, MS analysis performed on NF-YC2 and NF-YB2 epitope tagged lines found strong evidence of this interaction *in planta.* Results obtained on different Co-IP experiments carried out on independent overexpressor NF-YC2 and NF-YB2 GFP or FLAG tagged lines, were consistent, identifying identical NF-Y interactor proteins. Interestingly, Co-IP of NF-YC2 protein pulled down not only NF-YB2 but also NF-YB1 and NF-YB10, raising the possibility that these NF-YB proteins may participate in the formation of the functional transcriptional complex with NF-YC2 protein in a combinatorial manner, in order to regulate the transcription of specific genes. This is in agreement with Calvenzani et al. (2012) where Y2H methodology was used to systematically analyze the ability of each member of NF-YB and NF-YC family to interact in pair with each other. The result showed that in general most NF-YB and NF-YC subunits are able to dimerize, and in particular NF-YC2 subunit can strongly interact with NF-YB2, NF-YB1 and NF-YB10. In support to this result, it has been reported that NF-YB1 as well as NF-YC2 mediate the response to drought stress and endoplasmic reticulum (ER) stress. Together with the transcription factor bZIP28, NF-Y binds to the *endoplasmic reticulum stress responsive element I* (ERSE-I) in combination with the CCAAT-box element (Hackenberg et al. 2012). Moreover, a bioinformatics search on STRING database (https://string-db.org), which shows known and predict protein-protein interactions, confirmed the interactions between NF-YC2 and NF-YB10.

The reciprocal Co-IP experiment performed on NF-YB2 tagged protein, showed a similar result to the Co-IP experiment carried out on NF-YC2. Hence, the MS identified that NF-YC2 together with NF-YC9, NF-YC4 and NF-YC1 was pulled down with NF-YB2 as bait protein. Previous studies reported that NF-YC9 and NF-YC4 have an overlapping functionality in flowering time, since CONSTANS (CO) requires these NF-YC subunits to trigger the transcriptional activation of FT gene (Kumimoto et al. 2010). Furthermore, Kumimoto et al. (2010) showed that NF-YC3, NF-YC4 and NF-YC9 can physically interact with NF-YB2 in the Y2H analysis, being consistent with the results obtained by MS analysis performed in this

chapter. Previous study reported that NF-YC4 and NF-YC9 are the closest NF-YC homologs in the NF-YC family (Petroni et al., 2012), however the MS identified unique peptides for each protein. Siefers et al. (2009) revealed that *NF-YC4* and *NF-YC9* are expressed in light- and dark-grown young *Arabidopsis* seedlings. Additionally, a most recent study demonstrated that NF-YC4, and NF-YC9 function as positive regulators of photomorphogenesis in *Arabidopsis* (Myers et al., 2016). The MS results obtained in this study suggest that perhaps as a response to various environmental conditions, NF–Y combinatorial diversity could provide unique platforms for the gene fine-tuning during plant stress or developmental responses. In addition, NF–Y subunit heterogeneity at a given promoter might also provide antagonistic gene regulation. For example, there may be both positive and negative NF–Y complexes competing for regulation of the same gene promoter. The diverse roles of NF-YCs, together with those of the other two NF-Y subunits NF-YA and NF-YB, imply the widely flexible formation of NF-Y complexes spatially and temporally regulated by diverse developmental and growth conditions.

However, it is also important to consider that the lines used in this study are not functional complementation lines since they were not produced using the NF-Y KO mutant as transgenic host, which should have contained the respectively tagged NF-Y protein. In fact most of the analysis were performed on overexpressor NF-YA2, NF-YB2 and NF-YC2 mutants, using the 35S promoter which enabled a better detection of the protein, since it is known that this promoter increase the levels of gene expression (Odell et al. 1985). This means that the expression levels of each subunits analyzed is altered from physiological level, so the interactions detected by MS analysis lead to artefacts. Indeed, this could cause a stoichiometric alteration during the formation of the complex determining non-canonical protein aggregations.

It would have been useful generate Arabidopsis transgenic lines with NF-Y genes under the regulation of their native promoter to create a plant system very similar to reality.

5.4.3 Why is NF-YA2 so difficult to detect?

Conversely, NF-YA2 or any NF-YA subunit, was not identified by MS in all Co-IP experiment performed on NF-YC2 and NF-YB2 epitope tagged lines. Additionally, Co-IP carried out on Arabidopsis lines stably expressing NF-YA2 GFP and FLAG tag was very problematic; indeed, no signal indicating the presence of tagged NF-YA2 could be observed in western blot analysis. This result was consistent across all the NF-YA2 tagged lines generated in this study. Three main reasons could explain these results. The first one is due to technical issues: the NF-YA2 gene in the epitope tagged lines generated in this study could not be functional because of the steric hindrance of the tag or because the insertion of the construct did not occur. Although this is unlikely since to circumvent these problems, independent lines with different tags in different orientation were generated. Additionally, the presence of the NF-YA2 construct and the gene expression level was checked in all lines using PCR and qRT-PCR respectively (Chapter 3).

The second reason could depend on the fact that NF-YA2 protein is degraded during the protein extraction process, even if protease inhibitors were used. While the third reason consider that NF-YA2 protein is not always expressed in plant or it is expressed at very low level. In fact, Leyva-Gonzalez et al. (2012) reported that NF-YA2 gene is the most tightly post-transcriptionally regulated member of the NF-YAs. They have proposed a hypothetical molecular model in which the expression of NF-YAs in wild type plants growing under non-stress conditions is low due to the presence of high level of miR169, a conserved micro-RNA (miRNA) family involved in plant development and stress induced responses, which inhibit the expression of NF-YAs. On the contrary under stress conditions, such as Pi deprivation, the level of miR169 is reduced allowing the transcript level of NF-YAs to increase. Hence, they used qRT-PCR to evaluate the transcript level of several NF-YA subunits (NF-YA5, NF-YA3, NF-YA2, NF-YA10) in HEN1 KO mutants (*hen 1-1)*, which have a constitutive reduction of mature miR169 (Li J. et al. 2005), grown in media containing sufficient and low Pi. qRT-PCR showed that

NF-YA transcript levels in *hen 1-1* mutants were higher than wild type regardless of sufficient or deficient Pi conditions, confirming that NF-YA is post transcriptional regulated by miR169. Additionally, because NF-YA2 showed to have the higher transcript level compared to the other NF-YAs tested, it was hypothesized that it is the most tightly post-transcriptionally regulated member (Leyva-Gonzalez et al. 2012). Moreover, MS analysis performed on NF-YA2-FLAG OE line identified many post-transcriptional regulation proteins supporting the hypothesis by which NF-YA2 in plant is tightly post-transcriptionally regulated.
In addition, Sorin et al. (2014) showed that knocking-out miR169, the level of NF-YA2 increase considerably in Arabidopsis, this suggest a more sophisticated approach to generate lines overexpressing NF-YA2. It would be useful to create functional mutants with just a point mutation in the miR169 binding site for NF-YA2, this would allow to increase the level of NF-YA2, leaving the rest of the proteins levels unchanged. It is also important to consider that the use of Arabidopsis overexpressor mutants could alter the normal functionality of the plant cell. For this reason, *nf-ya2*::*p*NF-YA2:NF-YA2-GFP line was created in this study, introducing *p*NF-YA2:NF-YA2-GFP construct in *nf-ya2* KO mutant complementing the loss-of-function. However, even if this line was functional, allowing to localize the NF-YA2 subunit in the nucleus, qPCR analysis demonstrate that the level of NF-YA2 was really low, not comparable with Col-0 (Figure 3.8) suggesting that the mutant complementation was only partial. Hence, the NF-YA2 protein was not detectable in Co-IP experiment.

5.4.4 Conclusion

In this chapter, strong evidences were found about the existence *in planta* of NF-YB2 and NF-YC2 heterodimer, and other NF-YB and NF-YC complexes. However, the detection of NF-YA2 was not possible due to technical problems probably related with low expression level of this protein in physiological conditions. As described here, multiple technical issues still limit the understanding about NF-Ys. This encourage to look for alternative and novel methods to characterize NF-

Y families. Further research on the putative trimer (NF-YA2/NF-YB2/NF-YC2) will be necessary to overcome experimental issue using innovative approach providing a better understanding of its functionality, specificity and mechanism of action.

Chapter 6

6. Genome-wide expression analysis of tomato and lettuce *NF-Y* genes during *Botrytis cinerea* infection

6.1 Introduction

In the past 20 years, plant scientists have chosen to use *Arabidopsis thaliana* as a model system, thanks to its small size, small genome, amenability to genetic manipulations and reasonably short generation time. This important spin-off allowed the developing of essential tools, resources and experimental approaches that have significantly inspired plant biological studies (Somerville and Koornneef 2002), as well as faster testing of hypotheses. Critically a model plant should facilitate biological insight into other plant species and reduce the time taken for production of improved crops. Comparative genomics and genetics has provided strong evidence that much of the information gained on Arabidopsis is relevant to other higher plant species, particularly crop plants (Irish and Benfey 2004), hence, the organization of genes within plant genomes has remained conserved over millions of years of evolution (Gale and Devos 1998). For example, Brassica species are certainly the most closely related crops to Arabidopsis having a largely conserved genome (O'Neill and Bancroft 2000, Paterson et al. 2001). Significant similarity has also been observed between Arabidopsis and soybean (Grant et al. 2000) and Arabidopsis and tomato (Mysore et al. 2001), and chromosomal synteny was used to investigate genes function. Also, the whole-genome analyses of Arabidopsis provided a better understanding of other agronomically important crops such as rice and cereal (Izawa et al. 2003, Rensink and Buell 2004, Ware and Stein 2003).

6.1.1 Gene families and homologues

Based on sequence similarity most genes can be classified into gene families. Several factors such as gene duplication and gene deletion can change the size of gene families, and this variation is important for the adaptation of different species in various environments (Guo 2013). Many studies have reported that whole genome duplications (polyploidy) are the main feature leading plant genome evolution (Adams and Wendel 2005, Soltis et al. 2015). Despite some of the duplicated genes being lost during the evolution, some are kept in the genome as homologues. These homologous genes can have the same function as the ancestor (subfunctionalization) or they can develop new functions (neofunctionalization) through a mutation in the open reading frame of a gene or due to the presence of the protein in different temporal or spatial environments in the cell (Freeling 2008, Lynch and Conery 2000, Moore and Purugganan 2005). Homologous genes are defined orthologues when they descend from a single gene in the last common ancestor, and paralogues when they diverged via duplication before this ancestor (Fitch 1970, Jensen 2001, Sonnhammer and Koonin 2002). With the rapid increase of sequenced genomes, orthologue identification is becoming an important part of functional genomics research. Indeed, orthologues often have the same or similar functions in different species (Li L. et al. 2015).

6.1.2 Comparative approach: from model systems to other species.

Surely model plants have provided an excellent basis to identify molecular pathways involved in different processes, however, despite the examples above, applying this information to other crops can be challenging. The overall approach has been to recognize key genes in model plants and identify their orthologues in other species, but this simple strategy brings along many difficulties. Specifically, over evolutionary time gene duplication produces functionally redundant copies of genes and these copies are more likely to accumulate polymorphisms and

evolve new, or varying, functions since they are not under selective pressure (Krakauer and Nowak 1999). This phenomenon can make it problematic to identify true functional orthologues between different species. Functional analysis, to experimentally test the gene of interest, is easy to carry out in Arabidopsis, but can be difficult to perform in non-model plants. For this reason, analyzing and comparing the expression patterns of potential orthologues between Arabidopsis and other species can be a useful tool to predict the function of a certain gene in its native context. Several comparative expression analyses have been performed, for example, the comparison of microarray expression profiles between Arabidopsis and rice (*Oryza sativa*) from seedlings grown under different light qualities has shown that very similar gene expression patterns were observed in both species with only a few species-specific differences. Also in the same study, global expression profiles between the two species has shown a higher correlation of genome expression patterns in constant light than in darkness, suggesting that genes involved in the photomorphogenesis are more conserved (Jiao et al. 2005, Ma et al. 2005). Similarly, a cross-species transcriptomics approach between Arabidopsis and *poplar* was used to identify genes with a key role in leaf development. Specifically, a large collection of microarray data and network-clustering analysis based on similar gene expression pattern were used to identify transcription factors associated with leaf development in *Populus*. This approach revealed that conserved gene expression pattern between the two species suggest their conserved function (Street et al. 2008). Hence, comparing gene expression profiles between different species represents a powerful tool to investigate conserved gene function under different conditions.

6.1.3 The problem of *Bortytris cinerea* in lettuce and tomato.

As described previously Grey mold is a very common fungal disease caused by the ubiquitous necrotrophic fungal pathogen *Botrytis cinerea.* Tomato (*Solanum lycopersicum L.*) and lettuce (*Lactuca sativa*) are particularly susceptible to this

pathogen which finds the best conditions in greenhouse environments, where it can cause severe losses, attacking leaves, flowers and fruits, compromising the commercial value of the product and ultimate leading to plant death (Dik et al. 1999).

6.2 Chapter aims

In this chapter, the overarching goal was to use transcriptome data to predict functional *NF-Y* orthologues genes that influence the susceptibility to *B. cinerea*. Gene expression profiles of tomato (*Solanum lycopersicum*) leaves during the necrotrophic pathogen infection were generated and compared to existing transcriptome data available in Arabidopsis and lettuce (*Lactuca sativa* cv. Saladin). Such comparison will help to better understand the conserved role of NF-Y TFs during the plant defense response across different crops species.

6.3 Results

6.3.1 Identification of lettuce and tomato *NF-Y* genes

The Lettuce genome sequence was published in 2017 (Reyes-Chin-Wo et al. 2017). The authors used Pfam domain to determine sequence orthologues of the NF-Y subunits identified in Arabidopsis (Table 6.1). Meanwhile NF-Y orthologues genes in *Solanum lycopersicum* were downloaded from the Plant Transcription Factor Database (PlantTFDB, http://planttfdb.cbi.pku.edu.cn/) (Table 6.2). 34 NF-Y genes were identified in lettuce (8 NF-YAs, 19 NF-YBs and 7 NF-YCs) and 59 NF-Y genes in tomato (10 NF-YAs, 29 NF-YBs and 20 NF-YCs), including NF-YB11, NF-YB13, NF-YC10, NF-YC11 and NF-YC13. In previous classification these genes were considered within the NF-Y gene family (Siefers et al. 2009), however Petroni et al. (2012) reclassified them as negative cofactors 2α/β (NC2) (Mermelstein et al. 1996) and as DNA POLYMERASE II SUBUNIT B3/B4 (DPB3/4) (Ohya et al. 2000), since they do not overlap with NF-Y domain regions (Petroni et al. 2012), hence in this chapter they will be excluded from further analysis related to NF-Y gene families.

6.3.2 Chromosome distribution of *NF-Y* genes in the tomato and lettuce genome.

All three species analyzed in this chapter are diploid (2n) having two copies of pairs of homologous chromosomes. Specifically, *Arabidopsis thaliana* has a haploid chromosome number of 5 (2n=10), tomato (*Solanum lycopersicum*) of 12 (2n=24) and Lettuce (*Lactuca sativa L.*) of 9 (2n=18). In Arabidopsis, tomato and lettuce NF-Y orthologues genes are distributed across all chromosomes. It appears that the pattern of NF-Y genes across these plant genomes is uneven and that the distribution varies among the different species. In tomato chromosome 1 contain three NF-YA genes, while chromosomes 4 to 7 and chromosome 9 do not contain any genes from this sub-group. Meanwhile, chromosome 5 contain the largest number of NF-YB genes, with a total of 10 NF-Y genes and

chromosome 3 contains the largest number of NF-YC genes, six (Li et al. 2016). In lettuce, most of the NF-Y are distributed across chromosome 1, 2, 4, 5, 6, 7. In particular chromosome 2, 5, 6 and 7contain the largest number of NF-Y orthologues genes, with respectively seven, four, five and four NF-Ys.

NF-YA subunit	Lettuce gene ID
NF-YA1	Lsat_1_v5_gn_2_97800
NF-YA2	Lsat_1_v5_gn_2_54241 Lsat_1_v5_gn_6_34921
NF-YA3	Lsat_1_v5_gn_1_37160
NF-YA7	Lsat_1_v5_gn_1_117081
NF-YA8	Lsat_1_v5_gn_7_34841
NF-YA9	Lsat_1_v5_gn_4_31560 Lsat_1_v5_gn_6_47121

NF-YB subunit	Lettuce gene ID
NF-YB3	Lsat_1_v5_gn_2_65440 Lsat_1_v5_gn_5_1080 Lsat_1_v5_gn_5_122040 Lsat_1_v5_gn_7_96781
NF-YB5	Lsat_1_v5_gn_6_16641 Lsat_1_v5_gn_9_2061 Lsat_1_v5_gn_9_123081
NF-YB6	Lsat_1_v5_gn_4_63880 Lsat_1_v5_gn_7_13001
NF-YB7	Lsat_1_v5_gn_1_82020 Lsat_1_v5_gn_2_37460
NF-YB8	Lsat_1_v5_gn_1_53800
NF-YB10	Lsat_1_v5_gn_2_109681 Lsat_1_v5_gn_2_115161 Lsat_1_v5_gn_6_29620 Lsat_1_v5_gn_9_67940

NF-YC subunit	Lettuce gene ID
NF-YC1	Lsat_1_v5_gn_5_12561
NF-YC2/NF-YC9	Lsat_1_v5_gn_2_64201 Lsat_1_v5_gn_5_74780 Lsat_1_v5_gn_6_87100

Table 6.1 - Genes in *Lactuca sativa* orthologous to NF-Y subunits in Arabidopsis according to Reyes-Chin-Wo et al. (2017). Pfam domain was used to determine lettuce NF-Y subunits.

NF-YA subunit	Tomato gene ID
NF-YA1	Solyc01g008490 Solyc11g065700
NF-YA2	Solyc01g006930
NF-YA3	Solyc03g121940 Solyc12g009050
NF-YA7	Solyc10g079150 Solyc02g069860
NF-YA8	Solyc08g062210
NF-YA9	Solyc01g087240
NF-YA10	Solyc10g081840

NF-YB subunit	Tomato gene ID
NF-YB2	Solyc07g065500 Solyc12g006120
NF-YB3	Solyc04g054150
NF-YB5	Solyc01g067130 Solyc01g099320 Solyc06g009010 Solyc09g074760
NF-YB6	Solyc02g032180 Solyc02g032190 Solyc04g015060 Solyc05g005350 Solyc05g005360 Solyc05g005380 Solyc05g005390 Solyc05g005440 Solyc05g015550 Solyc07g065570 Solyc07g065580 Solyc10g009440 Solyc11g012750
NF-YB7	Solyc12g027650
NF-YB8	Solyc04g009520 Solyc04g049910
NF-YB10	Solyc09g007290

NF-YC subunit	Tomato gene ID
NF-YC1	Solyc03g110860 Solyc03g111450 Solyc03g111460 Solyc06g072040
NF-YC2/NF-YC9	Solyc01g079870
NF-YC3	Solyc08g007960
NF-YC4	Solyc00g107050 Solyc02g021330 Solyc02g091030 Solyc03g110840 Solyc03g110850 Solyc03g111470 Solyc11g016910 Solyc11g016920

Table 6.2 - Genes in *Solanum lycopersicum* orthologous to NF-Y subunits in Arabidopsis. Tomato orthologues genes were downloaded from PlantTFDB database (http://planttfdb.cbi.pku.edu.cn/).

6.3.3 Analysis of the evolutionary relationships between tomato, lettuce and Arabidopsis NF-Y family subunits.

To assist with functional prediction and to understand the evolutionary relationship between Arabidopsis *NF-Ys* and their orthologues genes in tomato and lettuce, a phylogenetic tree for each sub-family (NF-YA, NF-YB, NF-YC) was generated using the full-length tomato, lettuce and Arabidopsis NF-Y protein sequences.

The unrooted tree was constructed by the neighbor-joining method, generated with MEGA7 software, after the alignment of the NF-Y amino acid sequences of Arabidopsis, tomato and lettuce genes (Figure 6.1, 6.3, 6.5). The evolutionary relationship between individual Arabidopsis NF-YAs, NF-YBs and NF-YCs shown in Siefers et al. (2009) corresponds with the evolutionary relationships found in this study, proving the reliability of this analysis. Moreover each tree confirmed the putative orthologues found in Table 6.1 and 6.2. Comparative functional analysis between Arabidopsis, where the referred NF-Y genes are well characterized (Quach et al. 2015), and other crops such as tomato and lettuce, where only a few publications on NF-Y orthologous genes have been published, is crucial to predict genes function across species (Gabaldon 2008). In this approach, functional predictions are based on identifying different levels of similarity between the gene of interest and the characterized genes. The similarity can be estimated considering primary DNA sequence, motifs, protein domains, secondary and three-dimensional protein structure. In this study, the evolutionary relationship analysis was performed by comparing full length proteins of Arabidopsis NF-Y and their putative orthologues in tomato and lettuce. However, despite sequence similarity, genes can be considered NF-Y orthologues only if they contain the canonical NF-Y domains. Hence, to support the hypothesis of functional conservation between specific Arabidopsis, tomato and lettuce NF-Y orthologues genes, multiple alignment were generated using Clustal omega tool (https://www.ebi.ac.uk/Tools/msa/clustalo/) (Figure 6.2, 6.4, 6.6). The protein sequence alignment, were performed for each subunit family (NF-YA, NF-YB, NF-

YC), which showed extensive conserved homologous motifs, essential for subunit interactions and DNA binding in yeast and mammals (McNabb et al. 1997, Sinha et al. 1996, Xing et al. 1994).

6.3.3.1 NF-YA family

The phylogenetic tree of NF-YA orthologues genes using full length proteins of Arabidopsis, tomato and lettuce, identified two main clades based on common ancestor represented by a single branch on the tree (Figure 6.1). It is possible to identified one clade containing 7 members (4 Arabidopsis genes, 2 tomato genes and 1 lettuce gene) and another one containing 18 members within 2 subgroups, one with 6 genes (2 Arabidopsis, 2 tomato and 2 lettuce) and the other with 12 genes (4 Arabidopsis, 5 tomato and 3 lettuce). A group composed by 2 lettuce genes and 1 tomato gene can also be identified in the tree, which may represent outliers since they do not belong to a particular group. The NF-YA tree confirmed the putative orthologues showed in Table 6.1 and 6.2. In fact these orthologues are evolutionary close in the phylogenic tree and they belong the same clade (Table 6.3). For example *NF-YA1*|*AT5G12840*, *Solyc11g065700*, *Solyc01g008490* and *Lsat1v5gn297800* are in the same clade as *NF-YA9*|*AT3G20910*, *Solyc01g087240*, *Lsat_1_v5_gn_4_31560* and *Lsat_1_v5_gn_6_47121*, since they all seem to descend from the same ancestor. However three orthologues genes, such as *Solyc12g009050*, *Lsat_1_v5_gn_1_117081* and *Lsat_1_v5_gn_7_34841*, which in the tree are clustered in a separate group, were not identified as orthologues of NF-YA3, NF-YA7 and NF-YA8 respectively.

Previous studies have shown that functional groups for each clade can be identified. For example, Arabidopsis *NF-YA2* is important in nodule development and nitrogen nutrition (Zhao M. et al. 2011), hence in other plant species orthologous genes having highly similar sequence to *NF-YA2*, such as *GmNF-YA1*, *GmNF-YA3* and *GmNF-YA10* in soybean, *MtNF-YA1* in *M. truncatula* (Combier et al. 2006) and *LjNF-YA1* in *Lotus japonicus* have shown to have the same function. Moreover to support the reliability of this phylogenetic analysis, the NF-YA tree

generated in this study was compared to the Arabidopsis NF-YA tree generated in Siefers et al. (2009), showing the same evolutionary relationships between NF-YA subunits.

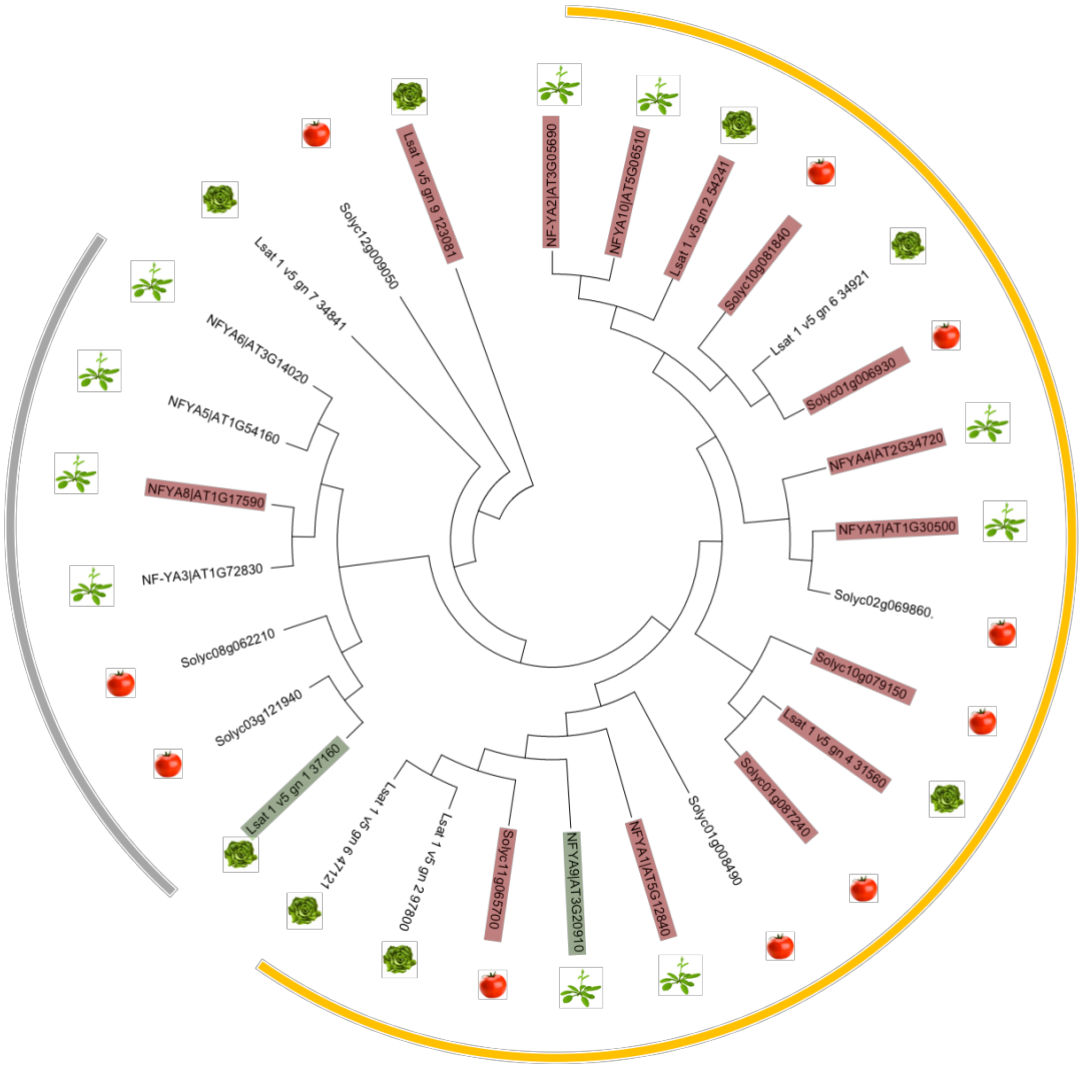

Figure 6.1 – Phylogenetic analysis of Arabidopsis, tomato (*Solanum lycopersicum*) and lettuce (*Lactuca sativa*) NF-YA proteins. Phylogenetic tree of NF-YA was constructed by neighbor joining using MEGA7 software. The tree was generated using full length proteins. Red and green boxes indicate respectively downregulated and upregulated genes during *B. cinerea* infection (24hpi). Yellow and gray lines indicate different clades.

Table 6.3 - Genes in tomato (*Solanum lycopersicum)* and lettuce *(Lactuca sativa)* orthologous to NF-YA subunit in Arabidopsis.

NF-YA subunit	Tomato gene ID	Lettuce gene ID
NF-YA1	Solyc01g008490 Solyc11g065700	Lsat_1_v5_gn_2_97800
NF-YA2	Solyc01g006930	Lsat_1_v5_gn_2_54241 Lsat_1_v5_gn_6_34921
NF-YA3	Solyc03g121940 Solyc12g009050	Lsat_1_v5_gn_1_37160
NF-YA7	Solyc10g079150 Solyc02g069860	Lsat_1_v5_gn_1_117081
NF-YA8	Solyc08g062210	Lsat_1_v5_gn_7_34841
NF-YA9	Solyc01g087240	Lsat_1_v5_gn_4_31560 Lsat_1_v5_gn_6_47121
NF-YA10	Solyc10g081840	

The alignment of tomato and lettuce NF-YA genes were observed to have the characteristic NF-YA conserved domain of 20 amino acids, which represent the surface for the binding of NF-YB/NF-YC heterodimer (Hackenberg et al. 2012) and a DNA binding domain of 21 amino acids (Figure 6.2) (Quach et al. 2015). Also, among Arabidopsis, tomato and lettuce NF-Y proteins, only NF-YA subunits have a nuclear localization signal, having all three groups of basic amino acid residues, required for nuclear targeting (Kahle et al. 2005). However, regions flanking the NF-YA conserved domain have a limited amino acid sequence conservation, generally rich in Gln (Q) and Ser/Thr (S/T) residues, which are involved in transcriptional activation (Coustry et al. 1996, de Silvio et al. 1999).

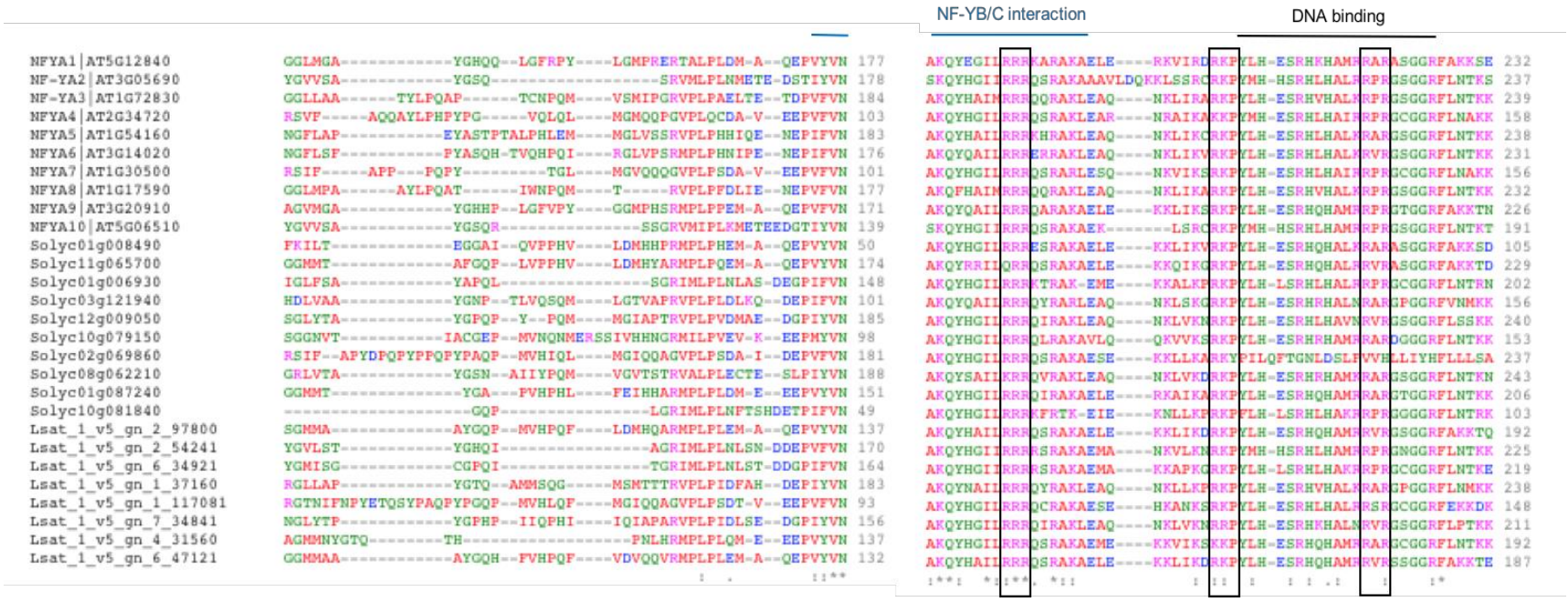

Figure 6.2 – Alignment of tomato (*Solanum lycopersicum*) and lettuce (*Lactuca sativa*) NF-YA domains. The reference sequence are from Arabidopsis NF-YAs. The amino acids that are predicted to be important for DNA binding and subunit interaction are based on Quach et al. (2015). The three boxes are the residual clusters required for nuclear targeting (Peng et al. 1998). Lines above highlight the conserved domain involved in DNA binding and in NF-YB and NF-YC subunits interaction. Numbers on the left indicate the amino acid position on the protein.

6.3.3.2 NF-YB family

The phylogenetic tree of NF-YB orthologues genes in tomato, lettuce and Arabidopsis, identified two clades (Figure 6.3): one containing 17 members (2 Arabidopsis genes, 13 tomato genes, 2 lettuce genes) and another one containing 32 members within 3 subgroups, one with 9 genes (2 Arabidopsis, 4 tomato and 3 lettuce), one with 6 genes (1 Arabidopsis, 2 tomato and 3 lettuce) and one with 17 genes (5 Arabidopsis genes, 5 tomato genes, 7 lettuce genes). The putative orthologues illustrated in Table 6.1 and 6.2 are confirmed in the NF-YB phylogenetic tree (Table 6.4). For instance *NF-YB5*|*AT2G47810* and its orthologues genes in tomato (*Solyc01g067130*, *Solyc01g099320*, *Solyc06g009010*, *Solyc09g074760*) and lettuce (*Lsat_1_v5_gn_6_16641*, *Lsat_1_v5_gn_9_2061*, *Lsat_1_v5_gn_9_123081*) are represented in the same clade and this suggest a very high protein sequence similarity between them. Phylogenetic analysis can be used to predict the function of members belonging to the same clade. For example Arabidopsis *NF-YB6*, also called *LEAFY COTYLEDON 1-LIKE* (*L1L*), is an important regulator involved in embryogenesis and ABA signaling (Kwong et al. 2003, Warpeha et al. 2007), which accumulated in seed and flower. The *L1L* homologue genes in *Solanum lycopersicum* (*Solyc05g005370; Solyc05g005360; Solyc02g032190; Solyc05g005380; Solyc05g015550; Solyc10g009440; Solyc05g005390; Solyc04g015060; Solyc11g012750*) showed to have similar expression pattern in flower, seed and developing fruit and also the same function (Hilioti et al. 2014). Moreover, the analogy of NF-YB phylogenetic tree generated in this study with the Arabidopsis NF-YB tree generated in Siefers et al. (2009), reinforce the consistency of this analysis.

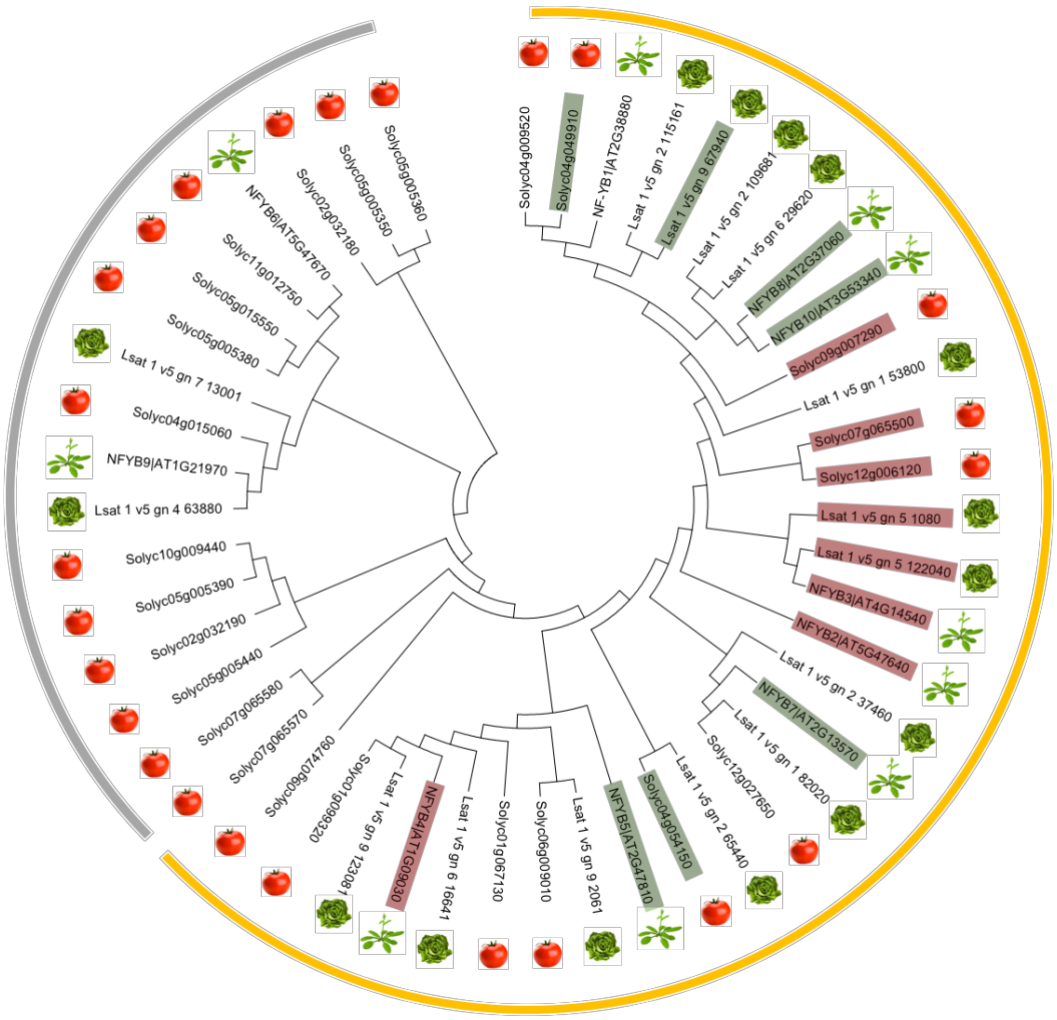

Figure 6.3 – Phylogenetic analysis of Arabidopsis, tomato (*Solanum lycopersicum*) and lettuce (*Lactuca sativa*) NF-YB proteins. Phylogenetic tree of NF-YB was constructed by neighbor joining using MEGA7 software. The tree was generated using full length proteins. Red and green boxes indicate respectively downregulated and upregulated genes during *B. cinerea* infection (24hpi). Yellow and gray lines indicate different clades.

Table 6.4 - Genes in tomato (*Solanum lycopersicum) and lettuce (Lactuca sativa)* orthologous to NF-YB subunit in Arabidopsis.

NF-YB subunit	Tomato gene ID	Lettuce gene ID
NF-YB2	Solyc07g065500 Solyc12g006120	
NF-YB3	Solyc04g054150	Lsat_1_v5_gn_2_65440 Lsat_1_v5_gn_5_1080 Lsat_1_v5_gn_5_122040 Lsat_1_v5_gn_7_96781
NF-YB5	Solyc01g067130 Solyc01g099320 Solyc06g009010 Solyc09g074760	Lsat_1_v5_gn_6_16641 Lsat_1_v5_gn_9_2061 Lsat_1_v5_gn_9_123081
NF-YB6	Solyc02g032180 Solyc02g032190 Solyc04g015060 Solyc05g005350 Solyc05g005360 Solyc05g005380 Solyc05g005390 Solyc05g005440 Solyc05g015550 Solyc07g065570 Solyc07g065580 Solyc10g009440 Solyc11g012750	Lsat_1_v5_gn_4_63880 Lsat_1_v5_gn_7_13001
NF-YB7	Solyc12g027650	Lsat_1_v5_gn_1_82020 Lsat_1_v5_gn_2_37460
NF-YB8	Solyc04g009520 Solyc04g049910	Lsat_1_v5_gn_1_53800
NF-YB10	Solyc09g007290	Lsat_1_v5_gn_2_109681 Lsat_1_v5_gn_2_115161 Lsat_1_v5_gn_6_29620 Lsat_1_v5_gn_9_67940

The alignment of Arabidopsis, tomato and lettuce NF-YB orthologous genes have shown to have the conserved domains, consisting in 90 amino acids, involved in the DNA binding and in the interaction with NF-YA and NF-YC subunits (Sinha et al. 1996) (Figure 6.4). Regions flanking this conserved domain protein sequences were variable in amino acid length and composition. Figure 6.4 also shows that two tomato NF-YB orthologues genes (*Solyc02g032180* and *Solyc02g032190*) seem to lack conserved domain for NF-YC interaction, suggesting that these two subunits could potentially form non-canonical NF-Y complexes, interacting with other TFs and not with an NF-YC subunit.

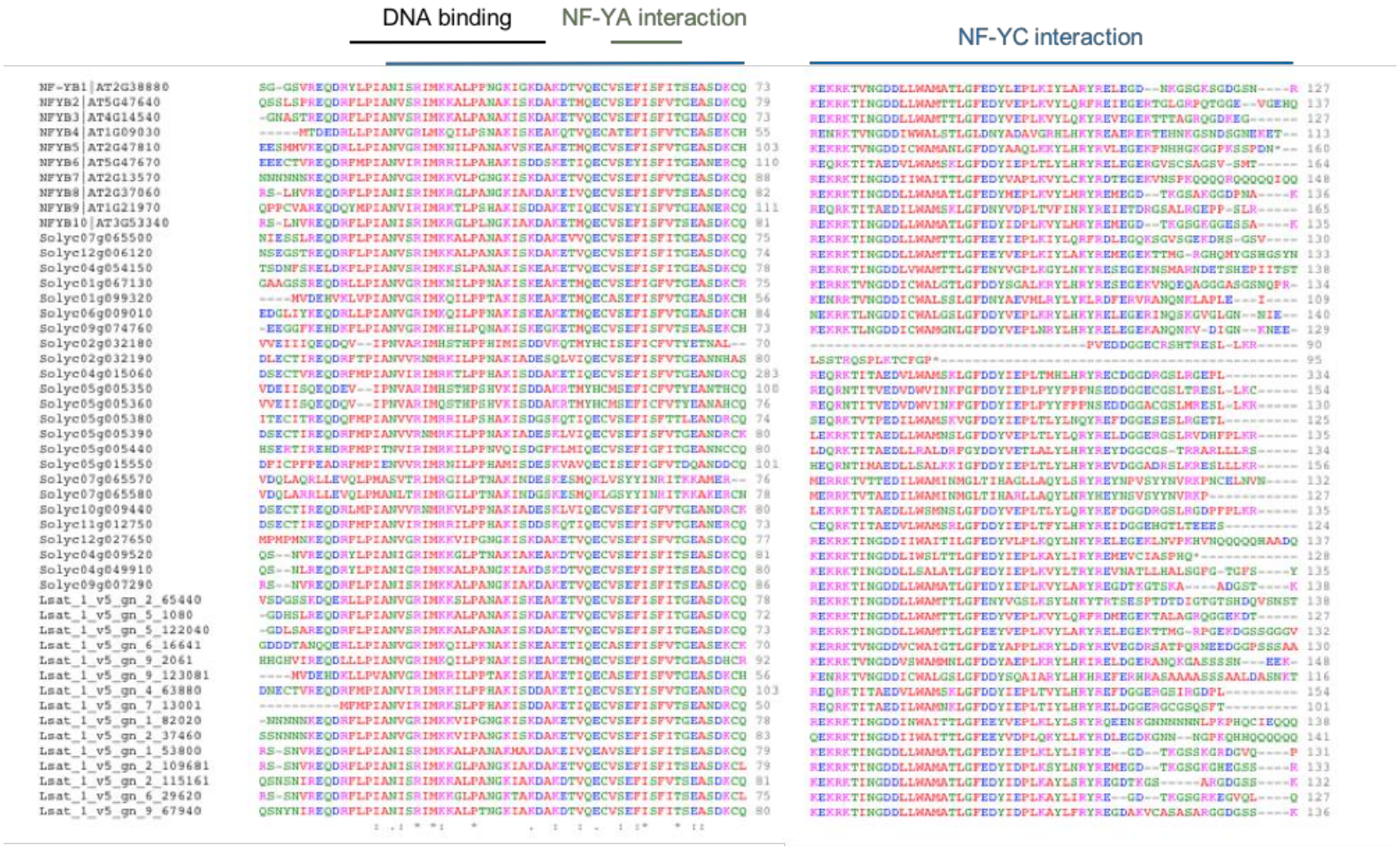

Figure 6.4 – Alignment of tomato(*Solanum lycopersicum*) and lettuce (*Lactuca sativa*) NF-YB domains. The reference sequence are from Arabidopsis NF-YBs. The amino acids that are predicted to be important for DNA binding and subunit interaction are based on Quach et al. (2015). Lines above highlight the conserved domain involved in DNA binding and in NF-YA and NF-YC subunits interaction. Numbers on the left indicate the amino acid position on the protein.

6.3.3.3 NF-YC family

The phylogenetic tree of NF-YC orthologues genes in Arabidopsis, tomato and lettuce, identified two main clades (Figure 6.5): one containing 18 members and another one containing 8 members. In the first clade, it is possible to identify 3 subgroups: one composed by 8 tomato genes; a second one constituted by 4 Arabidopsis genes and 1 tomato gene and a third one containing 3 Arabidopsis genes, 2 tomato genes and 1 lettuce gene. Table 6.5 shows a correlation between the putative orthologues genes illustrated in Table 6.1 and 6.2 and the NF-YC orthologues genes in the phylogenetic tree (Figure 6.5). For example *NF-YC1|AT3G48590* and its orthologues genes *Solyc03g110860*, *Solyc03g111450*, *Solyc03g111460*, *Solyc06g072040* and *Lsat_1_v5_gn_5_12561* descend from a common ancestor since they are in the same clade. Not many papers are available about single NF-YC in Arabidopsis, however function prediction for tomato and lettuce genes can be based on gene homology to the referred characterized Arabidopsis proteins. For example, Arabidopsis NF-YC3, NF-YC4 and NF-YC9 are essential for flowering, interacting with CONSTANS (CO) and they are required for the activation of FLOWERING LOCUS T (FT) during floral initiation (Kumimoto et al. 2010). *Solyc01g079870, Solyc03g110860* and *Solyc06g072040* the tomato homologues gene of *NF-YC3*, *NF-YC4* and *NF-YC9*, have shown to be involved in fruit ripening, being consistent with the NF-YC Arabidopsis function (Li S. et al. 2016). Also for the NF-YC subunit there is a correspondence between the NF-YC phylogenetic tree in Figure 6.5 and the Arabidopsis NF-YC tree (Siefers et al 2009).

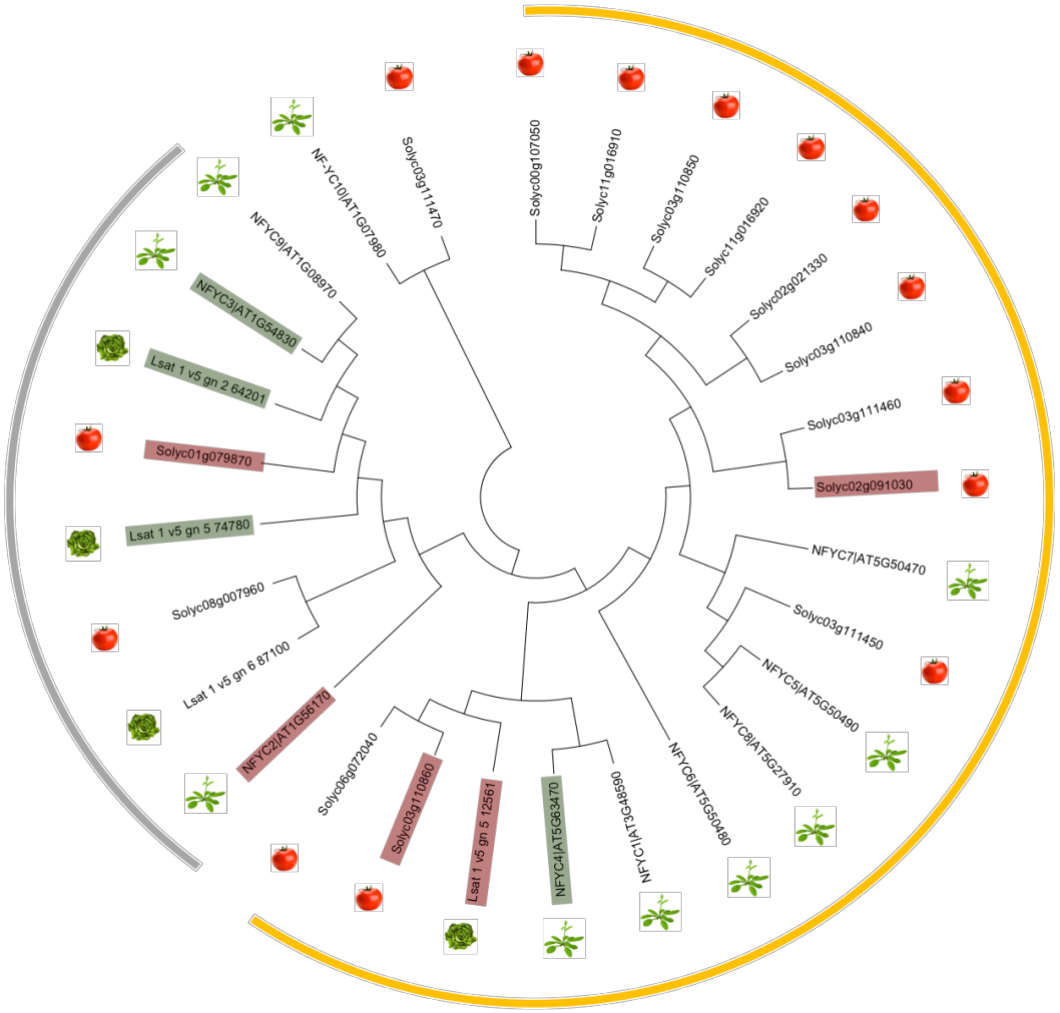

Figure 6.5 – Phylogenetic analysis of Arabidopsis, tomato (*Solanum lycopersicum*) and lettuce (*Lactuca sativa*) NF-YC proteins. Phylogenetic tree of NF-YC was constructed by neighbor joining using MEGA7 software. The tree was generated using full –length proteins. Red and green boxes indicate respectively downregulated and upregulated genes during *B. cinerea* infection (24hpi). Yellow and gray lines indicate different clades.

Table 6.5 - Genes in tomato (*Solanum lycopersicum)* and lettuce *(Lactuca sativa)* orthologous to NF-YC subunit in Arabidopsis.

NF-YC subunit	Tomato gene ID	Lettuce gene ID
NF-YC1	Solyc03g110860 Solyc03g111450 Solyc03g111460 Solyc06g072040	Lsat_1_v5_gn_5_12561
NF-YC2/NF-YC9	Solyc01g079870	Lsat_1_v5_gn_2_64201 Lsat_1_v5_gn_5_74780 Lsat_1_v5_gn_6_87100
NF-YC3	Solyc08g007960	
NF-YC4	Solyc00g107050 Solyc02g021330 Solyc02g091030 Solyc03g110840 Solyc03g110850 Solyc03g111470 Solyc11g016910 Solyc11g016920	

The alignment of Arabidopsis, tomato and lettuce NF-YC subunits revealed an highly conserved domain, approximately 80 amino acids, which has been shown to be necessary for NF-YA and NF-YB interaction and DNA binding (Romier et al. 2003) (Figure 6.6). NF-YC were shown to be rich in Gln (Q), a characteristic that determines transcriptional activation (Coustry et al. 1996, de Silvio et al. 1999) in Arabidopsis (Siefers et al. 2009) and other plant species (Petroni et al. 2012). However, the alignment indicates that two putative NF-YC4 tomato orthologues *Solyc03g111470* and *Solyc11g016910* do not overlap in the domain regions suggesting a different gene function (Figure 6.5). Specifically, *Solyc03g111470* is missing all the canonical NF-YC domain regions, while *Solyc11g016910* seems to lack conserved domain for NF-YB interaction, suggesting that it might be able to form complexes with other TFs instead of NF-YB subunit.

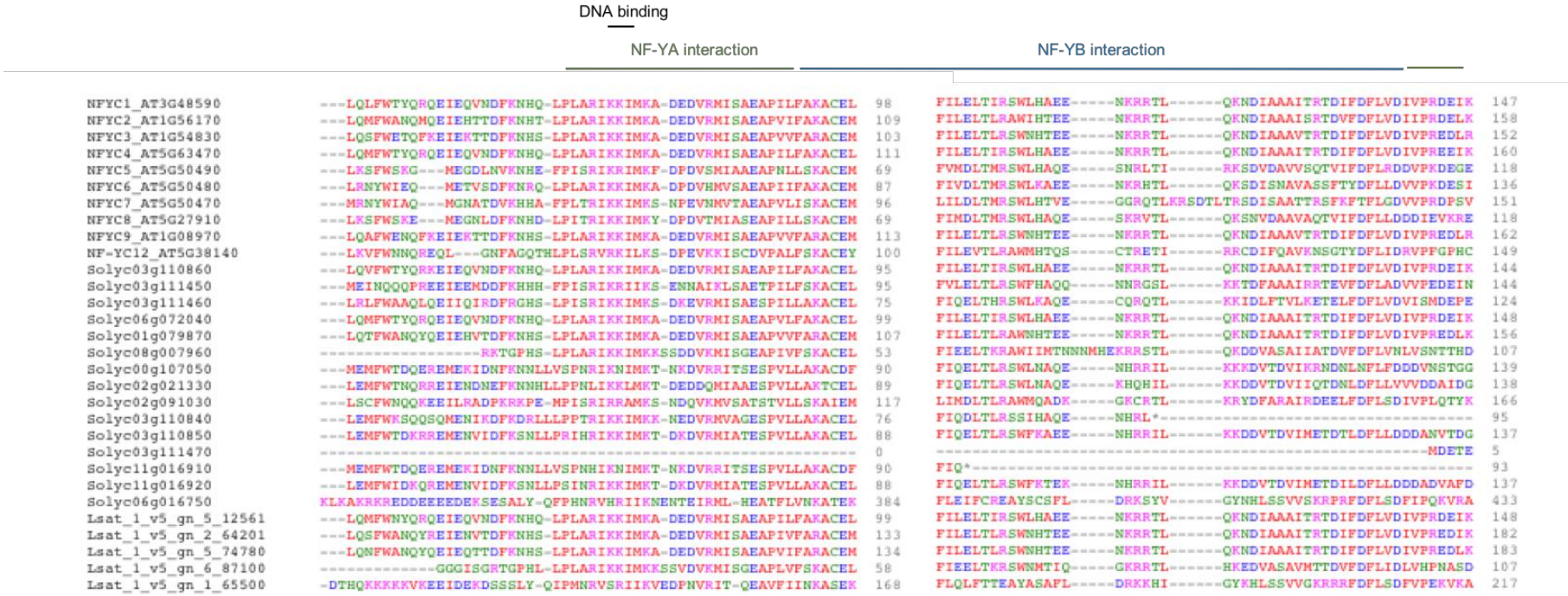

Figure 6.6 – Alignment of tomato (*Solanum lycopersicum*) and lettuce (*Lactuca sativa*) NF-YC domains. The reference sequence are from Arabidopsis NF-YCs. The amino acids that are predicted to be important for DNA binding and subunit interaction are based on Quach et al. (2015). Lines above highlight the conserved domain involved in DNA binding and in NF-YA and NF-YB subunits interaction. Numbers on the left indicate the amino acid position on the protein.

Identification of putative orthologues genes is an essential task in comparative genomics for transferring the knowledge of NF-Y proteins function from the model plant Arabidopsis to tomato and lettuce. Hence, based on the phylogenetic trees generated in this study orthologues genes for most of NF-Y TFs have been assigned. However, in few cases the identification of orthologues genes can be ambiguous and because gene orthology implies similar gene function, looking at the expression pattern could provide further information on conserved function of NF-Y genes in other species.

6.3.4 RNA-Seq expression profile analysis in tomato leaves during *Botrytis cinerea* infection

To look at NF-Y gene expression in tomato after *B. cinerea* infection, a similar experimental approach to a published data set in Arabidopsis and an unpublished lettuce data set (A. Talbot, unpublished) was used. Total RNA was extracted from tomato (*Solanum lycopersicum cv. Ailsa craig*) detached 5 weeks old leaves, inoculated with multiple droplets of *B. cinerea* spore suspension at even spacing, to ensure uniform infection, or mock inoculated with sterile media at similar spacing. The whole leaf was harvested at 26 hpi and 48 hpi and four replicates for each time point and each treatment were analyzed (Figure 6.7). RNA sequencing was carried out to investigate gene expression during infection. These time points were chosen because in the Arabidopsis time-series experiment (Windram et al. 2012) at 26 hpi the number of genes started to be differentially expressed, while at 48 hpi nearly one-third of the Arabidopsis genome was shown to be differentially expressed. However most of changes in gene expression occur before significant lesion development.

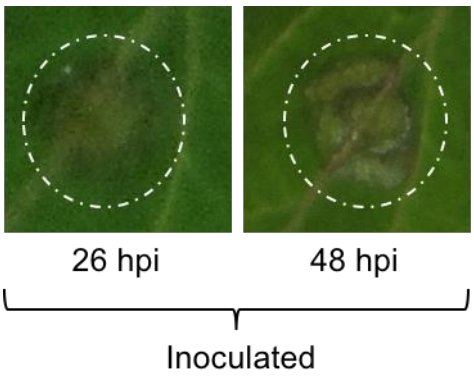

Figure 6.7 - *B. cinerea* infection on detached tomato leaves after 26 and 48 hours post infection. Lesion development after inoculation of tomato detached leaves inoculated with 10 µL droplets of *B. cinerea* spore suspension ($1x10^5$ per mL^{-1}). The two images show the same leaf after 26 and 48 hours post infection. The white circle indicate the lesion. Hpi = hours post infection.

6.3.4.1 Quality control of RNA-Seq data

Quality control of tomato RNA-Seq dataset was performed by Adam Talbot. Approximately 20 million reads were aligned to the tomato genome (Tomato Genome 2012) from both mock and inoculated across all replicates (Table 6.6). FastQC was used to confirm reads were of sufficient quality for analysis. This program produces a quality scores (Phred score) for each base pair, underscoring machine sequencing errors and poor quality reads. A score < 20 indicates low quality data, a score between 20 and 30 indicate intermediate quality data and a score > 30 indicates high quality data. Also, FastQC detects over-represented sequences, indicating the presence of contaminants and adaptors.

In this study, all samples presented a good per base sequence quality and GC content as illustrated in Figure 6.8 where representative plots are shown.

Table 6.6 – Total aligned reads and library size for each tomato sample.

Sample	Treatment	Total aligned reads
1	Mock 26 hpi	19134194
2	Mock 26 hpi	26356778
3	Mock 26 hpi	21694795
4	Mock 26 hpi	19866582
5	Infected 26 hpi	18734931
6	Infected 26 hpi	26526487
7	Infected 26 hpi	17343392
8	Infected 26 hpi	23397460
9	Mock 48 hpi	20359750
10	Mock 48 hpi	24850915
11	Mock 48 hpi	21101854
12	Mock 48 hpi	18926782
13	Infected 48 hpi	24810381
14	Infected 48 hpi	22473058
15	Infected 48 hpi	23542870
16	Infected 48 hpi	22622808

Figure 6.8 – Representative plots of FastQC per base sequence quality (26 hours post infection). Top left and top right represent a mock sample (forward and reverse respectively). Bottom left and right represent an infected sample (forward and reverse respectively). Phred score is represented on the y-axis.

Reads were aligned to the tomato genome and quantified using the pseudo-alignment software Kallisto (Bray et al. 2016). Pseudo-count data was transformed using a log-CPM transformation in Voom (Law et al. 2014). Differentially expressed genes were determined using a general linear model in Linear Models for Microarray and RNA-Seq Data (Limma) by Dr. Adam Talbot (Ritchie et al. 2015). Samples were checked for the presence of tomato rRNA, filtered (Figure 6.9) and normalized. Filtering was carried out using the limma-voom pipeline: genes with less than 64 reads were excluded from the analysis. The mean-variance relationship of log-CPM (log count per million) values illustrated in Figure 6.9 shows acceptable filtering of reads, since no drop in variance levels is observed at the low end of the expression scale. Multi-Dimensional Scaling (MDS) plots of log-CPM values was used to visualize similarity between samples over two dimensions (Figure 6.10). The plot shows distinct variation between treatment and time points. The treatment and time variables cluster together, with the time variable segregating by the first dimension and the treatment appears to segregate on the second dimension. This analysis illustrates that gene expression profile is stable across samples underling the same treatment, while there are differences between samples belonging different treatment and time point.

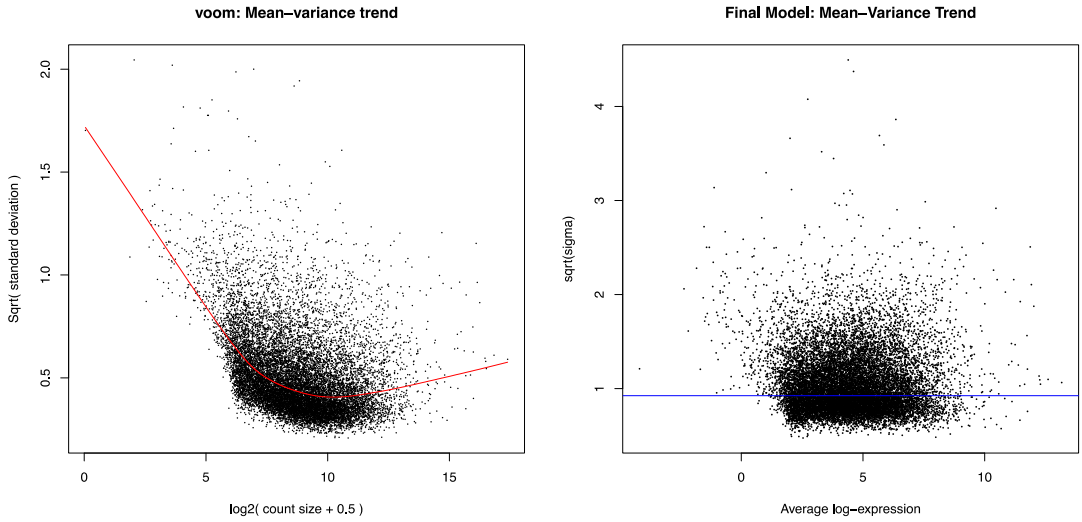

Figure 6.9 – The plot on the left shows the relation between means (x-axis) and variances (y-axis) of each gene before limma-voom is applied to the data. Plot on the right represent how the trend is removed after voom precision weights are applied to the data. The voom function was used to extract residual variances from fitting linear models to log-CPM transformed data (plot on the left). Subsequently variances are rescaled to quarter-root variances and plotted against the mean expression of each gene. The means are log2-transformed mean-counts with an offset of 0.5. PlotSA was used to generate the plot on the right, this function plots log2residual standard deviations against mean log-CPM values. The horizontal blue line represents the average log2 residual standard deviation. In both plots, each black dot represents a gene and a red curve is fitted to these points.

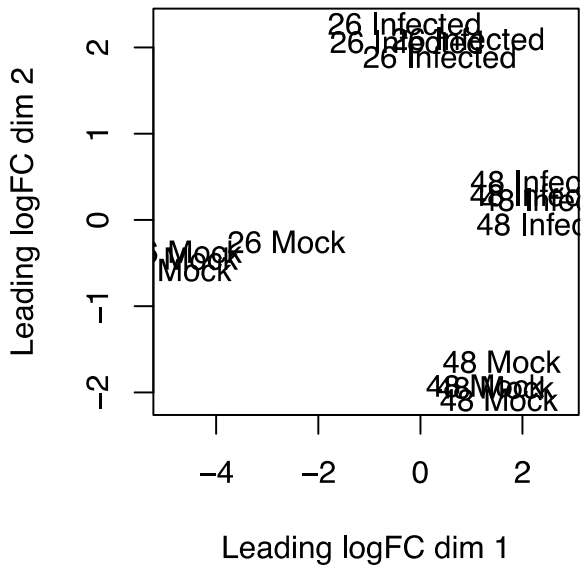

Figure 6.10 - MDS plots of log-CPM values over dimensions 1 and 2 with samples labeled by sample treatment. Distances on the plot correspond to the leading fold-change, which is the average (root-mean-square) log2-fold-change for the 500 genes most divergent between each pair of samples by default.

6.3.4.2 Transcriptome profiling of *S. lycopersicum* in response to *B. cinerea*

To evaluate genes expression changes in tomato during *B. cinerea* infection, transcriptome of *S. lycopersicum* plants infected with *B. cinerea* was compared with mock inoculated plants with time treated as a covariat. Differential expression ($p < 0.05$ after false discovery adjustment(Benjamini et al. 2001)) was evident for 11193 genes in total, 5241 genes were upregulated and 5952 genes were downregulated at 26 hpi. Meanwhile at 48 hpi 6330 genes, showed differential expression, having 3128 downregulated and 3202 upregulated genes. Therefore, 35% of the 31760 genes in tomato genome (version SL3.0) are differentially expressed (Tomato Genome 2012) at 26 hpi, while only 20% at 48 hpi, probably because by that time-point the necrotrophic pathogen has caused a severe leaf tissue damage. This result is consistent with what was observed in Arabidopsis where one third of the genome is upregulated or downregulated during the first 48 hours after *B. cinerea* infection (Windram et al. 2012) with the majority of changes in gene expression occurring by 24 hpi. Arabidopsis and

tomato leaves infected by *B. cinerea* induce a considerable transcriptional reprogramming in the host, as demonstrated by transcriptional profiling studies, suggesting that key regulators are involved in this process (AbuQamar et al. 2006, Ferrari et al. 2003, Rowe et al. 2010). Hence, many transcription factors regulate host defenses against various plant pathogens. Specifically, TF families that in Windram et al. (2012) were shown to be significantly differentially expressed at each time point during *B. cinerea* infection showed to be differentially expressed in the tomato transcriptome at 26 hpi (Figure 6.11). This analysis confirmed that WRKY and ARF families, with around 40% of differentially expressed genes, are the most regulated TF group involved in *B. cinerea* plant immunity (AbuQamar et al. 2006, Birkenbihl et al. 2012, Lai et al. 2011, Xu X. et al. 2006), since a very large number of these orthologues genes in tomato showed expression change during the infection. WRKYs are often associate with plant immunity and are known as positive or negative regulators in the plant defense responses (Eulgem and Somssich 2007). Moreover, some auxin-related genes, such as ARFs have been documented as involved in plant immunity (Jiang et al. 2016). Specifically, publicly available Arabidopsis transcriptome data revealed that a significant portion (around 65%) of these genes are down-regulated during Arabidopsis infection with *B. cinerea*. These results indicate role of ARF genes in regulating biotic stress signaling pathways (Llorente et al. 2008).

Also, many members of CO-LIKE family in tomato were differentially expressed during the pathogen attack, suggesting that this family may be involved in plant defense responses. Because in Arabidopsis and other cereals CO-like genes control flowering time (Griffiths et al. 2003), it can be assumed that the pathogen infection may influence time to flower to affect plant tolerance and to enhance plant resistance. Another large TF family represented by MYB, seems to be involved in controlling responses to biotic stresses, since these genes show changes in gene expression during the infection. This is in agreement with previous studies where it was reported that in Arabidopsis MYB TFs are implicated in JA-dependent defense responses (Ambawat et al. 2013). In Figure 6.11 it is also

visible that a good percentage of C3H (for zinc finger domain) TFs, are differentially expressed in tomato during the infection. This is consistent with previous reports showing up or down regulation of C3H genes during biotic and abiotic stress conditions (Shaik and Ramakrishna 2014). Interestingly also a good portion, corresponding to more than 20% of tomato NF-Y TF genes revealed to be differentially expressed during *B. cinerea* infection. This is in agreement with what was observed in Arabidopsis, where 8 NF-Y genes were shown to be upregulated and 10 downregulated during the fungal pathogen attack (Figure 1.10). Therefore, this family of TFs appears to be key determinants of regulatory specificity during the plant defense responses, suggesting NF-Y TFs as important players in plant immunity.

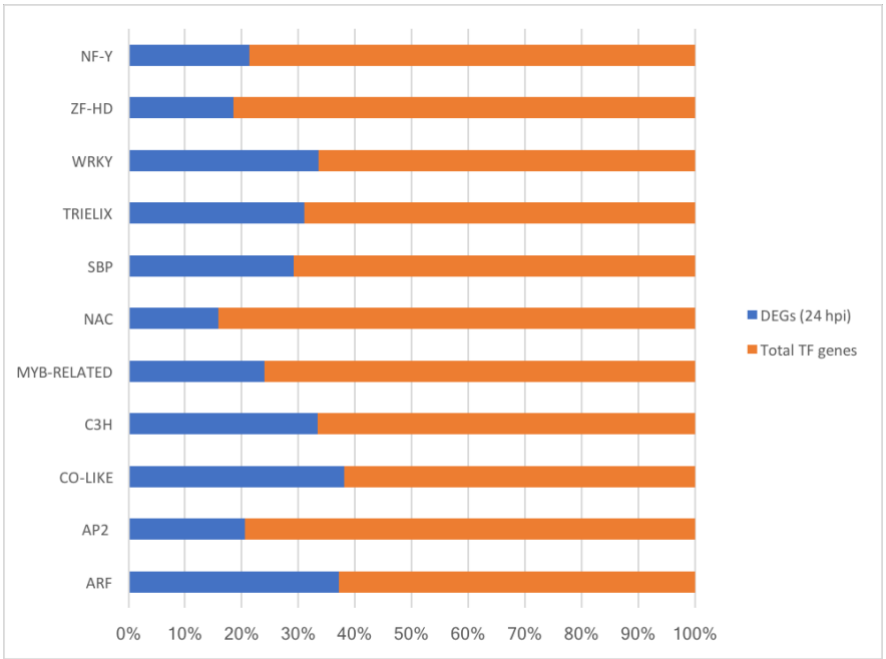

Figure 6.11 – Percentage of differentially expressed tomato genes for each of the major TF families at 26 hpi. Each bar represents a TF family. The blue bar is the percentage of differentially expressed genes related to the total number of genes (orange bar).

6.3.4.3 Expression pattern of *NF-Y* genes in tomato and lettuce during *B. cinerea i*nfection.

Transcriptomic analysis using RNA-Seq or microarray allows for analysis of the gene expression profiles of all genes in a genome. This consent to compare different data sets and allows to identify gene expression patterns across species associated with a specific stress. Many members of tomato NF-Y family were shown to be differentially expressed at 26 hpi (Table 6.7), while at 48 hpi less NF-Y genes showed expression changes in response to *B. cinerea* infection, probably due to tissue damage caused by the necrotrophic pathogen. For this reason, only 26 hpi time point was used in the following analysis. Moreover, to compare tomato expression data, obtained in this study, to previous Arabidopsis and lettuce dataset, only 24 hpi was considered in both species. In tomato 13 NF-Y subunits (5 members of NF-YA, 5 members of NF-YB and 3 members of NF-YC) showed to be differentially expressed in response to *B. cinerea* infection (Figure 6.1, 6.2, 6.3), which correspond to 22% of total NF-Y orthologues genes. Table 6.7 shows the Log2 (1) FC, the P value and the direction of the expression of each NF-Y tomato orthologous gene.

Meanwhile in lettuce the number of differential expressed NF-Y genes is 10, (4 members of NF-YA, 3 members of NF-YB and 3 members of NF-YC), corresponding to 29% of the total NF-Y family members (Figure 6.1, 6.2, 6.3). However, in Arabidopsis the portion of NF-Y genes involved in the plant defense response is higher, indeed 56% of them are up or downregulated during the infection (Figure 1.10). This because the number of NF-Y orthologues genes in tomato and lettuce is larger than Arabidopsis, so some are probably redundant in the genome, due to gene duplication during the evolution process and only few NF-Y orthologue genes show conserved function across species. Interestingly, in all three species more members of NF-YA subunits are differentially expressed during the infection and most of them are shown to be downregulated. This could suggest a conserved key role of NF-YA subunits in the plant defense response. The differential expression of NF-Ys during *B. cinerea* infection suggests that this TF family could

have an important role in the Arabidopsis, tomato and lettuce defense response. For example, Figures 6.1, 6.3, 6.5 show the direction of expression change for each NF-Y orthologue genes. Figure 6.1 shows a cluster of NF-YA orthologues genes which have the same expression profile. Specifically, Arabidopsis *NF-YA1*, *NF-YA2*, *NF-YA4*, *NF-YA7*, *NF-YA8*, *NF-YA10* and their orthologues in tomato *Solyc11g065700*, *Solyc01g006930*, *Solyc10g079150*, *Solyc10g081840* and lettuce *Lsat_1_v5_gn_2_54241*, *Lsat_1_v5_gn_1_117081* are downregulated during the infection. However, Arabidopsis *NF-YA9* is upregulated and its orthologues (*Solyc01g087240* and *Lsat_1_v5_gn_4_31560*) are downregulated in both crops. Also, Figure 6.3 displays a consistency in NF-YB gene expression profile between Arabidopsis, tomato and lettuce. Hence, during the infection Arabidopsis *NF-YB2*, *NF-YB3* and *NF-YB4* are downregulated as their orthologues *Solyc07g065500*, *Solyc12g006120*, *Lsat_1_v5_gn_5_1080*, *Lsat_1_v5_gn_5_122040*, while Arabidopsis *NF-YB5*, *NF-YB7*, *NF-YB8* and *NF-YB10* are upregulated as their orthologues *Solyc04g049910* and *Lsat_1_v5_gn_9_67940*. However, there are some exception since *Solyc04g054150* (*NF-YB3* homologue) shows to be upregulated and *Solyc09g007290* (*NF-YB10* homologue) is downregulated. Based on this RNA-Seq expression profile analysis, putative key defense response genes were hypothesized. Specifically, Arabidopsis NF-YA2 and its orthologues in both tomato (*Solyc01g006930)* and lettuce (*Lsat_1_v5_gn_2_54241*) showed to have the same expression pattern during the infection, suggesting a conserved gene function across the three species. Also, Arabidopsis NF-YB2 and its homologue NF-YB3, very closely related proteins sharing 94% amino acid identity in their conserved domains (Siefers et al. 2009), showed a downregulated expression at 26 hpi as their orthologues genes in tomato (*Solyc07g065500, Solyc12g006120)* and lettuce *(Lsat_1_v5_gn_5_1080)* being consistent with the hypothesis of a role in the defense response. The gene expression of *Solyc01g006930 and Solyc07g06550* was further evaluated by real time quantitative RT-PCR analysis on Micro-Tom, a tomato model cultivar, which showed to be downregulated

during the defense response (Figure 6.12), reinforcing the theory of a conserved gene function of NF-YA2 and NF-YB2 across different species.

On the other hand, NF-YC orthologues genes revealed contrasting expression profiles. For example, Figure 6.5 shows that Arabidopsis *NF-YC4* is upregulated during the infection, while *Solyc02g091030* is downregulated. Another example is represented by Arabidopsis *NF-YC2* and its orthologues in tomato *Solyc01g079870,* which are both downregulated in response to the pathogen attack, while lettuce orthologues (*Lsat_1_v5_gn_5_74780* and *Lsat_1_v5_gn_2_64201*) are upregulated. All these discrepancies can be caused by the differentiation of function between orthologue genes or depends on the fact that orthologues identified by BLAST analysis are not always true orthologues (Street et al. 2008), because they have different function.

Table 6.7 – Differentially expressed tomato NF-Y genes during *B. cinerea* infection. Log2 (1) FC and the P value are reported for each gene. Arrows indicates the direction of the gene expression (red arrows = downregulated genes; green arrows = upregulated genes).

Tomato gene	Orthologue Arabidopsis gene	Log FC	P value adjusted	Direction of gene expression
Solyc11g065700	NF-YA1	-0.3317	0.0193196	↓
Solyc01g006930	NF-YA2	-1.5233	0.0003484	↓
Solyc10g079150	NF-YA7	-2.2928	0.0102456	↓
Solyc01g087240	NF-YA9	-1.8719	8.80E-06	↓
Solyc10g081840	NF-YA10	-2.484	0.0272935	↓
Solyc07g065500	NF-YB2	-1.9737	5.50E-06	↓
Solyc12g006120	NF-YB2	-2.3956	0.0010537	↓
Solyc04g054150	NF-YB3	3.0569	5.00E-06	↑
Solyc04g049910	NF-YB8	0.2595	0.0493153	↑
Solyc09g007290	NF-YB10	-0.4146	0.0055892	↓
Solyc03g110860	NF-YC1	-1.6946	1.80E-06	↓
Solyc01g079870	NF-YC2/NF-YC9	-1.3013	2.84E-05	↓
Solyc02g091030	NF-YC3	-0.8307	0.0183638	↓

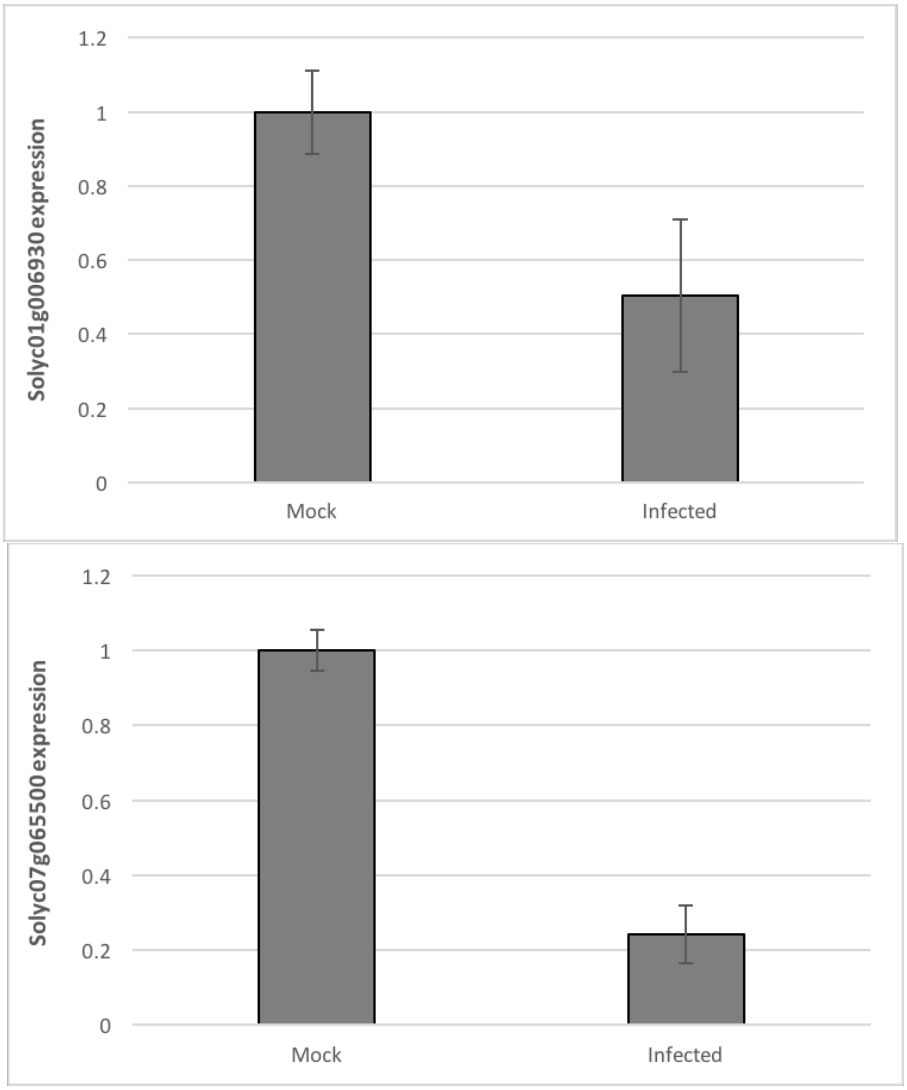

Figure 6.12 – q-PCR expression analysis of tomato Micro-Tom NF-YA2 (*Solyc01g006930*) and NF-YB2 (*Solyc07g065500*) showed to be differentially expressed during *B. cinerea* infection. Detached leves from 4 weeks old Micro-Tom plants were inoculated with B. cinerea spores in 0.5% grape juice (Infected) and 0.5% grape juice only (Mock). Tissue was harvested at 26 hpi. Gene transcript levels were calculated using the comparative 2-ΔΔC(T) method (Livak and Schmittgen 2001) and normalized to the expression of the two housekeeping genes alpha-Tubulin and (Tuba) and Ubiquitin (UBQ5). Mock infected values were arbitrarily set to 1. Data are presented as relative expression from 3 technical replicates and 3 biological. The analysis was performed on pooled multiple plants leaf material.

6.4 Discussion

6.4.1 Comparison between differentially expressed genes in Arabidopsis, tomato and lettuce.

This chapter presented a gene expression profile during infection of tomato leaves by the fungal pathogen *B. cinerea*. Analysis of this transcriptome has shown that nearly one-third of the tomato genome changes in expression during the first 26 h after infection. This result is consistent with published analyses of the Arabidopsis transcriptome after *B. cinerea* infection which shows that the majority of changes in gene expression have occurred by 24 h after infection, when the pathogen has penetrated leaf epidermis but lesions are not yet visible (Windram et al. 2012).

A comparative analysis of gene expression patterns between the model plant Arabidopsis and two other crops, tomato and lettuce, have been carried out. This analysis has revealed a trend of changes in the transcriptome between orthologous genes across the three species. The RNA-Seq analysis in tomato identified 11193 differential expressed genes at 26 hpi after inoculation with *B. cinerea* spores, corresponding to 35% of the whole tomato genome, with around 50% of these genes upregulated and 50% downregulated. A similar result was obtained analyzing RNA-Seq data on lettuce leaves inoculated with *B. cinerea* spores at 24 hpi. The expression profiling identified 13923 differentially expressed lettuce genes (36.8% of the total), 6432 upregulated and 7492 downregulated, between infected and mock inoculated leaves (personal communication, A. Talbot; unpublished), given 37828 predicted genes in total (Reyes-Chin-Wo et al. 2017). In Arabidopsis, the same percentage of upregulated or downregulated genes during *B. cinerea* infection was observed. Hence the time series expression profile identified 9838 differentially expressed genes at 24 hpi, which are around 35% of the total genes during the infection (Windram et al. 2012). Overall, these analyses suggest that there is significant conservation in terms of number of differentially expressed genes across different plant species apparently

phylogenetic distant such as Arabidopsis, tomato and lettuce. This fundamental knowledge should provide a good start for following gene functional studies.

6.4.2 Identification of key NF-Y during *B. cinerea* infection

In contrast to the well-known function of NF-Y Arabidopsis genes in controlling plant growth and development (Ballif et al. 2011, Laloum et al. 2013), very little information is available about their role during defense against pathogen attack (Zanetti et al. 2017). To overcome this deficiency a combination of phylogenetic and gene expression profile analysis during *B. cinerea* infection was used to predict NF-Y gene function in tomato and lettuce. The phylogenetic analysis discovered similarities and conservation of NF-Y genes between Arabidopsis, tomato and lettuce and helped to identify candidate NF-Y genes involved in the plant defense response. In this study, some evidences have revealed that single NF-Y subunits, specifically belonging NF-YA and NF-YB sub-families, have an important role during the plant defense response. Indeed, a large number of tomato and lettuce NF-YA and NF-YB genes were differentially expressed in response to the pathogen attack and they can be possibly involved in the defense response (Figure 6.1 and 6.3). Hence, tomato and lettuce NF-YA family appears to have half NF-YA orthologues genes (Figure 6.1) and around a quarter of NF-YB orthologues genes (Figure 6.3) induced by the fungal infection. Specifically, many members of NF-YA subunit were downregulated during the infection in all three species. This expression pattern may highlight a still unknown conserved role of NF-YA subunits in the plant defense against *B. cinerea*. Also the differential expression of NF-YB orthologues genes across the three species, suggest a conserved function of this subunit during the infection. A consistent down regulation tendency of NF-YA2 and NF-YB2/NF-YB3 across Arabidopsis, tomato and lettuce suggested these NF-Y subunits as the best candidate genes involved in the plant defense response. Indeed, the same expression pattern was found using qRT-PCR analysis on Micro-Tom, supporting such a role during the infection across different tomato cultivar.

According to the tree showed in Figure 6.3, Arabidopsis NF-YB2 does not have a clear orthologue, while NF-YB3 seems to have several orthologues genes which are differentially expressed during pathogen attack. However it is important to consider that NF-YB2 and NF-YB3 are very similar proteins with 94% amino acid identity in their conserved domains (Siefers et al. 2009), hence NF-YB3 is homologue to NF-YB2 with probably the same function. This hypothesis is reinforced by Kumimoto et al. (2008) where NF-YB2 and NF-YB3 were shown to be redundant players in photoperiod-related floral transitions.

Looking at the evidence, the cross-species approach used in this study identified important NF-Y candidates comparing Arabidopsis genes with their orthologues in other species. This method suggested that NF-Y TFs can have a key role in the transcriptional regulation of tomato and lettuce defense response highlighting the importance of this TF family, which is involve in many plant molecular mechanism but it is still underestimate and not well studied.

6.4.3 Conclusion

In this work, the relationship between NF-Y orthologues genes in Arabidopsis, tomato and lettuce was analysed using a phylogenetic approach and also the expression patterns of each genes were characterized. Among all these NF-Y genes in both crops, based on the expression profile it was hypothesized that two members of NF-YA family in tomato and lettuce (*Solyc01g006930, Lsat_1_v5_gn_2_54241)* and three members of NF-YB *(Solyc07g065500, Solyc12g006120, Lsat_1_v5_gn_5_1080),* represent putative key genes during *B. cinerea* infection. These candidate genes probably play an important role in the plant defence response and this provides a starting point for further investigation of their biological function.

Because closely related proteins do not always share the same function, it is important to clarify if orthologous genes in different species play the same role or if they have evolved different function. To understand this, it is crucial to perform further gene functional studies. For this reason, the next step of this

research would be obtained *NF-Y* gene knockout crops to investigate the effect of gene loss in the mutant. It would be also useful to perform transcriptional analysis in other species, to investigate the NF-Y family conservation in different crops during the evolutionary process.

Chapter 7

7. General discussion

One of the most important questions about the NF-Y TF family in plants is to determine functional complexes *in planta*. Individual NF-Y subunits are not capable of regulating gene transcription, instead they have to combine in hetero-trimers composed by NF-YA, NF-YB and NF-YC subunits (Zhao H. et al. 2016) or hetero-dimers formed by NF-YB and NF-YC subunits which are able to interact with other TFs forming non-canonical NF-Y complexes. These NF-Y hybrid complexes eschew NF-YA and bind the DNA at different elements other than CCAAT (Liu and Howell 2010, Wenkel et al. 2006), increasing functional complexity. As described previously, in Arabidopsis and other plants each NF-Y subunit is encoded by large families and for this reason identifying active NF-Y complexes is particularly challenging. In fact, this provides multiple combinations between NF-YA, NF-YB and NF-YC members, which may assemble in a specific manner according to different developmental plant stage or environmental conditions.

Based on the putative hetero-trimer hypothesized in this study (NF-YA2/NF-YB2/NF-YC2), the possibility that the NF-YB2/NF-YC2 dimer can potentially interact not only with a NF-YA subunit but with many other TFs, dramatically increases the number of possible combinations and NF-YA competitors. For example, several studies through Y2H system have found that NF-YB and NF-YC proteins are able to interact with other TFs like MADS18, bZIP28, CO and CO-like (Liu and Howell 2010, Masiero et al. 2002, Wenkel et al. 2006, Yamamoto et al. 2009) as described in previous chapters. In line with this, the MS performed in this study revealed that NF-YC2 can interact *in planta* not only with NF-YB2 but also with NF-YB1 and NF-YB10, while NF-YB2 can form hetero-dimer with NF-YC9, NF-YC4 and NF-YC1*,* in agreement with previous studies which identified these interactions using Y2H system (Calvenzani et al. 2012).

This confirms the capability of each NF-Y members to combine with different subunits, expanding the combinatorial complexity and providing a significant challenge in detecting complete hetero-trimeric complexes *in planta*.

Confocal analysis performed on transiently transformed *N. benthamiana* and stably transformed Arabidopsis leaf cells revealed that NF-YB2 and NF-YC2 are localized in the cytoplasm while NF-YA2 is exclusively localized in the nucleus, in agreement with the widely-accepted mechanism of NF-Y complex assembly proposed by Kahle et al. (2005). Additionally, strong evidence for dimerization of NF-YB2 and NF-YC2 *in planta* were provided using BiFC and MS assays, in line with previous Y2H analysis carried out by Calvenzani et al. (2012). These results perfectly match with what was revealed by crystallography structure analysis of NF-YB and NF-YC in mouse. It was found that their ability to form a complex derives from hydrophobic residues in the α2 helix of the HFD, core of the dimerization surface, which establish hydrophobic contact between the two subunits (Romier et al. 2003). However, still no NF-YA2 or any NF-YAs were detected, so no evidence of the existence of the putative hetero-trimer NF-YA2/NF-YB2/NF-YC2 or any NF-YA2 interactors were discovered in this research. Many hypothesis can lead to this result, for example it was reported in previous studies that the expression of NF-YA subunits is inhibited by miR169 in non-stress conditions (Li J. et al. 2005, Sorin et al. 2014), so the protein level of NF-YA subunits is normally low in plant. Hence, the fact that NF-YA members are tightly regulated and localized only in the nucleus could cause difficulties in the detection. Moreover, it is important to consider that in this study most of the analysis were performed on overexpressor mutants, having NF-YA2, NF-YB2 and NF-YC2 under the 35S promoter, and this could lead to artefacts. Hence, the overexpression of a protein member of a complex generates a stoichiometry imbalance creating atypical protein aggregation (Abruzzi et al. 2002). These promiscuous protein-protein interactions could cause pathway alterations due to the sequestration of proteins, essential for a specific complex, by the aggregation

with non-physiological partner proteins. This perhaps provides another reason for the missing NF-YA subunits in the NF-YB2 and NF-YC2 pull down experiments.

In order to move forward in our understanding of the function of NF-Y genes, it would have been useful to detect the NF-YA2 subunit and the protein associated with it, to unravel the target genes they control and other regulatory proteins they interact with in multimeric complexes. Windram et al. (2012) found that in Arabidopsis NF-YA transcripts exhibit significant alterations during the defense response against *B. cinerea*. This result together with the significantly enhanced susceptibility of *nf-ya2* KO mutants during the infection with the necrotrophic fungal pathogen and the reduced level of JA observed in this mutant in a previous study (Breeze at al. in preparation), indicate that NF-YA2 subunit may act as key regulator in the plant defense response. Additionally, the lack of altered phenotype of NF-YA2 KO and OE mutants during *Hpa* and *P. syringae* infection suggests that NF-YA2 subunit could play an exclusive role during the plant defense response against *B. cinerea* infection. This is in line with the hypothesis that NF-YA, as in mammals (Manni et al. 2008), represent the regulatory subunits of the trimer and so, different NF-YAs specifically bind the CCAAT box of a target gene allowing transcriptional fine-tuning under different environmental conditions. However, the functional specificity of NF-Y complexes is largely still unknown. Chromatine immunoprecipitation followed by PCR (Chip-Seq) would be required to identify the set of genes containing CCAAT boxes in their promoter representing direct targets of each NF-YA member *in vivo* under different endogenous and exogenous stimuli. This investigation in combination with transcriptome analysis should shed some light on the function and specificity of different NF-Y complexes. Also, the use of Y3H system would help to elucidate putative NF-YA2 trimeric complexes, to narrow down all possible combinations, which can be then confirmed *in planta*.

In this research, it was also shown that Arabidopsis *nf-yb2* mutant did not display altered susceptibility against *B. cinerea* and *Hpa* compared to wild type plants, while *nf-yb2/nf-yb3* double mutant showed to be significantly more resistant than

Col-0. This suggests an overlapping functionality between NF-YB3 and NF-YB2, hence only when both subunits are absent it is possible to observe an altered phenotype. These results raised an important question about whether different NF-Y genes in plant, belonging to the same subfamily, have evolved new functions or have an overlapping functionality with other NF-Y members.

Furthermore, to expand our knowledge on NF-Y TFs in other crops a cross-species approach was used to identify key NF-Y orthologues genes based on the information gained in the model plant Arabidopsis. However, in the case of large TFs families such as NF-Ys, where functional redundant copies of each genes are present, identifing true functional orthologues based on protein sequence can be problematic. For this reason we performed a comparative expression analysis under a specific stress condition between the model plant and other species, represented a useful tool to predict the function of a certain gene. RNA-Seq analysis were carried out, and based on gene expression profiles it was found that large number of tomato and lettuce NF-YA and NF-YB orthologues genes were differentially expressed in response to *B. cinerea* infection. This is in agreement with what was observed in Arabidopsis where NF-YA and NF-YB members showed to be the subunits which undergo significant alteration in the expression pattern during the necrotrophic pathogen attack, suggesting a possible conserved function of these NF-Y subfamilies across different species.

Moreover, in this study it was determined that five NF-Y orthologues genes in tomato and lettuce, including two members of the NF-YA subfamily (*Solyc01g006930, Lsat_1_v5_gn_2_54241)* and three members of the NF-YB subfamily *(Solyc07g065500, Solyc12g006120, Lsat_1_v5_gn_5_1080)* could possibly influence plant defense response, based on their conserved expression profile across the three species, providing candidates for further gene functional studies in other crops than Arabidopsis.

Having looked carefully at the data obtained, the research presented here gives strong evidence concerning the role of NF-Y TFs during the plant defense against the necrotrophic pathogen *B. cinerea*. This is a novel function of NF-Y TFs, since,

so far, they were mainly associated with developmental and physiological responses, such as flowering time, embryogenesis and abiotic stresses (Swain et al. 2017), with only few study reporting their role in plant immunity (Alam et al. 2015, Hanemian et al. 2016, Rey et al. 2016). Moreover, according to the result showed in this research it can be hypothesized a model where during *B. cinerea* infection miR169, a microRNA family involved in plant development and stress-induced responses. is repressed. This enhance the expression level of NF-YA2 subunit, which is normally very low in physiological condition due to post transcriptional regulation. Hence, it was reported that the level of miR169/AGO1 complex, which target NF-YA mRNA, decreased during different stress condition. NF-YA2 is then translocated into the nucleus where it binds NF-YB2/NF-YC2 dimer, forming the NF-Y complex which regulate the expression of key defense genes probably involved in the JA pathway, since *nf-ya2* KO mutant have present altered level of JA. Additionally, other dimer combinations are possible between NF-YB and NF-YC subunits, such as NF-YC2/NF-YB10, NF-YC2/NF-YB1, NF-YB2/NF-YC9, NF-YB2/NF-YC4, NF-YB2/NF-YC4, which are potentially NF-YB2/NF-YC2 competitors preventing the formation of this dimer. This competition could regulate defence gene through the formation of different NF-Y complex, acting as positive or negative regulator of plant immunity. The activator complex NF-YA2/NF-YB2/NF-YC2, which positively regulate the expression of defense genes and the repressor complex formed by different NF-YB and NF-YC subunits preventing NF-YA2 to join the complex and bind the promoter in the CCAAT element.

7.1 Conclusion

In conclusion, this research improved our understanding of NF-Y assembly mechanism in plant. Firstly, it allowed to localize each subunit of the putative trimer in the plant cell and identified where the dimerization between NF-YB2 and NF-YC2 occur. Secondly, it discovered potential leaf complexes, such as NF-YB2/NF-YC9, NF-YB2/NF-YC4, NF-YB2/NF-YC1, NF-YC2/NF-YB1 and NF-YC2/NF-

YB10 as well as confirmed the interaction between NF-YB2 and NF-YC2 *in planta*. Thirdly, it found a conserved expression patterns of different NF-Y orthologues genes during *B. cinerea* across different crops, suggesting a conserved function of some NF-YA and NF-YB orthologues genes in tomato and lettuce.

Hence this study proposed a methodology which combines BiFC, MS and transcriptomics analysis to systematically identify NF-Y protein complexes *in planta,* which could be a powerful system since so far, the identification of NF-Y complexes was mainly carried out using Y3H assay. However, technical challenges still limit our understanding of NF-Y hetero-trimeric complexes, one example is represented by the functional redundancy of NF-Ys, which is problematic when NF-Y KO mutants are used. Also, the tight regulation of NF-YA subunits is an issue for the detection of these proteins in plants. Hence, looking for alternative methodologies is fundamental to characterize NF-Y complexes. This would elucidate our understanding in many areas of plant-environment interactions, stress responses and plant development and would allow the production of pathogen resistant crops using NF-Y as candidate genes for genetic engineering experiment.

Still many questions need to be answered, for example the transcriptional regulation and post-transcriptional modification of NF-Y in plant need to be investigate, together with understand differences and similarities between animal and plant to better explain why plants have many NF-Y TFs for each subfamily. Specifically, it is important to elucidate whether different NF-Y have developed new functions or they are redundant genes in the genome. The research presented here provides a starting point for further investigation about the functional and combinatorial role of NF-Y in physiological condition and during the plant defense response, focusing not just on the model plant Arabidopsis but also in other economically important crops such as tomato and lettuce.

Bibliography

Abruzzi KC, Smith A, Chen W, Solomon F. 2002. Protection from free beta-tubulin by the beta-tubulin binding protein Rbl2p. Mol Cell Biol 22:138-147.

AbuQamar S, Chen X, Dhawan R, Bluhm B, Salmeron J, Lam S, Dietrich RA, Mengiste T. 2006. Expression profiling and mutant analysis reveals complex regulatory networks involved in Arabidopsis response to Botrytis infection. Plant J 48:28-44.

Adams KL, Wendel JF. 2005. Polyploidy and genome evolution in plants. Curr Opin Plant Biol 8:135-141.

Aktar MW, Paramasivam M, Sengupta D, Purkait S, Ganguly M, Banerjee S. 2009. Impact assessment of pesticide residues in fish of Ganga river around Kolkata in West Bengal. Environ Monit Assess 157:97-104.

Alam MM, et al. 2015. Overexpression of a rice heme activator protein gene (OsHAP2E) confers resistance to pathogens, salinity and drought, and increases photosynthesis and tiller number. Plant Biotechnol J 13:85-96.

Alfano JR. 2009. Roadmap for future research on plant pathogen effectors. Mol Plant Pathol 10:805-813.

Ambawat S, Sharma P, Yadav NR, Yadav RC. 2013. MYB transcription factor genes as regulators for plant responses: an overview. Physiol Mol Biol Plants 19:307-321.

Asai T, Tena G, Plotnikova J, Willmann MR, Chiu WL, Gomez-Gomez L, Boller T, Ausubel FM, Sheen J. 2002. MAP kinase signalling cascade in Arabidopsis innate immunity. Nature 415:977-983.

Atkinson NJ, Urwin PE. 2012. The interaction of plant biotic and abiotic stresses: from genes to the field. J Exp Bot 63:3523-3543.

Audenaert K, De Meyer GB, Hofte MM. 2002. Abscisic acid determines basal susceptibility of tomato to Botrytis cinerea and suppresses salicylic acid-dependent signaling mechanisms. Plant Physiol 128:491-501.

Ballif J, Endo S, Kotani M, MacAdam J, Wu Y. 2011. Over-expression of HAP3b enhances primary root elongation in Arabidopsis. Plant Physiol Biochem 49:579-583.

Bardas GA, Veloukas T, Koutita O, Karaoglanidis GS. 2010. Multiple resistance of Botrytis cinerea from kiwifruit to SDHIs, QoIs and fungicides of other chemical groups. Pest Manag Sci 66:967-973.

Bardoel BW, van der Ent S, Pel MJ, Tommassen J, Pieterse CM, van Kessel KP, van Strijp JA. 2011. Pseudomonas evades immune recognition of flagellin in both mammals and plants. PLoS Pathog 7:e1002206.

Bebber DP, Holmes T, Smith D, Gurr SJ. 2014. Economic and physical determinants of the global distributions of crop pests and pathogens. New Phytol 202:901-910.

Bechtold U, et al. 2013. Arabidopsis HEAT SHOCK TRANSCRIPTION FACTORA1b overexpression enhances water productivity, resistance to drought, and infection. J Exp Bot 64:3467-3481.

Benatti P, Chiaramonte ML, Lorenzo M, Hartley JA, Hochhauser D, Gnesutta N, Mantovani R, Imbriano C, Dolfini D. 2016. NF-Y activates genes of metabolic pathways altered in cancer cells. Oncotarget 7:1633-1650.

Benatti P, Dolfini D, Vigano A, Ravo M, Weisz A, Imbriano C. 2011. Specific inhibition of NF-Y subunits triggers different cell proliferation defects. Nucleic Acids Res 39:5356-5368.

Benjamini Y, Drai D, Elmer G, Kafkafi N, Golani I. 2001. Controlling the false discovery rate in behavior genetics research. Behav Brain Res 125:279-284.

Berrocal-Lobo M, Molina A, Solano R. 2002. Constitutive expression of ETHYLENE-RESPONSE-FACTOR1 in Arabidopsis confers resistance to several necrotrophic fungi. Plant J 29:23-32.

Birkenbihl RP, Diezel C, Somssich IE. 2012. Arabidopsis WRKY33 is a key transcriptional regulator of hormonal and metabolic responses toward Botrytis cinerea infection. Plant Physiol 159:266-285.

Block A, Alfano JR. 2011. Plant targets for Pseudomonas syringae type III effectors: virulence targets or guarded decoys? Curr Opin Microbiol 14:39-46.

Boller T, Felix G. 2009. A renaissance of elicitors: perception of microbe-associated molecular patterns and danger signals by pattern-recognition receptors. Annu Rev Plant Biol 60:379-406.

Bolognese F, et al. 1999. The cyclin B2 promoter depends on NF-Y, a trimer whose CCAAT-binding activity is cell-cycle regulated. Oncogene 18:1845-1853.

Bontinck M, Van Leene J, Gadeyne A, De Rybel B, Eeckhout D, Nelissen H, De Jaeger G. 2018. Recent Trends in Plant Protein Complex Analysis in a Developmental Context. Front Plant Sci 9:640.

Bouche N, Bouchez D. 2001. Arabidopsis gene knockout: phenotypes wanted. Curr Opin Plant Biol 4:111-117.

Bracha-Drori K, Shichrur K, Katz A, Oliva M, Angelovici R, Yalovsky S, Ohad N. 2004. Detection of protein-protein interactions in plants using bimolecular fluorescence complementation. Plant J 40:419-427.

Bray NL, Pimentel H, Melsted P, Pachter L. 2016. Near-optimal probabilistic RNA-seq quantification. Nat Biotechnol 34:525-527.

Braybrook SA, Harada JJ. 2008. LECs go crazy in embryo development. Trends Plant Sci 13:624-630.

Breeze E. 2014. Action of the NF-Y Transcription Factors in Plant Stress Responses. University of Warwick.

Breeze E, et al. 2011. High-resolution temporal profiling of transcripts during Arabidopsis leaf senescence reveals a distinct chronology of processes and regulation. Plant Cell 23:873-894.

Bruckner A, Polge C, Lentze N, Auerbach D, Schlattner U. 2009. Yeast two-hybrid, a powerful tool for systems biology. Int J Mol Sci 10:2763-2788.

Brutus A, Sicilia F, Macone A, Cervone F, De Lorenzo G. 2010. A domain swap approach reveals a role of the plant wall-associated kinase 1 (WAK1) as a receptor of oligogalacturonides. Proc Natl Acad Sci U S A 107:9452-9457.

Bu Q, Jiang H, Li CB, Zhai Q, Zhang J, Wu X, Sun J, Xie Q, Li C. 2008. Role of the Arabidopsis thaliana NAC transcription factors ANAC019 and ANAC055 in regulating jasmonic acid-signaled defense responses. Cell Res 18:756-767.

Calvenzani V, Testoni B, Gusmaroli G, Lorenzo M, Gnesutta N, Petroni K, Mantovani R, Tonelli C. 2012. Interactions and CCAAT-binding of Arabidopsis thaliana NF-Y subunits. PLoS One 7:e42902.

Cao S, Kumimoto RW, Gnesutta N, Calogero AM, Mantovani R, Holt BF, 3rd. 2014. A distal CCAAT/NUCLEAR FACTOR Y complex promotes chromatin looping at the FLOWERING LOCUS T promoter and regulates the timing of flowering in Arabidopsis. Plant Cell 26:1009-1017.

Cao S, Kumimoto RW, Siriwardana CL, Risinger JR, Holt BF, 3rd. 2011. Identification and characterization of NF-Y transcription factor families in the monocot model plant Brachypodium distachyon. PLoS One 6:e21805.

Chae HD, Yun J, Bang YJ, Shin DY. 2004. Cdk2-dependent phosphorylation of the NF-Y transcription factor is essential for the expression of the cell cycle-regulatory genes and cell cycle G1/S and G2/M transitions. Oncogene 23:4084-4088.

Chen L, Zhang L, Yu D. 2010. Wounding-induced WRKY8 is involved in basal defense in Arabidopsis. Mol Plant Microbe Interact 23:558-565.

Citovsky V, Gafni Y, Tzfira T. 2008. Localizing protein-protein interactions by bimolecular fluorescence complementation in planta. Methods 45:196-206.

Clough SJ, Bent AF. 1998. Floral dip: a simplified method for Agrobacterium-mediated transformation of Arabidopsis thaliana. Plant J 16:735-743.

Coates ME, Beynon JL. 2010. Hyaloperonospora Arabidopsidis as a pathogen model. Annu Rev Phytopathol 48:329-345.

Combier JP, et al. 2006. MtHAP2-1 is a key transcriptional regulator of symbiotic nodule development regulated by microRNA169 in Medicago truncatula. Genes Dev 20:3084-3088.

Cottier S, Monig T, Wang Z, Svoboda J, Boland W, Kaiser M, Kombrink E. 2011. The yeast three-hybrid system as an experimental platform to identify proteins interacting with small signaling molecules in plant cells: potential and limitations. Front Plant Sci 2:101.

Coustry F, Maity SN, Sinha S, de Crombrugghe B. 1996. The transcriptional activity of the CCAAT-binding factor CBF is mediated by two distinct activation domains, one in the CBF-B subunit and the other in the CBF-C subunit. J Biol Chem 271:14485-14491.

Croucher DR, et al. 2016. Bimolecular complementation affinity purification (BiCAP) reveals dimer-specific protein interactions for ERBB2 dimers. Sci Signal 9:ra69.

Cui F, Brosche M, Sipari N, Tang S, Overmyer K. 2013. Regulation of ABA dependent wound induced spreading cell death by MYB108. New Phytol 200:634-640.

Cunnac S, Lindeberg M, Collmer A. 2009. Pseudomonas syringae type III secretion system effectors: repertoires in search of functions. Curr Opin Microbiol 12:53-60.

De Miccolis Angelini RM, Masiello M, Rotolo C, Pollastro S, Faretra F. 2014. Molecular characterisation and detection of resistance to succinate dehydrogenase inhibitor fungicides in Botryotinia fuckeliana (Botrytis cinerea). Pest Manag Sci 70:1884-1893.

de Silvio A, Imbriano C, Mantovani R. 1999. Dissection of the NF-Y transcriptional activation potential. Nucleic Acids Res 27:2578-2584.

Dean R, et al. 2012. The Top 10 fungal pathogens in molecular plant pathology. Mol Plant Pathol 13:414-430.

Denby KJ, Kumar P, Kliebenstein DJ. 2004. Identification of Botrytis cinerea susceptibility loci in Arabidopsis thaliana. Plant J 38:473-486.

Dik AJ, Koning G, Kohl J. 1999. Evaluation of microbial antagonists for biological control of Botrytis cinerea stem infection in cucumber and tomato. European Journal of Plant Pathology 105:115-122.

Dolfini D, Gatta R, Mantovani R. 2012. NF-Y and the transcriptional activation of CCAAT promoters. Crit Rev Biochem Mol Biol 47:29-49.

Dolfini D, Zambelli F, Pavesi G, Mantovani R. 2009. A perspective of promoter architecture from the CCAAT box. Cell Cycle 8:4127-4137.

Dolfini D, Zambelli F, Pedrazzoli M, Mantovani R, Pavesi G. 2016. A high definition look at the NF-Y regulome reveals genome-wide associations with selected transcription factors. Nucleic Acids Res 44:4684-4702.

Dyson MR, Shadbolt SP, Vincent KJ, Perera RL, McCafferty J. 2004. Production of soluble mammalian proteins in Escherichia coli: identification of protein features that correlate with successful expression. BMC Biotechnol 4:32.

El Yahyaoui F, et al. 2004. Expression profiling in Medicago truncatula identifies more than 750 genes differentially expressed during nodulation, including many potential regulators of the symbiotic program. Plant Physiol 136:3159-3176.

Eshed Y, Baum SF, Perea JV, Bowman JL. 2001. Establishment of polarity in lateral organs of plants. Curr Biol 11:1251-1260.

Eulgem T, Somssich IE. 2007. Networks of WRKY transcription factors in defense signaling. Curr Opin Plant Biol 10:366-371.

Fabro G, et al. 2011. Multiple candidate effectors from the oomycete pathogen Hyaloperonospora arabidopsidis suppress host plant immunity. PLoS Pathog 7:e1002348.

FAO. 2009. Global agricolture towards 2050. Report no.

Feng ZJ, He GH, Zheng WJ, Lu PP, Chen M, Gong YM, Ma YZ, Xu ZS. 2015. Foxtail Millet NF-Y Families: Genome-Wide Survey and Evolution Analyses Identified Two Functional Genes Important in Abiotic Stresses. Front Plant Sci 6:1142.

Ferrari S, Galletti R, Denoux C, De Lorenzo G, Ausubel FM, Dewdney J. 2007. Resistance to Botrytis cinerea induced in Arabidopsis by elicitors is independent of salicylic acid, ethylene, or jasmonate signaling but requires PHYTOALEXIN DEFICIENT3. Plant Physiol 144:367-379.

Ferrari S, Plotnikova JM, De Lorenzo G, Ausubel FM. 2003. Arabidopsis local resistance to Botrytis cinerea involves salicylic acid and camalexin and requires EDS4 and PAD2, but not SID2, EDS5 or PAD4. Plant J 35:193-205.

Fields S, Song O. 1989. A novel genetic system to detect protein-protein interactions. Nature 340:245-246.

Fiil BK, Petersen M. 2011. Constitutive expression of MKS1 confers susceptibility to Botrytis cinerea infection independent of PAD3 expression. Plant Signal Behav 6:1425-1427.

Filichkin SA, Priest HD, Givan SA, Shen R, Bryant DW, Fox SE, Wong WK, Mockler TC. 2010. Genome-wide mapping of alternative splicing in Arabidopsis thaliana. Genome Res 20:45-58.

Fitch WM. 1970. Distinguishing homologous from analogous proteins. Syst Zool 19:99-113.

FitzGerald PC, Shlyakhtenko A, Mir AA, Vinson C. 2004. Clustering of DNA sequences in human promoters. Genome Res 14:1562-1574.

Food and Agriculture Organization of the United Nations. 2013. Report of the FAO Workshop on Bycatch Management and Low-impact Fishing : Kuwait City, the State of Kuwait, 9-12 December 2012. Food and Agriculture Organization of the United Nations.

Fornari M, Calvenzani V, Masiero S, Tonelli C, Petroni K. 2013. The Arabidopsis NF-YA3 and NF-YA8 genes are functionally redundant and are required in early embryogenesis. PLoS One 8:e82043.

Freeling M. 2008. The evolutionary position of subfunctionalization, downgraded. Genome Dyn 4:25-40.

Frontini M, Imbriano C, Manni I, Mantovani R. 2004. Cell cycle regulation of NF-YC nuclear localization. Cell Cycle 3:217-222.

Gabaldon T. 2008. Comparative genomics-based prediction of protein function. Methods Mol Biol 439:387-401.

Gale MD, Devos KM. 1998. Plant comparative genetics after 10 years. Science 282:656-659.

Galletti R, Ferrari S, De Lorenzo G. 2011. Arabidopsis MPK3 and MPK6 play different roles in basal and oligogalacturonide- or flagellin-induced resistance against Botrytis cinerea. Plant Physiol 157:804-814.

Gao W, Liu W, Zhao M, Li WX. 2015. NERF encodes a RING E3 ligase important for drought resistance and enhances the expression of its antisense gene NFYA5 in Arabidopsis. Nucleic Acids Res 43:607-617.

Gingras AC, Gstaiger M, Raught B, Aebersold R. 2007. Analysis of protein complexes using mass spectrometry. Nat Rev Mol Cell Biol 8:645-654.

Glazebrook J. 2005. Contrasting mechanisms of defense against biotrophic and necrotrophic pathogens. Annu Rev Phytopathol 43:205-227.

Global Food Security. 2015. Global Food Security. (http://www.foodsecurity.ac.uk/issue/global.html)

Goulson D. 2014. Ecology: Pesticides linked to bird declines. Nature 511:295-296.

Govrin EM, Levine A. 2002. Infection of Arabidopsis with a necrotrophic pathogen, Botrytis cinerea, elicits various defense responses but does not induce systemic acquired resistance (SAR). Plant Mol Biol 48:267-276.

Gramzow L, Theissen G. 2010. A hitchhiker's guide to the MADS world of plants. Genome Biol 11:214.

Grant D, Cregan P, Shoemaker RC. 2000. Genome organization in dicots: genome duplication in Arabidopsis and synteny between soybean and Arabidopsis. Proc Natl Acad Sci U S A 97:4168-4173.

Griffiths S, Dunford RP, Coupland G, Laurie DA. 2003. The evolution of CONSTANS-like gene families in barley, rice, and Arabidopsis. Plant Physiol 131:1855-1867.

Guo YL. 2013. Gene family evolution in green plants with emphasis on the origination and evolution of Arabidopsis thaliana genes. Plant J 73:941-951.

Gurr SJ, Rushton PJ. 2005. Engineering plants with increased disease resistance: how are we going to express it? Trends Biotechnol 23:283-290.

Gusmaroli G, Tonelli C, Mantovani R. 2001. Regulation of the CCAAT-Binding NF-Y subunits in Arabidopsis thaliana. Gene 264:173-185.

Hackenberg D, Wu Y, Voigt A, Adams R, Schramm P, Grimm B. 2012. Studies on differential nuclear translocation mechanism and assembly of the three subunits of the Arabidopsis thaliana transcription factor NF-Y. Mol Plant 5:876-888.

Han X, Tang S, An Y, Zheng DC, Xia XL, Yin WL. 2013. Overexpression of the poplar NF-YB7 transcription factor confers drought tolerance and improves water-use efficiency in Arabidopsis. J Exp Bot 64:4589-4601.

Hanemian M, et al. 2016. Arabidopsis CLAVATA1 and CLAVATA2 receptors contribute to Ralstonia solanacearum pathogenicity through a miR169-dependent pathway. New Phytol 211:502-515.

Hayes TB, et al. 2006. Pesticide mixtures, endocrine disruption, and amphibian declines: are we underestimating the impact? Environ Health Perspect 114 Suppl 1:40-50.

Hein I, Gilroy EM, Armstrong MR, Birch PR. 2009. The zig-zag-zig in oomycete-plant interactions. Mol Plant Pathol 10:547-562.

Hilioti Z, Ganopoulos I, Bossis I, Tsaftaris A. 2014. LEC1-LIKE paralog transcription factor: how to survive extinction and fit in NF-Y protein complex. Gene 543:220-233.

Hou X, Zhou J, Liu C, Liu L, Shen L, Yu H. 2014. Nuclear factor Y-mediated H3K27me3 demethylation of the SOC1 locus orchestrates flowering responses of Arabidopsis. Nat Commun 5:4601.

Howell LA, Gulam R, Mueller A, O'Connell MA, Searcey M. 2010. Design and synthesis of threading intercalators to target DNA. Bioorg Med Chem Lett 20:6956-6959.

Huang M, Hu Y, Liu X, Li Y, Hou X. 2015a. Arabidopsis LEAFY COTYLEDON1 controls cell fate determination during post-embryonic development. Front Plant Sci 6:955.

---. 2015b. Arabidopsis LEAFY COTYLEDON1 Mediates Postembryonic Development via Interacting with PHYTOCHROME-INTERACTING FACTOR4. Plant Cell 27:3099-3111.

Immink RG, Kaufmann K, Angenent GC. 2010. The 'ABC' of MADS domain protein behaviour and interactions. Semin Cell Dev Biol 21:87-93.

Ingle RA, Carstens M, Denby KJ. 2006. PAMP recognition and the plant-pathogen arms race. Bioessays 28:880-889.

Irish VF, Benfey PN. 2004. Beyond Arabidopsis. Translational biology meets evolutionary developmental biology. Plant Physiol 135:611-614.

Izawa T, Takahashi Y, Yano M. 2003. Comparative biology comes into bloom: genomic and genetic comparison of flowering pathways in rice and Arabidopsis. Curr Opin Plant Biol 6:113-120.

Jensen RA. 2001. Orthologs and paralogs - we need to get it right. Genome Biol 2:INTERACTIONS1002.

Jiang Z, Dong X, Zhang Z. 2016. Network-Based Comparative Analysis of Arabidopsis Immune Responses to Golovinomyces orontii and Botrytis cinerea Infections. Sci Rep 6:19149.

Jiao Y, Ma L, Strickland E, Deng XW. 2005. Conservation and divergence of light-regulated genome expression patterns during seedling development in rice and Arabidopsis. Plant Cell 17:3239-3256.

Jin H, Martin C. 1999. Multifunctionality and diversity within the plant MYB-gene family. Plant Mol Biol 41:577-585.

Jin J, Zhang H, Kong L, Gao G, Luo J. 2014. PlantTFDB 3.0: a portal for the functional and evolutionary study of plant transcription factors. Nucleic Acids Res 42:D1182-1187.

Jones JD, Dangl JL. 2006. The plant immune system. Nature 444:323-329.

Jones-Rhoades MW, Bartel DP. 2004. Computational identification of plant microRNAs and their targets, including a stress-induced miRNA. Mol Cell 14:787-799.

Junker A, et al. 2012. Elongation-related functions of LEAFY COTYLEDON1 during the development of Arabidopsis thaliana. Plant J 71:427-442.

Kahle J, Baake M, Doenecke D, Albig W. 2005. Subunits of the heterotrimeric transcription factor NF-Y are imported into the nucleus by distinct pathways involving importin beta and importin 13. Mol Cell Biol 25:5339-5354.

Kerppola TK. 2008. Bimolecular fluorescence complementation (BiFC) analysis as a probe of protein interactions in living cells. Annu Rev Biophys 37:465-487.

Kloek AP, Verbsky ML, Sharma SB, Schoelz JE, Vogel J, Klessig DF, Kunkel BN. 2001. Resistance to Pseudomonas syringae conferred by an Arabidopsis thaliana coronatine-insensitive (coi1) mutation occurs through two distinct mechanisms. Plant J 26:509-522.

Kodama Y, Hu CD. 2012. Bimolecular fluorescence complementation (BiFC): a 5-year update and future perspectives. Biotechniques 53:285-298.

Kondou Y, Higuchi M, Matsui M. 2010. High-throughput characterization of plant gene functions by using gain-of-function technology. Annu Rev Plant Biol 61:373-393.

Konig AC, et al. 2014. The Arabidopsis class II sirtuin is a lysine deacetylase and interacts with mitochondrial energy metabolism. Plant Physiol 164:1401-1414.

Korolev N, Mamiev M, Zahavi T, Elad Y. 2011. Screening of Botrytis cinerea isolates from vineyards in Israel for resistance to fungicides. European Journal of Plant Pathology 129:591-608.

Krakauer DC, Nowak MA. 1999. Evolutionary preservation of redundant duplicated genes. Semin Cell Dev Biol 10:555-559.

Kranz HD, et al. 1998. Towards functional characterisation of the members of the R2R3-MYB gene family from Arabidopsis thaliana. Plant J 16:263-276.

Kubala MH, Kovtun O, Alexandrov K, Collins BM. 2010. Structural and thermodynamic analysis of the GFP:GFP-nanobody complex. Protein Sci 19:2389-2401.

Kumimoto RW, Adam L, Hymus GJ, Repetti PP, Reuber TL, Marion CM, Hempel FD, Ratcliffe OJ. 2008. The Nuclear Factor Y subunits NF-YB2 and NF-YB3 play additive roles in the promotion of flowering by inductive long-day photoperiods in Arabidopsis. Planta 228:709-723.

Kumimoto RW, Siriwardana CL, Gayler KK, Risinger JR, Siefers N, Holt BF, 3rd. 2013. NUCLEAR FACTOR Y transcription factors have both opposing and additive roles in ABA-mediated seed germination. PLoS One 8:e59481.

Kumimoto RW, Zhang Y, Siefers N, Holt BF, 3rd. 2010. NF-YC3, NF-YC4 and NF-YC9 are required for CONSTANS-mediated, photoperiod-dependent flowering in Arabidopsis thaliana. Plant J 63:379-391.

Kwong RW, Bui AQ, Lee H, Kwong LW, Fischer RL, Goldberg RB, Harada JJ. 2003. LEAFY COTYLEDON1-LIKE defines a class of regulators essential for embryo development. Plant Cell 15:5-18.

Lai Z, Vinod K, Zheng Z, Fan B, Chen Z. 2008. Roles of Arabidopsis WRKY3 and WRKY4 transcription factors in plant responses to pathogens. BMC Plant Biol 8:68.

Lai Z, Wang F, Zheng Z, Fan B, Chen Z. 2011. A critical role of autophagy in plant resistance to necrotrophic fungal pathogens. Plant J 66:953-968.

Laloum T, De Mita S, Gamas P, Baudin M, Niebel A. 2013. CCAAT-box binding transcription factors in plants: Y so many? Trends Plant Sci 18:157-166.

Latorre BA, Torres R. 2012. Prevalence of isolates of Botrytis cinerea resistant to multiple fungicides in Chilean vineyards. Crop Protection 40:49-52.

Law CW, Chen Y, Shi W, Smyth GK. 2014. voom: Precision weights unlock linear model analysis tools for RNA-seq read counts. Genome Biol 15:R29.

Lee H, Fischer RL, Goldberg RB, Harada JJ. 2003. Arabidopsis LEAFY COTYLEDON1 represents a functionally specialized subunit of the CCAAT binding transcription factor. Proc Natl Acad Sci U S A 100:2152-2156.

Lee H, Yoo SJ, Lee JH, Kim W, Yoo SK, Fitzgerald H, Carrington JC, Ahn JH. 2010. Genetic framework for flowering-time regulation by ambient temperature-responsive miRNAs in Arabidopsis. Nucleic Acids Res 38:3081-3093.

Lee K, Kang H. 2016. Emerging Roles of RNA-Binding Proteins in Plant Growth, Development, and Stress Responses. Mol Cells 39:179-185.

Leuzinger K, Dent M, Hurtado J, Stahnke J, Lai H, Zhou X, Chen Q. 2013. Efficient agroinfiltration of plants for high-level transient expression of recombinant proteins. J Vis Exp.

Lewis LA, et al. 2015. Transcriptional Dynamics Driving MAMP-Triggered Immunity and Pathogen Effector-Mediated Immunosuppression in Arabidopsis Leaves Following Infection with Pseudomonas syringae pv tomato DC3000. Plant Cell 27:3038-3064.

Leyva-Gonzalez MA, Ibarra-Laclette E, Cruz-Ramirez A, Herrera-Estrella L. 2012. Functional and transcriptome analysis reveals an acclimatization strategy for abiotic stress tolerance mediated by Arabidopsis NF-YA family members. PLoS One 7:e48138.

Li J, Yang Z, Yu B, Liu J, Chen X. 2005. Methylation protects miRNAs and siRNAs from a 3'-end uridylation activity in Arabidopsis. Curr Biol 15:1501-1507.

Li L, Ji G, Ye C, Shu C, Zhang J, Liang C. 2015. PlantOrDB: a genome-wide ortholog database for land plants and green algae. BMC Plant Biol 15:161.

Li S, Li K, Ju Z, Cao D, Fu D, Zhu H, Zhu B, Luo Y. 2016. Genome-wide analysis of tomato NF-Y factors and their role in fruit ripening. BMC Genomics 17:36.

Li WX, Oono Y, Zhu J, He XJ, Wu JM, Iida K, Lu XY, Cui X, Jin H, Zhu JK. 2008. The Arabidopsis NFYA5 transcription factor is regulated transcriptionally and posttranscriptionally to promote drought resistance. Plant Cell 20:2238-2251.

Li YJ, Fang Y, Fu YR, Huang JG, Wu CA, Zheng CC. 2013. NFYA1 is involved in regulation of postgermination growth arrest under salt stress in Arabidopsis. PLoS One 8:e61289.

Liu JX, Howell SH. 2010. bZIP28 and NF-Y transcription factors are activated by ER stress and assemble into a transcriptional complex to regulate stress response genes in Arabidopsis. Plant Cell 22:782-796.

Livak KJ, Schmittgen TD. 2001. Analysis of relative gene expression data using real-time quantitative PCR and the 2(-Delta Delta C(T)) Method. Methods 25:402-408.

Llorente F, Muskett P, Sanchez-Vallet A, Lopez G, Ramos B, Sanchez-Rodriguez C, Jorda L, Parker J, Molina A. 2008. Repression of the auxin response pathway increases Arabidopsis susceptibility to necrotrophic fungi. Mol Plant 1:496-509.

Lobell DB, Gourdji SM. 2012. The influence of climate change on global crop productivity. Plant Physiol 160:1686-1697.

Lopez-Molina L, Mongrand S, Chua NH. 2001. A postgermination developmental arrest checkpoint is mediated by abscisic acid and requires the ABI5 transcription factor in Arabidopsis. Proc Natl Acad Sci U S A 98:4782-4787.

Lorenzo O, Piqueras R, Sanchez-Serrano JJ, Solano R. 2003. ETHYLENE RESPONSE FACTOR1 integrates signals from ethylene and jasmonate pathways in plant defense. Plant Cell 15:165-178.

Lu D, Wu S, Gao X, Zhang Y, Shan L, He P. 2010. A receptor-like cytoplasmic kinase, BIK1, associates with a flagellin receptor complex to initiate plant innate immunity. Proc Natl Acad Sci U S A 107:496-501.

Lynch M, Conery JS. 2000. The evolutionary fate and consequences of duplicate genes. Science 290:1151-1155.

Ma L, et al. 2005. A microarray analysis of the rice transcriptome and its comparison to Arabidopsis. Genome Res 15:1274-1283.

Maity SN, de Crombrugghe B. 1992. Biochemical analysis of the B subunit of the heteromeric CCAAT-binding factor. A DNA-binding domain and a subunit interaction domain are specified by two separate segments. J Biol Chem 267:8286-8292.

---. 1998. Role of the CCAAT-binding protein CBF/NF-Y in transcription. Trends Biochem Sci 23:174-178.

Manni I, Caretti G, Artuso S, Gurtner A, Emiliozzi V, Sacchi A, Mantovani R, Piaggio G. 2008. Posttranslational regulation of NF-YA modulates NF-Y transcriptional activity. Mol Biol Cell 19:5203-5213.

Mantovani R. 1999. The molecular biology of the CCAAT-binding factor NF-Y. Gene 239:15-27.

Maruyama Y, Yamoto N, Suzuki Y, Chiba Y, Yamazaki K, Sato T, Yamaguchi J. 2013. The Arabidopsis transcriptional repressor ERF9 participates in resistance against necrotrophic fungi. Plant Sci 213:79-87.

Masiero S, Imbriano C, Ravasio F, Favaro R, Pelucchi N, Gorla MS, Mantovani R, Colombo L, Kater MM. 2002. Ternary complex formation between MADS-box transcription factors and the histone fold protein NF-YB. J Biol Chem 277:26429-26435.

Massonnet C, et al. 2010. Probing the reproducibility of leaf growth and molecular phenotypes: a comparison of three Arabidopsis accessions cultivated in ten laboratories. Plant Physiol 152:2142-2157.

Masters SC. 2004. Co-immunoprecipitation from transfected cells. Methods Mol Biol 261:337-350.

McLoughlin AG, Wytinck N, Walker PL, Girard IJ, Rashid KY, de Kievit T, Fernando WGD, Whyard S, Belmonte MF. 2018. Identification and application of exogenous dsRNA confers plant protection against Sclerotinia sclerotiorum and Botrytis cinerea. Sci Rep 8:7320.

McNabb DS, Tseng KA, Guarente L. 1997. The Saccharomyces cerevisiae Hap5p homolog from fission yeast reveals two conserved domains that are essential for assembly of heterotetrameric CCAAT-binding factor. Mol Cell Biol 17:7008-7018.

Mendes A, Kelly AA, van Erp H, Shaw E, Powers SJ, Kurup S, Eastmond PJ. 2013. bZIP67 regulates the omega-3 fatty acid content of Arabidopsis seed oil by activating fatty acid desaturase3. Plant Cell 25:3104-3116.

Mengiste T, Chen X, Salmeron J, Dietrich R. 2003. The BOTRYTIS SUSCEPTIBLE1 gene encodes an R2R3MYB transcription factor protein that is required for biotic and abiotic stress responses in Arabidopsis. Plant Cell 15:2551-2565.

Mermelstein F, Yeung K, Cao J, Inostroza JA, Erdjument-Bromage H, Eagelson K, Landsman D, Levitt P, Tempst P, Reinberg D. 1996. Requirement of a corepressor for Dr1-mediated repression of transcription. Genes Dev 10:1033-1048.

Miya A, Albert P, Shinya T, Desaki Y, Ichimura K, Shirasu K, Narusaka Y, Kawakami N, Kaku H, Shibuya N. 2007. CERK1, a LysM receptor kinase, is essential for chitin elicitor signaling in Arabidopsis. Proc Natl Acad Sci U S A 104:19613-19618.

Mnif W, Hassine AI, Bouaziz A, Bartegi A, Thomas O, Roig B. 2011. Effect of endocrine disruptor pesticides: a review. Int J Environ Res Public Health 8:2265-2303.

Moffat CS, Ingle RA, Wathugala DL, Saunders NJ, Knight H, Knight MR. 2012. ERF5 and ERF6 play redundant roles as positive regulators of JA/Et-mediated defense against Botrytis cinerea in Arabidopsis. PLoS One 7:e35995.

Moore RC, Purugganan MD. 2005. The evolutionary dynamics of plant duplicate genes. Curr Opin Plant Biol 8:122-128.

Moriya H. 2015. Quantitative nature of overexpression experiments. Mol Biol Cell 26:3932-3939.

Mu J, Tan H, Hong S, Liang Y, Zuo J. 2013. Arabidopsis transcription factor genes NF-YA1, 5, 6, and 9 play redundant roles in male gametogenesis, embryogenesis, and seed development. Mol Plant 6:188-201.

Mysore KS, Tuori RP, Martin GB. 2001. Arabidopsis genome sequence as a tool for functional genomics in tomato. Genome Biol 2:REVIEWS1003.

Nagai T, Ibata K, Park ES, Kubota M, Mikoshiba K, Miyawaki A. 2002. A variant of yellow fluorescent protein with fast and efficient maturation for cell-biological applications. Nat Biotechnol 20:87-90.

Nakamura S, et al. 2010. Gateway binary vectors with the bialaphos resistance gene, bar, as a selection marker for plant transformation. Biosci Biotechnol Biochem 74:1315-1319.

Nardini M, et al. 2013. Sequence-specific transcription factor NF-Y displays histone-like DNA binding and H2B-like ubiquitination. Cell 152:132-143.

Nelson DE, et al. 2007. Plant nuclear factor Y (NF-Y) B subunits confer drought tolerance and lead to improved corn yields on water-limited acres. Proc Natl Acad Sci U S A 104:16450-16455.

Nicaise V, Joe A, Jeong BR, Korneli C, Boutrot F, Westedt I, Staiger D, Alfano JR, Zipfel C. 2013. Pseudomonas HopU1 modulates plant immune receptor levels by blocking the interaction of their mRNAs with GRP7. EMBO J 32:701-712.

Nicolopoulou-Stamati P, Maipas S, Kotampasi C, Stamatis P, Hens L. 2016. Chemical Pesticides and Human Health: The Urgent Need for a New Concept in Agriculture. Front Public Health 4:148.

O'Neill CM, Bancroft I. 2000. Comparative physical mapping of segments of the genome of Brassica oleracea var. alboglabra that are homoeologous to sequenced regions of chromosomes 4 and 5 of Arabidopsis thaliana. Plant J 23:233-243.

Odell JT, Nagy F, Chua NH. 1985. Identification of DNA sequences required for activity of the cauliflower mosaic virus 35S promoter. Nature 313:810-812.

Ohad N, Shichrur K, Yalovsky S. 2007. The analysis of protein-protein interactions in plants by bimolecular fluorescence complementation. Plant Physiol 145:1090-1099.

Ohya T, Maki S, Kawasaki Y, Sugino A. 2000. Structure and function of the fourth subunit (Dpb4p) of DNA polymerase epsilon in Saccharomyces cerevisiae. Nucleic Acids Res 28:3846-3852.

Oldfield AJ, Yang P, Conway AE, Cinghu S, Freudenberg JM, Yellaboina S, Jothi R. 2014. Histone-fold domain protein NF-Y promotes chromatin accessibility for cell type-specific master transcription factors. Mol Cell 55:708-722.

Page DR, Grossniklaus U. 2002. The art and design of genetic screens: Arabidopsis thaliana. Nat Rev Genet 3:124-136.

Pant BD, Musialak-Lange M, Nuc P, May P, Buhtz A, Kehr J, Walther D, Scheible WR. 2009. Identification of nutrient-responsive Arabidopsis and rapeseed microRNAs by comprehensive real-time polymerase chain reaction profiling and small RNA sequencing. Plant Physiol 150:1541-1555.

Paterson AH, Lan TH, Amasino R, Osborn TC, Quiros C. 2001. Brassica genomics: a complement to, and early beneficiary of, the Arabidopsis sequence. Genome Biol 2:REVIEWS1011.

Pel MJ, Wintermans PC, Cabral A, Robroek BJ, Seidl MF, Bautor J, Parker JE, Van den Ackerveken G, Pieterse CM. 2014. Functional analysis of Hyaloperonospora arabidopsidis RXLR effectors. PLoS One 9:e110624.

Peng WT, Lee YW, Nester EW. 1998. The phenolic recognition profiles of the Agrobacterium tumefaciens VirA protein are broadened by a high level of the sugar binding protein ChvE. J Bacteriol 180:5632-5638.

Perdivara I, Deterding LJ, Przybylski M, Tomer KB. 2010. Mass spectrometric identification of oxidative modifications of tryptophan residues in proteins: chemical artifact or post-translational modification? J Am Soc Mass Spectrom 21:1114-1117.

Pertl-Obermeyer H, Schulze WX, Obermeyer G. 2014. In vivo cross-linking combined with mass spectrometry analysis reveals receptor-like kinases and Ca(2+) signalling proteins as putative interaction partners of pollen plasma membrane H(+) ATPases. J Proteomics 108:17-29.

Petroni K, Kumimoto RW, Gnesutta N, Calvenzani V, Fornari M, Tonelli C, Holt BF, 3rd, Mantovani R. 2012. The promiscuous life of plant NUCLEAR FACTOR Y transcription factors. Plant Cell 24:4777-4792.

Pieterse CM, Van der Does D, Zamioudis C, Leon-Reyes A, Van Wees SC. 2012. Hormonal modulation of plant immunity. Annu Rev Cell Dev Biol 28:489-521.

Pre M, Atallah M, Champion A, De Vos M, Pieterse CM, Memelink J. 2008. The AP2/ERF domain transcription factor ORA59 integrates jasmonic acid and ethylene signals in plant defense. Plant Physiol 147:1347-1357.

Qi Y, Katagiri F. 2009. Purification of low-abundance Arabidopsis plasma-membrane protein complexes and identification of candidate components. Plant J 57:932-944.

Qiu JL, et al. 2008. Arabidopsis MAP kinase 4 regulates gene expression through transcription factor release in the nucleus. EMBO J 27:2214-2221.

Quach TN, Nguyen HT, Valliyodan B, Joshi T, Xu D, Nguyen HT. 2015. Genome-wide expression analysis of soybean NF-Y genes reveals potential function in development and drought response. Mol Genet Genomics 290:1095-1115.

Ramirez V, Garcia-Andrade J, Vera P. 2011. Enhanced disease resistance to Botrytis cinerea in myb46 Arabidopsis plants is associated to an early down-regulation of CesA genes. Plant Signal Behav 6:911-913.

Ransone LJ. 1995. Detection of protein-protein interactions by coimmunoprecipitation and dimerization. Methods Enzymol 254:491-497.

Rasmussen MW, Roux M, Petersen M, Mundy J. 2012. MAP Kinase Cascades in Arabidopsis Innate Immunity. Front Plant Sci 3:169.

Ren D, Liu Y, Yang KY, Han L, Mao G, Glazebrook J, Zhang S. 2008. A fungal-responsive MAPK cascade regulates phytoalexin biosynthesis in Arabidopsis. Proc Natl Acad Sci U S A 105:5638-5643.

Rensink WA, Buell CR. 2004. Arabidopsis to rice. Applying knowledge from a weed to enhance our understanding of a crop species. Plant Physiol 135:622-629.

Rey T, Laporte P, Bonhomme M, Jardinaud MF, Huguet S, Balzergue S, Dumas B, Niebel A, Jacquet C. 2016. MtNF-YA1, A Central Transcriptional Regulator of Symbiotic Nodule Development, Is Also a Determinant of Medicago truncatula Susceptibility toward a Root Pathogen. Front Plant Sci 7:1837.

Reyes-Chin-Wo S, et al. 2017. Genome assembly with in vitro proximity ligation data and whole-genome triplication in lettuce. Nat Commun 8:14953.

Riechmann JL, et al. 2000. Arabidopsis transcription factors: genome-wide comparative analysis among eukaryotes. Science 290:2105-2110.

Ripodas C, Castaingts M, Clua J, Blanco F, Zanetti ME. 2014. Annotation, phylogeny and expression analysis of the nuclear factor Y gene families in common bean (Phaseolus vulgaris). Front Plant Sci 5:761.

Ritchie ME, Phipson B, Wu D, Hu Y, Law CW, Shi W, Smyth GK. 2015. limma powers differential expression analyses for RNA-sequencing and microarray studies. Nucleic Acids Res 43:e47.

Robson F, Costa MM, Hepworth SR, Vizir I, Pineiro M, Reeves PH, Putterill J, Coupland G. 2001. Functional importance of conserved domains in the flowering-time gene CONSTANS demonstrated by analysis of mutant alleles and transgenic plants. Plant J 28:619-631.

Romier C, Cocchiarella F, Mantovani R, Moras D. 2003. The NF-YB/NF-YC structure gives insight into DNA binding and transcription regulation by CCAAT factor NF-Y. J Biol Chem 278:1336-1345.

Rowe HC, Walley JW, Corwin J, Chan EK, Dehesh K, Kliebenstein DJ. 2010. Deficiencies in jasmonate-mediated plant defense reveal quantitative variation in Botrytis cinerea pathogenesis. PLoS Pathog 6:e1000861.

Sanborn M, Kerr KJ, Sanin LH, Cole DC, Bassil KL, Vakil C. 2007. Non-cancer health effects of pesticides: systematic review and implications for family doctors. Can Fam Physician 53:1712-1720.

Sato H, et al. 2014. Arabidopsis DPB3-1, a DREB2A interactor, specifically enhances heat stress-induced gene expression by forming a heat stress-specific transcriptional complex with NF-Y subunits. Plant Cell 26:4954-4973.

Schneider CA, Rasband WS, Eliceiri KW. 2012. NIH Image to ImageJ: 25 years of image analysis. Nat Methods 9:671-675.

Schumacher J. 2012. Tools for Botrytis cinerea: New expression vectors make the gray mold fungus more accessible to cell biology approaches. Fungal Genet Biol 49:483-497.

Schweighofer A, et al. 2007. The PP2C-type phosphatase AP2C1, which negatively regulates MPK4 and MPK6, modulates innate immunity, jasmonic acid, and ethylene levels in Arabidopsis. Plant Cell 19:2213-2224.

Shaik R, Ramakrishna W. 2014. Machine learning approaches distinguish multiple stress conditions using stress-responsive genes and identify candidate genes for broad resistance in rice. Plant Physiol 164:481-495.

Sheard LB, et al. 2010. Jasmonate perception by inositol-phosphate-potentiated COI1-JAZ co-receptor. Nature 468:400-405.

Shi H, Ye T, Zhong B, Liu X, Jin R, Chan Z. 2014. AtHAP5A modulates freezing stress resistance in Arabidopsis through binding to CCAAT motif of AtXTH21. New Phytol 203:554-567.

Siefers N, Dang KK, Kumimoto RW, Bynum WEt, Tayrose G, Holt BF, 3rd. 2009. Tissue-specific expression patterns of Arabidopsis NF-Y transcription factors suggest potential for extensive combinatorial complexity. Plant Physiol 149:625-641.

Simillion C, Vandepoele K, Van Montagu MC, Zabeau M, Van de Peer Y. 2002. The hidden duplication past of Arabidopsis thaliana. Proc Natl Acad Sci U S A 99:13627-13632.

Singh K, Talla A, Qiu W. 2012. Small RNA profiling of virus-infected grapevines: evidences for virus infection-associated and variety-specific miRNAs. Funct Integr Genomics 12:659-669.

Sinha S, Kim IS, Sohn KY, de Crombrugghe B, Maity SN. 1996. Three classes of mutations in the A subunit of the CCAAT-binding factor CBF delineate functional domains involved in the three-step assembly of the CBF-DNA complex. Mol Cell Biol 16:328-337.

Siriwardana CL, Gnesutta N, Kumimoto RW, Jones DS, Myers ZA, Mantovani R, Holt BF, 3rd. 2016. NUCLEAR FACTOR Y, Subunit A (NF-YA) Proteins Positively Regulate Flowering and Act Through FLOWERING LOCUS T. PLoS Genet 12:e1006496.

Soltis PS, Marchant DB, Van de Peer Y, Soltis DE. 2015. Polyploidy and genome evolution in plants. Curr Opin Genet Dev 35:119-125.

Somerville C, Koornneef M. 2002. A fortunate choice: the history of Arabidopsis as a model plant. Nat Rev Genet 3:883-889.

Son GH, Wan J, Kim HJ, Nguyen XC, Chung WS, Hong JC, Stacey G. 2012. Ethylene-responsive element-binding factor 5, ERF5, is involved in chitin-induced innate immunity response. Mol Plant Microbe Interact 25:48-60.

Son O, Kim S, Shin YJ, Kim WY, Koh HJ, Cheon CI. 2015. Identification of nucleosome assembly protein 1 (NAP1) as an interacting partner of plant ribosomal protein S6 (RPS6) and a positive regulator of rDNA transcription. Biochem Biophys Res Commun 465:200-205.

Sonnhammer EL, Koonin EV. 2002. Orthology, paralogy and proposed classification for paralog subtypes. Trends Genet 18:619-620.

Sorin C, Declerck M, Christ A, Blein T, Ma L, Lelandais-Briere C, Njo MF, Beeckman T, Crespi M, Hartmann C. 2014. A miR169 isoform regulates specific NF-YA targets and root architecture in Arabidopsis. New Phytol 202:1197-1211.

Stege JT, Guan X, Ho T, Beachy RN, Barbas CF, 3rd. 2002. Controlling gene expression in plants using synthetic zinc finger transcription factors. Plant J 32:1077-1086.

Stephenson TJ, McIntyre CL, Collet C, Xue GP. 2007. Genome-wide identification and expression analysis of the NF-Y family of transcription factors in Triticum aestivum. Plant Mol Biol 65:77-92.

Strayer C, Oyama T, Schultz TF, Raman R, Somers DE, Mas P, Panda S, Kreps JA, Kay SA. 2000. Cloning of the Arabidopsis clock gene TOC1, an autoregulatory response regulator homolog. Science 289:768-771.

Street NR, Sjodin A, Bylesjo M, Gustafsson P, Trygg J, Jansson S. 2008. A cross-species transcriptomics approach to identify genes involved in leaf development. BMC Genomics 9:589.

Sutherland BW, Toews J, Kast J. 2008. Utility of formaldehyde cross-linking and mass spectrometry in the study of protein-protein interactions. J Mass Spectrom 43:699-715.

Swain S, Myers ZA, Siriwardana CL, Holt BF, 3rd. 2017. The multifaceted roles of NUCLEAR FACTOR-Y in Arabidopsis thaliana development and stress responses. Biochim Biophys Acta 1860:636-644.

Takatsuji H. 1998. Zinc-finger transcription factors in plants. Cell Mol Life Sci 54:582-596.

Tao Y, Xie Z, Chen W, Glazebrook J, Chang HS, Han B, Zhu T, Zou G, Katagiri F. 2003. Quantitative nature of Arabidopsis responses during compatible and incompatible interactions with the bacterial pathogen Pseudomonas syringae. Plant Cell 15:317-330.

Testa A, Donati G, Yan P, Romani F, Huang TH, Vigano MA, Mantovani R. 2005. Chromatin immunoprecipitation (ChIP) on chip experiments uncover a widespread distribution of NF-Y binding CCAAT sites outside of core promoters. J Biol Chem 280:13606-13615.

Thirumurugan T, Ito Y, Kubo T, Serizawa A, Kurata N. 2008. Identification, characterization and interaction of HAP family genes in rice. Mol Genet Genomics 279:279-289.

Thomma BP, Eggermont K, Penninckx IA, Mauch-Mani B, Vogelsang R, Cammue BP, Broekaert WF. 1998. Separate jasmonate-dependent and salicylate-dependent defense-response pathways in Arabidopsis are essential for resistance to distinct microbial pathogens. Proc Natl Acad Sci U S A 95:15107-15111.

Thomma BP, Eggermont K, Tierens KF, Broekaert WF. 1999. Requirement of functional ethylene-insensitive 2 gene for efficient resistance of Arabidopsis to infection by Botrytis cinerea. Plant Physiol 121:1093-1102.

Tian G, Lu Q, Zhang L, Kohalmi SE, Cui Y. 2011. Detection of protein interactions in plant using a gateway compatible bimolecular fluorescence complementation (BiFC) system. J Vis Exp.

Tiwari SB, et al. 2010. The flowering time regulator CONSTANS is recruited to the FLOWERING LOCUS T promoter via a unique cis-element. New Phytol 187:57-66.

Tomato Genome C. 2012. The tomato genome sequence provides insights into fleshy fruit evolution. Nature 485:635-641.

Vasilescu J, Guo X, Kast J. 2004. Identification of protein-protein interactions using in vivo cross-linking and mass spectrometry. Proteomics 4:3845-3854.

Vavouri T, Semple JI, Garcia-Verdugo R, Lehner B. 2009. Intrinsic protein disorder and interaction promiscuity are widely associated with dosage sensitivity. Cell 138:198-208.

Viola IL, Gonzalez DH. 2016. Chapter 2 - Methods to Study Transcription Factor Structure and Function. Pages 13-33. Plant Transcription Factors. Boston: Academic Press.

Vitale A, Ceriotti A. 2004. Protein quality control mechanisms and protein storage in the endoplasmic reticulum. A conflict of interests? Plant Physiol 136:3420-3426.

Voinnet O, Rivas S, Mestre P, Baulcombe D. 2003. An enhanced transient expression system in plants based on suppression of gene silencing by the p19 protein of tomato bushy stunt virus. Plant J 33:949-956.

Walhout AJ, Vidal M. 2001. High-throughput yeast two-hybrid assays for large-scale protein interaction mapping. Methods 24:297-306.

Walter M, et al. 2004. Visualization of protein interactions in living plant cells using bimolecular fluorescence complementation. Plant J 40:428-438.

Wan J, Zhang XC, Neece D, Ramonell KM, Clough S, Kim SY, Stacey MG, Stacey G. 2008. A LysM receptor-like kinase plays a critical role in chitin signaling and fungal resistance in Arabidopsis. Plant Cell 20:471-481.

Wang X, Basnayake BM, Zhang H, Li G, Li W, Virk N, Mengiste T, Song F. 2009. The Arabidopsis ATAF1, a NAC transcription factor, is a negative regulator of defense responses against necrotrophic fungal and bacterial pathogens. Mol Plant Microbe Interact 22:1227-1238.

Ware D, Stein L. 2003. Comparison of genes among cereals. Curr Opin Plant Biol 6:121-127.

Warpeha KM, Upadhyay S, Yeh J, Adamiak J, Hawkins SI, Lapik YR, Anderson MB, Kaufman LS. 2007. The GCR1, GPA1, PRN1, NF-Y signal chain mediates both blue light and abscisic acid responses in Arabidopsis. Plant Physiol 143:1590-1600.

Weiberg A, Wang M, Lin FM, Zhao H, Zhang Z, Kaloshian I, Huang HD, Jin H. 2013. Fungal small RNAs suppress plant immunity by hijacking host RNA interference pathways. Science 342:118-123.

Wenkel S, Turck F, Singer K, Gissot L, Le Gourrierec J, Samach A, Coupland G. 2006. CONSTANS and the CCAAT box binding complex share a functionally important domain and interact to regulate flowering of Arabidopsis. Plant Cell 18:2971-2984.

Windram O, et al. 2012. Arabidopsis defense against Botrytis cinerea: chronology and regulation deciphered by high-resolution temporal transcriptomic analysis. Plant Cell 24:3530-3557.

Windram O, Stoker C, Denby K. 2015. Overview of Plant Defence Systems: Lessons from Arabidopsis - Botrytis cinerea Systems Biology in Publishing SI, ed. Botrytis – the Fungus, the Pathogen and its Management in Agricultural Systems. Switzerland.

Wray GA. 2003. Transcriptional regulation and the evolution of development. Int J Dev Biol 47:675-684.

Xing Y, Zhang S, Olesen JT, Rich A, Guarente L. 1994. Subunit interaction in the CCAAT-binding heteromeric complex is mediated by a very short alpha-helix in HAP2. Proc Natl Acad Sci U S A 91:3009-3013.

Xu L, Lin Z, Tao Q, Liang M, Zhao G, Yin X, Fu R. 2014a. Multiple NUCLEAR FACTOR Y transcription factors respond to abiotic stress in Brassica napus L. PLoS One 9:e111354.

Xu MY, Zhang L, Li WW, Hu XL, Wang MB, Fan YL, Zhang CY, Wang L. 2014b. Stress-induced early flowering is mediated by miR169 in Arabidopsis thaliana. J Exp Bot 65:89-101.

Xu X, Chen C, Fan B, Chen Z. 2006. Physical and functional interactions between pathogen-induced Arabidopsis WRKY18, WRKY40, and WRKY60 transcription factors. Plant Cell 18:1310-1326.

Yamamoto A, Kagaya Y, Toyoshima R, Kagaya M, Takeda S, Hattori T. 2009. Arabidopsis NF-YB subunits LEC1 and LEC1-LIKE activate transcription by interacting with seed-specific ABRE-binding factors. Plant J 58:843-856.

Yoshida H, Okada T, Haze K, Yanagi H, Yura T, Negishi M, Mori K. 2000. ATF6 activated by proteolysis binds in the presence of NF-Y (CBF) directly to the cis-acting element responsible for the mammalian unfolded protein response. Mol Cell Biol 20:6755-6767.

---. 2001. Endoplasmic reticulum stress-induced formation of transcription factor complex ERSF including NF-Y (CBF) and activating transcription factors 6alpha and 6beta that activates the mammalian unfolded protein response. Mol Cell Biol 21:1239-1248.

Yun J, Chae HD, Choi TS, Kim EH, Bang YJ, Chung J, Choi KS, Mantovani R, Shin DY. 2003. Cdk2-dependent phosphorylation of the NF-Y transcription factor and its involvement in the p53-p21 signaling pathway. J Biol Chem 278:36966-36972.

Zander M, La Camera S, Lamotte O, Metraux JP, Gatz C. 2010. Arabidopsis thaliana class-II TGA transcription factors are essential activators of jasmonic acid/ethylene-induced defense responses. Plant J 61:200-210.

Zanetti ME, Ripodas C, Niebel A. 2017. Plant NF-Y transcription factors: Key players in plant-microbe interactions, root development and adaptation to stress. Biochim Biophys Acta 1860:645-654.

Zemzoumi K, Frontini M, Bellorini M, Mantovani R. 1999. NF-Y histone fold alpha1 helices help impart CCAAT specificity. J Mol Biol 286:327-337.

Zhang JZ. 2003. Overexpression analysis of plant transcription factors. Curr Opin Plant Biol 6:430-440.

Zhang L, Kars I, Essenstam B, Liebrand TW, Wagemakers L, Elberse J, Tagkalaki P, Tjoitang D, van den Ackerveken G, van Kan JA. 2014. Fungal

endopolygalacturonases are recognized as microbe-associated molecular patterns by the arabidopsis receptor-like protein RESPONSIVENESS TO BOTRYTIS POLYGALACTURONASES1. Plant Physiol 164:352-364.

Zhang M, Hu X, Zhu M, Xu M, Wang L. 2017. Transcription factors NF-YA2 and NF-YA10 regulate leaf growth via auxin signaling in Arabidopsis. Sci Rep 7:1395.

Zhang W, Fraiture M, Kolb D, Loffelhardt B, Desaki Y, Boutrot FF, Tor M, Zipfel C, Gust AA, Brunner F. 2013. Arabidopsis receptor-like protein30 and receptor-like kinase suppressor of BIR1-1/EVERSHED mediate innate immunity to necrotrophic fungi. Plant Cell 25:4227-4241.

Zhang Y, Gao P, Yuan JS. 2010. Plant protein-protein interaction network and interactome. Curr Genomics 11:40-46.

Zhao H, Wu D, Kong F, Lin K, Zhang H, Li G. 2016. The Arabidopsis thaliana Nuclear Factor Y Transcription Factors. Front Plant Sci 7:2045.

Zhao M, Ding H, Zhu JK, Zhang F, Li WX. 2011. Involvement of miR169 in the nitrogen-starvation responses in Arabidopsis. New Phytol 190:906-915.

Zhao Y, Wei T, Yin KQ, Chen Z, Gu H, Qu LJ, Qin G. 2012. Arabidopsis RAP2.2 plays an important role in plant resistance to Botrytis cinerea and ethylene responses. New Phytol 195:450-460.

Zheng S, Chen B, Qiu X, Chen M, Ma Z, Yu X. 2016. Distribution and risk assessment of 82 pesticides in Jiulong River and estuary in South China. Chemosphere 144:1177-1192.

Zhou X, Wang G, Sutoh K, Zhu JK, Zhang W. 2008. Identification of cold-inducible microRNAs in plants by transcriptome analysis. Biochim Biophys Acta 1779:780-788.

Zhu Z, et al. 2011. Derepression of ethylene-stabilized transcription factors (EIN3/EIL1) mediates jasmonate and ethylene signaling synergy in Arabidopsis. Proc Natl Acad Sci U S A 108:12539-12544.